Doctor of Philosophy

Modelling Metabolomic changes in human Bone Marrow derived Mesenchymal Stem Cells during Osteogenic Differentiation via Genome Scale Metabolic Modelling to further their use in Regenerative Medicine

Þóra Björg Sigmarsdóttir

September, 2021

VERKFRÆÐIDEILD
DEPARTMENT OF ENGINEERING

Modelling Metabolomic changes in human Bone Marrow derived Mesenchymal Stem Cells during Osteogenic Differentiation via Genome Scale Metabolic Models to further their use in Regenerative Medicine

by

Þóra Björg Sigmarsdóttir

Doctor of Philosophy

September 2021

Biomedical Engineering

Reykjavík University

Ph.D. Dissertation

Modelling metabolomic changes in human Bone Marrow derived Mesenchymal Stem Cells during Osteogenic Differentiation via Genome scale metabolic models to further their use in Regenerative Medicine

Dissertation submitted to the School of Science and Engineering
at Reykjavík University in partial fulfilment of the
requirements for the degree of
Doctor of Philosophy (Ph.D.) in Engineering

September 2021

Thesis Committee:

Dr. Ólafur Eysteinn Sigurjónsson, Supervisor
Professor, Reykjavík University, Iceland

Dr. Óttar Rólfsson, Co-Supervisor
Professor, University of Iceland, Iceland

Dr. Sarah McGarrity, Co-Supervisor
University of Iceland, Iceland

Dr. James Yurkovich, Co-Supervisor University
of California San Diego, La Jolla, CA, USA

Igor Marín de Mas, Examiner,
Novo Nordisk Foundation Center for Biosustainability Autoflow, Denmark

September 2021

ISBN 978-9935-9620-1-0 electronic version
ISBN 978-9935-9620-0-3 printed version
ORCID: 0000-0002-4737-4646

Modelling metabolomic changes in human Bone Marrow derived Mesenchymal Stem Cells during Osteogenic Differentiation via Genome scale metabolic models to further their use in Regenerative Medicine

Þóra Björg Sigmarsdóttir
September 2021

Abstract

In recent years the fields of regenerative and translational medicine have become the subjects of significantly growing interest due to their offer of previously unimaginable therapeutics.

Within these fields are several novel tools believed to hold the keys to furthering existing and new developments and one of those tools is human mesenchymal stem cells. One of the applications hMSCs have been studied for is enhanced osteogenic regeneration or reconstruction of new bone tissue. Although various studies have been performed and some strides been made towards a plausible clinical application there is still lot left to be discovered.

A methodical studying and relatively detailed *in silico* genome scale metabolic model modelling occurring changes and the accompanying metabolic phenotypes could provide a means to fill in the existing knowledge gaps (from the protein level all the way to the genomic level) and, additionally, a means to perform hypotheses testing with a significant reduction when it comes to the accompanying cost.

The objective of this thesis was to study the metabolomic changes in hMSCs during osteogenic differentiation using original transcriptomic, intracellular and extracellular metabolomic data in order try and define possible metabolic stages over the course of the differentiation and use genome scale network reconstruction to create *in silico* models.

In the first part of this work extracellular and intracellular data were used to define possible stages to osteogenic differentiation and hypothesise which pathways may characterise the different metabolic phenotypes. Three stages were suggested based on the data and labelled intracellular metabolomics indicated a decrease in glycolytic dependencies throughout the differentiation period with an increase in mitochondria related energy producing functions as the osteogenesis progressed. This will help focus specific time points of interest and relevance when it comes to mapping the significant metabolomic changes.

In the second part of this work extracellular metabolomic data collected from BM-hMSCs during proliferation, adipogenic and osteogenic differentiation was used along with experimentally specific data to create three directly comparable genome scale metabolic models, two of which have no comparable predecessors, for those cell lineages during the first 7 days of cell culture. Models were biologically feasible and showed all lineage specific characteristic reactions as active. By analysis and comparison, the various enriched subsystems and pathways most significant for each lineage were found. Results were varied for proliferating cells, which matches that they have to synthesise various metabolites and substances to expand, whilst fatty acid oxidation and fatty acid synthesis was most prominent in adipogenesis with fatty acid oxidation as well as transport reactions characteristic for osteogenesis. These models can be used for model-driven experimental design to engineer osteogenesis and, with modifications, to create disease model for osteoporosis.

In the third part presented we summarized the various characteristics and possibilities that lie in using MSCs as a tool in tissue engineering and regenerative medicine and how, via implementation of genome scale metabolic model reconstruction, their possibilities could

possibly be taken much further in a faster, more methodical manner while reducing the related experimental cost.

To summarise, this work has provided real strides when it comes to closing the existing gap regarding metabolomic changes during differentiation of hMSCs as well as providing novel tools that can be used to make further studies more efficient and cost effective.

Keywords: Metabolism, MSCs, osteogenesis, metabolic models, tissue engineering

Bygging erfðafræðilegra tölvulíkana sem módela efnaskiptabreytingar við beinsérhæfingu í mennskum mesenkýmal stofnfrumum einangruðum úr beinmerg.

Þóra Björg Sigmarsdóttir
September 2021

Útdráttur

Á undanförnum árum hafa sviðin endurnýjunar og tilfærslu lækningar vakið sífellt meiri áhuga vegna möguleikanna sem í þeim felast er varða nýjungar í læknavísindum. Innan þeirra má finna ýmis tól sem talin eru vera lykilatriði þegar kemur að því að finna og þróa ný meðferðarúrræði, og er eitt þessara tóla notkun mesenkýmal stofnfrumna (MSF). MSF hafa verið rannsakaðar m.t.t. ýmissa þátta þ.á.m. getu þeirra til að bæta endurnýjun beina og endurbyggingu beinvefs. Þrátt fyrir margvíslegar rannsóknir og meðfylgjandi framfarir í áttina að mögulegri klínískri notkun er margt sem er enn óljóst er varðar virkni og möguleika þessara frumna.

Nákvæm og skipulögð rannsókn ásamt tiltölulega nákvæmum tölvulíkönum sem geta hermt eftir efnaskiptabreytingum og líkt eftir samfylgjandi svipgerðum gætu verið leiðir til að stoppa upp í núverandi göt í þekkingu hvað varðar efnaskiptabreytingar, frá tjáningu gena til framleiðslu próteina, ásamt því að veita möguleika á tilgátuprófunum án meðfylgjandi kostnaðar.

Markmið verkefnisins sem hér er kynnt var að rannsaka efnaskiptabreytingar í mennskum MSF við beinsérhæfingu til að reyna að skilgreina mögulega efnaskipta fasa sem beinsérhæfingartímabilið væri samsett úr og búa til *in silico* módel byggð á genatengdum upplýsingum til að líkja eftir breytingunum.

Í fyrsta hluta þessa verkefnis var notast við innan- og utanfrumu metabolómísk gögn til að skilgreina möguleg mismunandi stig beinsérhæfingar og hvaða efnaskiptabrautir geta legið þar að baki. Eftir greiningu gagna var lögð var fram tilgáta um tilveru þriggja mismunandi fasa og merkt innanfrumu gögn bentu til dvínandi virkni í glýkólýsu í gegnum sérhæfingartímann á sama tíma og aukningu gætti í hvatbera tengdum orkugefandi ferlum eftir því sem leið á. Þessar niðurstöður geta hjálpað með að finna tímapunkta sem eru af sérstökum áhuga er varðar kortlagningu mikilvægra efnaskiptabreytinga.

Í öðrum hluta verkefnisins var notast við utanfrumu metabólómísk gögn sem safnað var frá mennskum MSF einangruðum úr beinmerg sem ræktaðar voru við venjulega skiptingu, fitu- og beinsérhæfingu, og þau notuð ásamt sértækum tilraunatengdum gögnum til að búa til þrjú sambærileg *in silico* módel, þau fyrstu sinnar gerðar, er líkja eftir efnaskiptabreytingum þessara þriggja frumugerða fyrstu 7 daga ræktunar. Módelin voru öll líffræðilega möguleg og sýndu af sér öll helstu einkennandi hvörf sem virk. Við greiningu og samanburð á módelunum fundust helstu breyttu undirkerfi og efnaskiptaferlar er voru einkennandi fyrir hverja frumugerð fyrir sig. Í tilviki frumna í venjulegri skiptingu voru breytt kerfi mjög fjölbreytt sem endurspeglar þær fjölbreyttu kröfur sem fruma þarf að uppfylla við að búa til annað eintak af sér, í tilviki fitusérhæfingar var nýmyndun og oxun fitusýra hvað mest áberandi og oxun fitusýra ásamt flutnings hvörfum einkenndu beinsérhæfingu. Þessi módel má nota til að sigta úr og setja upp ákjósanlegar tilraunir til að besta beinsérhæfingu og með breytingum mætti búa til sjúkdómsmódel til að líkja eftir beinþynningu.

Í þriðja þætti verkefnisins sem hér er kynnt hafa verið tekið saman þau margvíslegu einkenni og fjölmörgu möguleikar er felast í MSF sem tóli til að nýta í endurnýjunar lækningum og vefjaverkfræði og hvernig, með notkun *in silico* efnaskiptamódela byggðum á genaupplýsingum, þá möguleika mætti þróa áfram á skilvirkari og hraðari máta samtímis því að lækka tilraunatengdan kostnað.

Þetta verkefni hefur lagt sitt af mörkum er kemur að því að minnka núverandi eyðu þekkingar er varðar efnaskiptabreytingar er eiga sér stað í gegnum beinsérhæfingu mennskra MSF og

hefur komið með að borðinu ný tól sem geta nýst til frekari rannsókna á sama sviði meðfram því að geta gert þær skilvirkari og hagkvæmari.

Lykilorð: Efnaskipti, mesenkýmal stofnfrumur, beinsérhæfing, tölvulíkön, vefjaverkfræði

The undersigned hereby certify that they recommend to the School of Science and Engineering at Reykjavík University for acceptance this Dissertation entitled

Modelling metabolomic changes in human Bone Marrow derived Mesenchymal Stem Cells during Osteogenic Differentiation via Genome scale metabolic models to further their use in Regenerative Medicine

sub- mitted by **Þóra Björg Sigmarsdóttir** in partial fulfilment of the requirements for the degree of **Doctor of Philosophy (Ph.D.) in Engineering**

date

Ólafur Eysteinn Sigurjónsson,
Supervisor Professor,
Reykjavík University, Iceland

Óttar Rólfsson,
Co-Supervisor Professor,
University of Iceland, Iceland

Sarah McGarrity,
Co-Supervisor
University of Iceland, Iceland

James Yurkovich,
Co-Supervisor
University of California San Diego. La Jolla, CA, USA

Igor Marín de Mas, Examiner,
Novo Nordisk Foundation Center for Biosustainability Autoflow, Denmark

I dedicate this to my family and friends, who have never, ever stopped believing in me.

Acknowledgements

I want to give a particular and heartfelt thanks to my Ph.D. committee. I was fortunate to get a chance to study and grow under the guidance of such a great group made up of incredibly versatile and talented people. They became not only mentors but also friends from whom I learnt how to evolve as a scientist and a person. I owe them all (and have a feeling they wouldn't mind payment in one beer or two) but despite that I want to mention in particular my lead supervisor, Professor Ólafur Eysteinn Sigurjónsson, who saw something in me way before I ever could and never gave up on me (even when I felt like it) and talked me of the ledge a few times. And there were quite a few times, especially in the beginning (a Ph.D. really should come with a health warning). I also want to give special thanks to Sarah McGarrity, but having a team-member of such skill but still so close in age made quite a difference when things on the personal front got tough.

I also want to give my family and friends the written equivalence of a tremendous applause for their never failing belief and encouragement throughout my whole academic career. They never possessed a single doubt of if I would be able to reach my goal or not. It was just a matter of time to them. And without such belief (and in some cases quite extreme and lavish bouts of compliments from my best friend, Gróa, that would make anyone red in the face) I don't think I would have come out the other side of all of this as put together as I am. Though I guess some would debate the integrity of that "put together-ness", however that is another matter.

I also want to give thanks to the Icelandic Bloodbank and its staff, that has provided me with facilities to perform my research and work since 2017 and where I have spent many weekends and some late nights, as well as DeCode genetics and some of the talented people there whose help played a large role in my presented work.

This work was funded by the Icelandic Research Fund (grant number 217005), and for that I will be forever grateful as it is (sadly) not the common position to be in to be able to get paid to perform this kind of research work and studies, even though the hours far exceed the standardized 8 hour workday. My hope is that science and the people devoted to furthering our knowledge, in almost whichever field, of it will one day get the recognition that they (or should I now say we?) deserve as well as the funding to go along with it. Because, after all, where would the world be without science?

Thank you everyone, I can hardly believe this whole thing happened. Who ever planned on doing a Ph.D.?! I for sure did not!

Preface

This dissertation is original work by the author, Þóra Björg Sigmarsdóttir. Portions of the introductory text are used with permission from Sigmarsdóttir et al [1] of which I am an author.

Contents

Acknowledgements ..... **x**
Preface ..... **xi**
List of Figures ..... **xv**
List of Tables ..... **xvi**
List of Abbreviations ..... **xvii**
1 Introduction **1**
1.1 Biology of Mesenchymal Stem Cells (MSCs) 4
1.1.1 Differentiation on MSCs 5
1.1.2 Immunomodulation of MSCs 6
1.1.3 Homing effects of MSCs 7
1.1.4 MSCs in regenerative medicine 8
1.1.5 Cell engraftment vs. Paracrine Factors 9
1.1.6 Existing Challenges and Problems 10
1.2 Metabolism of MSCs 10
1.2.1 Function is linked to Metabolism 11
1.2.2 Mitochondrial Impact on MSC function 12
1.2.3 Possible Manipulation of Metabolism 12
1.3 Metabolomics and Transcriptomics 13
1.3.1 Mass Spectrometry 14
1.3.2 Techniques to Separate Metabolites 15
1.3.3 LC-MS data analysis 16
1.3.4 RNA-Sequencing (RNAseq) 17
1.3.5 RNA data analysis 18
1.4 Genome Specific Metabolic Models 20
1.4.1 Mathematical Modelling of Human Metabolism 20
1.4.1.1 A brief overview of the mathematical representation of a metabolic network 22
1.4.1.2 Current Human Metabolic Reconstruction – Recon3D 23
1.4.1.3 Current State-of-the-Art Application 23
1.4.2 Benefits of integration of varied -omics data 24
1.4.3 The value of Cell Specific and Circumstance specific Metabolic Models 25
1.4.3.1 Deeper Insights into Metabolism 26
1.4.3.2 Uncovering Changes over Time 26
1.5 What the future holds 27

2 Purpose **29**
3 Materials and Methods **31**
3.1 Cell culturing 31
3.1.1 Seeding, harvesting and expanding MSCs 31

3.1.2 Osteogenic Differentiation 31
3.1.3 Adipogenic Differentiation 32
3.1.4 Osteogenic differentiation for labelled extracellular metabolomic and intracellular metabolomics sampling 32
3.1.5 Osteogenic differentiation for unlabelled intracellular metabolomics sampling and BCA protein assay 32
3.1.6 Osteogenic differentiation for RNA-sequence sampling 33
3.1.7 Quality Control Assays for Osteo- and Adipogenesis 33
3.1.7.1 Reflection – How could cell culture experiment planning be changed to enhance precision and usefulness of downstream work? 33
3.2 Metabolomic measurements 34
3.2.1 Non-MS Metabolite measurement - Paper I 34
3.2.1.1 Data normalisation and processing - Paper I 34
3.2.2 Extracellular Metabolite Extraction – Paper I and II 35
3.2.3 Intracellular labelled and unlabelled Metabolite Extraction – Paper I 36
3.3 UPLC-MS -Paper I and II 36
3.4 RNA-sequence measurement, data processing and normalisation – Paper I 37
3.5 LC-MS Data Processing and Normalisation 38
3.5.1 Extracellular targeted data processing using TargetLynx – Paper II 38
3.5.2 Intracellular untargeted data processing using XCMS -Paper I 38
3.5.2.1 Mummichog pathway and network analysis 39
3.5.2.2 Targeted Ms-MS analysis to confirm Mummichog metabolite prediction 39
3.5.3 BCA Protein Assay 39
3.6 Statistical Analysis 40
3.6.1 LC-MS data 40
3.6.2 RNA sequence data 40
3.7 Genome Scale Metabolic Modelling 40
3.8 Model Comparison 41

4 Results and Discussion 43

4.1 Paper I: Using measurements of key metabolites to define metabolic stages during osteogenic differentiation of mesenchymal stromal cells 43
4.2 Paper II: Analysing metabolic states of adipogenic and osteogenic differentiation in human mesenchymal stem cells via genome scale metabolic model reconstruction 46
4.3 Paper III: Current Status and Future Prospects of Genome-Scale Metabolic Modelling to Optimize the Use of Mesenchymal Stem Cells in Regenerative Medicine 50

5 Conclusions and Future Directions 53

5.1 Conclusions 53
5.2 Challenges and Limitation 55
5.3 Future Directions 57

References **61**
Paper I **81**
Paper II **115**
Paper III **131**
Appendix A **157**

List of Figures

Figure 1: Characterisation of MSCs. 5
Figure 2: RNA data analysis workflow. 19
Figure 3: Phases of osteogenic differentiation. 44
Figure 4: PLSDA visualization of m/z values with significantly different ion intensities during osteogenic differentiation. 45
Figure 5: Estimates optimal fluxes for ATP production from various key carbon sources 49
Figure 6: Relative mean fluxes (compared to expansion model) from various reactions – 49

List of Tables

Table 1: Immunomodulation of hMSCs. 7

Table 2: Showing subsystems that have a significantly overrepresented. 50

List of Abbreviations

RM – Regenerative Medicine
TE – Tissue Engineering
HA – Hydroxyapatite
CPC – Calcium Phosphate Cement
MSCs – Mesenchymal Stem Cells
RNA - Ribonucleic Acid
GEM – Genome scale metabolic model
HT – High Throughput
DNA – Deoxyribonucleic Acid
hMSCs – Human Mesenchymal Stem Cells
BM – Bone Marrow
ISCT – International Society for Cellular Therapy
BMP – Bone Morphogenic Protein
LPL – Lipoprotein Lipase
ALP – Alkaline Phosphate
RUNX2 – Runt-related transcription factor 2
OD – Osteogenic Differentiation
AD – Adipogenic Differentiation
NK – Natural Killer Cell
IS – Immune System
BM-hMSCs – Bone Marrow derived human Mesenchymal Stem Cells
Ad-hMSCs – Adipose derived human Mesenchymal Stem Cells
GvHD – Graft versus Host Disease
GMP – Good Manufacturing Practise
OxPhos – Oxidative Phosphorylation
PPP – Pentose Phosphate Pathway
HIF-1 – Hypoxia Inducible factor 1
IFNγ – Interferon gamma
CK – Creatine Kinase
NADP-IDH – Reversible mitochondrial adenine dinucleotide dependent reaction of isocitrate dehydrogenase
ROS – Reactive Oxygen Species
NMR – Nuclear Magnetic Resonance
MS – Mass Spectrometry
LC-MS – Liquid Chromatography Mass Spectrometry
LC-QTOF-MS - Liquid Chromatography quadrupole time-of-flight mass spectrometry
DC – Direct Current
RF-AC – Alternating Radio Frequency Current
HPLC – High performance Liquid Chromatography
UPLC – Ultra performance Liquid Chromatography

EI – Electrospray Ionisation
APCI – Atmospheric Pressure Chemical Ionisation
RNAseq – RNA sequencing
PCR – Polymerase Chain Reaction
cDNA – Complimentary Deoxyribonucleic Acid
EST – Expressed Sequencing Tags
NGS – Next Generation Sequencing
RPKM – Read Per Kilobase Million
FPKM – Fragments Per Kilobase Million
TPM – Transcripts Per Million
CBMs – Constraint Based Models
FBA – Flux Balance Analysis
BiGG – Biochemical, genetic and genomic [database]
S – Stoichiometric Matrix
ATP – Adenosine Triphosphate
IEM – Inborn Errors of Metabolism
MTA – Metabolic Transformation Algorithm
dFBA – Dynamic Flux Balance Analysis
uFBA – Unsteady-state Flux Balance Analysis
SOP – Standard of Practice
SBML – Systems Biology Mark-up Language
FVA – Flux Variability Analysis
CRISPR – Clustered Regularly Interspaced Short Palindromic Repeats
Cas9 – CRISPR-associated protein 9
FBS – Foetal Bovine Serum
PIPL – Platelet Inactivated Platelet Lysate
WHO – World Health Organisation
OCR – Oxygen Consumption Rate
ECAR – Extracellular Acidification Rate
OoC – Organ on a Chip

1 Introduction

''Any sufficiently advanced
technology is indistinguishable from magic. ''

Arthur C. Clarke, British Science-Fiction writer (1917-2008).

The skeleton is the foundation upon which a body stands. Its function is by and large six-fold; protection, support, movement, production of blood cells, storage of minerals and endocrine regulation [2]. From this it is fair to say that strong, stable, well-functioning bones are precious and important to a person's wellbeing and a necessity to be able to maintain an active role in modern society.

Bone is a dynamic structure, it is constantly renewing and changing throughout a person's lifespan in order to mend microfractures and adjust to the ever changing load that it is put under [3].

There are various factors that can negatively impact the skeletons' integrity (e.g. drugs, hormonal changes, and physical activities) but the one that is most prevalent is age. With increased age this important foundation becomes brittle; a combination of the ever ongoing remodelling process becoming less efficient and a decrease in loading stimulus in the aged are thought to be the primary causes [4]. Osteoporosis and even osteoarthritis start to gain leverage, often in such a manner that intervention is needed. The fields of regenerative medicine (RM) and tissue engineering (TE) have been developing possible treatments for use in such instances, but the field of RM seeks solutions for the restoration of structure and function of tissues and organs that have in some way become permanently damaged [5], [6]. As of yet more often than not the chosen intervention or therapeutic is only partially successful [7], [8].

Age does not even have to get a hold in order to compromise mechanical properties of bones. The body can only mend fractures that are below a certain critical size on its own and so bone defects created either by accidents or necessary surgical intervention (e.g. due to osteosarcoma) may in many cases need external aid in order to heal [9]. This aid can range from metal screws to fasten bone fractures to bone grafts or implantations meant to bridge an otherwise unbridgeable gap [10].

Bone grafts and bone related substitutes are used in various applications during orthopaedic surgeries, with approximately two million bone grafts performed globally in the year 2017 [11] and the market for such applications only expected to continue to rise with an annual growth rate of 5% at least until the year 2028 [12].

There are a few key factors that are driving the market growth in bone graft and bone substitute demand (e.g. growing prevalence of orthopaedic defects and transition towards minimally invasive surgeries) but the main reason is an unprecedented growth of the aging global population [12]. It is predicted that by the year 2050 the number of people over the age of 60 will have gone from 900 million (recorded in 2015) to over 2 billion [13], and the currently available materials all come with various risks and limitations.

Currently, a varied array of bone related substitutes exist, ranging from being in the early stages of development to being relatively common and in clinical use [14]. Roughly they can be divided into two groups, synthetic and natural materials. In the synthetic material group substances such as ceramics, bone cement and polymers can be found whilst in the group spanning natural materials biological substitutes are more prevalent, i.e. autografts, allografts and demineralised bone matrixes to name a few [14], [15].

Currently hydroxyapatite (HA) and bone cement (calcium-phosphate cement (CPC) in particular) are the most common materials in clinical use today but natural materials, with autografts in the lead, are overall preferred due to their osteogenic potential and are often considered to be the gold standard for bone substitution [14].

However, with each and every one of the available substitutes come some risks and limitations. With bone cements the risk of cement fragmentation, foreign body reaction due to wear debris and potential allergic reactions follow its use whilst with natural materials such as autografts the rather great potential risk of donor site morbidity problems due to the highly invasive surgeries required for material gathering is presented along with possibilities of donor-host problems (applicable if using e.g. allografts) and a very limited material supply relative to synthetic materials [8], [11], [15]. Due to all of these existing problems regarding available material, along with the rising demand of bone grafts and substitutes the use of mesenchymal stem cells (MSCs), as a way to enhance the use of already available therapeutics and aid in development of new ones has been on the rise in TE and RM [16]–[19]. Mesenchymal stem or stromal cells (MSCs) are post-natal, self-renewing, multipotent cells with stem cell like abilities that can be isolated from various adult tissues (e.g. peripheral blood, bone-marrow and adipose tissue) as well as neonatal tissue types (e.g. Wharton's jelly and umbilical cord blood) found within the body [20], [21], [22]. They are defined e.g. by their ability to differentiate into cells of the mesodermal origin (e.g. chondrocytes, adipocytes and osteoblasts) whilst maintaining their proliferation abilities, their remarkable immunomodulatory capabilities and homing effects [17], [23] and they are currently one of the most common type of cell used in TE and RM related research [16]–[18], [24]–[26]. In this regard MSC metabolism has for the past decade been of an ever growing interest due to accumulation of evidence suggesting that metabolic manipulation of the cells may allow for enhanced therapeutic uses via augmented cell retention, cell survival, differentiation and immunoregulation to name but a few ways [27]–[36]. However, despite there being a partial success when it comes to research where MSCs are used in bone replacement focused TE [37][38][39] there are certain problems that keep turning up and need to be addressed in a methodical and decisive manner in order to enable a continued and greater use of these cells in a way that is more efficient when it comes to both cost and therapeutical manner.

All cell focused applications in regenerative medicine require a relatively large amount of cells (though optimal amount is still unclear) [40] but prolonged expansion can have adverse effect of the quality of function desired from the cells [41] even though it has been shown that transplantation of expanded cells is not in itself harmful [42], [43].

In order to reduce costs related to cell focused therapies it will be necessary to create a focused and efficient way to expand and differentiate the cells *in vitro* whilst keeping their characteristics and functionality as optimal as possible.

Another problem that needs addressing and for which cell focused therapies are a good candidate is osteoporosis. Osteoporosis is a quite common and sometimes severe age or lifestyle related disease that can go unnoticed up until a major fraction occurs. A certain "malfunction" of MSCs in osteoporosis pushes cells towards adipogenesis, resulting in adipose accretion in the bone marrow. This happens at the expense of osteoblast formation which indicates that in this disease condition the cell behaviour is altered, and their microenvironment disturbed. A similar occurrence has been observed when under microgravity conditions [44]–[47].

Both proliferation (expansion of cells) and the progress of differentiation of MSCs have been directly linked to their metabolic states and those states have been shown to change throughout the different processes[30], [31], [34], [48]–[51].Cellular metabolism comprises a very intricate and complex system, involving various pathways, metabolites, enzymatic reactions and cofactors that all have numerous effects on both the cell and its immediate microenvironment [32], [52]–[54]. The interplay between these aspects down to the way genes, RNA and proteins connect and interact, is extremely complicated and as of yet unclear in its various aspects to the research community.

By gaining a more thorough understanding of how various factors affect the apparent metabolic change a greater optimisation of both expansion methods and initial *in vitro* differentiation methods for MSCs could be made possible and development of more effective standardized culturing methods might be pushed. Additionally the undesired shift from osteogenesis to adipogenesis that occasionally seems to happen upon *in vivo* implantation and that is at least partially to blame for osteoporosis development [4], [7], [44], [55] might be prevented. A more grounded understanding could additionally give better focus to research aimed at developing or advancing therapeutics for such diseases as osteoporosis and osteonecrosis – disease states that both seem to be dependent upon metabolically linked changes in the body's' osteoprogenitor cell capabilities [56], [57].

In order to get closer to this and do it with the additional hopes of reducing future experimental cost, implementation of genome scale metabolic models (GEMs) [58] is reasonable way to go.

As a wholistic systems biology approach GEMs acknowledge that biological systems, such as cells or cell metabolism, are made up of a network of networks and with the advent of high throughput (HT) –omics technologies the detailing that genome scale metabolic networks entail has been enabled [59]–[61].

Over the course of the last few years, it has become clearer that data analysis and interpretation is becoming the most prevalent bottleneck when it comes to any kind of biological discovery due to increasingly more efficient ways in generating HT data. A robust modelling and analysis formalism such as GEMs are can be used to organise and interpret the HT data as they serve as a model concentric databases built upon current DNA sequencing technologies as well as the HT data and so provide a framework for wholistic studies of cellular metabolism [59]–[61].

Whilst some form of constraint based models focus on metabolism at the reaction level GEMs allow its study at the gene level by accounting for individual fluxes of enzymes encoded by each gene [62][63], [64]. This makes it easier to study the mechanistic link

between a cell phenotype and a genotype through the complex gene-protein reaction association.

This is in large part done by combination of various types of -omics data that together form stoichiometric, thermodynamic, enzyme capacity and in some instances kinetic constraints [59]–[62], [65].

Metabolic or metabolomic data can provide a biochemical snapshot of a global metabolic state within a system but it does not manage to account for any reactions nor enzymes that are producing the governing state. Conversely, genomic data only shows the potential of a cell without any information regarding its current functional state [66]. By integrating these types of data, along with other ones (e.g. proteomics and genomics), in a unified modelling framework such as a genome scale reconstruction one can obtain a much more distinctive understanding not just of the observed state of metabolism at a particular point in time but of how a cell achieves the observed metabolic state. These types of models are generally built through reverse engineering a network structure, making it more condition specific via integration of the previously mentioned types of data [59], [60], [67], [68].

Through creation of the kind of models that focus on metabolic changes of human mesenchymal stem cells (hMSCs), as are described in this thesis, an *in silico* laboratory can be built capable of aiding in experimental design for cell culture laboratories that have higher probability of success and so aid in cost reduction as well as provide insights into complex internal workings of MSCs thus allowing for a better understanding of ways to implement them in an efficient therapeutic manner in regenerative medicine and tissue engineering.

1.1 Biology of Mesenchymal Stem Cells (MSCs)

Mesenchymal stem or stromal cells (MSCs) are believed to have been originally discovered in the year 1976 by Freidenstein and colleagues [69] though evidence of the presence of nonhematopoietic stem cells in bone marrow date back to the year 1867 [70]. The term *mesenchymal stem cell* was first proposed by Caplan in the early 90s as term to be used for progenitor cells isolated from human adult bone marrow (BM) and though the definition of it has widened through the years it maintains it wide spread popularity [71].

Mesenchymal stem cells comprise non-hematopoietic cell that originate from the mesodermal germ layer [18], [72]. They are classified as multipotent cells with stem cell like abilities, capable of both self-renewal and multilineage differentiation into various tissues of the mesodermal origin [72] (figure 1).

These multipotent cells can be isolated from various adult tissues types, in additional to bone marrow, (e.g. skin, peripheral blood, adipose tissue) as well as neonatal tissues (e.g. umbilical cord blood, Wharton‘s jelly) [20].

Currently there does not exist any definitive historical concensus regarding methods of isolation, proliferation and characterisation of hMSCs, however the International Society for Cellular Therapy (ISCT) has produced a criteria that in a minimal way defines hMSCs [17], [23]. In order to be classified as hMSCs, the cells must be able to:

i. Adhere to plastic and develop as fibroblast colony-forming units and differentiate in to cells of the mesodermal origin (i.e. osteocytes, chondrocytes and adipocytes) when cultured *in vitro*.
ii. Lack expression of surface markers CD11b, CD14, CD19, CD34, CD45 and HLA-DR surface markers when cultured for proliferation *in vitro*.
iii. Express surface markers CD73, CD90 and CD105 when cultured for proliferation *in vitro.*

This criterion is likely to evolve and change over time with continued study and discovery relating to hMSCs.

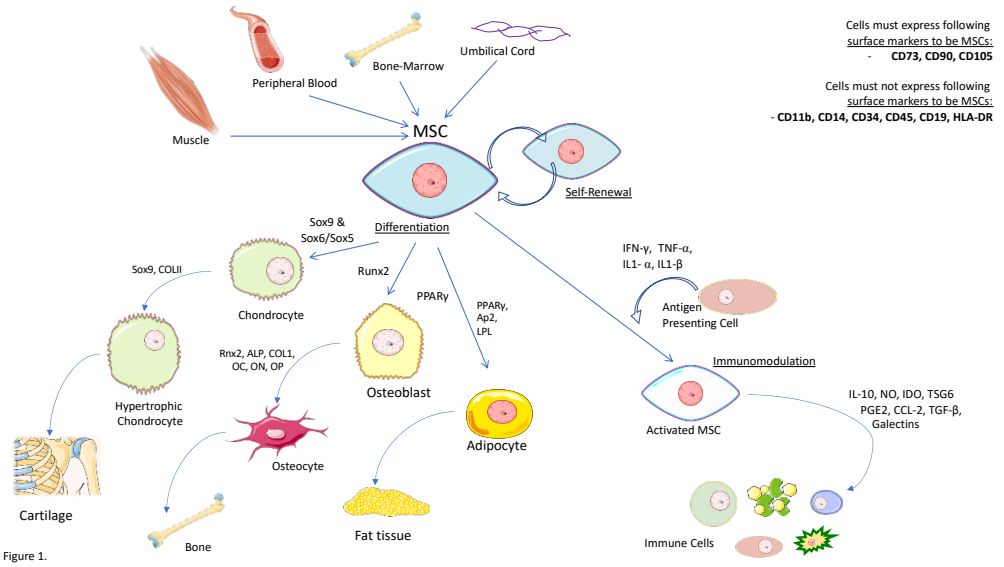

Figure 1: Characterisation of MSCs. MSCs can be isolated from various tissues, e.g. muscles and bone marrow, they can differentiate, are capable of self-renewal and immunomodulation (when activated) by secreting various factors. Figure created by author, adapted from [73]. Created using Biorender.com.

1.1.1 Differentiation on MSCs

One of the most identifying characteristics of hMSCs is their ability to differentiate into cells of the mesodermal origin.

Though the hallmark trilineage differentiation (i.e. osteogenic, chondrocyte and adipogenic differentiation) is probably the one most researched there have been reports of hMSC differentiation into cells of the ectodermal and endodermal origin. This includes tenocytes, cardiomyocytes, skeletal myocytes, smooth muscle cells and neurons. There is however an ongoing debate about the functionality of the end product of these trans-differentiations.

Under standard *in vitro* conditions differentiation of hMSCs is induced via various media supplementation. There are also instances of inducing differentiation through the use of scaffolds with varying modules of elasticity or surface modifications and mechanical stimulation [74], [74]–[76].

Different supplements are required for the varying differentiations. Chondrogenesis requires additions of e.g. ascorbate 2-phosphate, dexamethasone and linoleic acid [77]–[79]. Osteogenesis is most often induced through supplementation of dexamethasone, ascorbic acid, β-glycerophosphate and bone morphogenic protein (BMP) 2 [18], [80], [81] and adipogenesis via dexamethasone, insulin and indomethacin to name but a few of the required additions [81]. A more comprehensive list of differentiation inducing components and methods that have been registered for a few varying differentiations of MSCs can be seen in **table 1**.

Progression of the differentiation process is checked and verified throughout the culturing period to establish a successful culture. This is done by checking the expression levels of characteristic cell type markers that are different in each case. A common marker to check in the case of chondrogenesis is e.g. Sox9, in adipogenesis it is lipoprotein lipase (LPL) or peroxisome proliferator- activated receptor γ (PPAR γ) and for osteogenesis it most commonly is alkaline phosphatase (ALP) or runt-related transcription factor 2 (RUNX2) [79], [81].
Differentiation is in many cases a multi-phased process, controlled throughout by interlinked set of regulatory molecules that together form highly complex signalling pathways. For the most part each type of differentiation has its own distinct signalling pathways but there can be found overlapping areas of some importance. This is true e.g. for the processes of adipogenic (AD) and osteogenic differentiation (OD). The integrated signalling network involved in those differentiation maintains a delicate balance between the processes with activation or induction towards one having inhibitory effects on the other.

1.1.2 Immunomodulation of MSCs

As well as their differentiation potential, hMSCs have important immunomodulatory properties that have been gaining an increased focus when it comes to cell mediated therapeutics [82]. The immunomodulation enables the cells to either inhibit or promote immune responses of the host's body through a combination of direct inhibitory effects and indirect regulatory effects. Largely this regulatory response entails decreased natural killer (NK) cell activation as well as dendritic cell maturation, inhibition of various cytokine production and inhibition of B- and T-cell proliferation [83]–[86].

Immunomodulatory effects of hMSCs are not steadily ongoing, the cells are only activated through inflammatory cytokines that are secreted by T-cells and other antigen-presenting cells [82], [87], [88]. When activated hMSCs secret soluble immune factors that, by mediating the resulting regulatory response of the target cell in question, can affect both the adaptive and innate immune systems (figure 1). The combination of secreted factors determine the mediated immunoregulatory effects in each instance of activation [82], [87], [88][89]. In **table 1** a summary of inflammatory cytokines capable of activating the immunoregulatory state of hMSCs can be seen, along with the major known soluble paracrine factors that the cells secret and resulting biological functions.

Table 1: Immunomodulation of hMSCs. Summary of secreted factors and exerted effects.

Immunomodulation of hMSCs				
hMSC activating inflammatory cytokines	**Immune cell type**	**hMSC function**	**hMSC secreted immunosuppressive factors**	**Biological functions exerted by hMSC secreted factors**
IFN-γ, IL-1α, IL-1β, TNF-α	DCs (innate IS)	Inhibit migration, activation, differentiation, maturation and endocytosis	CCL2	Promotion of monocyte migration. Suppression of activation and mitigation of TH17 cells
	NK cells (innate IS)	Inhibit migration, proliferation, differentiation, maturation and activation	Galectins	Suppression of Tcell immunomodulatory effects
	Macrophages (innate IS)	Activate M2 polarization in general, activate M1 polarization in specific microenvironments	IDO	Suppression of effects and proliferation of immune cells
	T cells (adaptive IS)	Inhibit cell survival proliferation, differentiation, maturation and activation, accelerate cell recruitment	IL-10	Suppression of immune cell apoptosis
	B cells (adaptive IS)	Inhibit proliferation, differentiation, maturation, chemotaxis and activation	NO	Promotion of immune cell apoptosis. Suppression of T cell proliferation and modulation
			PGE2	Suppression of NK cell cytolytic activity and T cell proliferation
			TSG6	Overall anti-inflammatory effect
			TGF-β	Inhibition of NK cell activation and proliferation, Treg induction and mast cell degranulation

During the past few years there has been accumulation of emerging data that suggests that the immunoregulatory effects that hMSCs exert could become a promising tool in such therapeutical applications as tissue repair, inflammatory diseases (e.g. Graft versus Host Disease, Chron's, Type 1 Diabetes) and immune disorders (e.g. Systemic Lupus Erythematosus) though many issues still need settling before common clinical application can take place [86].

1.1.3 Homing effects of MSCs

In addition to secreting immunosuppressive factors, hMSCs secrete paracrine factors that promote tissue repair. As a response to tissue related damage hMSCs secrete factors that allow their navigation to the injured site, an effect commonly referred to as homing [90], [91].

This effect is generally considered as beneficial to tissue repair because of hMSC interaction with the damaged tissue through secretion of both trophic and paracrine factors. It is through a combination of this homing effect as well as direct cell delivery that enables engrafting or migration of hMSCs in experimental settings[90], [92]. Over 40 different migration and homing molecules have been recorded to be expressed on hMSCs [91].

Both homing effect and the following migration of hMSCs has been observed in experimental setting, but the mechanisms that lie behind it are as of yet ill understood and only a small proportion of systematically administrated cells actually manages to reach target

tissue and remain[91], [92]. Several factors are believed to be involved in causing this low success rate.

The expression of homing molecules on hMSCs is fairly limited and it seems that *in vitro* expansion of the cells diminishes this low expression even further. Cultural and expressional heterogeneity of the cells and molecules also seems to be problem, but hMSCs derived from different sources seem to express different homing molecule profile. There are several ongoing researches aimed at improving the efficiency and retention of hMSCs homing to further their retention after systemic administration and strategies that either have or are in development are e.g. modification of the mode of administration, pre-treatment or priming of cells or culture conditions and genetic modification [91].

1.1.4 MSCs in regenerative medicine

Regenerative medicine, a term widely considered to have been coined in 1999 by William Haseltine, is considered to be novel frontier when it comes to medical research [5], [6], [93]. It is a field that combines the knowledge and application of tissue engineering, stem cell biology, cell transplantation, biochemistry, prosthetics and biology with the aim to either replace or restore human cells, tissues and organs that have become permanently damaged back to their original normal functions [6].

There are a variety of regenerative medicine therapies available [92], [94]–[99], though at different stages in clinical development, but the associated success is so far very limited. This limitation is for the most part due to functional obstacles that in some way or form reduce the therapeutic efficacy and increase risk of harm towards patients.

Though some applications have shown both progress and promise there is a great room for improvement, by targeting the above mentioned limiting factors.

The hMSC characteristics, i.e. their multipotency, differentiation abilities, high proliferation potential, immunomodulatory activity and paracrine effect [17], [18], [100], have made these cells a focus of many researches as a possible novel tool to be developed for use in regenerative medicine. Included in this is immunotherapy and tissue engineering.

At the beginning there were a few fundamental challenges that needed to be overcome in order to enable use of MSCs. Recent advancements have targeted this and now there are numerous clinical trials that have assessed hMSC safety and found that cell transfusions are safe [42], [43], [101]. Various methods of isolation and culturing have been developed as studies of these cells have continued and along with study of possible mechanisms of delivery. These studies have managed to demonstrate that a relatively long-term culture of hMSCs is possible without loss of morphological, phenotypical or functional features, though cell senescence presents a problem [102], [103].

Another aspect of hMSCs that has worked to increase interest in them within the field of biomedicine is growing availability. The most popular and commonly researched hMSCs in tissue engineering and cell-based medicine currently, despite the relatively invasive procedure required for collection, are derived from either bone marrow (BM-hMSCs) or adipose tissue (Ad-hMSCs)[100]. The reasons working in their favour are varied [100]:

i. The total cell number that can be harvested at each time is higher compared to other types of stem cell.
ii. The frequency of cells that are of interest is higher compared that with other stem cells.
iii. Ad-hMSC harvesting can additionally be performed as a part of elective cosmetic surgery (e.g. liposuction).

In addition to BM-hMSCs and Ad-hMSCs, placenta and umbilical cord derived hMSCs are of a growing interest. This is largely because the associated tissues are usually discarded as waste products at birth and so there is relatively high availability and a resulting waste reduction [92].

The variance in phenotypic properties of the differently derived cells (if any) is still an open question and currently under research to some extent.

Ad-hMSCs have been shown to have comparatively increased capacity for adipogenic differentiation *in vitro*, while BM-hMSCs show an increased trend towards osteogenesis and chondrogenesis [104]. A comparative study focused on the immunomodulatory abilities of hMSCs derived from these different tissues within the same donor showed Ad-hMSCs to have a greater capacity for inhibiting differentiation of dendritic cells compared to BM-hMSCs, while the latter group seemed to have a higher capacity for NK cell cytotoxic activity inhibition [105]. These findings have been supported by several independent groups [106], [107].

All of this indicates that choosing the right cell source may prove to be paramount to the success of particular clinical application.

1.1.5 Cell engraftment vs. Paracrine Factors

For the majority of the last several decades the focus of hMSCs therapeutic potential has been on the cell transplantation aspect, i.e. adding hMSCs to a recipient donor site in the hopes of aiding in repair of tissue damage via regeneration and differentiation[108]. Through co-culturing studies done in animals it has already been shown that hMSCs, up to a certain extent, can enable tissue regeneration via infiltration and replacement in the damaged or injured tissues [109]–[112].

Lately, however, increasing attention has been focused on the possibilities that lie in the immunomodulatory and suppressive abilities of hMSCs. This holds especially true for the autocrine and paracrine factors of the cells [85], [88], [89], [113].

It has now been recognised that hMSCs exert majority of their healing effects through paracrine signalling and cell-to-cell contact, not by replacement [100].

A few notable examples have been recorded where this is utilised in symptom relief for immune disorders (e.g. graft versus host disease (GvHD) [114], arthritis [115], Crohn‘s [116]), skin healing [117], ischemic stroke treatments [85], neurovascular and musculoskeletal therapies [118] and recently there have been notions of using hMSCs in the search of cancer vaccinations, an increasingly active research topic, precisely because of their paracrine and immunomodulatory properties [113]. The newest suggested therapeutic use for hMSCs and their related secretome is in relation to the recent COVID-19 pandemic, but

reports have been made that claim hMSC infusion is proving to be both safe and effective in patients suffering from COVID-19 induced pneumonia [119].

The reported success of the above mentioned studies as well as others (see e.g. [120]–[122] indicate that the secretome of hMSCs possess therapeutically beneficial effects that may well be exploited for enhancement and development of future applications.

1.1.6 Existing Challenges and Problems

As mentioned there have already been reports of successes in both animal-studies and early-stage clinical trials when it comes to both safety and efficacy of hMSC based therapeutic applications. However, there are a number of existing challenges and problems as well as numerous questions that still go unanswered and that need to be addressed and resolved to move this aspect of regenerative medicine further.

Cell source availability is still an existing problem though more tissue types are being studied[100], [123]. Possible variance between cells from different donors and isolation sites may be effecting experimental outcomes in a yet ill-understood manner [108], [124] and lack of knowledge regarding optimal administration timing [125]–[127] , frequency and technique of cells adds yet another factor with unknown effects on therapeutic efficacy [108], [128], [129].

Senescence of cells is an additional problem that has to be addressed if hMSCs are ever to be a standard tool in tissue engineering and regenerative medicine. Despite being proven to be able to retain their functionality and characteristics over long-term proliferation [130] hMSCs, like other cells, eventually become senescent [131]. This means that they have undergone functional changes to some degree (decrease in differentiation potential, reduced migration and homing-related abilities, compromised secretome profile) which can lead to exacerbated inflammatory response at a systemic level and promotion of migrating or proliferating cancer cells [131].

Other problems include clinical grade production compliance with GMP [132], scalability [100], polarisation control [133], cell retention *in vivo* [108], [134], engraftment rate [127], localisation post-transplant and tissue persistence [108], [134],[135].

1.2 Metabolism of MSCs

The use of hMSCs in regenerative medicine holds a great promise for the future development of the field.

Several challenges to their implementation have already been mentioned in section 1.1.6., but it can be reasoned that one of the greatest barriers to potentially prevent a widespread and successful implementation of such cells as a form of therapeutics is a critical gap in knowledge and understanding of hMSCs metabolism. This gap presents an opportunity for advancement as accumulating evidence suggest that metabolism is tightly linked to functional capabilities of hMSCs.

Throughout adipogenic and osteogenic differentiations a metabolic shift has been observed, where hMSCs go from being almost solely glycolysis dependant towards using a mix of glycolysis, beta fatty acid oxidation and oxidative phosphorylation in their energy production.

Additionally, in order for hMSCs to be able to exert their immunomodulatory effects it seems that they must maintain their primarily glycolytic state.

Even further, knowledge about the way that energy metabolism in early vs. late stages of the varying differentiations changes and to what extent as well as how cell source and age may affect it, will undoubtedly impact how hMSCs can be used both *in vitro* and *in vivo.*

And so, focusing attentions on the intricate effects metabolism may have on all hMSCs characteristics is likely to turn up possible ways to manipulate cells to further therapeutic applications.

1.2.1 Function is linked to Metabolism

The hMSCs‘ functions of immunomodulation, proliferation and differentiation have, through varied studies, all been found to be linked to metabolism [31], [136], [137].

Mounting evidence (from studies performed primarily on Ad- and BM-hMSCs) suggest that hMSCs are metabolically heterogenous and the difference shows itself to impact the cells` functionalities, such as differentiation ability and immunomodulatory capacity [54], [138].

There exist compelling evidence suggesting that proliferating hMSCs are primarily reliant upon glycolysis when it comes to energy production. This has been shown for BM-hMSCs [29], [30], [32], [36] during proliferation but the cells seem to lean toward a more oxygen dependant metabolism when moving into osteogenic and adipogenic differentiation (OD, AD) such as oxidative phosphorylation (OxPhos) [32], [50]. Similar finding have been reported for Ad-hMSCs [34], [50].

Ad-hMSCs also seem to prefer glycolysis for energy production when proliferating, even when under aerobic conditions but when during OD the cells have been observed to increase both glycolysis and mitochondria linked metabolism (this includes OxPhos and fatty acid β-oxidation). When undergoing AD, however, the cells have been recorded to show decreased pentose phosphate pathway (PPP) capacity as well as decreased glycolysis whilst an increase was observed in mitochondrial enzyme activities [34], [50].

Consistent with these observations, it has also been noted that in addition to having a glycolytic phenotype, undifferentiated hMSCs have high levels of hypoxia-inducible factor 1 (HIF-1). This is a transcriptional regulator central to regulation of genes involved in hypoxic processes and a crucial physiological regulator of anaerobic metabolism [139]. Cells that undergo OD downregulate HIF-1 and that downregulations seems to be required on order to activate mitochondrial OxPhos, which is an oxygen dependant pathway [140]. From this it can be deduced that hMSCs ability to differentiate is greatly impacted by mitochondrial functions [134].

The metabolic phenotype of these cells has also been suggested to impact their immunomodulatory capabilities. A maintenance of a glycolytic phenotype seems to be a requirement for hMSCs to maintain and sustain secretion of immunosuppressive factors [138]. In 2019 Liu et al. [138] demonstrated this by utilizing IFN-γ to induce immune polarisation but hMSCs only start secreting immunomodulatory factors upon activation e.g. with IFN-γ. This led to remodelling of metabolic pathways towards glycolysis, reducing TCA cycle metabolism. The polarised cells were measured to have increased lactate levels, glucose

consumption and acidification rate. Increased expression was also observed of glucose transporter 1 and hexokinase isoform 2 (both are key enzymes in glycolysis), along with reduced OxPhos and electron transport. All of these points are indicative of increased glycolytic activity [138].

1.2.2 Mitochondrial Impact on MSC function

As has been touched upon in 1.2.1. active mitochondria are necessary for successful differentiation. Both mitochondrial enzymes and regulatory pathways are important to hMSCs in both their proliferating and differentiating states [27], [30], [134]. If not for active mitochondria, hMSCs would not be able to produce sufficient ATP to support e.g. OD. This happens via promotion of β-catenin signalling and acetylation due to active mitochondria. Increased β-catenin acetylation is a mechanism of osteogenesis that is driven by mitochondrial OxPhos [141] and it seems that acetylation increases throughout osteogenesis (at least for BM-hMSCs).

There is other enzymatic activity that further supports this importance of mitochondrial activation, e.g. creatine kinase (CK) activity [34], reversible mitochondrial adenine dinucleotide (NADP)- dependent reaction of isocitrate dehydrogenase (NADP-IDH) [142] and activity related to reactive oxygen species (ROS) [134], [143].

1.2.3 Possible Manipulation of Metabolism

As functionality and survival of hMSCs is greatly affected by changes in metabolism, a potential for therapeutic efficacy enhancement is present via metabolic manipulation.

Like many other cell types hMSCs can effectively reconfigure their functionality in response to stimuli. This applies to metabolism as well, but hMSCs can reconfigure their metabolism to respond to biochemical demands issued during tissue repair, be it secretion of immunomodulatory factors or integration and differentiation towards specific cell types [144]–[146].

As it is, the currently most researched subtypes of hMSCs are the Ad-hMSCs and BM-hMSCs, but even in those subtypes the research cannot be described as exhaustive.

It has already been mentioned that both enzymes and pathways relating to mitochondrial functions seem to have significant impact on proliferation and differentiation of hMSCs [27], [30], [134] but in addition to that external mechanisms (e.g. mechanical and biochemical) such as microenvironment composition and scaffold stiffness can significantly influence the internal workings of the cells [147]. Previous work has explored various ways of affecting hMSCs functionality and mechanisms by impacting and controlling their metabolic function. Oxygen manipulation (see [30], [31], [134], [136], [137], [148]–[150]), chemical stimuli manipulation (see [151]–[153]) and gene knock-outs and knock-ins (see [154]–[156]) are some of the approaches that have been tried.

As has been mentioned and demonstrated in this thesis so far metabolism of hMSCs is a very complex and dynamic system, and there are several gaps present in the collective knowledge on this subject that are actively being addressed by the research community. Only by gaining further insight into workings of the primary energy-generating pathways

utilised during proliferation and differentiation can effective manipulation be achieved. In order to get to that stage a holistic perspective is needed, one that integrates knowledge on the varying biological levels (using varied types of data) of hMSC differentiation in order to gain how these cells work as a whole.

One of the most prominent ways of doing this is through the use of -omics data and genome scale metabolic modelling such as has been done for this dissertation.

1.3 Metabolomics and Transcriptomics

Metabolomics, defined as the comprehensive and quantitative analysis of the full suite of small molecules in a biological specimen, is relatively new field of research within systems biology. „Metabolome“ first emerged as a term in 1998 and up to 2010 metabolomics was still considered as an emerging field [157], [158].

In its practice metabolomics are a challenge when it comes their analysis because of how disparate physical properties the molecules involved have, going from very nonpolar lipids all the way to very water soluble organic acids [159]. This makes the metabolome field very different from other present in systems biology, like genomic and proteomic, that usually only require a single analytical run to acquire extensive coverage. Methods that deal with metabolomics have to be chosen based on what subset of molecules within the metabolome are to be analysed and each of the method introduces a certain bias both for and against each class, generating a sort of patchwork of results for the metabolome [157]. Because of the way the metabolome is analysed and the ever continuous evolvement of analytical methods, precision and reproducibility will most often not be the same for all measured metabolites [160].

Transcriptomics, also a field within system biology, is defined as the study of an organisms transcriptome [161]. The aims of transcriptomics are generally written as: 1) record all types of transcripts (i.e. mRNAs, non-coding RNAs, small RNAs); 2) determining the transcriptional structure of genes (e.g. start sites, splicing patterns, post-transcriptional modifications) and 3) quantify expression levels changes in each transcript during development and condition changes [162].

The transcriptome (a term normally attributed to Charles Auffray [163]) is the complete set of RNA transcripts produced by the genome under a specific circumstance and connects the genome to gene function. The comparison of transcriptomes enables identification of differently expressed genes between either distinct cell populations, different cell states or different treatments. Modern day transcriptomics is possible due to high-throughput (HT) methods that analyse multiple transcripts [164], [165].

There are several methods available for use when it comes to studying the metabolome and generate a metabolomic profile but the ones that are the most common are spectroscopic techniques like nuclear magnetic resonance (NMR) and the hyphenated mass spectrometry (MS) techniques that couple together on-line metabolite separation and mass spectrometry [166]. Metabolomic (extracellular and intracellular) data analysis done for this dissertation (Paper I and II) was done using liquid chromatography MS (LC-MS). More precisely liquid

chromatography coupled with quadrupole time-of-flight mass spectrometry (LC-QTOF-MS), and this method will be described in a bit more detail later in this section of the dissertation.

As with the metabolome there exists a few methods to analyse and study the transcriptome, e.g. DNA microarray and RNA-seq [164], [167]. The latter one is a fairly recent addition to the method scope available for transcriptome analysis, it uses next-generation sequencing platforms, and this is the methods that was used in generating and analysing the transcriptomic data used in Paper I.

1.3.1 Mass Spectrometry

Characterization of whole intact biomolecules using mass spectrometry (MS) has been possible since roughly the mid-1980s'[168]. The MS technique is a widely used instrumental technique based on ionization and fragmentation of sample molecules in the gas phase. Molecules fragment in a unique manner so the resulting ion fragmentation patterns can be used to obtain structural information. In other terms the MS technique, in its most basic principle, generates and measures multiple ions from the same sample that is under investigation. It measures and separates the ions according to their specific mass-to-charge ratio and its results are usually presented as a mass spectrum with intensity as a function of the mass-to-charge ratios [168], [169].

A mass spectrometer in its basic form consists of a sample-introduction system, ionization source, mass analyser and an ion detector. The sample size that is required for MS analysis is much lower than that of the NMR spectroscopy (few microliters for the MS vs. 30-600 µl for the NMR). The MS also has a higher resolution (meaning it is better suited to distinguish between compounds with small mass differences) compared to NMR and it can be coupled with a separation technique (e.g. CE, LC or GC) [170], [171].

The most common MSs used for studying the metabolome are time-of-flight MS (TOF-MS), the quadrupole MS, ion trap MS and the Fourier-transform ion cyclotron resonance MS [172].

The MS that was used in the metabolomic analysis for this dissertation was a combination of two of the above-mentioned common MS, TOF-MS and the quadrupole MS and so they will be introduced further.

In TOF-MS, the ion mass-to-charge ratio is determined through time-of-flight measurements – i.e. the time it takes ion to travel a fixed distance in a vacuum. Electric field (located in the „pusher" or acceleration-region of the analyser) is used to accelerate the gaseous ions, giving ions with the same charge the same amount of kinetic energy.

As according to the physical laws that govern anything and everything, the ion's velocity will be in inverse proportions to their mass and so the time it takes the ion to go from „pusher" to detector will tell the mass-to-charge ratio [168], [172].

The quadrupole MS consists, as the name gives away, of four cylindrical rods set in parallel and it separates the ions based on the stability of their flight trajectory through an oscillating electric field. This field is generated by applying both direct current (DC) potential and alternating radio frequency current (RF-AC) potential to the rods. The ions follow flight trajectories specific to their mass-to-charge ratios when inside the space between the rods. By applying specific values of DC and RF-AC it is possible to only allow a very narrow ratio

range to have a stable flight trajectory within the field and so reach the detector, with all ratios outside the range colliding before being detected. The quadrupole MS can thus be used as a sort of filter when it comes to analysis [172], [173].

As mentioned, the MS used in this dissertation was a MS/MS configuration, also known as tandem MSs, made up of a quadrupole MS and a TOF MS or Q-TOF MS. Generally, the Q-TOF-MS is the most commonly used MS in untargeted metabolomics i.e., discovery-based analysis focused on global detection and relative quantitation of small molecules. Targeted metabolomics on the other hand is a validation-based analysis that focuses in measuring well defined groups of metabolites and allows for absolute quantitation. Targeted metabolomics was the focus of this dissertation, though some untargeted analysis was performed on the data as well [174].

It is quite common now a days to use more than one MS analysers in this sort of a "row" - configuration (as is the case in this instance).

This is done in order to increase the specificity of the analysis and aids with specific protein targeting. The coupling, normally done by using a collision cell, makes the latter analyser data dependant (i.e. dependant on the data of the first one). E.g. often the first MS is a quadrupole MS, which filters all ions outside of a narrow ratio range out, and the filtered ions are then fragmented before moving on to the second MS. The second analyser then measures the mass-to-charge ratios of the fragments and the fragmentation is reproducible. How highly depends on the molecular structure of the ions.

So, instead of only being able to measure the precursor ion as is possible in MS configuration, in tandem MS/MS it is possible to analyse the product ions of the precursor ion. This can mean increased sensitivity and/or the possibility to gain more structural information on the analyte used (depending on what type of MSs are set up in tandem) [175].

1.3.2 Techniques to Separate Metabolites

As mentioned in section 1.3, samples that are to be measured for metabolomic analysis are more often than not of high compositional complexity, and so in order for the MS to be able gather a good analysis it can be advantageous to sperate the metabolites beforehand. Chromatography is a technique that does this kind of separation and relies on differences in partitioning behaviour between a mobile phase and a stationary phase [176].

The most common ways currently used to achieve separation are liquid or gas chromatography (LC, GC).

In GC all compound intended for analysis must be sufficiently volatile and thermally stable as all samples need to be vaporized before being separated. Upon vaporization the sample is swept into a column by a carrier gas (e.g. helium or argon) where it is separated due to the interaction between the gas (mobile phase) and the interior coating of the column (stationary phase). Later part of the column then passes through a heated transfer line and ends at the entrance of an ion source [177]–[179].

In LC the mobile phase is a liquid in which ion samples or molecules are dissolved. The sample passes through a column (or a plane, dependent upon the type of LC) packed with

stationary regularly or spherically shaped particles that enables the separation of molecules due to their inherent difference in ion-exchange, adsorption, partitioning and size.

This gives different transmit times to different molecules. After being eluted from the column (or plane), the metabolites are converted from a soluble to a gas and ionized, after which they are ready to be measured by the MS [180], [181].

Now it is common to use high pressure to separate the metabolites, resulting in a detection and quantification technique known as high-performance LC (HPLC) that gives very high resolution and fast analysis time, however yet another technique has emerged that is considered to give an even better result. This is known as ultra-performance LC (UPLC). The UPLC operates at a higher pressure (15.000 psi generally vs. 6000 psi for HPLC) which allows for even shorter run times, lower solvent consumption and smaller particle size in the column, i.e. greater analyte separation and so detection [176].

1.3.3 LC-MS data analysis

LC part of the LC-MS or MS/MS systems is very beneficial when it comes to capability of separating complex mixtures, but it is not applicable to obtain material structural information [181], [182].

Despite being widely used at present in metabolomic analysis, the coupling of LC and MS was not an easy feat to accomplish. This was mainly due to fact that maintenance of the high vacuum that MS requires was hard to contain because of the high liquid flows in the LC, i.e. one instrument operates in a condensed phase but the other under vacuum. This had to be solved using the correct interface between the LC and the MS or MS/MS systems – the two most commonly used ones are electrospray ionisation (EI) and atmospheric pressure chemical ionisation (APCI) [181].

EI (often termed as a very soft ionisation technique), under optimal conditions, introduces the analyte to the source at flow rate around 1 µl min^{-1} and generates intact gas-phase ions by applying high voltage to the liquid, creating an aerosol. In other words the liquid (charged) is formatted and sprayed, in order to evaporate the solvent, ion formation occurs in the fission of the charged droplets because of high field intensity. EI is very useful for analysing ionic compounds and compounds with high molecular weight [183], [184].

Atmospheric pressure chemical ionisation (APCI), in its optimised format, has a mixture of both analyte and solvent molecules go through a corona discharge after a gas phase drying. Then the molecules in the solvent are ionised in order to create charged solvent ions, and that charge then transfers to analyte molecules crating analyte ions. This interface is often used to analyse nonpolar molecules of a more moderate weight than is done using EI [183].

Combining LC and MS techniques then enables the physical separation of molecules in a liquid phase (that the LC part brings) as well as the mass analysis of the MS that is done via identification of the mass-to-charge ratios of gaseous ions in an electric and magnetic fields [168], [181], [185]. This kind of analysis method is able to produce a considerable amount of data in one experimental set up and the data points are known as three dimensional. This stems from each measurement containing information on the metabolites chromatographic

retention time, signal intensity, and the frequently talked about mass-to-charge ratio [186]. On top of this comes the fact that, aside from the large amount of metabolites contained within a system at each given time of sampling, each metabolite or primary ion is often fragmented in the run process so there are several resulting fragments and then there is the possibility of addition of adduct formation between the ions.

Due to the scale of the data that is produced in metabolomics the identification of the metabolites often presents itself as a limiting, time consuming factor. Use of specific algorithms (e.g. TargetLynx from Waters [187] , XCMS [188]–[190]) is therefore needed to sort through the raw data and collect information about the sought after metabolites. This works when doing targeted metabolomics, where only known metabolites are being identified (often with known retention times, fragmentation patterns and mass-to-charge ratios) as this only reports information about them

As already mentioned, the MS instrument used for this dissertation was of the UPLC-Q-TOF-MS variety. Using this kind of a tandem MS set up enables provision of structural information (enable identification of unknown compounds), it increases specificity of the targeted analysis, and helps with achieving determination of high-sensitive trace levels [185].

Additionally, by using complex but complementary instrument setup such as this, greater sample throughput is achieved as the LC-MS set up markedly reduces the need for sample clean up strategies.

1.3.4 RNA-Sequencing (RNAseq)

Classified as a kind of an umbrella term for next-generation sequencing strategies that can be used to map the transcribed, RNAseq enables whole genome sequencing with a wide dynamic range of expression levels in a relatively easy manner which facilitates new molecular marker or novel transcript identification and could render polymerase chain reaction (PCR) unnecessary [162], [191], [192].

This technique can be used to produce an almost complete snapshot of the mRNA in form of small tags corresponding to fragments of the transcripts. Other older sequencing methods that are still in current use, such as those that use complementary deoxyribonucleic acid (cDNA) clones to generate expressed sequencing tags (EST), are only able to detect the more abundant transcripts present. RNAseq methods however, when applied with enough sequencing depth (100-1000 reads/base pair/transcript) can deliver an almost complete transcriptome capture [164].

The general method used by this kind of technology is converting a population of RNA to a library of cDNA fragments with adaptors attached to both ends of the fragment strands. Next, each molecule (whether it is amplified or not) is sequenced in a HT-manner in order to obtain either single or pair-end sequencing. Any HT-sequencing technology can be used but the type chosen will affect the depth of the reads [162], [164]. For this dissertation Illumina HiSeq System was used.

Following sequencing the reads can be either aligned (if using a reference genome) or assembled *de novo* without a guiding sequence if the desire is to produce a genome-scale

transcription map consisting of either one or both; structure of the transcriptome and the expression level for each gene [162].

To give a bit better overview of the run of a typical RNA-seq experiment, the steps can be divided and described largely as follows [165], [193]:

1) RNA purification and isolation
    a. Here the RNA is also broken into small fragments, but RNA transcripts can be thousands of bases long whilst sequencing machines only sequence 200-300 bp fragments).
2) Library preparation.
    a. RNA is converted to cDNA which is more stable than RNA and sequencing adaptors are added. The adaptors purpose is to allow the machines to recognise the fragments and to allow the sequencing of multiple different samples at the same time, but different samples can use different adaptors. The addition of adaptors can be a problem as it does not work 100% of the time. Samples with adaptors are amplified in a PCR step and then a quality controls steps verifies library concentration and fragment lengths.
3) Next generation sequencing (NGS) platform performs the sequencing itself.
4) Resulting reads are analysed.

Note that the precise configuration of each step as well as how the NGS run is performed is dependent upon the specific method.

The key advantages of using RNAseq technology are that it is not limited to detecting transcript corresponding to existing genomic sequences, it can reveal the precise location of transcription boundaries, short reads from RNAseq can give information regarding the connection of two exons and it can aid with discovery of sequence variations in transcribed regions. It also has a very low background signal.

These points, along with others, make RNAseq the first sequencing-based method that enables entire transcriptome observation in a HT and quantitative manner.

1.3.5 RNA data analysis

The typical steps of an RNA-seq experiment were gone through in section 1.3.4, the analysis of the resulting data itself also usually follows quite a structured process.

It can in essence be broken down into six steps [165], [194]:

1) Initial processing
2) *De novo* assembly
3) Mapping reads
4) Transcript annotation
5) Normalization
6) Downstream analysis.

During initial processing of the data the sequencing reads are demultiplexed (usually done as a part of the sequencing device‘s software), trimmed (the adaptors are removed) and run through a quality filtration where garbage reads (reads with low quality base calls or that are artifacts of chemistry) are filtered out.

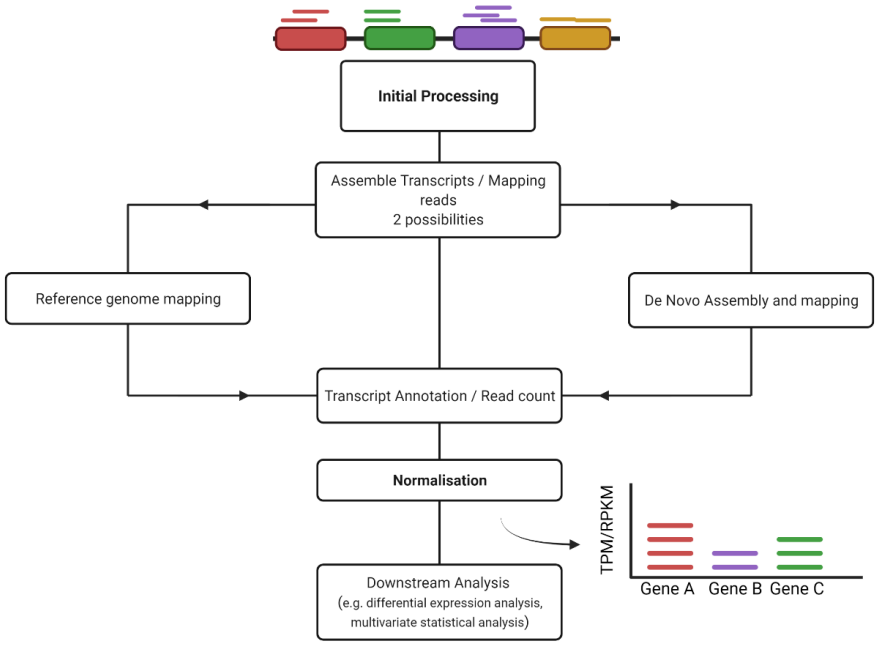

Figure 2: RNA data analysis workflow. The process can be split into six main steps – 1) Initial processing 2) Transcript assembly 3) Either Reference genome mapping or De Novo Assembly and mapping 4) Transcript annotation or Read count 5) Normalisation of data and 6) Various downstream analysis. Created with BioRender.com

The second step, *de novo* assembly, is only necessary if a reference genome is not available. Then it is necessary to construct it out of RNA-seq reads.

Mapping of the reads, also known as aligning RNA-seq reads to a reference genome is the next step. Here the genome and genome sequence is split into small fragments (allows alignment of read even if they are not exact matches to the genome) and index is created containing all the fragments and their locations on the genome. The sequence read is then, just as the genome, split into small fragments and the seq-read fragments are matched to the genome fragments. This determines the genome location of the fragment (both the chromosome and position on it, where applicable).

Once position of a read is determined it is possible to see if it falls within a coordinate of a gene (or an interesting feature). The read counts per gene is summarized and the results are given as a matrix – this matrix (col 1 = gene names, read counts = counts for each samples sequenced). For this dissertation so called „bulk“RNA-sequencing was performed, resulting in a smaller matrix than if a „single-cell“RNA-sequencing were to have been done.

Next comes the normalization of the data, but each sample will likely have a different number of reads assigned to it because one sample may have more low quality reads

compared to another or some samples may even just have a bit higher concentration in the machinery‘s flow cell. This normalisation step is supposed to try and account for both within and between sample variations. Normalised read counts used to be reported as either Read Per Kilobase Million (RPKM) or Fragments Per Kilobase Million (FPKM) but a more novel approach (that is being used ever more widely) was used for this thesis or Transcripts Per Million (TPM). The normalised read counts that this method gives have been normalised to count for both sequencing depth and the length of the gene. When using the TPM method one normalises for gene length first (each gene count is divided by gene length in Kb) and the sequencing depth second (read counts for each replicate are summed up, that sum is divided by million and the read counts are divided by the resulting scaling factor). TPM is by many considered a better method of normalisation than RPKM and FPKM because it gives a clearer indication of how large proportion of reads for a gene were mapped to a replicate because the sum of total normalised reads in each column of the data matrix (i.e. in each replicate) is always the same. Since RNA-seq is essentially all about being able to compare relative proportions of reads TPM has been found to be very useful. This method was used e.g. in Paper I**.**

When normalisation of the data has been completed the downstream analysis can take place (this includes e.g. differential expression analysis, multivariate statistical analysis and visualisation). See paper I for more detailed downstream analysis performed.

1.4 Genome Specific Metabolic Models

Generic constraint-based modelling, an aspect of systems biology and biomedical engineering, has been around for roughly 30 years. During this time it has gone from an initial interest of theory and basic conception into a predictive biological practice where number of ongoing studies are combining the use of HT data and these models in a search for answers to relevant biological questions [195].

Genome scale metabolic models (GEMs) or genome scale metabolic networks are reconstructions that first were presented in 1999 (*Haemophilus influenzae* RD) [196] and contain a comprehensively curated and systemized information on cellular metabolism of a given organism[195]. Since the presentation of the first GEM advances have been made to develop and reconstruct models that cover an increasing number of organisms reaching across the realms of bacteria, archaea and eukarya [66]. These reconstructions can be put into a mathematical format that follow the same principles are standard constraint based models (CBMs) except for where CBMs focus on metabolism at the reaction level, GEMs work at the gene-level and so account for the complex gene-protein reaction association [196]. Models like GEMs can be used to study the intricate genotype-phenotype relationship when it comes to cellular metabolism and function, which is a key factor when it comes to manipulation of cells to enhance their use in tissue engineering and regenerative medicine.

1.4.1 Mathematical Modelling of Human Metabolism

A bottom-up (going from fundamental units e.g. DNA, RNA, metabolites and protein to the organism as a complex whole) systems biology approach allows for a grounded, thorough mechanistic understanding of a system [197]. Models created in such a mathematical manner

can be used to predict potential interventions and so insight into possible ways to successfully manipulate hMSCs for therapeutic applications. As has been mentioned in previous sections of this dissertation, various individual components of hMSCs have been studied (in varying detail), but in order to be able to predict a cell‘s realistic phenotype a wholistic approach must be taken. An understanding of all systemic interactions of both environmental and cellular components that contribute in some manner to that phenotype has to be involved to get an accurate picture [61].

A combination of HT –omics technologies (e.g. proteomics, metabolomics, transcriptomics), enabling collections of very large data sets, along with improved computational modelling methods that enable a better holistic analysis of said data have made systems biology in its present format possible [60], [198].

Generally speaking the first step in modelling metabolism at the genomic level, as is done in GEMs, is to reverse engineer the network structure [60], [61], [199], [200].

The reconstruction process starts with collection of all genome and experimental evidence relating to biochemical reactions of the organism of interest [66]. This generates what can be called the base model. In this thesis the base model is the Recon3D [201] model, a base human genome reconstruction that covers all known metabolic reactions in *Homo sapiens.* These base models are generally too large and not focused enough to be used in search for an answer to a specific biological question, which are most aimed at a certain tissue or cell type. So, further constraints are placed upon the network based on existing biochemical knowledge – this includes stoichiometric constraints (e.g. mass and charge balance of reactions), thermodynamic constraints (e.g. directionality of reactions), and enzymatic capacity constraints (e.g. the maximum possible flux rates of reactions) [58], [66], [199], [202]. This eventually results in a GEM of metabolism.

Transcriptomic and proteomic data is then used to learn and select which of the reactions are actually active in a given phenotype, based on the presence of the enzyme that catalyses the reaction (a chosen threshold value usually supports and enables this).

Metabolomic data may then be used to constrain which metabolites should be either consumed or produced by the cell or organism being modelled [61].

Resulting GEM can then be used to determine the flux state or pathway usage of the entire metabolic network via varied computation approaches (e.g. flux balance analysis (FBA) [203]).

The ability of integrating information from multiple types of -omics data with detailed biochemical data that has been previously acquired makes this kind of metabolic modelling a very powerful and effective technique to answer biological questions regarding how phenotypes occur because of genetic mutation, functional changes or environmental perturbation [204].

A more specific example of how a GEM can be reconstructed in steps can be seen in the method section of Paper II.

While constraint-based models such as GEMs are intrinsically quantitative (i.e. provide numerical values for all fluxes present in the network) they can answer both qualitative and quantitative questions relating to the metabolic behaviour of the cell. Predictions that are

focused on qualitative aspects usually require less physiological information (results being qualitatively insensitive to the imposed enzyme capacity constraints) but if quantitative predictions are the goal more physiological data is needed to properly constrain the model [205].

As more and more data are obtained a model will represent the intended physiological conditions more closely, and the new and improved model can be used to produce some novel hypotheses that can affect what experimental directions are taken.

This established back and forth feedback between the experimental design and data gathering and then the computational evaluation is important and enables a better understanding of how organisms, like hMSCs, organize their metabolic systems in response to shifts in either functional demand and environmental circumstances [60], [199]. In addition, the ability to contextualize models based on information at various levels (going from genomic to environmental) has the potential to allow them to inform the ever more desired personalization of medicine e.g., predicting potential genetic markers of a successful MSC donor.

1.4.1.1 A brief overview of the mathematical representation of a metabolic network

As described in section 1.4.1. network reconstructions such as GEMs, and other *in silico* models, are generally created in a bottom-up fashion. Based on both genomic and bibliomic data they can represent a biochemical, genetic and genomic (usually shortened to BiGG) knowledge base for the specific targeted organism. It is this reconstruction that is converted into a mathematical format.

In this mathematical representation the metabolic network is converted into a stoichiometric matrix (**S**) were each column in the matrix represents a reaction in the network and each row represent a metabolite ($\mathbf{S}_{\text{metabolite, reaction}}$). If the matrix coefficient in question is represented by a negative number that means it is a substrate (i.e. that metabolite in that specific reaction is being consumed) whilst positive numbers represent a product (i.e. that metabolite in that specific reaction is being produced). Metabolites that partake in a reaction have a non-zero entry in the **S** matrix. This is what makes the format of the metabolic network actually computer readable.

In order for proper mathematical representation of the holistic network to be possible and correct reaction fluxes, definition of system boundaries is needed. This is especially important when it comes to exchange reactions – that is all metabolites that can be either consumed or secreted by the cell itself. These can be added at a later stage of the reconstruction as a further definition of environmental conditions. Common reactions to have in a reconstruction are e.g. exchange reactions (define extracellular environment), extracellular reactions (denoted with an [e]), intracellular reactions (reactions happening completely within the cell, denoted with a [c]) and transport reactions (reactions moving metabolites from extracellular to intracellular or vice versa, denoted with [e] ↔ [c]). Metabolites in the stoichiometric matrix, **S**, are also denoted by the compartment they are located in.

Then it comes to the constraints (as described in section 1.4.1). With mass conservation being the basic physical law that models adhere to the steady state of the model can be described by the equation $S * v = 0$, where v is a vector representing reaction fluxes. Adding

the previously mentioned stoichiometric, thermodynamic and enzyme capacity constraints lead to a more confined set of a feasible steady state flux solution existing in what is known as the solution space).

Once a constrained stoichiometric matrix has been defined in a proper manner an objective function (usually denoted by a vector $\boldsymbol{Z} = \boldsymbol{c}^{\boldsymbol{T}} * \boldsymbol{v}$, where c is a vector of weights indicating how much each reaction contributes to the objective function, and v is again a vector representing flux values for the reactions**)** can be defined and included in the matrix itself. This can also be a biological question of a sort. Most commonly this is the biomass reaction, a complex reaction that consists of the biomass precursors, is dominated by adenosine triphosphate (ATP) consumption, and returns the produced biomass (usually under optimised conditions). However, the objective function does not need to be constricted to biomass production, it can be focused on various other aspects (e.g. ATP production under specific circumstances, or production of other cellular components when specific additives have been put in the media). If only one specific reaction is the focus of either max-or minimization of the objective function then **c** is a vector of zeros with one (1) at the position of the reaction of interest [66], [206].

Linear programming is then used to solve the resulting linear equations and the flux state of the network computed.

1.4.1.2 Current Human Metabolic Reconstruction – Recon3D

As mentioned in the previous section the base human metabolic model used for this dissertation was the Recon3D [201] model, the latest update of the Recon family of human metabolic reconstructions. Its key novel attributes are mainly twofold; one is the inclusion of information regarding protein and metabolite structures and the other is the number of reactions. Recon3D has almost double the number of reactions compared to its predecessor or 13,453 total reactions and the inclusion of the 3D aspect has allowed its use to show that deleterious mutations map to specific areas of the genome. That specially has improved predictions of cancer related mutations compared to predictions made by previous Recon models, and the overall improvements of this newest addition have also enabled investigation of the metabolic effects of various drugs. This drug analysis has revealed that drug effect signatures often contained dissimilar functional domains and metabolites, indicating that drug effects can often be due to a compensatory downstream metabolic effect [201].

A global network reconstruction that includes all known reactions of a whole organisms, such as Recon3D is, can thus provide a starting point for production of tissue-, cell-, or condition-specific GEMs (just like has been done for this dissertation).

1.4.1.3 Current State-of-the-Art Application

As has already been mentioned, a base GEM can be utilised to produce general predictions about human metabolism as a whole. This provides useful insights into human health as is and predictions of human metabolic functions that are currently unknown.

For example, by analysing reactions in Recon1 [207] that were at the time defined as being present because of either genome annotation or literature data but that were not predicted to be active, and then adding surrounding reactions to activate them (in a sort of

„connect-the-missing-dots“ manner) making of predictions about previously unknown human metabolic functions has been enabled. Examples of this is the iduronic acid following glycan degradation, N-acetylglutamate in amino acid metabolism, and the human activity of glucokinase [208], [209].

Another aspect that GEMs can be used for is personalised disease diagnostics, e.g. to predict biomarkers for inborn errors of metabolism (IEM), a collection of hereditary metabolic defects found in most of the main human metabolic pathways [210]. Here the accuracy of previous predictions is used and fed into improving the new models. For diseases such as IEM early recognition and treatment is very important, and identification of good biomarkers is key when it comes to successful early diagnosis. GEMs provide a novel computational approach that can systematically predict altered or effected metabolic biomarkers and so extend the information that can be inferred from obtained data. It is this that enables the accurate diagnosis for each individual patient, further insights into IEM focused hot spots in human metabolism and discovery of novel IEM which expands the range of metabolites associated with a diseased state [211]–[215].

The gene-protein-reaction that GEMs are built on make metabolic pathways relevant to specific genotype-phenotype pair more feasible, meaning that disease-specific biological insights can be derived.

1.4.2 Benefits of integration of varied -omics data

Once the first step of a reconstruction has been taken (choosing the base model, e.g. Recon3D), there is a plethora of methods available that can be taken in order to make context-specific models, i.e. models that are specific to both a certain cell type and circumstances. This is done via integration of transcriptomic, proteomic, and metabolomics data – an integral step in generating the more holistic, intricate models able to make the more accurate predictions.

These context-specific models are able to provide much more detailed insights into human metabolism in the chosen cell type, and comparison of models (e.g. same cell type in different circumstances, as was done as a part of this dissertation for hMSCs in osteogenic differentiation and adipogenic differentiation) is particularly useful. Previous published context-specific human models have proven this by producing useful insights into healthy and diseased state metabolism.

Expression of enzymes defines the metabolic state of a cell, and both transcriptomic and proteomic data provide information about what enzymes are expressed under each circumstance and up to what extent (i.e. expression levels), although not in a perfect manner [116], [216].

The process of downsizing a reconstructed network is most often called “pruning”, and several methods have been developed that do this based on expression data like transcriptomics. There are quite a few technical differences between the methods, but all seek to balance retention of reactions that are either known to be or thought likely to be present in a particular cell type under a given circumstance based on expression data or prior knowledge gained from literature research. Reactions that are by this defined as extraneous are removed.

The most commonly used methods to do this are GIMME [217][92], iMAT and INIT [35], [63], [78], [218], and MBA, Fastcore, and mCADRE [18], [99], [100], [219]–[221], [17], [222].

As was mentioned briefly in section 1.4.1. another way to generate a context specific model is to use metabolomic data that is collected either by mass spectrometry (MS) [169] and nuclear magnetic resonance (NMR) spectroscopy [170].

This type of data creates a constraint on the values of metabolites that the model can either take up or secrete and makes them more realistic. Rate of metabolite secretion or uptake is determined by either measuring concentration changes of various metabolites in cell culture medium over time or by comparing relative values of metabolites at different times. The determined rates are then applied as additional constraints to the model and help with restricting possible predictions to be consistent with the metabolic data set [65].

These kind of constraints help with predictions of different sets of active and inactive intracellular reactions based on extracellular data (this was used in the model reconstruction done for this dissertation) and the process may follow protocol such as Metabotools [223] or a similar one. The Metabotool protocol has been used to obtain metabolic insights into the metabolic differences between different leukemic cell lines [224], [225].

The use of isotope labelled metabolomic data can yet again help with generating a more specific model by contributing even better constraints.

Cells, such as those that are being modelled, can be fed on medium containing either glucose or glutamine that are labelled with heavy isotopes of carbon or nitrogen. The proportions of various metabolites labelled with these heavy isotopes in the cells sampled and analysed at different relevant time points after the labelling treatment then allow for inferences to be made about their production. See [128], [226] for examples of using isotope labelling in GEM reconstructions and predictions.

Through this it is easy to see the value that the possibility of integration of varied types of data brings to the precision, holistic comprehension and focus of GEMs.

1.4.3 The value of Cell Specific and Circumstance specific Metabolic Models

When in search for answers regarding causes of a diseased state or changes in cell‘s functionality or characteristics the starting point is not always apparent, making defining an objective function difficult.

Then it can be invaluable to be able to generate metabolic network reconstructions that are specific to each type of cell or circumstance that can then be compared in order to find the differences between the metabolic pathways (expression values, flux values, pathway usage etc).

The discovered differences in the metabolic networks can then be used as guide posts when it comes to either discovery of drug or „treatment“-targets or targets for metabolic manipulation and possibly therapeutic enhancement.

1.4.3.1 Deeper Insights into Metabolism

Historically, many constraint-based metabolic analyses have relied upon an objective function (mentioned briefly in section 1.4.1.1). It is defined as the metabolic objective of the cell in question, and as previously stated in 1.4.1.1, flux through this function or reaction is either maximized or minimized in order to compute the pathway usage or „flux-state“, across the entire network given the specific goal.

When it comes to diseased metabolic states, such as cancer, where a well-defined objective-function is not present (cancer cells usually follow the goal of gross cellular growth) one needs algorithms that can create a cell or tissue specific networks without a particular objective function. An algorithm that has specifically been used with regard to cancer research is the metabolic transformation algorithm (MTA) [227]. This is an algorithm that uses GEMs to predict genetic perturbations that can shift a diseased metabolic state to a more healthy one, and has been used to determine reactions that are capable of shifting “old” muscles into “young” by providing possible targets that can reduce age related metabolic shifts. These have also been used to identify key reactions that when removed from network shift a model for Alzheimer’s disease to that of a network more similar to a healthy state [228], [229].

Obesity is another example of a circumstance specific metabolic disease state that has been addressed by using human metabolic reconstruction. In this case the reconstruction was used to identify pathways implicated in the disease process. When it comes to obesity, just as for many other diseases, pinpointing the cause (in the form of either a specific genetic or environmental marker) and finding an effective “treatment” is not a simple task and having an *in silico* laboratory of sorts can aid in potential target elimination without being too costly [65], [230]–[232].

Yet another valuable use for cell and circumstance specific GEMs can be found in the more cost-effective manner they offer when it comes to evaluating drug toxicity levels and side effects for both short and long periods of usage, see [232], [233].

1.4.3.2 Uncovering Changes over Time

Biological systems often change dynamically over time, either in a response to an internal or external stimulus (e.g. a hMSC going from proliferation into differentiation), and analysing how the changes come about can be a challenge. This challenge is now addressed by integrating time-course experimental data using approaches like dynamic flux balance analysis (dFBA) in order to give more accurate flux predictions [234]. This is done by providing a continuous prediction based on the changing inputs and outputs from the system over the time course.

Another approach, known as unsteady-state flux balance analysis (uFBA) [68], integrates absolutely quantified time-course metabolomic data to model cellular dynamics and has been used to explore how temporal dynamics can impact metabolism of stored red blood cells. That work lead to proposed improved storage solutions for blood [235].

Methods like dFBA and uFBA can be used for cell types like hMSCs to detect, examine and compare as functions of time the key metabolic shifts that occur during trilineage differentiation just as has been done for this thesis.

1.5 What the future holds

From the earlier sections of this introduction is should now be relatively easy for the scientific mind to gather what possibilities lie within the combination of GEMs, tissue engineering and cellular or regenerative medicine.

Previously, a metabolic model of MSCs has been reconstructed and used to predict a possibly better way to expand the cell culture. This is the GEM iMSC1255 [64], the first GEM created to model MSCs. This model, after first being reconstructed and validated, was subsequently used to computationally predict possible metabolic interventions that could be used to optimize both proliferation and chondrogenic differentiation of MSCs as well as investigate effects of hypoxia on proliferating MSCs, see [236] for more detailed information.

These studies both showed how a model of MSC metabolism can provide useful insights into MSC proliferation and differentiation. The model described in Paper II is to the authors best knowledge the only one of its kind that models hMSCs undergoing OD and is built on data gathered from cells grown with culture ingredients containing only human related additives.

Some of the other ways that GEMs can be of use to further clinical applications of cell-based medicine are 1) trials with faster *in silico* metabolic engineering ; 2) disease biomarker identification [210], [211], [237]; 3) drug target prediction, therapeutic window prediction [232], [233], [238], [239]; 4) experimental cost reduction via *in silico* result prediction e.g. optimizing cellular functions without having to go through the costly processes of cell expansion and differentiation; 5) multi cell models, e.g. to gain insight into how multiple types of cells residing within same environment interact [232], [240]; 6) age related exploration, to explore the effect of donor age on cellular functions [80], [241], [242]; 7) exploration of metabolic differences, to explore different capacities of hMSCs from different sources [22], [138], [243]–[246].

In general GEMs can bring the highly valued engineering aspect of *optimisation* and *overview* to fields like tissue engineering and cell-based medicine, which have to deal with a lot of complicated and often unexpected and unforeseen situations that can spring up out of nowhere.

2 Purpose

''Face the demands of life voluntarily.
Respond to a challenge, instead of bracing for a catastrophe. "

Jordan. B. Peterson,
Canadian Clinical Psychologist (B. 1962).
12 Rules for life.

The purpose of this project can be divided into three sections:

1) To identify temporal changes in metabolic activity of mesenchymal stem cells during the course of osteogenic differentiation through analysis of metabolomic and transcriptomic data to see if the progression can be split up into different phases, each with its own identifying metabotype. Such identification of timepoints where metabolic shifts of interest are occurring can aid in focusing the scope of future research aimed at mapping metabolism of osteogenesis and the optimisation of the process within tissue engineering.

2) To reconstruct an original and hitherto unseen trio of comparable genome scale metabolic models, modelling metabolism of mesenchymal stem cells during the first seven days of osteogenic and adipogenic differentiation as well as proliferation. The goal of these reconstructions is to create *in silico* metabolic models that can be used to compare metabolic states of the cell lineages and explore their differences as well as to be able to utilize the models as a virtual laboratory to explore e.g., possible ways to enhance osteogenic differentiation among other things.

3) To bring together the possibilities that lie within the fields of genome scale metabolic modelling, metabolomics and stem cell based medicine and highlight how they can all be combined in order to further the use of mesenchymal stem cells in tissue engineering and regenerative medicine.

3 Materials and Methods

''Order and method, and the little grey cells
That is all one needs, mon amie.''
-Hercule Poirot

Dame Agatha Mary Clarissa Miller/Agatha Christie,
British Author (B. 1890 – D. 1976).
The Big Four.

Main methods are summarised and presented in condensed versions in this section. For more detailed descriptions please refer to Papers I-II.

3.1 Cell culturing

3.1.1 Seeding, harvesting and expanding MSCs

Cells used for experimentation in all works done for this Ph.D. were BM-MSCs that were purchased from Lonza (Walkersville, MD, USA).

Prior to being subjected to differentiation conditions cell were seeded (500.000 cells/175cm3 culture vessel) and expanded (from cryo-storage in liquid nitrogen) for one passage to allow stabilisation from the shock cells are believed to experience during the initial seeding from cryo-storage. Media composition used for general BM-MSC expansion is described in Paper I.

Upon reaching desired confluency cells were harvested using trypsin and counted via trypan blue staining and haemocytometer (Assistant, Munich, Germany).

Harvested cells were then used for differentiation and quality control assays.

3.1.2 Osteogenic Differentiation

Cells (n = 4) used to gather extracellular metabolomic data were cultured in 25cm2 culture vessels (5000cells/cm2) using 5ml of osteogenic inducing medium (detailed media composition can be found in Paper I as per previously S.O.P established protocols [input reference].

Sampling was performed approximately every 24-36 hours for 28 days, with media change every 48 hours. Samples were stored at -80 C until prepared for mass spectrometry analysis. This data was both used in Paper I and in Paper II.

Blank (unused) medium was also collected from the original batch (0.5 ml) for use as a control when looking at metabolite change between time points.

3.1.3 Adipogenic Differentiation

Cells (n = 4) used to gather extracellular metabolomic data were cultured in 25cm2 culture vessels (10.000cells/cm2) using 5ml of adipogenic inducing medium (medium composition is described in Paper II) as per previously established S.O.P established protocols.

Sampling was performed approximately every 24-36 hours for 14 days with media change every 48 hours. Samples were stored at -80 C until prepared for mass spectrometry analysis. This data was used in Paper II.

Blank (unused) medium was also collected from the original batch (0.5 ml) for use as a control when looking at metabolite change between time points (to be used in later work).

3.1.4 Osteogenic differentiation for labelled extracellular metabolomic and intracellular metabolomics sampling

Cells (n = 3) used to gather labelled extracellular metabolomic data were cultured in 6 well plate culture vessels (15.600 cells/cm2). Extracellular labelled metabolite samples were collected from the same wells as the cells intended for labelled intracellular metabolite sample collection were cultured. This was done in order for the data to be completely comparable.

Five separate wells were used for cells from each donor to match the desired day of culture (extrapolated from data presented in Paper I). Upon seeding cells were immediately placed in regular osteogenic inducing media (for detailed composition refer to Paper I), with media change (1.5 ml) occurring every 48 hours. Approximately 48 hours before sample harvesting regular osteogenic inducing media was switched out for labelled osteogenic inducing media. Three different types of labelled osteoinducing media were used (glucose13 labelled, glutamine13 labelled and glutamine15N2 labelled). All in all, 15 wells were used for cells from each donor (5 for each type of media). Upon the day of harvesting (approximately 48 hours after labelled media was added to the cells) a media sample was collected (0.5ml -1 ml) before the used media was discarded in order to collect the intracellular sample.

Blank (unused) medium was also collected from each of the original batches (0.5 ml in each case) for use as a control when looking at metabolite change between time points.

3.1.5 Osteogenic differentiation for unlabelled intracellular metabolomics sampling and BCA protein assay

Cells (n = 3) used to gather unlabelled intracellular metabolomic data were cultured in 6 well plate culture vessels (15.600 cells/cm2). Five separate wells were used for cells from each donor to match the desired day of culture (extrapolated from data presented in Paper I). Upon seeding cells were immediately placed in regular osteogenic inducing media (for detailed composition refer to Paper I), with media change (1.5 ml) occurring every 48 hours until sample collection was performed.

Blank (unused) medium was also collected from each of the original batches (0.5 ml in each case) for use as a control when looking at metabolite change between time points.

3.1.6 Osteogenic differentiation for RNA-sequence sampling

Cells (n = 3) used to gather RNA sequencing metabolomic data were cultured in 6 well plate culture vessels. The initial seeding density was 15.600 cells/cm2, but that yielded too low total RNA quantity, so experiment was repeated with seeding density of 26.041 cells/cm2. Five separate wells were used for cells from each donor to match the desired day of culture (time points extrapolated from data and methods presented in Paper I).

Upon seeding cells were immediately placed in osteogenic inducing medium (2 ml because of cell number, for detailed composition of media refer to Paper I), with media change every 48 hours.

3.1.7 Quality Control Assays for Osteo- and Adipogenesis

In order to confirm that the cells in use were BM-MSCs capable of the desired differentiation quality control assays were performed.

In the case of osteogenic differentiation Alizarin Red staining and quantification was performed on days 0, 14 and 28 (measures deposition of minerals), along with Alkaline phosphatase assay on days 0, 7, 14 and 28 (increased activity of alkaline phosphatase is suggestive of active osteoblast formation in MSC cultures) and RT-qPCR to gain the gene expression levels of known osteogenic markers (like RUNX2 and COL1A2) on days 0 and 28.

For detailed description of the methods along with kits and primers used refer to Paper I.

In the case of adipogenic differentiation Oil Red O staining was used to assess and demonstrate the accumulation of lipid droplets within the cells and the gene expression of PPARG, a key gene in adipogenesis, was evaluated using RT-qPCR. More detailed description of methods can be found in Paper II.

3.1.7.1 Reflection – How could cell culture experiment planning be changed to enhance precision and usefulness of downstream work?

There are three points above others that come to mind when reflecting upon what was done and knowing more about the applied subjects that the author would now do differently. As they reflect things learned during the projects progress it feels appropriate to list them here.

They are the following:

During the cell culture used to gather exometabolomic data every 24 hours for the total of 28 days I would have taken an additional blank sample of the media each time it was changed. This would have accounted for any kind of metabolite degradation possible in the newly supplied media and thus would have provided less possibilities for drawing inaccurate conclusions from metabolite changes over time.

During that same cell culture, I would also have had a parallel cell culture of the same cells where I would have harvested those cells each time a used media sample was taken to perform a BCA protein assay (or another similar assay that can be used to assess cell number)

on the additional harvested cells. This would have provided a solid overview of the cell number progression during the time of osteogenic differentiation, but this is harder to assess for cells in differentiation compared to proliferating cells. This is mainly due to the changing nature of the cells, both in function and morphology – counting them becomes difficult. This would have provided a solid way to normalise the extracellular metabolomic data as well as possible to cell number which is a frequently requested addition for any statistical analysis. This would also have made all of the flux rate calculations in the GEMs more precise and so provided an even more stable base to build the models upon.

I would have logged the exchange-time to the second in the cases where I changed media during all of my cell cultures. This would have provided a more exact time frame to work with regarding rates of uptake and secretion of metabolites essential in model evaluation and so would have provided possibly more precise model prediction and function.

3.2 Metabolomic measurements

3.2.1 Non-MS Metabolite measurement - Paper I

Extracellular glucose and lactate were measured using ABL blood gas analysis (ABL90 Flex analyser, Radiometer Medical ApS, Denmark) with unused medium (blank medium) samples serving as control.

The extracellular glutamine, glutamate and ammonia were assayed in spent medium samples, collected every 24 to 36 hours as described in previous section, using colorimetric assays (Megazyme, Wicklow, Ireland). L-glutamine and ammonia were measured using a single assay (Megazyme), as per the manufacturer's instructions, via determining the decrease in absorbance of the reaction mixture at 340 nm using a Spectromax M3 plate reader (Molecular Devices, San Jose, CA). L-glutamic acid was measured with a separate assay (Megazyme), as per the manufacturer's instructions, via absorbance measurements at 492 nm. Unused medium samples (blank medium) served as the controls for these assays.

These methods of metabolite measurements were used for Paper I instead of the more accurate mass spectrometry (as is the case for remaining metabolomic data) as the data was needed for further experimental planning and access to mass spectrometry was not possible at the time due to equipment malfunction.

3.2.1.1 Data normalisation and processing - Paper I

Non-MS extracellular metabolite data processing and normalization was performed in R [247]. One day was found to be missing more than 50% of data points and removed from further analysis. Other data points below limit of detection or for other reasons were replaced with the minimum metabolite value measured. For each metabolite measured a generalized linear model was fitted using the gamm4 package in R [248, p. 4], this modelled the change in metabolite concentration by day of differentiation protocol accounting for donor variation and analysis batch effects as random variables. Other possible models were considered also accounting for the media dwell time, and PIPL batch nested in donor and passage number nested in donor as random effects, however the Akaike Information Criteria of these models (see Table A2 in Appendix A) were higher indicating poorer models, either less good fit or

more over fitting. One exception to this was adding the effect of media well time to the lactate model. However, this was only slightly better and given the desire for consistency across metabolites and the use of rate of change for other analyses, which incorporates this factor, it was decided not to use this model. Change point detection was performed using the ECP package for R to perform change point detection in multivariate data using the e divisive method with a required significance level of 0.05 [249]. This analysis was performed on the modelled values for each day after they had been converted to the hourly rate of change (i.e. the secretion or uptake rate) for each day.

The hourly rates of uptake and secretion were calculated by taking the difference of the absolute metabolite concentration levels between adjacent days and dividing by the appropriate number of hours that passed between media change and sample collection.

3.2.2 Extracellular Metabolite Extraction – Paper I and II

In order to extract extracellular metabolites from collected media samples the supernatants (previously stored at -80 C) were thawed and subsequently 200 µL of each sample was placed into a properly labelled Eppendorf tube (1.5 ml) along with 30 µL of previously mixed isotopically labelled internal standards (IS, see table 1 in the appendix for IS composition).

The IS, which in this case is a mixture of known concentrations of compounds that are chemically similar to the ones being analysed but ones that are not expected to be naturally present in the samples (therefore isotope labelled compounds are most often used), has to be added as early as possible in the process to the samples.

The main purpose of IS is to improve the accuracy and precision of quantitation and robustness of the analysis.

After, 500 µL of ice-cold methanol (MeOH) was added and the resulting solution vortexed for one minute. Samples were then centrifuged at 20817g and 4°C for 15 minutes.

Resulting supernatants were transferred to a new Eppendorf tube (1.5 ml) whilst precipitate was discarded. The supernatant samples were then evaporated by using a vacuum concentrator (MiVac) before adding 300 µL of a mixture containing dH2O and acetonitrile (ACN) in equal parts to reconstitute the dried residue left in the Eppendorf tubes

In 2 separate sets of twelve Eppendorf tubes, 200 µL of varying dilutions of previously prepared CC mix (see table 2 in the appendix for CC mix detailed composition and dilution ratios) were transferred. The CC mix, also known as a mixture of metabolite standards, is a dilution series that can be used for absolute quantification of metabolite concentration by generating an external calibration curve by least-squares linear regression. This curve is then used to estimate the absolute concentrations of the corresponding metabolites in the measured experiment samples.

The CC samples were put through the same evaporation and reconstitution procedure as the samples.

The reconstitutes samples as well as the two CC mixes were then filtered through a Pierce protein 96-well precipitation plate that had previously been prepared by wetting the filter (to facilitate correct filtration). The filtration was done via centrifugation for 30 minutes at 4 C and 2000rpm.

The filtered precipitation was then transferred to a labelled set of glass mass spectrometry vials with glass inserts in order to be put through the mass spectrometer.

3.2.3 Intracellular labelled and unlabelled Metabolite Extraction – Paper I

Upon sample collection all media left after necessary extracellular metabolite sample collection was discarded. After, cells were washed 3 times using 1 ml of PBS (input ref if needed). PBS was discarded using a pipette after each wash.

Next, 1 ml of 80% methanol solution (stored until needed at -20 C in order to keep it at the necessary cold temperature) was pipetted straight onto the cells and a cell scraper subsequently used to dislodge and scrape cells from the bottom of the culture vessel. The resulting methanol-cell suspension was placed in an Eppendorf tube and stored at -80 C until needed for metabolite extraction/preparation for mass spectrometry.

To extract intracellular metabolites collected samples (a cell suspension in 80% methanol solution, previously stored at -80 C) were thawed and 30 µL of previously mixed isotopically labelled internal standards (IS, see table 1 in Appendix for IS composition) subsequently added. The samples were then placed on a floating rack and into a sonicating water bath for 20 second sonication before being put on ice for up to 2 minutes. This was done for a total of 3 times. Icing was needed in order to hinder the samples from heating up. Subsequently 800 µL of ice cold methanol:dH2O (7:3 v/v) solution was added to each sample and samples vortexed for approximately 30 seconds.

The samples were then centrifuged at 20817g for 15 minutes at 4 C.

The resulting supernatant was then transferred into properly labelled Eppendorf tubes (2 ml) whilst the precipitate was again reconstituted with 900 µL of previously described methanol solution before being vortexed and centrifuged for the second time. Resulting supernatant was combined with the previous one and precipitates retained at – 80 C for later protein assay.

Similar to the extraction of extracellular metabolites, 200 µL of CC mix serial dilution were transferred to properly labelled Eppendorf tubes (1.5 mL).

All samples (CCmix serial dilutions and intracellular samples) were then transferred to a vacuum concentrator (MinVac) for evaporation before being reconstituted in 300 µL solution containing dH2O and ACN in equal parts.

The reconstitutes samples as well as the two CC mixes were then filtered through a Pierce protein 96-well precipitation plate that had previously been prepared by wetting the filter (to facilitate correct filtration). The filtration was done via centrifugation for 30 minutes at 4 C and 2000rpm.

The filtered precipitate was then transferred to a labelled set of glass mass spectrometry vials with glass inserts in order to be put through the mass spectrometer.

3.3 UPLC-MS -Paper I and II

All metabolite measurements based on mass spectrometry were performed using a gradient elution UPLC (ACQUITY) system (UPLC ACQUITY, Waters Corporation, Milford, MA) coupled with an ionization qTOF mass spectrometer (Synapt G2 HDMS, Waters Corporation, Manchester, U.K.) with an electrospray interface (ESI).

Gradient chromatographic separation was achieved by HILIC through an Aquity BEH amide column (2.1 mm x 150 mm, 1.7 µm particle size, Waters Corporation) at 45° C.

Two different chromatographic conditions were used in combination with HILIC column, an acidic mobile phase (phase A) and a basic mobile phase (phase B). In both cases the injection volume was 7.5 µL, the flow rate was 0.4 mL/min and the run time was 14 minutes. Mobile phase A conditions consisted of ACN with 0.1 % of formic acid and mobile phase B conditions consisted of dH2O with 1% formic acid.

The following gradient patterns (solvent B) was used in both cases: 0 minutes 1% B, 0.1 minutes 1% B, 6 minutes 60% B, 8 minutes 40% B, 8.5 minutes 1% B, 14 minutes 1% B.

Both positive and negative ESI modes were acquired. The capillary voltage and the cone voltage were 1.5 kV, the temperatures were 120 C and 500 C respectively and desolvation gas flow was 800 L/h.

3.4 RNA-sequence measurement, data processing and normalisation – Paper I

When collecting, isolating and extracting the RNA samples RNAzol [250], [251] was used in all instances and the accompanying protocol for total RNA solation/extraction used.
Upon collection used media was discarded and without washing 1 mL of RNAzol was pipetted into each culture well and the same pipette tip used to scrape and pipette in order to ensure lysis took place.

Samples were all stored at – 80 C until every time point had been collected.
Upon completion of the experiment all samples were thawed at room temperature for 5 minutes with regular mixing, after which 0.4 mL of dH2O was added to each sample.
The resulting solution was then shaken or vortexed for 15 seconds before being incubated for 15 minutes at room temperature, after which the samples were centrifuged for 15 minutes at 12.000g. Specific temperature was not dictated.

From the resulting supernatant 1 mL was collected and put into a new Eppendorf tube (2 mL) into which 1 mL of isopropanol was mixed. The resulting solution was then incubated at room temperature for 10 minutes before being centrifuged at 12.000g for 10 minutes. This causes the RNA to form a pellet, which is not really visible to the naked eye. Therefore, care had to be taken with the placement of the Eppendorf tubes in order to know on which side of the tube the small pellet would form. This was done in order to prevent the pellet to be accidentally pipetted loose and subsequently discarded in the next washing steps.

The washing step of the RNA isolation involved using 75% ethanol solution. Around 0.4 mL of the ethanol solution was pipetted into the Eppendorf tube (directly onto the side opposite the intended RNA pellet) and the subsequent centrifuging for 2 minutes at 8000g. Here the same care of tube placement in the centrifuge had to be taken in order to preserve the pellet. The wash solution was discarded between washes via careful pipetting.
The resulting RNA pellet was then submerged in 50 µL of RNAse free water, the RNA concentration measured using a nanodrop machine and a sample with the concentration of 20ng/µL created in order to be run through RNA sequencing.

All RNA transcripts were sequenced using Illumina equipment (located at DeCOde genetics) and resulting fastaq files quantified using Kallisto version 0.46.1 [252] using default

parameters and the Ensembl Homo sapiens GRCh38 reference transcriptome. The R program „Sleuth“[253] was used for all statistical calculations from values in Kallisto output files.

3.5 LC-MS Data Processing and Normalisation

3.5.1 Extracellular targeted data processing using TargetLynx – Paper II

The extracellular metabolomics analysis was run as a targeted analysis and based on an in-house library generated by the author of this thesis. The library was used to identify a certain group of expected metabolites based on both their m/z ration of ion adducts to fragments and their chromatographic retention times. The software used for the purpose of integrating the chromatographic peak area of identified metabolites was TargetLynx (v4.1, Waters). Normalisation of said peak area is then performed by dividing it with the peak area of a isotopically labelled internal standard (one that is closest to the same retention time as the metabolite in question).

In order to generate an absolute quantification, the previously mentioned dilution series of mixture of metabolite standards (also referred to as the CCmix) was used to obtain an external calibration curve by least-square standard linear regression which subsequently was used to estimate absolute concentrations of corresponding metabolites in all analytical samples.

This method was used for the expansion, osteogenic and adipogenic extracellular data used to generate and compare the models in paper II.

3.5.2 Intracellular untargeted data processing using XCMS -Paper I

The intracellular metabolomic data was all run as an untargeted analysis using the R package XCMS [188].

The first step of the process was conversion of the raw LC-MS data files but in order to be able to work with the data outside of MassLynx and TargetLynx it has to be converted to a MZdata format using MassWolf and a function called „water.convert.R“. That option is preferable to other like DataBridge and MSconvert since it supports MS^n data (unlike DataBridge) and adds lockmass calibrations to analyte measurements in the output files (unlike MZdata). XCMS can then correct such gaps by filling them using the nearest available analyte scan.

After the raw data conversion had been completed the centWave algorithm was used in order to detect chromatographic peaks, also known as ion features, automatically. In broad strokes, the centWave algorithm sequentially goes over each chromatographic scan and records all m/z peaks into vectors or variables called regions of interest (ROI). It starts with the first scan and as it moves along it refers to the one before it to see if the previously recorded ROI that is being looked at in the new file contains the same peaks (a certain ppm range of the m/z values of the peaks is used as a reference. If the function confirms that the peaks are found in both files it calculates the mean m/z value between the files. This is done for each ROI. If the ppm is outside of the desired/allowed ppm range the ROI is discarded.

If ROI are not found in a predetermined number of consecutive scans with a certain minimum predetermined intensity they are discarded. This is done through a filter function in

the centWave algorithm and for the purpose of this thesis it was decided that if 3 consecutive ROI did not contain a peak with intensity level of at least 100 it was discarded.

Within the centWave algorithm ones all ROIs have been found a continuous wavelet transformation (CWT) was used to detect chromatographic peaks with variable peak widths. Here a minimum and maximum peak width.

The obiwarp method was used to align retention times between samples and peak density method to group corresponding chromatographic peaks.

The R package CAMERA [254] was then used in order to decrease the complexity of the generated data set. It groups ion features such as adducts and fragments that can potentially stem from the same compound.

During the peak identification and peak picking process the data was processed in such a manner as to normalize with reference to donor variation.

The resulting data was then normalized using NOMIS (NormQC, a function found in R) method, then by protein content (BCA protein piercing assay - to account for cell number) and finally log-transformed. This data was used for the PCA, PLSDA, one way ANOVA and Tukey's Post-HOC analysis, all used in Paper I.

3.5.2.1 Mummichog pathway and network analysis

To search for enrichment patterns in metabolic networks and identify possible characteristic metabolites that were enriched for each stage we applied the Mummichog online software [255] in conjunction with the online database HMDB [256]. It bypasses the need for metabolite identification by using the organisation of metabolic networks in order to predict activity directly from supplied mass spectrometry data tables. The analysis was run as described in the protocol that follows the online software.

3.5.2.2 Targeted MS-MS analysis to confirm Mummichog metabolite prediction

The instrumentation used was an ACQUITY UPLC system (UPLC ACQUITY, Waters Corporation, Milford, MA) coupled to a qTOF mass spectrometer (Synapt G2 HDMS, Waters Corporation, Manchester, U.K.) with an electrospray interface (ESI). The gradient chromatographic separation was performed on an ACQUITY BEH Amide (2.1 mm × 150 mm, 1.7 µm particle size, Waters Corporation) at 45◦C. Mobile phase A was Acetonitrile and mobile phase B H2O both with 0.1% of formic acid. Injection volume was 7.5 µL, flow rate was 0.4 mL/min and run time was 14 min. The following gradient pattern (solvent B) was used: 0 min, 1% B; 0.1 min, 1% B; 6 min, 60%B; 8 min, 40% B; 8.5 min, 1%B; 14 min, 1% B. Chromatograms were acquired on scan mode for both positive (+) and negative (-) ionization. The capillary and cone voltage were 1.5 kV and 30 V, respectively. The source and desolvation temperature were 120 and 500 °C, respectively, and the desolvation gas flow was 800 L/h.

3.5.3 BCA Protein Assay

In order to evaluate cell quantity at each time point defined by change point analysis, that could then be used to normalize data with regards to cell count, a bicinchoninic acid (BCA)

protein assay was performed on the precipitates collected during the intracellular metabolite extractions (see section 3.2.3 – and Paper I).

In order to extract and dissolve protein content a dissolving buffer was created. It constituted bufferA (RIPA buffer):bufferB (200mM NaOH, 1% SDS) in 1:1 v/v. 100 µL of the dissolving buffer was added to the Eppendorf tubes containing the protein pellets and volume adjusted based on estimated protein amount. Afterwards the tubes were vortexed and put through a freeze/thaw cycle to try and aid with pellet breakdown. Next, the pellets were sonicated for 1 hour at 60◦C before being vortexed again to try and dissolve as much protein as possible. Of the resulting suspension 5 µL of each sample were used for the assay.

In performance of the assay itself (Pierce™ BCA Protein Assay) the accompanying kit protocol from Thermo Scientific™ was followed [257].

3.6 Statistical Analysis

All statistical analysis and related data work was performed in R.

3.6.1 LC-MS data

With regards to the intracellular metabolomics data the normalisation process was split up into several sections. During the peak identification and peak picking process the data was processed in such a manner as to normalize with reference to donor variation.

The resulting data was then normalized using NOMIS (NormQC, a function found in R) method, then by protein content (BCA protein piercing assay - to account for cell number) and finally log-transformed in order to bring all metabolites within a scale that would enable comparisons and resulting statistical analysis (e.g. ANOVA, PCA, PLSDA and heatmaps). This data was primarily used in Paper I and all statistical analysis can be seen there.

With regards to the extracellular targeted metabolomics data (both for OD and AD) used in Paper II no statistical analysis was performed on the data after it had been normalised as described in section 3.5.1 as it was only needed to constrain the genome scale metabolic models reconstructed and described in that paper. There are plans however to use the data to do statistical comparisons on differences between the two cell states, adipogenesis and osteogenesis.

3.6.2 RNA sequence data

For detailed description of gene expression quantification and analysis methods please see method section 2.9 in paper I.

3.7 Genome Scale Metabolic Modelling

For a more detailed version of methods used to generate the osteogenic and adipogenic GEMs presented in this thesis please refer to Paper II. Only a brief overview will be presented here.

The models presented in Paper II were built on previously available transcriptomic data sets gathered from ArrayExpress [258]. Data sets were selected based on their relevance to the experimental conditions described below for collection of uptake and secretion data.

The transcriptomic data generated by the author was used for other work in this thesis with an additional intended used discussed in section 5.3.

Selected transcriptomic data sets were processed using MATLAB (Mathworks, Natick, Massachusetts, USA) and those along with metabolomic data set generated both through UPLC-MS Analysis and ABL blood gas analysis were used in the construction of the models

The model construction itself was performed using the Constraint-based reconstruction and analysis (COBRA) Toolbox version 3[259] in MATLAB 2017b (Mathwork, Natick, MA, USA). The model chosen as a base reconstruction of the global human metabolic network was a thermodynamically feasible version of the Recon3 model [201], which was curated as necessary in order to resemble more a MSC cell specific model. Details of curation steps can be found in Paper II.

The resulting curated model was then constrained with known medium compositions (which are different for the different culture conditions), the list if additional metabolites detected by MS in the basic/non differentiating medium and data on cell weight and growth. This was done 3 times, a separate process for each cell state condition (proliferation, osteogenesis and adipogenesis).

The three media constrained models were then made more specific by transcriptomic data constraints where certain core reactions specific to each state (found thorough literature research) were kept at a maximum expression. This was done via the GIMME [260] algorithm in the COBRA Toolbox[259].

The transcriptomically constrained models then had uptake and secretion constraint added based on the mass spectrometry data with minimal relaxation of those added constraints to allow for feasible models.

Those versions of the models were then further pruned in order to give fully functional condition specific models which were subsequently checked for the inclusion of the core reactions and biological feasibility.

Both base models and the final models were tested using the memote Cobrapy package [261] in Python after being exported from MATLAB in systems biology mark-up language (SBML) format.

A previously existing MSC model (iMSC1255) modelling proliferating MSCs was used for comparison.

3.8 Model Comparison

Comparison between the newly reconstructed models was all performed using the COBRA Toolbox in MATLAB.

Genes and reactions necessary to ensure flux through the biomass reactions were determined for each model and random sampling, flux balance analysis (FBA)[203] and flux variability analysis (FVA)[262] used with the biomass function as the objective to determine the different ranges, probability of distribution and optimal fluxes through all model reactions in each model.

Possible reactions needed for optimisation of osteogenesis were explored and flux enrichment analysis used to explore what subsystems and gene rule had to be enriched or changed in order to get a model from proliferation or adipogenic state to an osteogenic one. A more detailed method description and the accompanying results can be found in Paper II.

4 Results and Discussion

''What you learn from a life in science
is the vastness of our ignorance. ''

David Eagleman,
American Neuroscientist (B. April 25, 1971).

4.1 **Paper I:** Using measurements of key metabolites to define metabolic stages during osteogenic differentiation of mesenchymal stromal cells

The aim of this work was dual. Firstly, to explore through the use of key extracellular metabolite measurements, the possibility of there existing different metabolic phenotypes for BM-MSCs during their course of 28-day osteogenic differentiation. Secondly, to build upon the gathered results with more expansive and elaborate intracellular mass spectrometry and RNA sequence data to further explore the metabolic shifts behind the proposed stages and gain insights into what metabolically linked transcription factors might be the ones contributing the most to the observed metabolic differences.

In the author`s previous experiments (unpublished), using results from extracellular glucose and lactate measurements from BM-MSCs cultured under similar conditions glucose/lactate consumption rate was different in magnitude between the first and latter half of the differentiation period. A similar behaviour was observed in another study done by a different member of the group using the same cell type but during adipogenic differentiation [269].

This along with literature research regarding an observed metabolic switch during MSCs transition from proliferation into differentiation, where cells move from being almost solely reliant upon glycolysis for energy production into a more mixed ATP production via initiation of mitochondrial activity, sparked the hypothesis of there existing more than one metabolic phenotype for BM-MSCs during osteogenic differentiation. Some research has explored things along similar lines [29], [31], [141] but to the groups best knowledge none that had systematically tried to establish and define such phenotypes nor explore where in the metabolic pathways the differences might lie.

In this work the group first used previously defined biomarkers to verify osteogenic differentiation. Next, we used key metabolite markers to track differentiation and define metabolic stages of osteogenic differentiation. Then untargeted and targeted metabolomic analysis was used to globally characterize these metabolic shifts. Finally, we reconstructed a gene regulatory network to explore the underlying mechanisms of the observed metabolic shifts.

To estimate changes in central carbon metabolism the group quantified extracellular glucose, lactate, glutamine, glutamate and ammonia concentrations in spent medium from MSCs undergoing osteogenic differentiation. Minor significant differences in concentration levels were observed, with lactate being the only metabolite that differed significantly from

that of measured blank or unused medium. Through the use of generalised linear modelling it was possible to observe minor trends in the other four metabolites. Similar things were found to be true when analysing the extracellular unlabeled data measured via UPLC-MS analysis. Donor variability, equipment measuring capacity and media evaporation over time most likely contributed to the small differences.

By performing multivariate change point analysis using the model normalised metabolite values (converted to hourly rate of change) the group was able to use the utilisation and production of the previously mentioned essential metabolites to hypothesise stages of osteogenic differentiation. Two statistically significant change points within the differentiation period, in addition to the beginning and the end were identified, suggesting a total of three possible metabolic phases of differentiation. Phase 1 occurred over Days 1 to 4, Phase 2 was between Days 5 and 15, and Phase 3 was from Day 16 to the end of the study period at Day 28. This analysis along with calculations of glucose/lactate, glutamine/glutamate and glutamine/ammonia ratios suggest different metabolic phases over the 28 days of osteogenic differentiation that are defined by changes to glycolysis and glutaminolysis (see Figure 3).

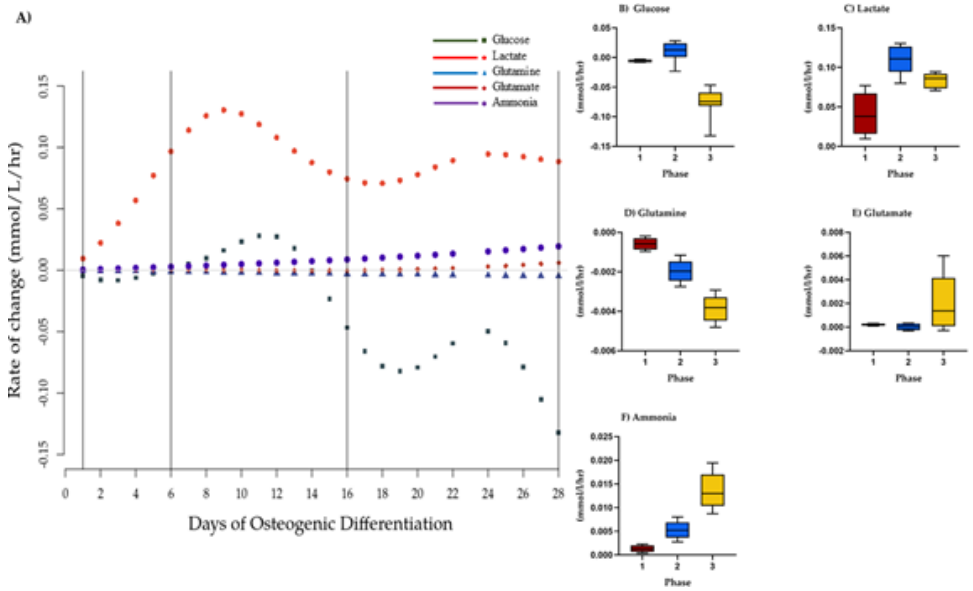

Figure 3: Phases of osteogenic differentiation. A) Change point analysis for glucose, lactate, glutamine, ammonia, and glutamate in spent medium from osteogenically differentiation MSCs between Days 1 and 28. Vertical lines indicate four possible change points separating the stages of differentiation. Points (various shapes) represent the model normalized rate of change on a given day (mmol/l/hr). Black lines represent the change points detected at less than p = 0.05. Grey line represents 0. Hourly rate of change of concentration of model normalized values (mmol/l/hr) per phase of osteogenic differentiation, mean and SEM of **B)** glucose, **C)** lactate **D)** glutamine, **E)** ammonia, and **F)** glutamate. Red = phase 1, blue = phase 2, yellow = phase 3.

To further expand upon this we used the results from untargeted intracellular metabolomic analysis (encompassing 1682 mz values in total gathered from samples from BM-MSCs in osteogenic differentiation at 5 different time points, chosen based on the above mentioned change point analysis) and visualised them via PLSDA (see figure 4). Separation with time

was captured by principle component 1. With respect to the three proposed metabolic phases from the changepoint analysis, grouping was observed between day 9 (phase 2) and day 28 (late phase 3). Day 9 (phase 2) however overlapped with day 16 (start of phase 3). A clear separation between day 3 and 6 (phase 1) with respect to day 28 was also seen. A slight overlap between day 6 and day 16 was also observed. In general the results support discrete metabolic phases during osteogenic differentiation.

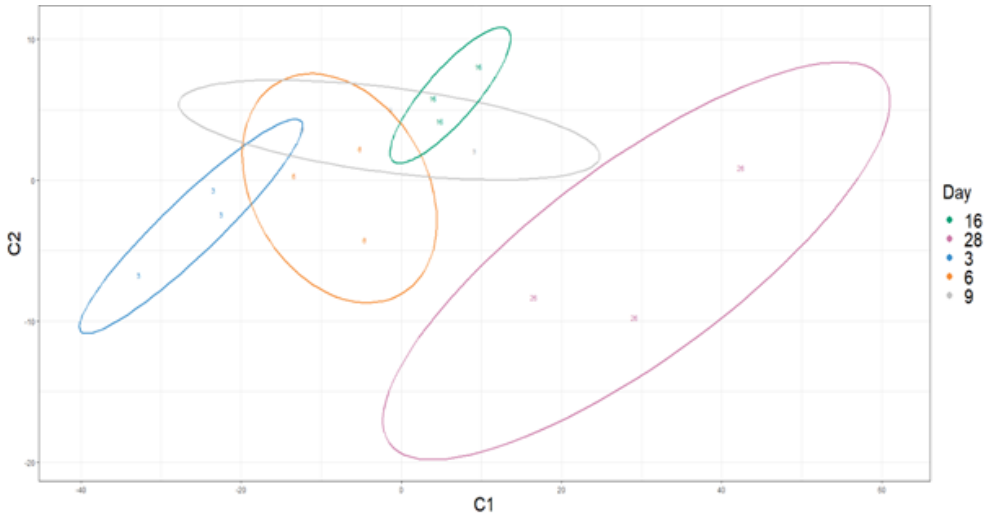

Figure 4: PLSDA visualization of m/z values with significantly different ion intensities during osteogenic differentiation. Ellipses indicate 95% confidence intervals. An overlap in confidence intervals is present for day 6, day 9 and day 16– however when observing day 3, day 9 and day 28 (timepoints firmly within the suggested phases) the overlap is less prominent. Data were normalized to protein abundance and scaled prior to analysis.

While offering good temporal resolution, our extracellular data lacked sensitivity. In order to support that altered metabolic phenotypes during osteogenic differentiation are defined by changes to glycolysis we fed cells with uniformly labelled ^{13}C glucose and, to investigate if changes could be associated with altered glutaminolysis, ^{13}C or ^{15}N glutamine. Looking at ^{13}C glucose label incorporation along with isotopolouge distribution in uridine diphosphate glucose (UDP-glucose) and UDP-N-Acetyl glucosamine we found indications of increased glycolytic flux coupled with decreased flux through the pentose phosphate pathway. This supports the notion of anaerobic switch following day 9 of osteogenic differentiation. Combining that with ^{13}C glucose label enrichment patterns in aspartate and glutamate (that can only be derived from glucose via oxaloacetate and alpha ketoglutarate and thus give indications of flux through the TCA cycle) the results are indicative of changes in glycolytic flux compared to PPP flux, with PPP decreasing over time whilst glycolytic flux increases as well as increased TCA cycle activity as osteogenesis increases. All support previous findings suggesting that cellular expansion decreases and eventually stops within the first two weeks of osteogenesis (reference), with an increase in mitochondrial functions as the energy demand of the differentiating cell seemingly increases.

An unexpected additional result, gathered from associating m/z values with metabolic pathways and specific metabolites through the use of the mummichog algorithm (input ref), revealed changes indicative of altered lipid metabolism in the cells and changes to their redox potential.

The changes related to the cellular redox potential via glutathione synthesis are consistent with changes to mitochondrial respiration during differentiation but the altered lipid metabolism was not an avenue we had anticipated and provides an intriguing future avenue to explore. For more detailed results please see Paper I of this thesis.

In conclusion, the changes observed in this study support distinct differences between early- and late-stage osteogenesis: there is an initial preparatory and proliferation stage, coinciding with high ALP activity, while later there is a plateau stage with lower ALP activity and possibly higher calcium accumulation. Our metabolomic analysis further supports these two stages, and preliminary results using general differential gene expression analysis indicate the possibility of three stages with a transcriptional state flip occurring between initial and last steps. Future functional work will be needed to fully define the relationships between transcriptomic, metabolic and functional changes. The current experiments also showed a high degree of inter-donor variability, with respect to both metabolism and osteogenic outcome. Further work to understand these differences will hopefully lead to the identification of metabolic biomarkers for successful osteogenesis, and possibly to interventions for increasing the success rate. Furthermore, it will be interesting to explore the observed metabolic changes in the area of lipidomics and related mitochondrial activity in a continuous manner around suggested time points of interest through such technology as Seahorse [263] technique and explore if by impacting the mitochondria in a positive manner can lead to a faster progression of osteogenesis. Such experiments would improve our understanding of how metabolism impacts the ability of cells to differentiate.

4.2 **Paper II:** Analysing metabolic states of adipogenic and osteogenic differentiation in human mesenchymal stem cells via genome scale metabolic model reconstruction

The aim of this work was to create 3 directly comparable genome scale metabolic models for BM-MSCs in 3 different cell states/lineages – proliferation, and early stage osteogenic and adipogenic differentiation – that were biologically feasible and to use the models to explore metabolic functions and main differences between these phenotypes.

Despite genome scale metabolic modelling (GEM) becoming more popular over the years as a tool in translational and regenerative medicine, only one other GEM modelling MSC functions has been reconstructed [64] and that was for cells solely undergoing proliferation.

As much interest in the research community lies within the differentiating MSC lineages and the current knowledge regarding metabolic function and differences is lacking, the group decided to bring forth something not seen before in order to try and start bridging the existing gap. By creating this set of equivalent but separate models, it is possible to create an *in silico* laboratory that helps to design experiments for the cell culture laboratory that have higher probability of success.

Using public transcriptomic data from ArrayExpress [258] (chosen based on relevance to experimental conditions present for collection of uptake and secretion data) along with new extracellular targeted metabolomic data (generated specifically for this work) and experimental data (such as media composition, specifically present in experiments done for this work) the 3 new metabolic networks were reconstructed via the COBRA Toolbox v3.0[259] with Recon3 [201] (a thermodynamically stable version of the global human network Recon3D) as the base model. This base was then manually refined before any cell specific reconstruction took place in order to have it more closely represent MSC metabolism. This included removal of extracellular bile acid metabolism, and drug metabolism as those are not of interest at this current point in time, and then the addition of a greater range of glycan and lipid metabolic sections back into the model along with appropriate links to make sure the results were still thermodynamically feasible.

The iterated base model was then constrained (separately for each cell state) using known medium composition, list of additional metabolites detected by mass spectrometry and data on cell weight and growth – producing three media constrained reconstructions that were then further constrained via transcriptomic data and with certain core reactions (defined through literature research as being characteristic for each cell state) increased to maximal expression. At each time point it was ensured that the models remained both mathematically and biologically feasible, with all core reactions included (those not present in the base model from the start were manually added and linked with necessary reaction to connect them into the model). Next constraining involved application of uptake and secretion rates based on mass spectrometry data and the resulting models were then pruned to give fully functional condition specific models that were validated against the original Recon3D model using Memote [261], [264].

During model comparisons (both new models against each other and them against the pre-existing iMSC1255) it was shown that these models could recapitulate known metabolic differences among the three cell subtypes but they both expand coverage of metabolic pathways when compared to iMSC1255 and accurately represent core metabolic fluxes. ATP molecule production for both glucose and glutamine was very close to the correct number (32 for aerobic glucose, 23 for aerobic glutamine and 2 for anaerobic conditions) and production from other important carbon sources was also generally close to theoretical values (see Figure 5).

By and large, mitochondrial function seemed to be a separating factor between proliferating and differentiating MSCs and flux rates of the PPP pathway seemed to distinguish between adipogenesis and osteogenesis (see Figure 6), but other reactions were looked at as well to determine differences and validate behaviour.

Through enrichment analysis on grouped reactions (by metabolic subsystems) an overview over differentially enriched metabolic subsystems was obtained for each cell type. This showed that in the case of proliferating cells, biotin metabolism, vitamin A metabolism, sphingolipid metabolism and fatty acid oxidation and synthesis are all significantly more active compared to the differentiating states. In the case of adipogenic differentiation fatty acid oxidation and fatty acid synthesis were both areas that were overrepresented in increased activity and in the case of osteogenic differentiation fatty acid oxidation especially showed increased activity (see Table 2).

As an additional point and a proof of the intended function, we used combined models of either osteogenic-adipogenic model or osteogenic-proliferating model to predict a possible way to increase osteogenesis, but metabolic modelling allows generation of hypothesise about means of optimizing one cell lineage over another. Through relaxation analysis a list of reactions was obtained that could be modified in order to move either model towards osteogenesis. Both lists indicate that alterations in the need for malate are changed, either with a reduced uptake or a switch to secretion being observed, and fatty acid and lipids involved in signalling, cell membranes and glycosylation are altered as well. The metabolites involved in these reactions could therefore be seen as possible metabolic markers for differentiation. One of the reactions that was highlighted is the need to increase transport of citrate from extracellular space to cytosol, and it has been shown that when growing cells on citrate rich materials they are encouraged to move towards osteogenesis [265], [266].

This discovery regarding citrate in combination with the enrichment of the exchange/demand reactions subsystem also suggests that other transporters may be interesting targets for future investigation when it comes to searching for new ways to increase osteogenesis of MSCs.

In this work three new genome-scale metabolic models of MSC metabolism, representing expansion, osteogenesis and adipogenesis differentiation, are presented. These newly reconstructed models are increased in scope compared to previous models of this cell type both in terms of the coverage of multiple lineages in models produced specifically for two new lineages and with the models due to usage of a new and much improved base human metabolic reconstruction (Recon3). We computed a variety of metabolic phenotypes, demonstrating that the models presented here accurately represent qualitative and quantitative cellular characteristics and important differences between the cell types. Having validated these models, we used them for model-driven experimental design with the goal to optimize *in vitro* osteogenesis. One of predicted solutions, the citrate transporter, concurs with a previously identified target which encourages further possibilities of similar predictions. Through the use of mechanistic models such as are presented here, we provide a blueprint for the application and engineering of regenerative medicine therapies where promising therapeutics like MSCs can be made more efficient and attainable.

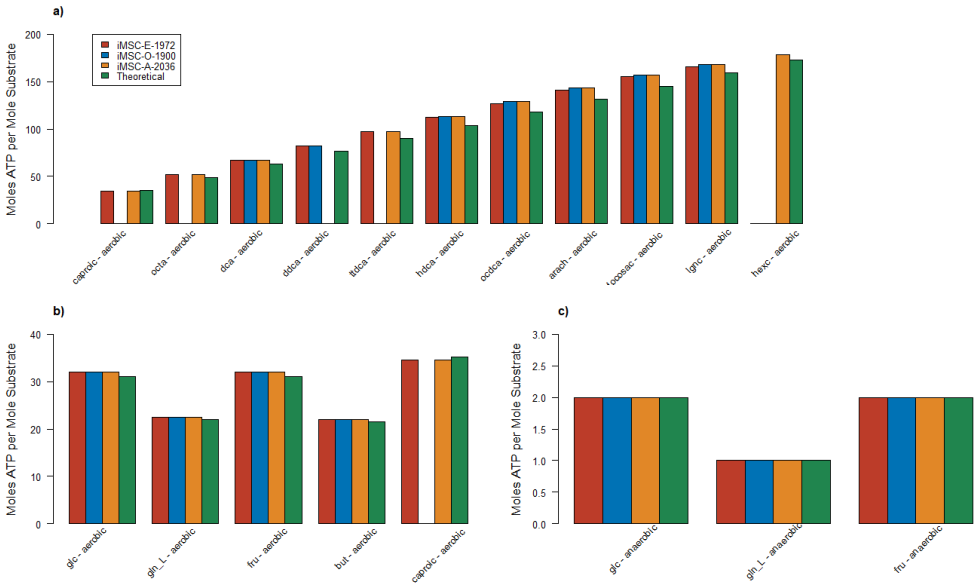

Figure 5: Estimates optimal fluxes for ATP production from various key carbon sources - a) Aerobic metabolism of the most energy dense substrates b) Aerobic metabolism of the least energy dense substrates c) Anaerobic metabolism.

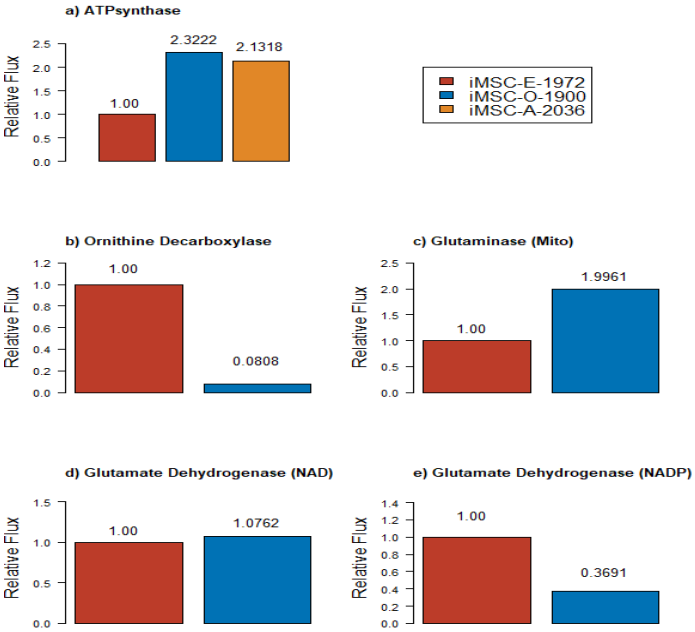

Figure 6: Relative mean fluxes (compared to expansion model) from various reactions –
a) ATPsynthase
b) Ornithine decarboxylase c) Mitochondrial glutaminase
d) NAD dependent glutamate dehydrogenase
e) NADP dependent glutamate dehydrogenase.

Table 2: Showing subsystems that have a significantly overrepresented (adjusted p-value < 0.05) number of more active reactions in the relevant model compared to the other differentiation lineage in the case of osteogenesis/adipogenesis or compared to the two differentiation models in the case of expansion.

Expansion			
Adjusted p-value	*Enriched set size*	*Total set size*	*Groups Increased*
0.000254	98	1368	Exchange/demand reaction
0.001831	65	961	Fatty acid oxidation
0.003348	9	242	Cholesterol metabolism
0.003348	9	240	Fatty acid synthesis
0.003348	1	105	Transport, lysosomal
0.003348	25	453	Transport, mitochondrial
0.006098	3	133	Sphingolipid, metabolism
0.011893	7	185	Bile acid synthesis
0.017589	11	47	Vitamin A metabolism
0.019096	5	12	Biotin metabolism
Osteogenesis			
Adjusted p-value	*Enriched set size*	*Total set size*	*Groups Increased*
7.09E-07	12	961	Fatty acid oxidation
8.6E-06	28	1368	Exchange/demand reaction
Adipogenesis			
Adjusted p-value	*Enriched set size*	*Total set size*	*Groups Increased*
1.64E-05	26	1368	Exchange/demand reaction
0.000253	16	961	Fatty acid oxidation
0.012651	1	240	Fatty acid synthesis

4.3 **Paper III:** Current Status and Future Prospects of Genome-Scale Metabolic Modelling to Optimize the Use of Mesenchymal Stem Cells in Regenerative Medicine

The aim of this work was to bring together a relatively comprehensive and, at that time point, up-to-date knowledge regarding MSCs, their characteristics, functions, limitation, current and possible future use in regenerative medicine and the concept and value that lies in constraint-based models (CBM), specifically GEMs (genome scale metabolic models) when it comes to developing and advancing those therapeutical uses.

It is intended as a review that can hopefully bring together two relatively different fields in the scientific community that do not necessarily realise the possible use and value that the other field can bring to their own.

Currently the number of scientists and laboratories that are well versed in, and implement, the use of GEMs in the purpose of advancing biological discoveries or reducing the cost that comes with such experimental work is growing. There are some excellent networks that have been reconstructed and used in cancer related research and drug target development but, if one looks at the increase in focus in cell based medicine and the popularity that MSCs have gathered as one of the best cell types to use in tissue engineering, it is a bit perplexing how relatively few have actually implemented the use of GEMs as a tool to further their application.

In this work, along with introducing both MSCs, CBM and GEMs we put forth possible ways to combine the subjects and how that combination may be used to further the therapeutic application of MSCs. Some of these possible ways include: 1) trials with *in silico* metabolic engineering (i.e. gene knock outs and knock ins); 2) identifying biomarkers of diseases; 3) predicting drug targets and therapeutic windows; 4) optimization of cellular functions without the cost of wet lab experimentation; 5) Age related exploration (i.e. the effect of cell donor age on clinical outcome and therefore application value of cells) and 6) multi-cell models (i.e. ways to provide insights into metabolic functions of interacting cell types residing within the same organism).

The overall use of GEMs to further therapeutics in regenerative medicine is on the rise and hopefully this work will aid in bringing the existing possibilities to further and wider notice.

5 Conclusions and Future Directions

''Impossible only means that you haven't found the solution yet. ''
-Anonymous

5.1 Conclusions

The possibilities of MSCs with regards to their application as additional tool in translational and regenerative medicine have been known for some time and various aspects of their characteristics have been studied; however, when it comes to looking into metabolism and metabolic changes the research has often been lacking in either scope or conciseness. In some parts this has been due to limitations of technology available at the time and in others it may be partially due to the near to overwhelming popularity of genomics and genetic discovery that was brought about with NGS techniques and the progression of CRISPR-Cas9[267], [268] that took focus away from the importance of metabolomics and metabolic changes when it comes to cellular function, progression, and so possible applications.

With such technology as CRISPR-Cas9 becoming more of a "everyday" tool in the arsenal of the scientific community and with ever better modern metabolomic techniques the generation of large scale quantitative metabolomic data sets is becoming less of an issue and the interpretation and discovery of biologically relevant knowledge from the data is taking its place. This requires that methods and research with the aim of unravelling to any extent the metabolic intricacies of cells to be focused whilst still having the means of looking at the changes in a holistic manner.

The aim of this thesis was to start methodically bridging the existing gap in knowledge when it comes to BM-MSC metabolism and its changes when the cells are changing states, specifically from proliferation into osteogenic differentiation, through the use of up to date metabolomics and transcriptomics techniques and to make the first such metabolic network reconstruction that can, down the line, be used to interpret the metabolomics data and give a better insight into the ongoing "behind-the-curtain" changes that can affect the way these cells may be employed in tissue engineering.

In the first work presented in this thesis we focused on, first, seeing if there was a plausible reason to believe (beyond results via literature research) that during the course of full 28 day osteogenic differentiation there might be different metabolic phenotypes ongoing and if yes where approximately during the time course the changes were occurring, and secondly to try and verify those hypotheses and see what metabolic subsystems within the cells were most likely to be behind it/most likely to be significantly enriched. One of the main contributions from this work is the enormous amount of both labelled and unlabelled intracellular and extracellular metabolomics data that was generated as well as the RNA transcriptomics data.

Another, more focused contribution, was the suggestion of BM-MSCs displaying three distinctive metabolic phenotypes over the course of 28-day osteogenic differentiation and the possible underlying metabolic pathways contributing to those phenotypic changes. This can help focus future metabolomic research on BM-MSCs and aid in understanding the most optimal ways of applying them in tissue engineering and regenerative medicine. The group/author does realize that further research is necessary for more intricate conclusions, e.g., to confirm or disregard the probability of ongoing gluconeogenesis and that lipidomics are the next logical step to further verify the three phases existence and notes that much of the necessary data is now ready and awaiting statistical analysis.

In the second work presented in this thesis the focus was to resolve the existing lack of genome scale metabolic network reconstruction that exists for MSCs by creating three new, directly comparable models modelling BM-MSCs in three cell states: proliferation, adipogenic differentiation and osteogenic differentiation. The reason behind this lineage choice is twofold, one, it is vital to understand the changes that are either driven by or drive the changes that happen when a cell changes its state (more precisely function) from being in proliferation to differentiation as it can greatly impact its survival and means of use and second, osteogenic and adipogenic differentiation pathways are interconnected and thus impact each other. With a more susceptibility towards adipogenic differentiation being one of the driving factors (it is believed) behind osteoporosis, the subsequent increase in yellow bone marrow and an ever-growing need for bone graft replacement material as well as adipogenic differentiation and lipid metabolism in general being of much interest with regards to various metabolomic diseases these differentiation choices presented themselves as obvious.

One of the main contributions from this work were the three new models, especially the adipogenic and osteogenic ones that before this did not exist. They present a new tool to use to interpret large scale metabolomic data and ways to predict which experimental outcomes may have a greater chance of being favourable and so reduce proper experimental cost. The model behaviour was in good agreement with literature and all most characteristic reactions presented themselves. The model analysis and the direct metabolic comparison offered insights into the existing metabolic differences between the cell lineages and offered a way to propose a probable method of enhancing osteogenic differentiation though that has still yet to be verified by experimentation.

The third work presented in this thesis, despite not being a presentation of original experimental work, had a very important goal. To bring to light the opportunities that lie in MSCs and genome scale network reconstructions that can be used to further the development of tissue engineering and other practices related to regenerative medicine. The combination of the two fields has not been implemented to any great extent the past decades and it is the authors believe that there goes a great opportunity unexplored and so this work was put together to try and bring together practitioners in very separate fields so that something new and exciting might be created as a result and which might be able to bridge, at least to some extent, the ever existing gap of knowledge regarding metabolic function and its impact on experimental and clinical results in the search for new cell based therapeutics in regenerative medicine.

In general, this thesis adds to the limited knowledge on MSC metabolism and its changes or differences in the instances of three distinct states of BM-MSCs. It also adds to the plethora of currently published GEMs with a trio of new ones, two of which currently have no president, and all have the potential to be used in predicting experimental outcomes.

The major reported findings, despite needing further verification in some instances, are e.g., that BM-MSCs seem to have 3 distinct metabolic phenotypes during 28-day osteogenic differentiation with a significant increase in secretion of extracellular lactate and measured increase in transcription factors related to mitochondrial functions. Another interesting find is the seemingly inverse relationship between proliferation and osteogenesis that seems to take place during the differentiation period, suggesting a cyclic behaviour in the cells which if true might be very interesting to investigate further with microenvironment survival in mind. That may impact retention and survival after transplantation if oxygen dependencies are markedly different. It is also worth mentioning that no experiments or cell cultures done for this thesis used animal products, such as foetal bovine serum (FBS) for their cell culture. Instead, pathogen inactivated platelet lysate (PIPL) harvested from human platelets obtained from the Bloodbank that would otherwise have been discarded was used. That bears significance as regulatory bodies such as the World Health Organisation (WHO) have considered banning the use of FBS entirely for cell therapy protocols and currently there are strict regulations being passed regarding its use [269], [270].

To conclude, this thesis contributes to the ever-growing knowledge regarding MSC metabolism as well as provide new tools that can be used to focus and hopefully accelerate future research within that field whilst allowing the needed cost to be directed towards endeavours more likely to have significant impact.

5.2 Challenges and Limitation

The work presented in this thesis had several limitations when it came to experimental setup, measurement methods or equipment and time restraints.

Limitations or presentation of things that the author would now have done differently, having gained further knowledge and experience, regarding cell culture experiment setup have already been presented in section 3.1.7.1 and so will not be listed here to limit repetition.

The only point related to the cell culture or cells that the author would like to address additionally is that all findings and model presented in the works done for this thesis were performed using BM-MSCs but there exists a great number of MSCs that are all harvested from different sources (e.g., adipose tissue, peripheral blood and neonatal tissues). There is evidence supporting the hypothesis that despite all being classified as MSCs (and the author finds that definition to be a bit broad) these differently sourced cells may behave in a somewhat different manner, perhaps with slightly different metabolic changes and be dissimilarly well suited for various tasks. So the reported findings in this thesis are not necessarily applicable to all types of MSCs.

The metabolomic methods that were implemented are by design more favourable when it comes to detection of hydrophilic compounds. Metabolites that are highly hydrophobic such

as phospholipid, steroids and other lipids are therefore either not measured at all or they measure very poorly and in an unreliable manner. Since MSCs can, as many other cells, utilize lipids in the case of energy production and literature research gives indications of shifts in lipid metabolism during proliferation and differentiation [271] the lack of quantitative lipid measurements in both extra and intracellular metabolomics adds an uncertainty when it comes to the network reconstruction but the addition of lipidomic data would undoubtedly increase the predictive capabilities of the reconstruction. It also causes a possible important blind spot that must be resolved when it comes to defining underlying pathways contributing towards suggested metabolic phenotypes. This has to be addressed in future studies.

In relation to absolute quantification of the metabolomic data there are two things that must be noted. For the processing of the targeted extracellular data (used e.g., to constrain the models) the method of using isotopically labelled internal standards and external calibration curves was used, however, this method is limited in its use by the disproportional number of metabolites that were measured compared to the number of internal standards but not all metabolites had their corresponding labelled isotope as internal standard. The "nearest neighbour" had to suffice. If all metabolites would have an isotopically labelled internal standard the accuracy if measurements would doubtlessly be improved, however the author does not believe that method to be currently realistic in such cases as were in employment here where the aim was to measure and quantify a great number of metabolites. For more targeted approach this might proof of great use.

For the processing of the untargeted intracellular data (e.g., used to discover contributing metabolic pathways towards phenotypic difference) there exists a more reliable way to normalise the data than through the use of limited number of internal standards. It uses the quality control samples or the "pool" samples to give the desired normalised output. In order to be able to use this method the sample order, when the mass spectrometry measurement is run, has to be very specific with a certain number of QC samples run before and after the measurement samples themselves. As this was not true in this case this method could not be implemented in this thesis. The difference and its effect are not definitive, but it would be recommended that sample order is well seen to in future mass spectrometry runs.

The next to last point of note that the author would like to make is with regards to the steady state assumption that is implemented in the metabolic reconstruction as well the growth assumption for the objective function used in most analyses. The former assumption effects the latter one but is necessary to allow for calculation and definition of the solution space but of course it bears no resemblance to the real-world situation (as is present when the intracellular metabolomic data is looked at). This is a note that has to be taken into account when the models or the ones built upon the presented ones will be validated and further curated using the intracellular data.

The last point that this author wants to address is the fact that presented model for osteogenesis only covers the first seven days of differentiation whilst similarly reporting (in a different paper) the metabolic differences that seem to occur between the various days and so the differences in metabolism between the three cell states are highly likely to become more pronounced and definitive with reconstruction of a further gone model.

5.3 Future Directions

As previously stated, MSCs are multipotent cells with stem cell like abilities that have proven over the course of the last decades to have a significant potential as a new tool in therapeutical development within regenerative medicine.

They are relatively easy to obtain (though the level of ease is dependent upon the desired source) and have various desirable characteristics. One of which is as enhancers of osteogenesis through paracrine factors or tissue replacement via transplantation. This application is however still hindered by various limitations and unknown factors such as ideal level or state of differentiation where the cells may have the best chance for survival *in vivo*, the optimal dosage or frequency of administration and how the progression of differentiation effects the functionality of the cells.

In order to cast light upon the last issue a wholistic overview is necessary and the approach must be methodical and precise.

By creating a genome scale reconstruction that models cellular behaviour during the various suggested phases of osteogenic differentiation the wholistic overview may be obtained and new insights into possible ways of cellular enhancement can be garnered. Such models would have to be directly comparable - meaning that the experimental circumstances would have to be identical, and they would have to be constructed and constrained using: 1) Transcriptomic data (RNAseq data) that would be generated in the aforementioned identical circumstances 2) Extracellular and intracellular labelled and unlabelled metabolomic data (this would have to come from an identical cell culture as the transcriptomic data) 3) Lipidomics 4) Experimentally related data (e.g. cell growth, medium composition etc.).

By using methods as have been described in the papers following this thesis directly comparable models could be generated, each modelling a suggested cellular phenotype for a separate phase in osteogenic differentiation that could then be used to explore from the genetic level upwards the differences in metabolic pathway activity and how similar manipulations may render different results depending on the state. This kind of a model has not been constructed to this group's best knowledge, just as is the case for the early day adipogenic and osteogenic models presented in Paper II. The author also wants to state that the reconstruction of these models has already begun (although in very early stages) and that all data excepting the lipidomic data has been generated and processed. Modelling the late stages of osteogenic differentiation has not been done before and to the groups best knowledge there doesn't even exist RNA sequenced data for BM-MSCs during those later stages which is necessary to build a thoroughly verified model aimed at modelling a specific cell state, so this would provide a novel tool for implementation in research related to bone engineering and osteoporosis treatment.

Another aspect that the group believes should be explored to hopefully validate further the suggestion of the three metabolic phases and the underlying metabolic activity is the use of the Agilent Seahorse XF Analyzer technology [272], [273]. This technology provides a fast way to measure oxygen consumption rate (OCR) and extracellular acidification rate (ECAR) at intervals of approximately 5-8 minutes so detailed monitoring of metabolic changes can be noticed. This can help identify global changes in glycolytic metabolism versus oxidative or mitochondrial metabolism and through the use if various available inhibitors that can be

implemented during the assay it is possible to obtain indication into what metabolites or substrates are contributing to the metabolic phenotype under observation. By incorporating labelling experiments, like 13-C metabolic flux analysis, it is also possible to map rather precisely which nutrients (e.g. glucose) are involved in specific metabolic fluxes and to which extent that nutrient gets incorporated in certain metabolites [263], [273]. By performing this kind of an assay during e.g. indicated timepoints of significant change it might be possible to observe more accurately where and when metabolic changes start happening. All additional knowledge provides a greater means for more accurate model prediction and therapeutical enhancement.

A more realistic culturing of the cell might also be beneficial i.e., to perform all previously mentioned cell culture experiment using same type of cells but seeded on a three-dimensional (3D) scaffolding and under the duress of perfusion and some sort of mechanical stimulation e.g. compression. This would allow cells to experience a more *in vivo* like microenvironment during their differentiation and so the data would be more likely to explain the "real life" function of BM-MSCs undergoing differentiation.

One of the ways this could be obtained would be through the use of the "Organ-On-a-Chip" (OoC) technology [274], [275]. The main principals and common design will not be introduced here, but these could be modified in order to design a chip specially for the growth of bone tissue micro-organ. Through proper design methods and applications this could be made so that continuous extracellular media sampling could be performed without disturbance of the cell culture at any given time and by designing multiple chips connected in parallel the possibility of performing multiple experiments at one time could be introduced. New technology such as nano engineering and fibre optic sensors [276]–[278] might even enable in situ single cell monitoring of certain intracellular functions, microscopic cameras could give visual conformation of morphological progression and micro-environmental sensors could monitor, log and maintain the desired set up without a break. A successful design of this kind of a system would also provide a way to model, enhance, and even personalise treatment possibilities in such types of bone related ailments. The OoC technology is being used in other parts of the world, like the U.S.A., to further drug development, disease modelling and personalized medicine but it has as of yet not been implemented anywhere in the Icelandic research or medical community. The author finds it an avenue worth exploring and believes that through the use of such cell culture environment the large-scale osteogenic models could be adjusted to give more precise and realistic predictions more likely to be translatable to *in vivo* circumstances. Such models might prove beneficial in a new avenue of bone tissue engineering that deals with studying the effects of situations like long term microgravity, as is prevalent during space flights, on bone function and how those negative effects may be prevented or haltered.

In short, the possibilities seem almost to be endless. This thesis has made notable strides in furthering existing knowledge regarding metabolism and metabolic changes in BM-MSCs and provided new tools to take that knowledge even further, but despite that there are numerous avenues left to explore and various challenges and limitations left to be addressed some of which will be attempted in future works of this group.

All this is done in the certainty that only through improved systemic knowledge of the topic of MSC metabolism can the therapeutic potential of these cells fully be realised and thus implemented properly in tissue engineering and cellular medicine with the hopes to improve quality of life for future generations.

> *"Science means constantly walking a tightrope*
> *between blind faith and curiosity;*
> *between expertise and creativity;*
> *between bias and openness;*
> *between experience and epiphany;*
> *between ambition and passion;*
> *and between arrogance and conviction*
> *– in short, between and old today and a new tomorrow."*
> — Henrich Rohrer
> Swiss Physicist (B. 6 June 1933 – 16 May 2013)

References

[1] Þ. Sigmarsdóttir, S. McGarrity, Ó. Rolfsson, J. T. Yurkovich, and Ó. E. Sigurjónsson, 'Current Status and Future Prospects of Genome-Scale Metabolic Modeling to Optimize the Use of Mesenchymal Stem Cells in Regenerative Medicine', *Front. Bioeng. Biotechnol.*, vol. 8, Mar. 2020, doi: 10.3389/fbioe.2020.00239.

[2] OpenStax, '6.1 The Functions of the Skeletal System', in *Anatomy and Physiology*, OpenStax, 2013. Accessed: Jun. 03, 2020. [Online]. Available: https://opentextbc.ca/anatomyandphysiology/chapter/6-1-the-functions-of-the-skeletal-system/

[3] D. J. Hadjidakis and I. I. Androulakis, 'Bone remodeling', *Ann. N. Y. Acad. Sci.*, vol. 1092, pp. 385–396, Dec. 2006, doi: 10.1196/annals.1365.035.

[4] B. Javaheri and A. A. Pitsillides, 'Aging and Mechanoadaptive Responsiveness of Bone', *Curr. Osteoporos. Rep.*, vol. 17, no. 6, pp. 560–569, Dec. 2019, doi: 10.1007/s11914-019-00553-7.

[5] J. Maienschein, 'Regenerative medicine's historical roots in regeneration, transplantation, and translation', *Dev. Biol.*, vol. 358, no. 2, pp. 278–284, Oct. 2011, doi: 10.1016/j.ydbio.2010.06.014.

[6] G. Sampogna, S. Y. Guraya, and A. Forgione, 'Regenerative medicine: Historical roots and potential strategies in modern medicine', *J. Microsc. Ultrastruct.*, vol. 3, no. 3, pp. 101–107, Sep. 2015, doi: 10.1016/j.jmau.2015.05.002.

[7] J. A. Sterling and S. A. Guelcher, 'Biomaterial scaffolds for treating osteoporotic bone', *Curr. Osteoporos. Rep.*, vol. 12, no. 1, pp. 48–54, Mar. 2014, doi: 10.1007/s11914-014-0187-2.

[8] G. Fernandez de Grado *et al.*, 'Bone substitutes: a review of their characteristics, clinical use, and perspectives for large bone defects management', *J. Tissue Eng.*, vol. 9, Jun. 2018, doi: 10.1177/2041731418776819.

[9] E. H. Schemitsch, 'Size Matters: Defining Critical in Bone Defect Size!', *J. Orthop. Trauma*, vol. 31 Suppl 5, pp. S20–S22, Oct. 2017, doi: 10.1097/BOT.0000000000000978.

[10] M. Nordin and V. H. Frankel, *Basic Biomechanics of the Musculoskeletal System*. Lippincott Williams & Wilkins, 2001.

[11] W. Wang and K. W. K. Yeung, 'Bone grafts and biomaterials substitutes for bone defect repair: A review', *Bioact. Mater.*, vol. 2, no. 4, pp. 224–247, Dec. 2017, doi: 10.1016/j.bioactmat.2017.05.007.

[12] ReportLinker, 'The global market of bone graft and substitute is estimated to grow at a CAGR of 4.89% during the estimated period of 2020-2028', *GlobeNewswire News Room*, Feb. 04, 2020. http://www.globenewswire.com/news-release/2020/02/04/1979346/0/en/The-global-market-of-bone-graft-and-substitute-is-estimated-to-grow-at-a-CAGR-of-4-89-during-the-estimated-period-of-2020-2028.html (accessed Jun. 03, 2020).

[13] 'Ageing and health'. https://www.who.int/news-room/fact-sheets/detail/ageing-and-health (accessed Jun. 03, 2020).

[14] H.-S. Sohn and J.-K. Oh, 'Review of bone graft and bone substitutes with an emphasis on fracture surgeries', *Biomater. Res.*, vol. 23, no. 1, p. 9, Mar. 2019, doi: 10.1186/s40824-019-0157-y.

[15] V. Campana *et al.*, ‘Bone substitutes in orthopaedic surgery: from basic science to clinical practice’, *J. Mater. Sci. Mater. Med.*, vol. 25, no. 10, pp. 2445–2461, 2014, doi: 10.1007/s10856-014-5240-2.
[16] R. S. Mahla, ‘Stem Cells Applications in Regenerative Medicine and Disease Therapeutics’, *Int. J. Cell Biol.*, vol. 2016, 2016, doi: 10.1155/2016/6940283.
[17] A. J. Rosenbaum, D. A. Grande, and J. S. Dines, ‘The use of mesenchymal stem cells in tissue engineering’, *Organogenesis*, vol. 4, no. 1, pp. 23–27, 2008.
[18] I. Ullah, R. B. Subbarao, and G. J. Rho, ‘Human mesenchymal stem cells - current trends and future prospective’, *Biosci. Rep.*, vol. 35, no. 2, Apr. 2015, doi: 10.1042/BSR20150025.
[19] R. E. B. Fitzsimmons, M. S. Mazurek, A. Soos, and C. A. Simmons, ‘Mesenchymal Stromal/Stem Cells in Regenerative Medicine and Tissue Engineering’, *Stem Cells International*, 2018. https://www.hindawi.com/journals/sci/2018/8031718/ (accessed May 01, 2019).
[20] C. Nombela-Arrieta, J. Ritz, and L. E. Silberstein, ‘The elusive nature and function of mesenchymal stem cells’, *Nat. Rev. Mol. Cell Biol.*, vol. 12, no. 2, pp. 126–131, Feb. 2011, doi: 10.1038/nrm3049.
[21] P. Bianco, M. Riminucci, S. Gronthos, and P. G. Robey, ‘Bone Marrow Stromal Stem Cells: Nature, Biology, and Potential Applications’, *STEM CELLS*, vol. 19, no. 3, pp. 180–192, May 2001, doi: 10.1634/stemcells.19-3-180.
[22] R. Hass, C. Kasper, S. Böhm, and R. Jacobs, ‘Different populations and sources of human mesenchymal stem cells (MSC): A comparison of adult and neonatal tissue-derived MSC’, *Cell Commun. Signal. CCS*, vol. 9, p. 12, May 2011, doi: 10.1186/1478-811X-9-12.
[23] C.-S. Lin, Z.-C. Xin, J. Dai, and T. F. Lue, ‘Commonly Used Mesenchymal Stem Cell Markers and Tracking Labels: Limitations and Challenges’, *Histol. Histopathol.*, vol. 28, no. 9, pp. 1109–1116, Sep. 2013.
[24] M. M. Bonab *et al.*, ‘Autologous mesenchymal stem cell therapy in progressive multiple sclerosis: an open label study’, *Curr. Stem Cell Res. Ther.*, vol. 7, no. 6, pp. 407–414, Nov. 2012.
[25] M. Duijvestein *et al.*, ‘Autologous bone marrow-derived mesenchymal stromal cell treatment for refractory luminal Crohn’s disease: results of a phase I study’, *Gut*, vol. 59, no. 12, pp. 1662–1669, Dec. 2010, doi: 10.1136/gut.2010.215152.
[26] J. Qin *et al.*, ‘Therapeutic potential of mesenchymal stem cells in gastrointestinal cancers – current evidence’, *Gastrointestinal Cancer: Targets and Therapy*, Sep. 08, 2016. https://www.dovepress.com/therapeutic-potential-of-mesenchymal-stem-cells-in-gastrointestinal-ca-peer-reviewed-fulltext-article-GICTT (accessed Apr. 04, 2019).
[27] C.-T. Chen, Y.-R. V. Shih, T. K. Kuo, O. K. Lee, and Y.-H. Wei, ‘Coordinated Changes of Mitochondrial Biogenesis and Antioxidant Enzymes During Osteogenic Differentiation of Human Mesenchymal Stem Cells’, *STEM CELLS*, vol. 26, no. 4, pp. 960–968, 2008, doi: 10.1634/stemcells.2007-0509.
[28] J. Croitoru-Lamoury *et al.*, ‘Interferon-γ Regulates the Proliferation and Differentiation of Mesenchymal Stem Cells via Activation of Indoleamine 2,3 Dioxygenase (IDO)’, *PLoS ONE*, vol. 6, no. 2, p. e14698, Feb. 2011, doi: 10.1371/journal.pone.0014698.
[29] G. Pattappa, H. K. Heywood, J. D. de Bruijn, and D. A. Lee, ‘The metabolism of human mesenchymal stem cells during proliferation and differentiation’, *J. Cell. Physiol.*, vol. 226, no. 10, pp. 2562–2570, Oct. 2011, doi: 10.1002/jcp.22605.

[30] L. B. Buravkova *et al.*, ‘Low ATP level is sufficient to maintain the uncommitted state of multipotent mesenchymal stem cells’, *Biochim. Biophys. Acta*, vol. 1830, no. 10, pp. 4418–4425, Oct. 2013, doi: 10.1016/j.bbagen.2013.05.029.
[31] J. Beegle *et al.*, ‘Hypoxic Preconditioning of Mesenchymal Stromal Cells Induces Metabolic Changes, Enhances Survival, and Promotes Cell Retention In Vivo’, *STEM CELLS*, vol. 33, no. 6, pp. 1818–1828, Jun. 2015, doi: 10.1002/stem.1976.
[32] L. C. Shum, N. S. White, B. N. Mills, K. L. de M. Bentley, and R. A. Eliseev, ‘Energy Metabolism in Mesenchymal Stem Cells During Osteogenic Differentiation’, *Stem Cells Dev.*, vol. 25, no. 2, p. 114, Jan. 2016, doi: 10.1089/scd.2015.0193.
[33] Q. Li, Z. Gao, Y. Chen, and M.-X. Guan, ‘The role of mitochondria in osteogenic, adipogenic and chondrogenic differentiation of mesenchymal stem cells’, *Protein Cell*, vol. 8, no. 6, pp. 439–445, Jun. 2017, doi: 10.1007/s13238-017-0385-7.
[34] J. Meyer, A. Salamon, S. Mispagel, G. Kamp, and K. Peters, ‘Energy metabolic capacities of human adipose-derived mesenchymal stromal cells in vitro and their adaptations in osteogenic and adipogenic differentiation’, *Exp. Cell Res.*, vol. 370, no. 2, pp. 632–642, Sep. 2018, doi: 10.1016/j.yexcr.2018.07.028.
[35] T. Vigo *et al.*, ‘IFNβ enhances mesenchymal stromal (Stem) cells immunomodulatory function through STAT1-3 activation and mTOR-associated promotion of glucose metabolism’, *Cell Death Dis.*, vol. 10, no. 2, Jan. 2019, doi: 10.1038/s41419-019-1336-4.
[36] J. Zhu and C. B. Thompson, ‘Metabolic regulation of cell growth and proliferation’, *Nat. Rev. Mol. Cell Biol.*, p. 1, Apr. 2019, doi: 10.1038/s41580-019-0123-5.
[37] A. Oryan, A. Kamali, A. Moshiri, and M. B. Eslaminejad, ‘Role of Mesenchymal Stem Cells in Bone Regenerative Medicine: What Is the Evidence?’, *Cells Tissues Organs*, vol. 204, no. 2, pp. 59–83, 2017, doi: 10.1159/000469704.
[38] S. Shanbhag, S. Suliman, N. Pandis, A. Stavropoulos, M. Sanz, and K. Mustafa, ‘Cell therapy for orofacial bone regeneration: A systematic review and meta-analysis’, *J. Clin. Periodontol.*, vol. 46, no. S21, pp. 162–182, 2019, doi: 10.1111/jcpe.13049.
[39] A. Battler and J. Leor, *Stem Cell and Gene-Based Therapy: Frontiers in Regenerative Medicine*. Springer Science & Business Media, 2007.
[40] N. M. Mount, S. J. Ward, P. Kefalas, and J. Hyllner, ‘Cell-based therapy technology classifications and translational challenges’, *Philos. Trans. R. Soc. B Biol. Sci.*, vol. 370, no. 1680, Oct. 2015, doi: 10.1098/rstb.2015.0017.
[41] K. Drela, L. Stanaszek, A. Nowakowski, Z. Kuczynska, and B. Lukomska, ‘Experimental Strategies of Mesenchymal Stem Cell Propagation: Adverse Events and Potential Risk of Functional Changes’, *Stem Cells Int.*, vol. 2019, Mar. 2019, doi: 10.1155/2019/7012692.
[42] J. Neman, A. Hambrecht, C. Cadry, and R. Jandial, ‘Stem cell-mediated osteogenesis: therapeutic potential for bone tissue engineering’, *Biol. Targets Ther.*, vol. 6, pp. 47–57, 2012, doi: 10.2147/BTT.S22407.
[43] Q. Zhao, H. Ren, and Z. Han, ‘Mesenchymal stem cells: Immunomodulatory capability and clinical potential in immune diseases’, *J. Cell. Immunother.*, vol. 2, no. 1, pp. 3–20, Mar. 2016, doi: 10.1016/j.jocit.2014.12.001.
[44] L. Han, B. Wang, R. Wang, S. Gong, G. Chen, and W. Xu, ‘The shift in the balance between osteoblastogenesis and adipogenesis of mesenchymal stem cells mediated by glucocorticoid receptor’, *Stem Cell Res. Ther.*, vol. 10, no. 1, p. 377, Dec. 2019, doi: 10.1186/s13287-019-1498-0.
[45] M. Zayzafoon, W. E. Gathings, and J. M. McDonald, ‘Modeled Microgravity Inhibits Osteogenic Differentiation of Human Mesenchymal Stem Cells and Increases

Adipogenesis', *Endocrinology*, vol. 145, no. 5, pp. 2421–2432, May 2004, doi: 10.1210/en.2003-1156.
[46] A. M. Pino, C. J. Rosen, and J. P. Rodríguez, 'In Osteoporosis, differentiation of mesenchymal stem cells (MSCs) improves bone marrow adipogenesis', *Biol. Res.*, vol. 45, no. 3, pp. 279–287, 2012, doi: 10.4067/S0716-97602012000300009.
[47] J. Phetfong *et al.*, 'Osteoporosis: the current status of mesenchymal stem cell-based therapy', *Cell. Mol. Biol. Lett.*, vol. 21, no. 1, p. 12, Aug. 2016, doi: 10.1186/s11658-016-0013-1.
[48] L. Shum, N. S White, B. Mills, K. Bentley, and R. Eliseev, 'Energy Metabolism in Mesenchymal Stem Cells During Osteogenic Differentiation', *Stem Cells Dev.*, vol. 25, Oct. 2015, doi: 10.1089/scd.2015.0193.
[49] J. M. G. Reyes *et al.*, 'Metabolic changes in mesenchymal stem cells in osteogenic medium measured by autofluorescence spectroscopy', *Stem Cells Dayt. Ohio*, vol. 24, no. 5, pp. 1213–1217, May 2006, doi: 10.1634/stemcells.2004-0324.
[50] A. V. Meleshina *et al.*, 'Probing metabolic states of differentiating stem cells using two-photon FLIM', *Sci. Rep.*, vol. 6, p. 21853, Feb. 2016, doi: 10.1038/srep21853.
[51] J. Bolander, T. Herpelinck, M. Chaklader, C. Gklava, L. Geris, and F. P. Luyten, 'Single-cell characterization and metabolic profiling of in vitro cultured human skeletal progenitors with enhanced in vivo bone forming capacity', *STEM CELLS Transl. Med.*, vol. 9, no. 3, pp. 389–402, Mar. 2020, doi: 10.1002/sctm.19-0151.
[52] S. G. Almalki and D. K. Agrawal, 'Key Transcription Factors in the Differentiation of Mesenchymal Stem Cells', *Differ. Res. Biol. Divers.*, vol. 92, no. 1–2, pp. 41–51, 2016, doi: 10.1016/j.diff.2016.02.005.
[53] R. J. DeBerardinis and C. B. Thompson, 'Cellular metabolism and disease: what do metabolic outliers teach us?', *Cell*, vol. 148, no. 6, pp. 1132–1144, Mar. 2012, doi: 10.1016/j.cell.2012.02.032.
[54] M. Agathocleous and W. A. Harris, 'Metabolism in physiological cell proliferation and differentiation', *Trends Cell Biol.*, vol. 23, no. 10, pp. 484–492, Oct. 2013, doi: 10.1016/j.tcb.2013.05.004.
[55] for the IOF CSA Inadequate Responders Working Group *et al.*, 'Treatment failure in osteoporosis', *Osteoporos. Int.*, vol. 23, no. 12, pp. 2769–2774, Dec. 2012, doi: 10.1007/s00198-012-2093-8.
[56] Q. Chen *et al.*, 'Fate decision of mesenchymal stem cells: adipocytes or osteoblasts?', *Cell Death Differ.*, vol. 23, no. 7, pp. 1128–1139, Jul. 2016, doi: 10.1038/cdd.2015.168.
[57] L. Hu, C. Yin, F. Zhao, A. Ali, J. Ma, and A. Qian, 'Mesenchymal Stem Cells: Cell Fate Decision to Osteoblast or Adipocyte and Application in Osteoporosis Treatment', *Int. J. Mol. Sci.*, vol. 19, no. 2, Jan. 2018, doi: 10.3390/ijms19020360.
[58] I. Rocha, J. Förster, and J. Nielsen, 'Design and Application of Genome-Scale Reconstructed Metabolic Models', in *Microbial Gene Essentiality: Protocols and Bioinformatics*, A. L. Osterman and S. Y. Gerdes, Eds. Totowa, NJ: Humana Press, 2008, pp. 409–431. doi: 10.1007/978-1-59745-321-9_29.
[59] J. L. Reed and B. Ø. Palsson, 'Thirteen Years of Building Constraint-Based In Silico Models of Escherichia coli', *J. Bacteriol.*, vol. 185, no. 9, pp. 2692–2699, May 2003, doi: 10.1128/JB.185.9.2692-2699.2003.
[60] O. Resendis-Antonio, 'Constraint-based Modeling', in *Encyclopedia of Systems Biology*, W. Dubitzky, O. Wolkenhauer, K.-H. Cho, and H. Yokota, Eds. New York, NY: Springer New York, 2013, pp. 494–498. doi: 10.1007/978-1-4419-9863-7_1143.

[61] A. Bordbar, J. M. Monk, Z. A. King, and B. O. Palsson, ‘Constraint-based models predict metabolic and associated cellular functions’, *Nat. Rev. Genet.*, vol. 15, no. 2, pp. 107–120, Feb. 2014, doi: 10.1038/nrg3643.
[62] A. M. Feist, M. J. Herrgård, I. Thiele, J. L. Reed, and B. Ø. Palsson, ‘Reconstruction of biochemical networks in microorganisms |’, *Nat. Rev. Microbiol.*, vol. 7, pp. 129–143, Dec. 2008.
[63] R. Agren, J. M. Otero, and J. Nielsen, ‘Genome-scale modeling enables metabolic engineering of Saccharomyces cerevisiae for succinic acid production’, *J. Ind. Microbiol. Biotechnol.*, vol. 40, no. 7, pp. 735–747, Jul. 2013, doi: 10.1007/s10295-013-1269-3.
[64] H. Fouladiha, S.-A. Marashi, and M. A. Shokrgozar, ‘Reconstruction and validation of a constraint-based metabolic network model for bone marrow-derived mesenchymal stem cells’, *Cell Prolif.*, vol. 48, no. 4, pp. 475–485, Aug. 2015, doi: 10.1111/cpr.12197.
[65] A. Bordbar, A. M. Feist, R. Usaite-Black, J. Woodcock, B. O. Palsson, and I. Famili, ‘A multi-tissue type genome-scale metabolic network for analysis of whole-body systems physiology’, *BMC Syst. Biol.*, vol. 5, no. 1, p. 180, Oct. 2011, doi: 10.1186/1752-0509-5-180.
[66] I. Thiele and B. Ø. Palsson, ‘A protocol for generating a high-quality genome-scale metabolic reconstruction’, *Nat. Protoc.*, vol. 5, no. 1, pp. 93–121, Jan. 2010, doi: 10.1038/nprot.2009.203.
[67] J. T. Yurkovich and B. O. Palsson, ‘Solving Puzzles With Missing Pieces: The Power of Systems Biology’, *Proc. IEEE*, vol. 104, no. 1, pp. 2–7, Jan. 2016, doi: 10.1109/JPROC.2015.2505338.
[68] A. Bordbar, J. T. Yurkovich, G. Paglia, O. Rolfsson, Ó. E. Sigurjónsson, and B. O. Palsson, ‘Elucidating dynamic metabolic physiology through network integration of quantitative time-course metabolomics’, *Sci. Rep.*, vol. 7, p. 46249, 07 2017, doi: 10.1038/srep46249.
[69] R. Mafi, S. Hindocha, P. Mafi, M. Griffin, and W. S. Khan, ‘Sources of adult mesenchymal stem cells applicable for musculoskeletal applications - a systematic review of the literature’, *Open Orthop. J.*, vol. 5 Suppl 2, pp. 242–248, 2011, doi: 10.2174/1874325001105010242.
[70] A. Mizukami and K. Swiech, ‘Mesenchymal Stromal Cells: From Discovery to Manufacturing and Commercialization’, *Stem Cells International*, Apr. 11, 2018. https://www.hindawi.com/journals/sci/2018/4083921/ (accessed Jun. 09, 2020).
[71] A. Mizukami and K. Swiech, ‘Mesenchymal Stromal Cells: From Discovery to Manufacturing and Commercialization’, *Stem Cells International*, Apr. 11, 2018. https://www.hindawi.com/journals/sci/2018/4083921/ (accessed Jun. 09, 2020).
[72] M. F. Pittenger *et al.*, ‘Multilineage Potential of Adult Human Mesenchymal Stem Cells’, *Science*, vol. 284, no. 5411, pp. 143–147, Apr. 1999, doi: 10.1126/science.284.5411.143.
[73] Þ. Sigmarsdóttir, S. McGarrity, Ó. Rolfsson, J. T. Yurkovich, and Ó. E. Sigurjónsson, ‘Current Status and Future Prospects of Genome-Scale Metabolic Modeling to Optimize the Use of Mesenchymal Stem Cells in Regenerative Medicine’, *Front. Bioeng. Biotechnol.*, vol. 8, 2020, doi: 10.3389/fbioe.2020.00239.
[74] R. M. Delaine-Smith and G. C. Reilly, ‘Mesenchymal stem cell responses to mechanical stimuli’, *Muscles Ligaments Tendons J.*, vol. 2, no. 3, pp. 169–180, Oct. 2012.

[75] A. J. Steward and D. J. Kelly, ‘Mechanical regulation of mesenchymal stem cell differentiation’, *J. Anat.*, vol. 227, no. 6, pp. 717–731, Dec. 2015, doi: 10.1111/joa.12243.
[76] A. M. Loye *et al.*, ‘Regulation of Mesenchymal Stem Cell Differentiation by Nanopatterning of Bulk Metallic Glass’, *Sci. Rep.*, vol. 8, no. 1, Art. no. 1, Jun. 2018, doi: 10.1038/s41598-018-27098-6.
[77] A. M. Mackay, S. C. Beck, J. M. Murphy, F. P. Barry, C. O. Chichester, and M. F. Pittenger, ‘Chondrogenic differentiation of cultured human mesenchymal stem cells from marrow’, *Tissue Eng.*, vol. 4, no. 4, pp. 415–428, 1998, doi: 10.1089/ten.1998.4.415.
[78] P. Antonitsis *et al.*, ‘Cardiomyogenic Potential of Human Adult Bone Marrow Mesenchymal Stem Cells in Vitro’, *Thorac. Cardiovasc. Surg.*, vol. 56, no. 2, pp. 77–82, Mar. 2008, doi: 10.1055/s-2007-989328.
[79] J. Li and S. Dong, ‘The Signaling Pathways Involved in Chondrocyte Differentiation and Hypertrophic Differentiation’, *Stem Cells International*, 2016. https://www.hindawi.com/journals/sci/2016/2470351/ (accessed May 11, 2019).
[80] J. Neves, P. Sousa-Victor, and H. Jasper, ‘Rejuvenating Strategies for Stem Cell-based Therapies in Aging’, *Cell Stem Cell*, vol. 20, no. 2, pp. 161–175, Feb. 2017, doi: 10.1016/j.stem.2017.01.008.
[81] A. W. James, ‘Review of Signaling Pathways Governing MSC Osteogenic and Adipogenic Differentiation’, *Scientifica*, vol. 2013, 2013, doi: 10.1155/2013/684736.
[82] M. Wang, Q. Yuan, and L. Xie, ‘Mesenchymal Stem Cell-Based Immunomodulation: Properties and Clinical Application’, *Stem Cells International*, Jun. 14, 2018. https://www.hindawi.com/journals/sci/2018/3057624/ (accessed Jun. 11, 2020).
[83] W. Deng, Q. Han, L. Liao, S. You, H. Deng, and R. C. H. Zhao, ‘Effects of Allogeneic Bone Marrow-Derived Mesenchymal Stem Cells on T and B Lymphocytes from BXSB Mice’, *DNA Cell Biol.*, vol. 24, no. 7, pp. 458–463, Jul. 2005, doi: 10.1089/dna.2005.24.458.
[84] O. K.-F. Ma and K. H. Chan, ‘Immunomodulation by mesenchymal stem cells: Interplay between mesenchymal stem cells and regulatory lymphocytes’, *World J. Stem Cells*, vol. 8, no. 9, pp. 268–278, Sep. 2016, doi: 10.4252/wjsc.v8.i9.268.
[85] C. J. Cunningham, E. Redondo-Castro, and S. M. Allan, ‘The therapeutic potential of the mesenchymal stem cell secretome in ischaemic stroke’, *J. Cereb. Blood Flow Metab.*, vol. 38, no. 8, pp. 1276–1292, Aug. 2018, doi: 10.1177/0271678X18776802.
[86] M. Wang, Q. Yuan, and L. Xie, ‘Mesenchymal Stem Cell-Based Immunomodulation: Properties and Clinical Application’, *Stem Cells International*, 2018. https://www.hindawi.com/journals/sci/2018/3057624/ (accessed Apr. 27, 2019).
[87] G. Ren *et al.*, ‘Mesenchymal Stem Cell-Mediated Immunosuppression Occurs via Concerted Action of Chemokines and Nitric Oxide’, *Cell Stem Cell*, vol. 2, no. 2, pp. 141–150, Feb. 2008, doi: 10.1016/j.stem.2007.11.014.
[88] K. Németh *et al.*, ‘Bone marrow stromal cells attenuate sepsis via prostaglandin E(2)-dependent reprogramming of host macrophages to increase their interleukin-10 production’, *Nat. Med.*, vol. 15, no. 1, pp. 42–49, Jan. 2009, doi: 10.1038/nm.1905.
[89] U. Kaundal, U. Bagai, and A. Rakha, ‘Immunomodulatory plasticity of mesenchymal stem cells: a potential key to successful solid organ transplantation’, *J. Transl. Med.*, vol. 16, Feb. 2018, doi: 10.1186/s12967-018-1403-0.
[90] M. Ullah, D. D. Liu, and A. S. Thakor, ‘Mesenchymal Stromal Cell Homing: Mechanisms and Strategies for Improvement’, *iScience*, vol. 15, pp. 421–438, May 2019, doi: 10.1016/j.isci.2019.05.004.

[91] A. De Becker and I. V. Riet, ‘Homing and migration of mesenchymal stromal cells: How to improve the efficacy of cell therapy?’, *World J. Stem Cells*, vol. 8, no. 3, pp. 73–87, Mar. 2016, doi: 10.4252/wjsc.v8.i3.73.
[92] A. Moreira, S. Kahlenberg, and P. Hornsby, ‘Therapeutic Potential of Mesenchymal Stem Cells for Diabetes’, *J. Mol. Endocrinol.*, vol. 59, no. 3, pp. R109–R120, Oct. 2017, doi: 10.1530/JME-17-0117.
[93] G. Sampogna, S. Y. Guraya, and A. Forgione, ‘Regenerative medicine: Historical roots and potential strategies in modern medicine’, *J. Microsc. Ultrastruct.*, vol. 3, no. 3, pp. 101–107, Sep. 2015, doi: 10.1016/j.jmau.2015.05.002.
[94] J. H. Lonner, S. Hershman, M. Mont, and P. A. Lotke, ‘Total Knee Arthroplasty in Patients 40 Years of Age and Younger With Osteoarthritis’, *Clin. Orthop. Relat. Res.*, vol. 380, p. 85, Nov. 2000.
[95] M. Blais, R. Parenteau-Bareil, S. Cadau, and F. Berthod, ‘Concise review: tissue-engineered skin and nerve regeneration in burn treatment’, *Stem Cells Transl. Med.*, vol. 2, no. 7, pp. 545–551, Jul. 2013, doi: 10.5966/sctm.2012-0181.
[96] X. Zhang *et al.*, ‘Experimental therapy for lung cancer: umbilical cord-derived mesenchymal stem cell-mediated interleukin-24 delivery’, *Curr. Cancer Drug Targets*, vol. 13, no. 1, pp. 92–102, Jan. 2013.
[97] E. Trushina and M. M. Mielke, ‘Recent advances in the application of metabolomics to Alzheimer’s Disease’, *Biochim. Biophys. Acta BBA - Mol. Basis Dis.*, vol. 1842, no. 8, pp. 1232–1239, Aug. 2014, doi: 10.1016/j.bbadis.2013.06.014.
[98] E. Björnson, J. Borén, and A. Mardinoglu, ‘Personalized Cardiovascular Disease Prediction and Treatment—A Review of Existing Strategies and Novel Systems Medicine Tools’, *Front. Physiol.*, vol. 7, 2016, doi: 10.3389/fphys.2016.00002.
[99] J. Archambault, A. Moreira, D. McDaniel, L. Winter, L. Sun, and P. Hornsby, ‘Therapeutic potential of mesenchymal stromal cells for hypoxic ischemic encephalopathy: A systematic review and meta-analysis of preclinical studies’, *PLOS ONE*, vol. 12, no. 12, p. e0189895, Dec. 2017, doi: 10.1371/journal.pone.0189895.
[100] R. E. B. Fitzsimmons, M. S. Mazurek, A. Soos, and C. A. Simmons, ‘Mesenchymal Stromal/Stem Cells in Regenerative Medicine and Tissue Engineering’, *Stem Cells International*, 2018. https://www.hindawi.com/journals/sci/2018/8031718/ (accessed May 01, 2019).
[101] V. K. Prasad *et al.*, ‘Efficacy and Safety of Ex Vivo Cultured Adult Human Mesenchymal Stem Cells (Prochymal™) in Pediatric Patients with Severe Refractory Acute Graft-Versus-Host Disease in a Compassionate Use Study’, *Biol. Blood Marrow Transplant.*, vol. 17, no. 4, pp. 534–541, Apr. 2011, doi: 10.1016/j.bbmt.2010.04.014.
[102] M. E. Bernardo and W. E. Fibbe, ‘Mesenchymal Stromal Cells: Sensors and Switchers of Inflammation’, *Cell Stem Cell*, vol. 13, no. 4, pp. 392–402, Oct. 2013, doi: 10.1016/j.stem.2013.09.006.
[103] Y. Gu *et al.*, ‘Changes in mesenchymal stem cells following long-term culture in vitro’, *Mol. Med. Rep.*, vol. 13, no. 6, pp. 5207–5215, Jun. 2016, doi: 10.3892/mmr.2016.5169.
[104] T. M. Liu, M. Martina, D. W. Hutmacher, J. H. P. Hui, E. H. Lee, and B. Lim, ‘Identification of common pathways mediating differentiation of bone marrow- and adipose tissue-derived human mesenchymal stem cells into three mesenchymal lineages’, *Stem Cells Dayt. Ohio*, vol. 25, no. 3, pp. 750–760, Mar. 2007, doi: 10.1634/stemcells.2006-0394.
[105] J. Valencia *et al.*, ‘Comparative analysis of the immunomodulatory capacities of human bone marrow- and adipose tissue-derived mesenchymal stromal cells from the same

donor', *Cytotherapy*, vol. 18, no. 10, pp. 1297–1311, 2016, doi: 10.1016/j.jcyt.2016.07.006.
[106] E. Ivanova-Todorova *et al.*, 'Adipose tissue-derived mesenchymal stem cells are more potent suppressors of dendritic cells differentiation compared to bone marrow-derived mesenchymal stem cells', *Immunol. Lett.*, vol. 126, no. 1–2, pp. 37–42, Sep. 2009, doi: 10.1016/j.imlet.2009.07.010.
[107] B. Blanco *et al.*, 'Immunomodulatory effects of bone marrow versus adipose tissue-derived mesenchymal stromal cells on NK cells: implications in the transplantation setting', *Eur. J. Haematol.*, vol. 97, no. 6, pp. 528–537, Dec. 2016, doi: 10.1111/ejh.12765.
[108] B. Lukomska, L. Stanaszek, E. Zuba-Surma, P. Legosz, S. Sarzynska, and K. Drela, 'Challenges and Controversies in Human Mesenchymal Stem Cell Therapy', *Stem Cells International*, 2019. https://www.hindawi.com/journals/sci/2019/9628536/ (accessed Jun. 24, 2019).
[109] R. A. Rose *et al.*, 'Bone marrow-derived mesenchymal stromal cells express cardiac-specific markers, retain the stromal phenotype, and do not become functional cardiomyocytes in vitro', *Stem Cells Dayt. Ohio*, vol. 26, no. 11, pp. 2884–2892, Nov. 2008, doi: 10.1634/stemcells.2008-0329.
[110] H. Qian *et al.*, 'Bone marrow mesenchymal stem cells ameliorate rat acute renal failure by differentiation into renal tubular epithelial-like cells', *Int. J. Mol. Med.*, vol. 22, no. 3, pp. 325–332, Sep. 2008.
[111] K.-A. Cho *et al.*, 'Mesenchymal stem cells showed the highest potential for the regeneration of injured liver tissue compared with other subpopulations of the bone marrow', *Cell Biol. Int.*, vol. 33, no. 7, pp. 772–777, Jul. 2009, doi: 10.1016/j.cellbi.2009.04.023.
[112] B. P. Sinder *et al.*, 'Engraftment of skeletal progenitor cells by bone-directed transplantation improves osteogenesis imperfecta murine bone phenotype', *STEM CELLS*, vol. 38, no. 4, pp. 530–541, 2020, doi: 10.1002/stem.3133.
[113] R. Shammaa, A. E.-H. El-Kadiry, J. Abusarah, and M. Rafei, 'Mesenchymal Stem Cells Beyond Regenerative Medicine', *Front. Cell Dev. Biol.*, vol. 8, Feb. 2020, doi: 10.3389/fcell.2020.00072.
[114] F. Gao *et al.*, 'Mesenchymal stem cells and immunomodulation: current status and future prospects', *Cell Death Dis.*, vol. 7, no. 1, p. e2062, Jan. 2016, doi: 10.1038/cddis.2015.327.
[115] J. Burke, M. Hunter, R. Kolhe, C. Isales, M. Hamrick, and S. Fulzele, 'Therapeutic potential of mesenchymal stem cell based therapy for osteoarthritis', *Clin. Transl. Med.*, vol. 5, Aug. 2016, doi: 10.1186/s40169-016-0112-7.
[116] H. Ibraheim, C. Giacomini, Z. Kassam, F. Dazzi, and N. Powell, 'Advances in mesenchymal stromal cell therapy in the management of Crohn's disease', *Expert Rev. Gastroenterol. Hepatol.*, vol. 12, no. 2, pp. 141–153, Feb. 2018, doi: 10.1080/17474124.2018.1393332.
[117] V. A. Solarte *et al.*, 'Function and Therapeutic Potential of Mesenchymal Stem Cells and Their Acellular Derivatives on Non-Healing Chronic Skin Ulcers', *J. Stem Cell Res. Ther.*, vol. 08, no. 04, 2018, doi: 10.4172/2157-7633.1000423.
[118] H. R. Hofer and R. S. Tuan, 'Secreted trophic factors of mesenchymal stem cells support neurovascular and musculoskeletal therapies', *Stem Cell Res. Ther.*, vol. 7, no. 1, p. 131, Sep. 2016, doi: 10.1186/s13287-016-0394-0.
[119] S. Öztürk, A. E. Elçin, and Y. M. Elçin, 'Mesenchymal Stem Cells for Coronavirus (COVID-19)-Induced Pneumonia: Revisiting the Paracrine Hypothesis with New

Hopes?', *Aging Dis.*, vol. 11, no. 3, pp. 477–479, Apr. 2020, doi: 10.14336/AD.2020.0403.
[120] R. Usategui-Martín, K. Puertas-Neyra, M.-T. García-Gutiérrez, M. Fuentes, J. C. Pastor, and I. Fernandez-Bueno, 'Human Mesenchymal Stem Cell Secretome Exhibits a Neuroprotective Effect over In Vitro Retinal Photoreceptor Degeneration', *Mol. Ther. Methods Clin. Dev.*, vol. 17, pp. 1155–1166, May 2020, doi: 10.1016/j.omtm.2020.05.003.
[121] Z. Zhou, L. Wang, H. Zhang, H. Liu, Y. Cui, and H. Nie, 'Participation of Mesenchymal Stem Cells in Acute Lung Injury/Acute Respiratory Distress Syndrome: Paracrine Effects and Transplantation', *Sci. Adv. Mater.*, vol. 12, no. 1, pp. 15–26, Jan. 2020, doi: 10.1166/sam.2020.3728.
[122] S. Maacha *et al.*, 'Paracrine Mechanisms of Mesenchymal Stromal Cells in Angiogenesis', *Stem Cells International*, Mar. 09, 2020. https://www.hindawi.com/journals/sci/2020/4356359/ (accessed Jun. 14, 2020).
[123] C. De Bari, F. Dell'Accio, P. Tylzanowski, and F. P. Luyten, 'Multipotent mesenchymal stem cells from adult human synovial membrane', *Arthritis Rheum.*, vol. 44, no. 8, pp. 1928–1942, Aug. 2001, doi: 10.1002/1529-0131(200108)44:8<1928::AID-ART331>3.0.CO;2-P.
[124] F. Bortolotti *et al.*, 'In Vivo Therapeutic Potential of Mesenchymal Stromal Cells Depends on the Source and the Isolation Procedure', *Stem Cell Rep.*, vol. 4, no. 3, pp. 332–339, Feb. 2015, doi: 10.1016/j.stemcr.2015.01.001.
[125] V. Tisato, K. Naresh, J. Girdlestone, C. Navarrete, and F. Dazzi, 'Mesenchymal stem cells of cord blood origin are effective at preventing but not treating graft-versus-host disease', *Leukemia*, vol. 21, no. 9, pp. 1992–1999, Sep. 2007, doi: 10.1038/sj.leu.2404847.
[126] D. Polchert *et al.*, 'IFN-gamma activation of mesenchymal stem cells for treatment and prevention of graft versus host disease', *Eur. J. Immunol.*, vol. 38, no. 6, pp. 1745–1755, Jun. 2008, doi: 10.1002/eji.200738129.
[127] K. Le Blanc *et al.*, 'Mesenchymal stem cells for treatment of steroid-resistant, severe, acute graft-versus-host disease: a phase II study', *Lancet Lond. Engl.*, vol. 371, no. 9624, pp. 1579–1586, May 2008, doi: 10.1016/S0140-6736(08)60690-X.
[128] W. D. Lee, D. Mukha, E. Aizenshtein, and T. Shlomi, 'Spatial-fluxomics provides a subcellular-compartmentalized view of reductive glutamine metabolism in cancer cells', *Nat. Commun.*, vol. 10, no. 1, p. 1351, 22 2019, doi: 10.1038/s41467-019-09352-1.
[129] A. Singh, A. Singh, and D. Sen, 'Mesenchymal stem cells in cardiac regeneration: a detailed progress report of the last 6 years (2010-2015)', *Stem Cell Res. Ther.*, vol. 7, no. 1, p. 82, Jun. 2016, doi: 10.1186/s13287-016-0341-0.
[130] M. E. Bernardo *et al.*, 'Human bone marrow derived mesenchymal stem cells do not undergo transformation after long-term in vitro culture and do not exhibit telomere maintenance mechanisms', *Cancer Res.*, vol. 67, no. 19, pp. 9142–9149, Oct. 2007, doi: 10.1158/0008-5472.CAN-06-4690.
[131] V. Turinetto, E. Vitale, and C. Giachino, 'Senescence in Human Mesenchymal Stem Cells: Functional Changes and Implications in Stem Cell-Based Therapy', *Int. J. Mol. Sci.*, vol. 17, no. 7, p. 1164, Jul. 2016, doi: 10.3390/ijms17071164.
[132] L. Sensebé, 'Clinical grade production of mesenchymal stem cells', *Biomed. Mater. Eng.*, vol. 18, no. 1 Suppl, pp. S3-10, 2008.
[133] R. S. Waterman, S. L. Tomchuck, S. L. Henkle, and A. M. Betancourt, 'A New Mesenchymal Stem Cell (MSC) Paradigm: Polarization into a Pro-Inflammatory MSC1

or an Immunosuppressive MSC2 Phenotype', *PLoS ONE*, vol. 5, no. 4, Apr. 2010, doi: 10.1371/journal.pone.0010088.
[134] Q. Li, Z. Gao, Y. Chen, and M.-X. Guan, 'The role of mitochondria in osteogenic, adipogenic and chondrogenic differentiation of mesenchymal stem cells', *Protein Cell*, vol. 8, no. 6, pp. 439–445, Jun. 2017, doi: 10.1007/s13238-017-0385-7.
[135] F. Tögel, Z. Hu, K. Weiss, J. Isaac, C. Lange, and C. Westenfelder, 'Administered mesenchymal stem cells protect against ischemic acute renal failure through differentiation-independent mechanisms', *Am. J. Physiol. Renal Physiol.*, vol. 289, no. 1, pp. F31-42, Jul. 2005, doi: 10.1152/ajprenal.00007.2005.
[136] F. dos Santos, P. Z. Andrade, J. S. Boura, M. M. Abecasis, C. L. da Silva, and J. M. S. Cabral, 'Ex vivo expansion of human mesenchymal stem cells: A more effective cell proliferation kinetics and metabolism under hypoxia', *J. Cell. Physiol.*, vol. 223, no. 1, pp. 27–35, Apr. 2010, doi: 10.1002/jcp.21987.
[137] J. C. Estrada *et al.*, 'Culture of human mesenchymal stem cells at low oxygen tension improves growth and genetic stability by activating glycolysis', *Cell Death Differ.*, vol. 19, no. 5, pp. 743–755, May 2012, doi: 10.1038/cdd.2011.172.
[138] D. Liu *et al.*, 'Activation of multiple signaling pathways during the differentiation of mesenchymal stem cells cultured in a silicon nanowire microenvironment', *Nanomedicine Nanotechnol. Biol. Med.*, vol. 10, no. 6, pp. 1153–1163, Aug. 2014, doi: 10.1016/j.nano.2014.02.003.
[139] J. M. Gaspar and L. A. Velloso, 'Hypoxia Inducible Factor as a Central Regulator of Metabolism – Implications for the Development of Obesity', *Front. Neurosci.*, vol. 12, 2018, doi: 10.3389/fnins.2018.00813.
[140] L. C. Shum, N. S. White, B. N. Mills, K. L. de Mesy Bentley, and R. A. Eliseev, 'Energy Metabolism in Mesenchymal Stem Cells During Osteogenic Differentiation', *Stem Cells Dev.*, vol. 25, no. 2, pp. 114–122, Jan. 2016, doi: 10.1089/scd.2015.0193.
[141] B. H. Shares, M. Busch, N. White, L. Shum, and R. A. Eliseev, 'Active mitochondria support osteogenic differentiation by stimulating β-catenin acetylation', *J. Biol. Chem.*, vol. 293, no. 41, pp. 16019–16027, 12 2018, doi: 10.1074/jbc.RA118.004102.
[142] K. Smolková and P. Ježek, 'The Role of Mitochondrial NADPH-Dependent Isocitrate Dehydrogenase in Cancer Cells', *International Journal of Cell Biology*, 2012. https://www.hindawi.com/journals/ijcb/2012/273947/abs/ (accessed May 16, 2019).
[143] Forrester Steven J., Kikuchi Daniel S., Hernandes Marina S., Xu Qian, and Griendling Kathy K., 'Reactive Oxygen Species in Metabolic and Inflammatory Signaling', *Circ. Res.*, vol. 122, no. 6, pp. 877–902, Mar. 2018, doi: 10.1161/CIRCRESAHA.117.311401.
[144] L. A. Mylotte *et al.*, 'Metabolic Flexibility Permits Mesenchymal Stem Cell Survival in an Ischemic Environment', *STEM CELLS*, vol. 26, no. 5, pp. 1325–1336, 2008, doi: 10.1634/stemcells.2007-1072.
[145] H. Zhu, A. Sun, Y. Zou, and J. Ge, 'Inducible metabolic adaptation promotes mesenchymal stem cell therapy for ischemia: a hypoxia-induced and glycogen-based energy prestorage strategy', *Arterioscler. Thromb. Vasc. Biol.*, vol. 34, no. 4, pp. 870–876, Apr. 2014, doi: 10.1161/ATVBAHA.114.303194.
[146] X. Yuan, T. M. Logan, and T. Ma, 'Metabolism in Human Mesenchymal Stromal Cells: A Missing Link Between hMSC Biomanufacturing and Therapy?', *Front. Immunol.*, vol. 10, 2019, doi: 10.3389/fimmu.2019.00977.
[147] A. B. Bloom and M. H. Zaman, 'Influence of the microenvironment on cell fate determination and migration', *Physiol. Genomics*, vol. 46, no. 9, pp. 309–314, May 2014, doi: 10.1152/physiolgenomics.00170.2013.

[148] N. Muñoz, J. Kim, Y. Liu, T. M. Logan, and T. Ma, 'Gas chromatography–mass spectrometry analysis of human mesenchymal stem cell metabolism during proliferation and osteogenic differentiation under different oxygen tensions', *J. Biotechnol.*, vol. 169, pp. 95–102, Jan. 2014, doi: 10.1016/j.jbiotec.2013.11.010.
[149] L. Li, X. Chen, W. E. Wang, and C. Zeng, 'How to Improve the Survival of Transplanted Mesenchymal Stem Cell in Ischemic Heart?', *Stem Cells Int.*, vol. 2016, 2016, doi: 10.1155/2016/9682757.
[150] M. Takarada-Iemata, T. Takarada, Y. Nakamura, E. Nakatani, O. Hori, and Y. Yoneda, 'Glutamate preferentially suppresses osteoblastogenesis than adipogenesis through the cystine/glutamate antiporter in mesenchymal stem cells', *J. Cell. Physiol.*, vol. 226, no. 3, pp. 652–665, 2011, doi: 10.1002/jcp.22390.
[151] I. Barbagallo *et al.*, 'Overexpression of heme oxygenase-1 increases human osteoblast stem cell differentiation', *J. Bone Miner. Metab.*, vol. 28, no. 3, pp. 276–288, May 2010, doi: 10.1007/s00774-009-0134-y.
[152] J. A. Araujo, M. Zhang, and F. Yin, 'Heme Oxygenase-1, Oxidation, Inflammation, and Atherosclerosis', *Front. Pharmacol.*, vol. 3, 2012, doi: 10.3389/fphar.2012.00119.
[153] M. François, I. B. Copland, S. Yuan, R. Romieu-Mourez, E. K. Waller, and J. Galipeau, 'Cryopreserved mesenchymal stromal cells display impaired immunosuppressive properties as a result of heat-shock response and impaired interferon-γ licensing', *Cytotherapy*, vol. 14, no. 2, pp. 147–152, Feb. 2012, doi: 10.3109/14653249.2011.623691.
[154] X. Xu *et al.*, 'Efficient homology-directed gene editing by CRISPR/Cas9 in human stem and primary cells using tube electroporation', *Sci. Rep.*, vol. 8, no. 1, Art. no. 1, Aug. 2018, doi: 10.1038/s41598-018-30227-w.
[155] X. Wu, Z.-D. Cai, L.-M. Lou, and Z.-R. Chen, 'The effects of inhibiting hedgehog signaling pathways by using specific antagonist cyclopamine on the chondrogenic differentiation of mesenchymal stem cells', *Int. J. Mol. Sci.*, vol. 14, no. 3, pp. 5966–5977, Mar. 2013, doi: 10.3390/ijms14035966.
[156] Q. Deng *et al.*, 'Activation of hedgehog signaling in mesenchymal stem cells induces cartilage and bone tumor formation via Wnt/β-Catenin', *eLife*, vol. 8, p. e50208, Sep. 2019, doi: 10.7554/eLife.50208.
[157] C. B. Clish, 'Metabolomics: an emerging but powerful tool for precision medicine', *Cold Spring Harb. Mol. Case Stud.*, vol. 1, no. 1, Oct. 2015, doi: 10.1101/mcs.a000588.
[158] 'History of Metabolomics', *News-Medical.net*, Mar. 08, 2017. https://www.news-medical.net/life-sciences/History-of-Metabolomics.aspx (accessed Jul. 15, 2020).
[159] N. L. Kuehnbaum and P. Britz-McKibbin, 'New Advances in Separation Science for Metabolomics: Resolving Chemical Diversity in a Post-Genomic Era', *Chem. Rev.*, vol. 113, no. 4, pp. 2437–2468, Apr. 2013, doi: 10.1021/cr300484s.
[160] O. Fiehn, 'Combining Genomics, Metabolome Analysis, and Biochemical Modelling to Understand Metabolic Networks', *Comp. Funct. Genomics*, vol. 2, no. 3, pp. 155–168, Jun. 2001, doi: 10.1002/cfg.82.
[161] 'What is transcriptomics?', *PHG Foundation*. https://www.phgfoundation.org/blog/what-is-transcriptomics (accessed Jul. 16, 2020).
[162] Z. Wang, M. Gerstein, and M. Snyder, 'RNA-Seq: a revolutionary tool for transcriptomics', *Nat. Rev. Genet.*, vol. 10, no. 1, Art. no. 1, Jan. 2009, doi: 10.1038/nrg2484.
[163] G. Piétu *et al.*, 'The Genexpress IMAGE knowledge base of the human brain transcriptome: a prototype integrated resource for functional and computational genomics', *Genome Res.*, vol. 9, no. 2, pp. 195–209, Feb. 1999.

[164] E. A. Milward, A. Shahandeh, M. Heidari, D. M. Johnstone, N. Daneshi, and H. Hondermarck, 'Transcriptomics', in *Encyclopedia of Cell Biology*, R. A. Bradshaw and P. D. Stahl, Eds. Waltham: Academic Press, 2016, pp. 160–165. doi: 10.1016/B978-0-12-394447-4.40029-5.
[165] F. Vafaee, H. Dashti, and H. Alinejad-Rokny, 'Transcriptomic Data Normalization', in *Encyclopedia of Bioinformatics and Computational Biology*, S. Ranganathan, M. Gribskov, K. Nakai, and C. Schönbach, Eds. Oxford: Academic Press, 2019, pp. 364–371. doi: 10.1016/B978-0-12-809633-8.20209-4.
[166] G. A. N. Gowda and D. Djukovic, 'Overview of Mass Spectrometry-Based Metabolomics: Opportunities and Challenges', *Methods Mol. Biol. Clifton NJ*, vol. 1198, pp. 3–12, 2014, doi: 10.1007/978-1-4939-1258-2_1.
[167] B. M. Kadakkuzha, X. Liu, S. Swarnkar, and Y. Chen, 'Chapter 18 - Genomic and Proteomic Mechanisms and Models in Toxicity and Safety Evaluation of Nutraceuticals', in *Nutraceuticals*, R. C. Gupta, Ed. Boston: Academic Press, 2016, pp. 227–237. doi: 10.1016/B978-0-12-802147-7.00018-8.
[168] H. Perreault and E. Lattová, '1.50 - Mass Spectrometry', in *Comprehensive Biotechnology (Second Edition)*, M. Moo-Young, Ed. Burlington: Academic Press, 2011, pp. 669–677. doi: 10.1016/B978-0-08-088504-9.00077-5.
[169] 'Mass Spectrometry :: Introduction, Principle of Mass Spectrometry, Components of Mass Spectrometer, Applications'. http://www.premierbiosoft.com/tech_notes/mass-spectrometry.html (accessed Jul. 14, 2020).
[170] 'NMR Spectroscopy'. https://www2.chemistry.msu.edu/faculty/reusch/VirtTxtJml/Spectrpy/nmr/nmr1.htm (accessed Jul. 14, 2020).
[171] A.-H. M. Emwas, 'The strengths and weaknesses of NMR spectroscopy and mass spectrometry with particular focus on metabolomics research', *Methods Mol. Biol. Clifton NJ*, vol. 1277, pp. 161–193, 2015, doi: 10.1007/978-1-4939-2377-9_13.
[172] C. Schaeffer-Reiss, 'A Brief Summary of the Different Types of Mass Spectrometers Used in Proteomics', in *Functional Proteomics: Methods and Protocols*, J. D. Thompson, M. Ueffing, and C. Schaeffer-Reiss, Eds. Totowa, NJ: Humana Press, 2008, pp. 3–16. doi: 10.1007/978-1-59745-398-1_1.
[173] D. J. Douglas, 'Linear quadrupoles in mass spectrometry', *Mass Spectrom. Rev.*, vol. 28, no. 6, pp. 937–960, 2009, doi: 10.1002/mas.20249.
[174] 'Untargeted metabolomics strategies – Challenges and Emerging Directions'. https://www.ncbi.nlm.nih.gov/pmc/articles/PMC5110944/ (accessed Jul. 17, 2020).
[175] null Loboda, null Krutchinsky, null Bromirski, null Ens, and null Standing, 'A tandem quadrupole/time-of-flight mass spectrometer with a matrix-assisted laser desorption/ionization source: design and performance', *Rapid Commun. Mass Spectrom. RCM*, vol. 14, no. 12, pp. 1047–1057, 2000, doi: 10.1002/1097-0231(20000630)14:12<1047::AID-RCM990>3.0.CO;2-E.
[176] 'Differences between HPLC and UPLC : Pharmaceutical Guidelines'. https://www.pharmaguideline.com/2018/04/differences-between-hplc-and-uplc.html#gsc.tab=0 (accessed Jul. 17, 2020).
[177] J. Abian, *JOURNAL OF MASS SPECTROMETRY J. Mass Spectrom. 34, 157È168 (1999) SPECIAL FEATURE: HISTORICAL The Coupling of Gas and Liquid Chromatography with Mass Spectrometry*¤.
[178] 'Bristol University - Gas Chromatography Mass Spectrometry (GC/MS)'. http://www.bris.ac.uk/nerclsmsf/techniques/gcms.html (accessed Jul. 17, 2020).

[179] ‘Gas chromatography’, *HiQ*. http://hiq.linde-gas.com/en/analytical_methods/gas_chromatography/index.html (accessed Jul. 17, 2020).
[180] ‘Liquid chromatography’, *HiQ*. http://hiq.linde-gas.com/en/analytical_methods/liquid_chromatography/index.html (accessed Jul. 17, 2020).
[181] C. Blasco and Y. Picó, ‘Chapter 14 - Liquid chromatography-mass spectrometry’, in *Food Toxicants Analysis*, Y. Picó, Ed. Amsterdam: Elsevier, 2007, pp. 509–559. doi: 10.1016/B978-044452843-8/50015-8.
[182] ‘Mass spectrometry (LC-MS)’, *HiQ*. http://hiq.linde-gas.com/en/analytical_methods/liquid_chromatography/mass_spectrometry.html (accessed Jul. 20, 2020).
[183] H.-R. Lee, S. Kochhar, and S.-M. Shim, ‘Comparison of Electrospray Ionization and Atmospheric Chemical Ionization Coupled with the Liquid Chromatography-Tandem Mass Spectrometry for the Analysis of Cholesteryl Esters’, *International Journal of Analytical Chemistry*, Mar. 19, 2015. https://www.hindawi.com/journals/ijac/2015/650927/ (accessed Jul. 20, 2020).
[184] ‘Bristol University - High Performance Liquid Chromatography Mass Spectrometry (HPLC/MS)’. http://www.bris.ac.uk/nerclsmsf/techniques/hplcms.html (accessed Jul. 20, 2020).
[185] B. Pang, Y. Zhu, L. Lu, F. Gu, and H. Chen, ‘The Applications and Features of Liquid Chromatography-Mass Spectrometry in the Analysis of Traditional Chinese Medicine’, *Evidence-Based Complementary and Alternative Medicine*, Nov. 10, 2016. https://www.hindawi.com/journals/ecam/2016/3837270/ (accessed Jul. 20, 2020).
[186] E. Gorrochategui, J. Jaumot, S. Lacorte, and R. Tauler, ‘Data analysis strategies for targeted and untargeted LC-MS metabolomic studies: Overview and workflow’, *TrAC Trends Anal. Chem.*, vol. 82, Jul. 2016, doi: 10.1016/j.trac.2016.07.004.
[187] ‘TargetLynx : Waters’. https://www.waters.com/waters/en_IS/TargetLynx-/nav.htm?cid=513791&locale=en_IS (accessed Jul. 20, 2020).
[188] C. A. Smith, E. J. Want, G. O’Maille, R. Abagyan, and G. Siuzdak, ‘XCMS: Processing Mass Spectrometry Data for Metabolite Profiling Using Nonlinear Peak Alignment, Matching, and Identification’, *Anal. Chem.*, vol. 78, no. 3, pp. 779–787, Feb. 2006, doi: 10.1021/ac051437y.
[189] H. P. Benton, E. J. Want, and T. M. D. Ebbels, ‘Correction of mass calibration gaps in liquid chromatography-mass spectrometry metabolomics data’, *Bioinforma. Oxf. Engl.*, vol. 26, no. 19, pp. 2488–2489, Oct. 2010, doi: 10.1093/bioinformatics/btq441.
[190] R. Tautenhahn, C. Böttcher, and S. Neumann, ‘Highly sensitive feature detection for high resolution LC/MS’, *BMC Bioinformatics*, vol. 9, no. 1, p. 504, Nov. 2008, doi: 10.1186/1471-2105-9-504.
[191] ‘RNA-seq: Basics, Applications and Protocol’, *Genomics Research from Technology Networks*. https://www.technologynetworks.com/genomics/articles/rna-seq-basics-applications-and-protocol-299461 (accessed Jul. 21, 2020).
[192] D. Singh, P. K. Singh, S. Chaudhary, K. Mehla, and S. Kumar, ‘Chapter Three - Exome Sequencing and Advances in Crop Improvement’, in *Advances in Genetics*, vol. 79, T. Friedmann, J. C. Dunlap, and S. F. Goodwin, Eds. Academic Press, 2012, pp. 87–121. doi: 10.1016/B978-0-12-394395-8.00003-7.
[193] ‘StatQuest: A gentle introduction to RNA-seq - YouTube’. https://www.youtube.com/watch?v=tlf6wYJrwKY (accessed Jul. 21, 2020).
[194] ‘Chapter 20209 - Transcriptomic Data Normalization | Elsevier Enhanced Reader’. https://reader.elsevier.com/reader/sd/pii/B9780128096338202094?token=871446916B

191A74574AF5BC7465DC605B7257C37738995B269B4235F3E2151C53965D4D63F70ADEEB2F78EF7876B916 (accessed Jul. 16, 2020).
[195] A. Bordbar, J. M. Monk, Z. A. King, and B. O. Palsson, 'Constraint-based models predict metabolic and associated cellular functions', *Nat. Rev. Genet.*, vol. 15, no. 2, Art. no. 2, Feb. 2014, doi: 10.1038/nrg3643.
[196] C. Gu, G. B. Kim, W. J. Kim, H. U. Kim, and S. Y. Lee, 'Current status and applications of genome-scale metabolic models', *Genome Biol.*, vol. 20, no. 1, p. 121, Jun. 2019, doi: 10.1186/s13059-019-1730-3.
[197] H. V. Westerhoff and B. O. Palsson, 'The evolution of molecular biology into systems biology', *Nat. Biotechnol.*, vol. 22, no. 10, pp. 1249–1252, Oct. 2004, doi: 10.1038/nbt1020.
[198] C. S. Henry, M. DeJongh, A. A. Best, P. M. Frybarger, B. Linsay, and R. L. Stevens, 'High-throughput generation, optimization and analysis of genome-scale metabolic models', *Nat. Biotechnol.*, vol. 28, no. 9, pp. 977–982, Sep. 2010, doi: 10.1038/nbt.1672.
[199] J. L. Reed and B. Ø. Palsson, 'Thirteen Years of Building Constraint-Based In Silico Models of Escherichia coli', *J. Bacteriol.*, vol. 185, no. 9, pp. 2692–2699, May 2003, doi: 10.1128/JB.185.9.2692-2699.2003.
[200] J. T. Yurkovich and B. O. Palsson, 'Solving Puzzles With Missing Pieces: The Power of Systems Biology', *Proc. IEEE*, vol. 104, no. 1, pp. 2–7, Jan. 2016, doi: 10.1109/JPROC.2015.2505338.
[201] E. Brunk *et al.*, 'Recon3D enables a three-dimensional view of gene variation in human metabolism', *Nat. Biotechnol.*, vol. 36, no. 3, pp. 272–281, Mar. 2018, doi: 10.1038/nbt.4072.
[202] M. A. Oberhardt, B. Ø. Palsson, and J. A. Papin, 'Applications of genome-scale metabolic reconstructions', *Mol. Syst. Biol.*, vol. 5, no. 1, p. 320, Jan. 2009, doi: 10.1038/msb.2009.77.
[203] J. D. Orth, I. Thiele, and B. Ø. Palsson, 'What is flux balance analysis?', *Nat. Biotechnol.*, vol. 28, no. 3, pp. 245–248, Mar. 2010, doi: 10.1038/nbt.1614.
[204] I. Thiele *et al.*, 'A community-driven global reconstruction of human metabolism', *Nat. Biotechnol.*, vol. 31, no. 5, pp. 419–425, May 2013, doi: 10.1038/nbt.2488.
[205] N. A. of S. Medicine Engineering, and, D. on E. and L. Studies, B. on C. S. and Technology, and C. S. Roundtable, *The Chemistry of Microbiomes: Proceedings of a Seminar Series*. National Academies Press, 2017.
[206] D. A. Cuevas, J. Edirisinghe, C. S. Henry, R. Overbeek, T. G. O'Connell, and R. A. Edwards, 'From DNA to FBA: How to Build Your Own Genome-Scale Metabolic Model', *Front. Microbiol.*, vol. 7, 2016, doi: 10.3389/fmicb.2016.00907.
[207] N. C. Duarte *et al.*, 'Global reconstruction of the human metabolic network based on genomic and bibliomic data', *Proc. Natl. Acad. Sci. U. S. A.*, vol. 104, no. 6, pp. 1777–1782, Feb. 2007, doi: 10.1073/pnas.0610772104.
[208] O. Rolfsson, B. Ø. Palsson, and I. Thiele, 'The human metabolic reconstruction Recon 1 directs hypotheses of novel human metabolic functions', *BMC Syst. Biol.*, vol. 5, p. 155, Oct. 2011, doi: 10.1186/1752-0509-5-155.
[209] G. Paglia *et al.*, 'Metabolic fate of adenine in red blood cells during storage in SAGM solution', *Transfusion (Paris)*, vol. 56, no. 10, pp. 2538–2547, Oct. 2016, doi: 10.1111/trf.13740.
[210] D. B. Kell and R. Goodacre, 'Metabolomics and systems pharmacology: why and how to model the human metabolic network for drug discovery', *Drug Discov. Today*, vol. 19, no. 2, pp. 171–182, Feb. 2014, doi: 10.1016/j.drudis.2013.07.014.

[211] T. Shlomi, M. N. Cabili, and E. Ruppin, ‘Predicting metabolic biomarkers of human inborn errors of metabolism’, *Mol. Syst. Biol.*, vol. 5, p. 263, Apr. 2009, doi: 10.1038/msb.2009.22.
[212] S. Sahoo, H. S. Haraldsdóttir, R. M. T. Fleming, and I. Thiele, ‘Modeling the effects of commonly used drugs on human metabolism’, *FEBS J.*, vol. 282, no. 2, pp. 297–317, Jan. 2015, doi: 10.1111/febs.13128.
[213] S. Sahoo, L. Franzson, J. J. Jonsson, and I. Thiele, ‘A compendium of inborn errors of metabolism mapped onto the human metabolic network’, *Mol. Biosyst.*, vol. 8, no. 10, pp. 2545–2558, Oct. 2012, doi: 10.1039/c2mb25075f.
[214] R. Mandal, D. Chamot, and D. S. Wishart, ‘The role of the Human Metabolome Database in inborn errors of metabolism’, *J. Inherit. Metab. Dis.*, vol. 41, no. 3, pp. 329–336, May 2018, doi: 10.1007/s10545-018-0137-8.
[215] M. Mussap, M. Zaffanello, and V. Fanos, ‘Metabolomics: a challenge for detecting and monitoring inborn errors of metabolism’, *Ann. Transl. Med.*, vol. 6, no. 17, p. 338, Sep. 2018, doi: 10.21037/atm.2018.09.18.
[216] H. Munir and H. M. McGettrick, ‘Mesenchymal Stem Cell Therapy for Autoimmune Disease: Risks and Rewards’, *Stem Cells Dev.*, vol. 24, no. 18, pp. 2091–2100, Sep. 2015, doi: 10.1089/scd.2015.0008.
[217] S. A. Becker and B. O. Palsson, ‘Context-Specific Metabolic Networks Are Consistent with Experiments’, *PLoS Comput. Biol.*, vol. 4, no. 5, May 2008, doi: 10.1371/journal.pcbi.1000082.
[218] H. Zur, E. Ruppin, and T. Shlomi, ‘iMAT: an integrative metabolic analysis tool’, *Bioinforma. Oxf. Engl.*, vol. 26, no. 24, pp. 3140–3142, Dec. 2010, doi: 10.1093/bioinformatics/btq602.
[219] ‘Model building algorithm (MBA) - Constraint-based analysis’. http://cobramethods.wikidot.com/mba (accessed Jun. 05, 2019).
[220] N. Vlassis, M. P. Pacheco, and T. Sauter, ‘Fast reconstruction of compact context-specific metabolic network models’, *PLoS Comput. Biol.*, vol. 10, no. 1, p. e1003424, Jan. 2014, doi: 10.1371/journal.pcbi.1003424.
[221] Y. Wang, J. A. Eddy, and N. D. Price, ‘Reconstruction of genome-scale metabolic models for 126 human tissues using mCADRE’, *BMC Syst. Biol.*, vol. 6, p. 153, Dec. 2012, doi: 10.1186/1752-0509-6-153.
[222] J. Neman, A. Hambrecht, C. Cadry, and R. Jandial, ‘Stem cell-mediated osteogenesis: therapeutic potential for bone tissue engineering’, *Biol. Targets Ther.*, vol. 6, pp. 47–57, 2012, doi: 10.2147/BTT.S22407.
[223] M. K. Aurich, R. M. T. Fleming, and I. Thiele, ‘MetaboTools: A Comprehensive Toolbox for Analysis of Genome-Scale Metabolic Models’, *Front. Physiol.*, vol. 7, 2016, doi: 10.3389/fphys.2016.00327.
[224] M. K. Aurich *et al.*, ‘Prediction of intracellular metabolic states from extracellular metabolomic data’, *Metabolomics Off. J. Metabolomic Soc.*, vol. 11, no. 3, pp. 603–619, 2015, doi: 10.1007/s11306-014-0721-3.
[225] A. von Bomhard, A. Elsässer, L. M. Ritschl, S. Schwarz, and N. Rotter, ‘Cryopreservation of Endothelial Cells in Various Cryoprotective Agents and Media - Vitrification versus Slow Freezing Methods’, *PloS One*, vol. 11, no. 2, p. e0149660, 2016, doi: 10.1371/journal.pone.0149660.
[226] E. Ahn, P. Kumar, D. Mukha, A. Tzur, and T. Shlomi, ‘Temporal fluxomics reveals oscillations in TCA cycle flux throughout the mammalian cell cycle’, *Mol. Syst. Biol.*, vol. 13, no. 11, p. 953, 06 2017, doi: 10.15252/msb.20177763.

[227] K. Yizhak, O. Gabay, H. Cohen, and E. Ruppin, ‘Model-based identification of drug targets that revert disrupted metabolism and its application to ageing’, *Nat. Commun.*, vol. 4, p. 2632, Oct. 2013, doi: 10.1038/ncomms3632.
[228] S. Stempler, K. Yizhak, and E. Ruppin, ‘Integrating Transcriptomics with Metabolic Modeling Predicts Biomarkers and Drug Targets for Alzheimer’s Disease’, *PLOS ONE*, vol. 9, no. 8, p. e105383, Aug. 2014, doi: 10.1371/journal.pone.0105383.
[229] B. W. M. Wone, J. M. Kinchen, E. R. Kaup, and B. Wone, ‘A procession of metabolic alterations accompanying muscle senescence in Manduca sexta’, *Sci. Rep.*, vol. 8, no. 1, p. 1006, Jan. 2018, doi: 10.1038/s41598-018-19630-5.
[230] L. Väremo, I. Nookaew, and J. Nielsen, ‘Novel insights into obesity and diabetes through genome-scale metabolic modeling’, *Front. Physiol.*, vol. 4, 2013, doi: 10.3389/fphys.2013.00092.
[231] C. Levian, E. Ruiz, and X. Yang, ‘The Pathogenesis of Obesity from a Genomic and Systems Biology Perspective’, *Yale J. Biol. Med.*, vol. 87, no. 2, pp. 113–126, Jun. 2014.
[232] B. V. Dougherty, T. J. Moutinho, and J. Papin, ‘Accelerating the Drug Development Pipeline with Genome-Scale Metabolic Network Reconstructions’, in *Systems Biology*, John Wiley & Sons, Ltd, 2017, pp. 139–162. doi: 10.1002/9783527696130.ch5.
[233] R. L. Chang, L. Xie, L. Xie, P. E. Bourne, and B. Ø. Palsson, ‘Drug Off-Target Effects Predicted Using Structural Analysis in the Context of a Metabolic Network Model’, *PLOS Comput. Biol.*, vol. 6, no. 9, p. e1000938, Sep. 2010, doi: 10.1371/journal.pcbi.1000938.
[234] J. A. Gomez, K. Höffner, and P. I. Barton, ‘DFBAlab: a fast and reliable MATLAB code for dynamic flux balance analysis’, *BMC Bioinformatics*, vol. 15, no. 1, p. 409, Dec. 2014, doi: 10.1186/s12859-014-0409-8.
[235] A. Bordbar *et al.*, ‘Identified metabolic signature for assessing red blood cell unit quality is associated with endothelial damage markers and clinical outcomes’, *Transfusion (Paris)*, vol. 56, no. 4, pp. 852–862, Apr. 2016, doi: 10.1111/trf.13460.
[236] H. Fouladiha, S.-A. Marashi, M. A. Shokrgozar, M. Farokhi, and A. Atashi, ‘Applications of a metabolic network model of mesenchymal stem cells for controlling cell proliferation and differentiation’, *Cytotechnology*, vol. 70, no. 1, pp. 331–338, Feb. 2018, doi: 10.1007/s10616-017-0148-6.
[237] O. Folger, L. Jerby, C. Frezza, E. Gottlieb, E. Ruppin, and T. Shlomi, ‘Predicting selective drug targets in cancer through metabolic networks’, *Mol. Syst. Biol.*, vol. 7, p. 501, Jun. 2011, doi: 10.1038/msb.2011.35.
[238] V. Raškevičius *et al.*, ‘Genome scale metabolic models as tools for drug design and personalized medicine’, *PLOS ONE*, vol. 13, no. 1, p. e0190636, Jan. 2018, doi: 10.1371/journal.pone.0190636.
[239] R. Agren, A. Mardinoglu, A. Asplund, C. Kampf, M. Uhlen, and J. Nielsen, ‘Identification of anticancer drugs for hepatocellular carcinoma through personalized genome-scale metabolic modeling’, *Mol. Syst. Biol.*, vol. 10, no. 3, Mar. 2014, doi: 10.1002/msb.145122.
[240] R. Levy and E. Borenstein, ‘Metabolic modeling of species interaction in the human microbiome elucidates community-level assembly rules’, *Proc. Natl. Acad. Sci.*, vol. 110, no. 31, pp. 12804–12809, Jul. 2013, doi: 10.1073/pnas.1300926110.
[241] M. S. Choudhery, M. Badowski, A. Muise, J. Pierce, and D. T. Harris, ‘Donor age negatively impacts adipose tissue-derived mesenchymal stem cell expansion and differentiation’, *J. Transl. Med.*, vol. 12, no. 1, p. 8, Jan. 2014, doi: 10.1186/1479-5876-12-8.

[242] P. Narbonne, 'The effect of age on stem cell function and utility for therapy', *Cell Med.*, vol. 10, Jun. 2018, doi: 10.1177/2155179018773756.
[243] R. Secunda, R. Vennila, A. M. Mohanashankar, M. Rajasundari, S. Jeswanth, and R. Surendran, 'Isolation, expansion and characterisation of mesenchymal stem cells from human bone marrow, adipose tissue, umbilical cord blood and matrix: a comparative study', *Cytotechnology*, vol. 67, no. 5, pp. 793–807, Oct. 2015, doi: 10.1007/s10616-014-9718-z.
[244] Y. Tachida *et al.*, 'Proteomic Comparison of the Secreted Factors of Mesenchymal Stem Cells from Bone Marrow, Adipose Tissue and Dental Pulp', *J. Proteomics Bioinform.*, Dec. 2015, doi: 10.4172/jpb.1000379.
[245] A. M. Billing *et al.*, 'Comprehensive transcriptomic and proteomic characterization of human mesenchymal stem cells reveals source specific cellular markers', *Sci. Rep.*, vol. 6, p. 21507, Feb. 2016, doi: 10.1038/srep21507.
[246] A. Bordbar, J. T. Yurkovich, G. Paglia, O. Rolfsson, Ó. E. Sigurjónsson, and B. O. Palsson, 'Elucidating dynamic metabolic physiology through network integration of quantitative time-course metabolomics', *Sci. Rep.*, vol. 7, no. 1, Art. no. 1, Apr. 2017, doi: 10.1038/srep46249.
[247] RStudio Team (2020), *RStudio: Integrated Development for R.* RStudio, PBC, Boston, MA. [Online]. Available: http://www.rstudio.com/.
[248] S. Wood and F. Scheipl, 'Package "gamm4": Generalized Additive Mixed Models using "mgcv" and "lme4"'. Apr. 03, 2020. [Online]. Available: https://cran.r-project.org/web/packages/gamm4/gamm4.pdf
[249] N. A. James and D. S. Matteson, 'ecp: An R Package for Nonparametric Multiple Change Point Analysis of Multivariate Data', *ArXiv13093295 Stat*, Nov. 2013, Accessed: Oct. 10, 2020. [Online]. Available: http://arxiv.org/abs/1309.3295
[250] P. Chomczynski, W. Wilfinger, A. Kennedy, M. Rymaszewski, and K. Mackey, 'RNAzol ® RT: a new single-step method for isolation of RNA', *Nat. Methods*, vol. 7, no. 12, Art. no. 12, Dec. 2010, doi: 10.1038/nmeth.f.315.
[251] 'RNAzol® RT R4533', *Sigma-Aldrich*. https://www.sigmaaldrich.com/catalog/product/sigma/r4533 (accessed Jan. 18, 2021).
[252] N. L. Bray, H. Pimentel, P. Melsted, and L. Pachter, 'Near-optimal probabilistic RNA-seq quantification', *Nat. Biotechnol.*, vol. 34, no. 5, Art. no. 5, May 2016, doi: 10.1038/nbt.3519.
[253] H. Pimentel, N. L. Bray, S. Puente, P. Melsted, and L. Pachter, 'Differential analysis of RNA-seq incorporating quantification uncertainty', *Nat. Methods*, vol. 14, no. 7, Art. no. 7, Jul. 2017, doi: 10.1038/nmeth.4324.
[254] C. Kuhl, R. Tautenhahn, C. Böttcher, T. R. Larson, and S. Neumann, 'CAMERA: An Integrated Strategy for Compound Spectra Extraction and Annotation of Liquid Chromatography/Mass Spectrometry Data Sets', *Anal. Chem.*, vol. 84, no. 1, pp. 283–289, Jan. 2012, doi: 10.1021/ac202450g.
[255] 'Mummichog'. https://shuzhao-li.github.io/mummichog.org/ (accessed Feb. 23, 2021).
[256] D. S. Wishart *et al.*, 'HMDB: the Human Metabolome Database', *Nucleic Acids Res.*, vol. 35, no. suppl_1, pp. D521–D526, Jan. 2007, doi: 10.1093/nar/gkl923.
[257] 'Pierce™ BCA Protein Assay Kit'. https://www.thermofisher.com/order/catalog/product/23225 (accessed Jan. 18, 2021).
[258] A. Athar *et al.*, 'ArrayExpress update – from bulk to single-cell expression data', *Nucleic Acids Res.*, vol. 47, no. D1, pp. D711–D715, Jan. 2019, doi: 10.1093/nar/gky964.

[259] L. Heirendt *et al.*, ‘Creation and analysis of biochemical constraint-based models using the COBRA Toolbox v.3.0’, *Nat. Protoc.*, vol. 14, no. 3, Art. no. 3, Mar. 2019, doi: 10.1038/s41596-018-0098-2.
[260] S. A. Becker and B. O. Palsson, ‘Context-Specific Metabolic Networks Are Consistent with Experiments’, *PLoS Comput. Biol.*, vol. 4, no. 5, p. e1000082, May 2008, doi: 10.1371/journal.pcbi.1000082.
[261] A. Ebrahim, J. A. Lerman, B. O. Palsson, and D. R. Hyduke, ‘COBRApy: COnstraints-Based Reconstruction and Analysis for Python.’, *BMC Syst. Biol.*, vol. 7, p. 74, Aug. 2013, doi: 10.1186/1752-0509-7-74.
[262] S. Gudmundsson and I. Thiele, ‘Computationally efficient flux variability analysis’, *BMC Bioinformatics*, vol. 11, no. 1, p. 489, Dec. 2010, doi: 10.1186/1471-2105-11-489.
[263] ‘How Agilent Seahorse XF Analyzers Work | Agilent’. https://www.agilent.com/en/products/cell-analysis/how-seahorse-xf-analyzers-work (accessed Jan. 13, 2021).
[264] C. Lieven *et al.*, *MEMOTE for standardized genome-scale metabolic model testing*, vol. 38. Nature Research, 2020. doi: 10.1038/s41587-020-0446-y.
[265] W. Wang *et al.*, ‘Enhancement of bone formation with a synthetic matrix containing bone morphogenetic protein-2 by the addition of calcium citrate’, *Knee Surg. Sports Traumatol. Arthrosc.*, vol. 21, no. 2, pp. 456–465, 2013, doi: 10.1007/s00167-012-1953-2.
[266] A. R. Irizarry *et al.*, ‘Defective enamel and bone development in sodium-dependent citrate transporter (NaCT) Slc13a5 deficient mice’, *PLoS ONE*, vol. 12, no. 4, Apr. 2017, doi: 10.1371/journal.pone.0175465.
[267] L. Cong *et al.*, ‘Multiplex genome engineering using CRISPR/Cas systems’, *Science*, vol. 339, no. 6121, pp. 819–823, Feb. 2013, doi: 10.1126/science.1231143.
[268] R. Jansen, J. D. A. van Embden, W. Gaastra, and L. M. Schouls, ‘Identification of genes that are associated with DNA repeats in prokaryotes’, *Mol. Microbiol.*, vol. 43, no. 6, pp. 1565–1575, Mar. 2002, doi: 10.1046/j.1365-2958.2002.02839.x.
[269] D. T.-B. Shih and T. Burnouf, ‘Preparation, quality criteria, and properties of human blood platelet lysate supplements for ex vivo stem cell expansion’, *New Biotechnol.*, vol. 32, no. 1, pp. 199–211, Jan. 2015, doi: 10.1016/j.nbt.2014.06.001.
[270] ‘A Challenging Future for Fetal Bovine Serum’, *BioProcess International*, Sep. 21, 2019. https://bioprocessintl.com/upstream-processing/biochemicals-raw-materials/challenging-future-for-fetal-bovine-serum/ (accessed Jan. 12, 2021).
[271] N. S. Alekos, M. C. Moorer, and R. C. Riddle, ‘Dual Effects of Lipid Metabolism on Osteoblast Function’, *Front. Endocrinol.*, vol. 11, Sep. 2020, doi: 10.3389/fendo.2020.578194.
[272] ‘XF Analyzers | Agilent’. https://www.agilent.com/en/product/cell-analysis/real-time-cell-metabolic-analysis/xf-analyzers (accessed Jan. 13, 2021).
[273] M. Wenes, P. Romero, and L. Zhang, ‘Chapter Five - Assessment of memory formation by metabolically engineered antigen-specific CD8 T cells’, in *Methods in Enzymology*, vol. 631, L. Galluzzi and N.-P. Rudqvist, Eds. Academic Press, 2020, pp. 77–90. doi: 10.1016/bs.mie.2019.10.021.
[274] Q. Wu *et al.*, ‘Organ-on-a-chip: recent breakthroughs and future prospects’, *Biomed. Eng. OnLine*, vol. 19, Feb. 2020, doi: 10.1186/s12938-020-0752-0.
[275] ‘Human Organs-on-Chips’, *Wyss Institute*, Aug. 05, 2017. https://wyss.harvard.edu/technology/human-organs-on-chips/ (accessed Jan. 13, 2021).

[276] J. Liu, J. Wen, Z. Zhang, H. Liu, and Y. Sun, ‘Voyage inside the cell: Microsystems and nanoengineering for intracellular measurement and manipulation’, *Microsyst. Nanoeng.*, vol. 1, no. 1, Art. no. 1, Sep. 2015, doi: 10.1038/micronano.2015.20.
[277] H. H. Chowdhury, ‘Differences in cytosolic glucose dynamics in astrocytes and adipocytes measured by FRET-based nanosensors’, *Biophys. Chem.*, vol. 261, p. 106377, Jun. 2020, doi: 10.1016/j.bpc.2020.106377.
[278] A. Alova *et al.*, ‘Prolonged oxygen depletion in microwounded cells of Chara corallina detected with novel oxygen nanosensors’, *J. Exp. Bot.*, vol. 71, no. 1, pp. 386–398, Jan. 2020, doi: 10.1093/jxb/erz433.
[279] L. A. Solchaga, K. J. Penick, and J. F. Welter, ‘Chondrogenic Differentiation of Bone Marrow-Derived Mesenchymal Stem Cells: Tips and Tricks’, *Methods Mol. Biol. Clifton NJ*, vol. 698, pp. 253–278, 2011, doi: 10.1007/978-1-60761-999-4_20.
[280] X. Guo *et al.*, ‘Cardiomyocyte differentiation of mesenchymal stem cells from bone marrow: new regulators and its implications’, *Stem Cell Res. Ther.*, vol. 9, Feb. 2018, doi: 10.1186/s13287-018-0773-9.
[281] B. Abd Emami *et al.*, ‘Mechanical and Chemical Predifferentiation of Mesenchymal Stem Cells Into Cardiomyocytes and Their Effectiveness on Acute Myocardial Infarction’, *Artif. Organs*, vol. 42, no. 6, pp. E114–E126, Jun. 2018, doi: 10.1111/aor.13091.
[282] A. Afshari, S. Shamdani, G. Uzan, S. Naserian, and N. Azarpira, ‘Different approaches for transformation of mesenchymal stem cells into hepatocyte-like cells’, *Stem Cell Res. Ther.*, vol. 11, no. 1, p. 54, Feb. 2020, doi: 10.1186/s13287-020-1555-8.
[283] A. Neve, A. Corrado, and F. P. Cantatore, ‘Osteoblast physiology in normal and pathological conditions’, *Cell Tissue Res.*, vol. 343, no. 2, pp. 289–302, Feb. 2011, doi: 10.1007/s00441-010-1086-1.

Paper I

- *Manuscript, in review at Bioengineering.*

Article

Using metabolomics and transcriptional changes to close in on metabolic stages during osteogenic differentiation of mesenchymal stromal cells

Thora Bjorg Sigmarsdottir[1], Sarah McGarrity[1,2], Adrian López García de Lomana[2], Snaevar Sigurðsson[5], James T. Yurkovich[3], Ottar Rolfsson[2], Olafur Eysteinn Sigurjonsson[*,1,4]

1 School of Science and Engineering, Reykjavík University, Reykjavik, Iceland
2 Center for Systems Biology, University of Iceland, Reykjavik, Iceland
3 Department of Bioengineering, University of California San Diego, La Jolla, CA, USA
4 The Blood Blank, Landspitali – the national University Hospital of Iceland, Reykjavik, Iceland
5 Biomedical Center, University of Iceland, Reykjavik, Iceland

* Dr. Olafur E. Sigurjonsson, M.Sc., Ph.D., Principal Investigator, School of Science and Engineering, Reykjavik University, Menntavegur 1, 102 Reykjavik, Iceland: oes@ru.is; Tel.: +354 543-5523; Mobile: +354-694-9427; Fax: +354-543-5532

Received: date; Accepted: date; Published: date

Abstract: Mesenchymal stromal cells (MSCs) are multipotent post-natal stem cells with applications in tissue engineering and regenerative medicine. MSCs can differentiate into osteoblasts, chondrocytes, or adipocytes, with functional differences in cells during osteogenesis accompanied by metabolic changes. The temporal dynamics of these metabolic shifts have not yet been fully characterized and are suspected to be of importance for therapeutic applications, such as osteogenesis optimization. Here, our goal was to characterize the metabolic shifts that occur during osteogenesis. We longitudinally profiled five key extracellular metabolites (glucose, lactate, glutamine, glutamate, and ammonia) from MSCs from four donors to classify osteogenic differentiation into three metabolic stages, defined by changes in the uptake and secretion rates of the metabolites in cell culture media. We used a combination of untargeted metabolomic analysis, targeted analysis of ^{13}C-glucose labelled intracellular data, and RNA-sequencing data to reconstruct the gene regulatory network and further characterize cellular metabolism. The metabolic stages identified in this proof-of-concept study provide a framework for more detailed investigations aimed at identifying biomarkers of osteogenic differentiation and small molecule interventions to optimize MSC differentiation for clinical applications.

Keywords: mesenchymal stromal cells (MSCs), osteogenic differentiation, metabolites, metabolism, metabolic changes, glycolysis, oxidative phosphorylation, gene regulatory network.

1. Introduction

Currently, around 2.2 million orthopaedic surgeries involving bone grafts are performed annually worldwide, a number expected to grow due to a global rise in the geriatric population. This increase will create an increased demand for graft material, which may pose a challenge because currently available sources all have limitations ranging from lack of safety or osteogenic potential to naturally limited supply [1]–[7]. In order to meet the ever-growing need for materials while eliminating risk to donors, the therapeutic application of mesenchymal stromal cells (MSCs) has been on the rise [6]. MSCs are multipotent, post-natal, self-renewing stem cells that can be isolated from various adult tissue types (e.g., fat, peripheral blood, and bone marrow) and are defined by the ability to differentiate *in vitro* into cells of mesodermal origin: osteoblasts, chondrocytes, and adipocytes [8]. The progression of differentiation depends on various factors, including hormonal and local factors, working together to form regulatory and metabolic pathways [9].

Osteogenic differentiation, or bone formation, occurs in three stages. First, the proliferation of osteoprogenitor cells is promoted by various growth factors, including insulin-like growth factor (IGF), transforming growth factor (TGF), and fibroblast growth factor (FGF). Next, differentiation into osteoblasts and the production of extracellular matrix takes place. This stage is promoted by both hormonal and growth factors, many of which act by increasing the activity of Runt related transcription factor 2 (RUNX2) and its downstream genes. Finally, progressive mineralization of bone matrix proteins within the extracellular matrix creates bone tissue that is capable of withstanding stress and strain [9].

We currently have an incomplete understanding of cellular metabolism during osteogenic differentiation—most of which is based on extracellular metabolite studies along with mapping of enzyme activity—based on indications of a specific metabolic phenotype amongst *in vitro* differentiated MSCs [10]–[13]. During proliferation, MSCs preferentially use anaerobic glycolysis for energy production, as indicated by low mitochondrial activity [11]. During osteogenic differentiation, it has been established that mitochondrial biogenesis increases and indicates a shift to aerobic energy production through oxidative phosphorylation [12], [14]. Imaging of changing mitochondrial distribution (from being centrally gathered around the nucleus to uniformly spaced throughout the cytoplasm) support this hypothesis [15]. A concurrent increase in the mitochondrial area of the cells could be due to increasing mitochondrial biogenesis [16], possibly upregulated by inhibiting hypoxia-inducible factor 1 (HIF-1), activating oxidative phosphorylation [12]. The metabolic shift from reliance on glycolysis to the activation of oxidative phosphorylation is important because it makes the survival of osteogenically differentiated MSCs more dependent upon oxygen; a reliance on oxygen may explain the reduced osteogenic differentiation under hypoxic conditions or under the typical oxygen levels present within human tissue. The activation of glutamine anaplerosis has been reported for cells in osteogenic differentiation, further indicating a greater reliance on mitochondrial energy production [16], [17]. Additionally, it has been demonstrated that various external factors used in regular practice in modern day labs, such as varying oxygen levels and the different osteoinductive agents, can have significant effects on the differentiation potential and/or metabolic pathway activity [18], [19]. However, we lack an understanding of the underlying basic metabolic mechanisms that govern the processes of proliferation and differentiation represents a barrier to the development of successful therapeutics that can manipulate the cells for implantation or reimplantation [6], [20]. Acquiring a firmly grounded understanding of aspects such as metabolic progression and changes in a biological system is a difficult undertaking due to the broad scope and expansive nature of metabolism, especially if one is looking at a long period of time. Defining time points of interest that can serve as initial focus points for comprehensive and detailed study might serve as a strategy to hone in on more detailed understanding.

In this study, we quantified changes in extracellular metabolites that contribute to energy production via oxidative phosphorylation, glycolysis, and anaplerosis to identify the metabolic phenotypes of osteogenesis. We profiled five metabolite biomarkers for cellular energy production—extracellular glucose, lactate, glutamine, glutamate, and ammonia—to study and further characterize the known change in metabolic activity levels between proliferation and differentiation. We observed three distinct metabolic stages during osteogenic differentiation, as defined by the temporal changes observed in the media concentrations of these five key metabolites that accompany MSC osteogenesis. We then performed both untargeted analysis of intracellular metabolomic data as well as targeted analysis of 13C-glucose labelled intracellular metabolomic data to validate these three stages and to identify which pathways were contributing to the observed functional difference. To elucidate the mechanistic underpinnings of these stages, we reconstructed a gene regulatory network from gene expression changes measured here using RNA-seq. This analysis allowed for insights into which genes were differentially expressed during the time course in question, which transcription factors regulated these changes, how the network topology changed, and whether any regulons were enriched for

metabolic enzymes. Taken together, this proof-of-concept study provides a molecular basis for the observed metabolic phenotypic shifts that we hope will serve as a foundation for future, more in-depth studies into the optimization of MSC osteogenic differentiation.

2. Materials and Methods

2.1. Cell Culture and Osteogenic Differentiation

Human bone marrow-derived MSCs from four donors were purchased from Lonza (Basel, Switzerland). All experiments were performed in triplicate and cells were cultured under normoxic conditions at 5% CO_2, 37 °C, and 95% humidity. Cells were maintained in basal growth medium (BGM). BGM was prepared by adding 5000 IU/ml of heparin (LEO Pharma A/Sm, Ballerup, Denmark), 1% penicillin/streptomycin (Gibco, Grand Island, NY) and 10% pathogen inactivated platelet lysate (PIPL) supernatant (Platome, Reykjavik, Iceland) into DMEM/F12 + Glutamax growth medium (Gibco, Grand Island, NY). The PIPL was centrifuged at 5000 rpm (4975 × g) for 10 min before the resulting supernatant was added to the medium.

Cells were used for osteogenic differentiation experiments at passages 2 – 5. Osteogenic differentiation was initiated using osteogenic culture medium (OM), prepared from 45 ml of BGM supplemented with dexamethasone (50 µl of 0.1 mM stock solution, Sigma, St. Louis, MO), Bone Morphogenetic Protein 2 (BMP-2, 50 µl of 50 ng/µl stock solution, Peprotech, Rocky Hill, USA), β-glycerophosphate (108 mg, Sigma), and ascorbic acid (50 µl of 50 mM stock solution, Sigma).

For collection of samples for metabolite analyses (glucose, lactate, glutamine, glutamic acid, and ammonia), cells were seeded at 5000 cells/cm² in 25 cm² culture flasks with 5 ml OM. Medium was changed approximately every 48 hours and samples of spent medium (0.5 ml) were taken in duplicate from each of the culture flasks approximately every 24 and 36 hours for cells under osteogenic differentiation. All samples were stored at -80 °C until analysis.

2.2. Alkaline Phosphatase Assay

Enzymatic activity of ALP during osteogenic differentiation was measured for all four donors using standard procedures. Cells were grown for 7, 14, or 28 days in 12-well plates at 3500 cells/cm² with 0.75 ml OM. For the Day 0 (control) samples, cells were collected from BGM prior to culturing. After the relevant culture period (0, 7, 14, and 28 days), cells were washed with phosphate-buffered saline (PBS) and then lysed for protein extraction with 0.02% Triton-100 (Sigma) in PBS. A liquid p-nitrophenyl phosphate solution was then added at a 1:1 ratio and incubated at 37 °C for 30 min in the dark before being measured using a Multiskan Spectrum spectrometer (Thermo Scientific, Helsinki, Finland) at wavelength of 400 nm. The ALP activity in terms of the conversion of p-nitrophenyl phosphate into p-nitrophenol was calculated using Equation 1.

$$ALP\ activity\ \left[\frac{\text{nmol}}{\text{min}}\right] = \frac{optical\ density}{18.8\ [\mu\text{mol}^{-1}] \cdot time\ [\text{min}]} \cdot 1000\ \left[\frac{\text{nmol}}{\mu\text{mol}}\right] \quad [1]$$

2.3. Alizarin Red Staining

Mineralization during osteogenic differentiation was determined by staining using Alizarin Red S indicator (Sigma-Aldrich) according to standard procedures. Cells for Alizarin Red staining were seeded at 3500 cells/cm² in a 12-well plate and grown for up to 28 days with 0.75 ml OM, with Day 0 samples cultured in BGM. Samples were collected after cells were grown for 0 (control), 14, or 28 days. After sampling, cells were washed with PBS and incubated for 15 min with paraformaldehyde. They were then washed again with deionized water before 2% Alizarin Red S solution (pH 4.1 – 4.3) was added. The samples were stained for 20 min on a rotating shaker then washed with deionized water and dried overnight. After drying, the samples were rehydrated by adding 1 ml of deionized water and

rehydrated overnight. After rehydration, 1 ml of 10% cetylpyridinium chloride solution was added to the cells and incubated for 15 min at 37 °C on a rotating shaker. The cell layer was then scraped, centrifuged for 10 min at 16,100 × g and 24 °C, and the resulting supernatant measured for optical density in a Multiskan Spectrum spectrometer (Thermo Scientific) at 562 nm.

2.4. Gene Expression/q-PCR Analysis

After culturing for 28 days, cells were harvested with trypsin and TRI reagent (Ambion, Austin, TX). All samples were kept in RNase-free microcentrifuge tubes at -80 °C until RNA isolation was performed. To perform the isolation, 150 µl of chloroform (Merck, Darmstadt, Germany) was added to all samples, after which they were centrifuged for 10 s at 12,000 × g and 4 °C and the resulting supernatant transferred to an RNase-free elution tube. Then 500 µl of isopropanol (Merck) was added, samples were centrifuged for 8 min at 12,000 × g and 10 °C, and the resulting supernatant discarded. Then 1 ml of 75% ethanol was added and samples were centrifuged for 5 min at 7500 × g and 22 °C. The RNA pellet was air dried before 50 µl of RNase-free water (Qiagen, Hilden, Germany) was added and the solution incubated at 58 °C on a PHMT Thermoshaker heat block (Grant Instruments, Shepreth, UK) for 12 min. Then 300 µl of RLT buffer (Qiagen) with 0.01% βb-mercaptoethanol (Sigma), and 350 µl of 70% ethanol (Gamla Apótekið, Reykjavik, Iceland) were added and samples transferred to an RNeasy spin column. The columns were centrifuged for 15 s at 16,100 × g and 24 °C, then 700 µl of RW1 buffer (Qiagen) was added and the columns centrifuged again for 15 s at 16,100 × g and 24 °C. 500 µl of RPE buffer (Qiagen) were then added to the columns and they were centrifuged again. After a final centrifugation step using the same settings, the column was placed in a new 1.5-ml collection tube and 50 µl of RNase-free water (Qiagen) was added to elute the RNA. The resulting flow-through samples were then stored at -80 °C until cDNA synthesis was performed.

For cDNA synthesis, isolated RNA samples were mixed in a new RNAse-free cDNA tube (Nunc, Roskilde, Denmark) at a 1:1 ratio with a master mix (8 µl nuclease-free H_2O, 5 µl 10X RT buffer, 5 µl 10X RT random primers, 2.5 µl RNase inhibitor, 2 µl 25X dNTP mix, and 2.5 µl MultiScribe™ Reverse transcriptase per sample) prepared from a High-Capacity cDNA Reverse Transcription Kit (Applied Biosystems, Foster City, CA) and nuclease-free H_2O (Qiagen). All samples and master mix components were thawed on ice prior to use. The mixed samples were centrifuged using a 96-well centrifuge adapter for a few seconds at 2500 rpm before being put into a thermal cycler (Applied Biosystems) operated under the following conditions: 27 °C for 10 min; 37 °C for 120 min; 85 °C for 5 s; 4 °C until use or storage at -20 °C.

Real-time qPCR analysis of the prepared cDNA was then performed, with RUNX2 and COL1A2 assayed as the genes of interest; both of these transcription factors are known and used to evaluate osteogenic differentiation. TATA box binding protein (TBP) was used as a housekeeping gene. 10X random primers were used (Applied Biosystems). All samples were mixed using an assay solution of 1 µl Taqman Assay and 10 µl Master Mix plus 2 µl cDNA. All RUNX2 primers and probes were obtained from Integrated DNA Technologies as premixed assays but for COL1A2 primers/probes were obtained separately from Integrated DNA Technologies. All relevant primer pairs can be found in Supplementary Table S1 online.

2.5. Cell culture and RNA isolation for RNAseq-data

Bone marrow derived human mesenchymal stem cells from three donors (Lonza, Basel, Switzerland) were taken from liquid nitrogen storage (-180°C) and seeded into 175 cm^2 culture flasks (Nunc, Penfield, NY, USA). About 500000 cells from each donor were used. Cells were expanded until about 85% confluency was reached – one donor in each culture flasks. The media used during proliferation phase was BGM (45ml), and media change was performed every 48 hours.

Upon reaching about 85% confluency the cells were harvested via trypsinization. Media was discarded from the culture flasks, 11.72 ml PBS (Gibco, Grand Island, NY, USA) used to remove remaining media before 11.72ml of 0.25% Trypsin (Gibco, Grand Island, NY, USA) was added. Culture flasks were incubated at 37°C (5% CO2, 95% H2O) for five minutes before 11.72 ml of BGM was added to neutralize and stop the trypsinization. Both BGM and 0.25% trypsin solution were warmed to 37°C before use.

Cell solution was transferred to 15ml falcon tubes using a pipette-boy and centrifuged at 1750 rpm (609g) for 5 minutes. The resulting supernatant was discarded and cells resuspended in 5 ml of BGM. Cells were then counted using a Neubauer hemocytometer (Assistant, Munich, Germany). For osteogenic differentiation of the cells OM (2ml/well) was used. Cells were seeded on to 6-well plates (200000 cells/well). Five separate wells were used for each donor in question, one per time point that was to be assessed (Day 3, 6, 9, 16, 28). Total of 15 wells were used. Media was changed every 48 hours. Upon day of assessment the medium was discarded using a pipette and 1ml of RNAzol® RT (Molecular Research Center, Inc., Cincinnati, OH, USA) added to the wells in question in order to lyse the cells. Repeated pipetting was used to dislodge and lyse cells completely before moving the resulting lysate to a 2-ml Eppendorf tube. In order to precipitate DNA, protein and polysaccharides 0.4 ml of water was added to the lysate, mixture shaken for 15sec and then stored at RT for 15 minutes. Samples were then centrifuged for 15 minutes at 12000g. About 75% of the resulting supernatant was moved to a new Eppendorf tube. In order to precipitate the total RNA 1ml of isopropanol was added to the supernatant collected in the previous step. Samples were then incubated at RT for 10 minutes before being centrifuged for 10 minutes at 12000g. This collected a small RNA pellet at the bottom of the Eppendorf tube. The supernatant was discarded and the resulting pellet washed twice by adding 0.5 ml 75% ethanol (care was taken to not dislodge the small RNA pallet in washing) to the Eppendorf tube and centrifuging for two minutes at 5000g. Alcohol solution was removed using a pipette. The pellet was then dissolved in 25µl of RNase-free water and nanodrop used to measure the resulting concentration. RNase free water was added as needed to gain 20 ng/µl concentration for RNA sequencing.

2.6. Cell culture and sample processing for intracellular metabolomics data

Cell cultures (n = 3) used to gather unlabeled intracellular metabolomic data were grown in 6 well plate culture vessels (15.600 cells/cm2). Five separate wells were used for cells from each donor to match the desired day of culture (selected based on change point analysis performed on extracellular metabolite data). Upon seeding cells were immediately placed in unlabeled OM, with media change (1.5 ml) occurring every 48 hours until sample collection took place.

Upon sample collection all media was discarded. Cells were then washed 3 times using 1 ml of PBS. PBS was discarded using a pipette after each wash.

Next, 1 ml of 80% methanol solution (stored until needed at -20 C in order to keep it at the necessary cold temperature) was pipetted straight onto the cells and a cell scraper subsequently used to dislodge and scrape cells from the bottom of the culture vessel. The resulting methanol-cell suspension was placed in an eppendorf tube and stored at -80 C until needed for metabolite extraction/preparation for mass spectrometry.

2.7. Glucose and Lactate Measurements

Extracellular glucose and lactate concentrations were determined in spent medium samples, collected every 24 to 36 hours as described above for metabolites, using an ABL90 FLEX blood gas analyzer (Radiometer Medical ApS, Denmark). Unused medium samples (blank medium) served as the controls.

2.8. Glutamine, Glutamic Acid, and Ammonia Measurements

Glutamine, glutamic acid, and ammonia were assayed in spent medium samples, collected every 24 to 36 hours as described for metabolites, using colorimetric assays (Megazyme, Wicklow, Ireland). L-glutamine and ammonia were measured using a single assay (Megazyme), as per the manufacturer's instructions, via determining the decrease in absorbance of the reaction mixture at 340 nm using a

Spectromax M3 plate reader (Molecular Devices, San Jose, CA). L-glutamic acid was measured with a separate assay (Megazyme), as per the manufacturer's instructions, via absorbance measurements at 492 nm.Unused medium samples (blank medium) served as the controls for these assays.

2.9. RNA sequencing

2.9.1. Gene expression quantification

The RNA transcript expression was quantified with Kallisto version 0.46.1 [21] using default parameters and the Ensembl Homo_sapiens GRCh38 reference transcriptome and generated FASTQ files as input.

2.9.2. Differential gene expression analysis

We used DESeq2 [22] version 1.26.0 to determine statistically significant differentially expressed genes (DEGs) across experimental conditions ($P < 0.05$ and Benjamini–Hochberg correction $\alpha = 0.1$ adjusted $P < 0.1$). We filtered out from downstream analysis those DEGs that across comparing conditions (i) were lowly expressed (< 2 TPM), (ii) showed relatively small fold-change (FC) differences (abs $\log_2$ FC < 1), and (iii) had highly variable expression across biological replicates (relative standard error of the mean > 1/2) and (iv) were inconsistent across donors (significant change for only one of the three patients). This filter resulted in a set of 1,106 response genes that we used as input for downstream analysis. We used the resource DoRothEA to annotate DEGs as transcription factors [23]; the human genome-scale metabolic network reconstruction Recon3D to annotate DEGs as metabolic genes [24].

2.9.3. Gene set ontology enrichment analysis

We used the gene ontology online tool AmiGO 2 (http://amigo.geneontology.org/amigo) to associate statistically significant pathway enrichments to gene sets of interest [25]. We selected the following options: "Reactome pathways" as annotation data set (Reactome version 65; released 2020-11-17), "Fisher's exact test" as test type and "False Discovery Rate" as multiple test correction. We downloaded results as JSON files and formatted them as tables using custom Python scripts.

2.9.4. Gene regulatory influence inference algorithm

First, we computed the expression z-score of the set of 1,106 response genes. Separately to upregulated and downregulated gene sets, we applied agglomerative clustering (sklearn.cluster.AgglomerativeClustering function) evaluating exhaustively the number of clusters (k) ranging from extreme values as low as 3 and as high as 114. Then, we quantified partition goodness using Silhouette, Calinski-Harabasz and Davies-Bouldin scores. Consistently optimal partitions ($k = 41$ and $k = 35$ for upregulated and downregulated gene sets, respectively) defined expression clusters. Next, we probed obtained clusters for enriched regulatory influences defined in DoRothEA regulons using hypergeometric tests [23]. We corrected multiple testing using Benjamini–Hochberg correction $\alpha = 0.1$. We then merged enriched gene sets that shared a common regulator. Finally, we evaluated if regulator expression profiles correlated (Pearson correlation coefficient > 0.8) with its identified target genes mean expression. We defined such sets as *regulons*. We assigned regulon activity for a particular condition as the gene expression mean over the target genes. We visualized clustered regulon activities in the form of a heatmap using the seaborn.clustermap function.

2.9.5. TF-TF regulatory influence network visualisation

We established a directed edge between two TFs if a regulator (tail) had as target gene another TF (head). We used Cytoscape [26] version 3.8.2 to visualize the inferred TF-TF influence network applying the hierarchical layout.

2.9.3. Code availability

All computational methods used for the analysis of RNA-seq data and beyond are available in the GitHub repository https://github.com/adelomana/osteo.

2.10. Intracellular labelled and unlabeled metabolite extraction

In order to extract intracellular metabolites collected samples (a cell suspension in 80% methanol solution, previously stored at -80 C) were thawed and 30 μL of previously mixed isotopically labelled internal standards subsequently added. The samples were then placed on a floating rack and into a sonicating water bath for 20 second sonication before being put on ice for up to 2 minutes. This was done for a total of 3 times. Icing prevented the samples from over heating. Subsequently 800 μL of ice cold methanol:dH2O (7:3 v/v) solution was added to each sample and samples vortexed for approximately 30 seconds. The samples were then centrifuged at 20817g for 15 minutes at 4 C.

The resulting supernatant was then transferred into properly labelled eppendorf tubes (2 ml) whilst the precipitate was again reconstituted with 900 μL of previously described methanol solution before being vortexed and centrifuged for the second time. The resulting supernatant was combined with the previous one and precipitates retained at – 80 C for later BCA protein assay (for data normalization purposes).

In 2 separate sets of twelve eppendorf tubes, 200 μL of varying dilutions of previously prepared CC mix were transferred. The CC mix, also known as a mixture of metabolite standards, is a dilution series that can be used for absolute quantification of metabolite concentration by generating an external calibration curve by least-squares linear regression. This curve is then used to estimate the absolute concentrations of the corresponding metabolites in the measured experiment samples.

All samples (CCmix serial dilutions and intracellular samples) were then transferred to a vacuum concentrator (MinVac) for evaporation before being reconstituted in 300 μL solution containing dH2O and ACN in equal parts.
The reconstituted samples as well as the two CC mixes were then filtered through a Pierce protein 96-well precipitation plate that had previously been prepared by wetting the filter (to facilitate correct filtration). The filtration was done via centrifugation for 30 minutes at 4 C and 2000rpm.

The filtered precipitation was then transferred to a labelled set of glass mass spectrometry vials with glass inserts in order to be put through the mass spectrometer (UPLC-MS).

2.11. BCA Protein Assay

In order to evaluate cell quantity at each time point defined by change point analysis, that could then be used to normalize data, a bicinchoninic acid (BCA) protein assay was performed on the precipitates collected during the intracellular metabolite extractions.
In order to extract and dissolve protein content a dissolving buffer was created. It constituted bufferA (RIPA buffer):bufferB (200mM NaOH, 1% SDS) in 1:1 v/v. 100 μL of the dissolving buffer was added to the eppendorf tubes containing the protein pellets and volume adjusted based on estimated protein amount. Afterwards the tubes were vortexed and put through a freeze/thaw cycle to try and aid with pellet breakdown. Next, the pellets were sonicated for 1 hour at 60◦C before being vortexed again to try and dissolve as much protein as possible. Of the resulting suspension 5 μL of each sample were used for the assay.
In performance of the assay itself (Pierce™ BCA Protein Assay) the accompanying kit protocol from Thermo Scientific™ was followed.

2.12. UPLC-MS set up and run configuration

All metabolite measurements based on mass spectrometry were performed using a gradient elution UPLC (ACQUITY) system (UPLC ACQUITY, Waters Corporation, Milford, MA) coupled with an ionization qTOF mass spectrometer (Synapt G2 HDMS, Waters Corporation, Manchester, U.K.) with an electrospray interface (ESI) as previously described. Briefly, gradient chromatographic separation of samples was achieved by HILIC through an Aquity BEH amide column (2.1 mm x 150 mm, 1.7 μm particle size, Waters Corporation) at 45 C. Two different chromatographic conditions were used in combination with HILIC column, an acidic mobile phase (phase A) and a basic mobile phase (phase B). In both cases the injection volume was 7.5 μL, the flow rate was 0.4 mL/min and the run time was 14 minutes. Mobile phase A conditions consisted of ACN with 0.1 % of formic acid and mobile phase B conditions consisted of dH2O with 1% formic acid. The following gradient patterns (solvent B) was used in both cases: 0 minutes 1% B, 0.1 minutes 1% B, 6 minutes 60% B, 8 minutes 40% B, 8.5 minutes 1% B, 14 minutes 1% B. Both positive and negative ESI modes were acquired. The capillary voltage and the cone voltage were 1.5 kV, the temperatures were 120 C and 500 C respectively and desolvation gas flow was 800 L/h.

2.13. Data Normalization and Processing

2.13.1. Extracellular metabolomic data

Data processing and normalization was performed in R [27]. One day was found to be missing more than 50% of data points and removed from further analysis. Other data points below limit of detection or for other reasons were replaced with the minimum metabolite value measured. For each metabolite measured a generalized linear model was fitted using the gamm4 package in R [28], this modelled the change in metabolite concentration by day of differentiation protocol accounting for donor variation and analysis batch effects as random variables. Other possible models were considered also accounting for the media dwell time, and PIPL batch nested in donor and passage number nested in donor as random effects, however the Akaike Information Criteria of these models (see Supplementary Table S2 online) were higher indicating poorer models, either less good fit or more over fitting. One exception to this was adding the effect of media well time to the lactate model. However, this was only slightly better and given the desire for consistency across metabolites and the use of rate of change for other analyses, which incorporates this factor, it was decided not to use this model. Change point detection was performed using the ECP package for R to perform change point detection in multivariate data using the e divisive method with a required significance level of 0.05 [29]. This analysis was performed on the modelled values for each day after they had been converted to the hourly rate of change (i.e. the secretion or uptake rate) for each day.

The hourly rates of uptake and secretion were calculated by taking the difference of the absolute metabolite concentration levels between adjacent days and dividing by the appropriate number of hours that passed between media change and sample collection.

2.13.2. Intracellular unlabeled metabolomic data

The unlabeled intracellular metabolomic data was all run as an untargeted analysis using the R package XCMS. The first step of the process was conversion of the raw LC-MS data files but in order to be able to work with the data outside of MassLynx and TargetLynx it has to be converted to a MZdata format using MassWolf an the „water.convert.R" function. MassWolf is preferable to similar packages, DataBridge and MSconvert, since it supports MS^n data (unlike DataBridge) and adds lockmass calibrations to analyte measurements in the output files (unlike MZdata). XCMS can then correct such gaps by filling them using the nearest available analyte scan.

After the raw data conversion had been completed the centWave algorithm was used to automatically detect chromatographic peaks, ion features. In this analysis 3 consecutive ROI with no peaks with intensity level of at least 100 were considered empty and discarded.

Within the centWave algorithm once all ROIs have been found a continuous wavelet transformation (CWT) was used to detect chromatographic peaks with variable peak widths. Here a minimum and maximum peak width is applied.
The obiwarp method was used to align retention times between samples and peak density method to group corresponding chromatographic peaks.
The R package CAMERA was then used in order to decrease the complexity of the generated data set by grouping ion features such as adducts and fragments that can potentially stem from the same compound.
During the peak identification and peak picking process the data was processed in such a manner as to normalize with reference to donor variation.
The resulting data was then normalized using NOMIS (NormQC, a function found in R) method, then by protein content (BCA protein piercing assay - to account for cell number) and finally log-transformed. This data was used for the PCA, PLSDA, one way ANOVA and Tukey's Post-HOC analysis.

2.13.3. Mummichog pathway and network analysis
To search for enrichment patterns in metabolic networks and identify possible characteristic metabolites that were enriched for each stage we applied the Mummichog online software [30]. It bypasses the need for metabolite identification by using the organisation of metabolic networks in order to predict activity directly from supplied mass spectrometry data tables. The analysis was run as described in the protocol that follows the online software.

2.13.4. Targeted MS-MS analysis to confirm Mummichog metabolite prediction
The instrumentation used was an ACQUITY UPLC system (UPLC ACQUITY, Waters Corporation, Milford, MA) coupled to a qTOF mass spectrometer (Synapt G2 HDMS, Waters Corporation, Manchester, U.K.) with an electrospray interface (ESI). The gradient chromatographic separation was performed on an ACQUITY BEH Amide (2.1 mm × 150 mm, 1.7 μm particle size, Waters Corporation) at 45°C. Mobile phase A was Acetonitrile and mobile phase B H_2O both with 0.1% of formic acid. Injection volume was 7.5 μL, flow rate was 0.4 mL/min and run time was 14 min. The following gradient pattern (solvent B) was used: 0 min, 1% B; 0.1 min, 1% B; 6 min, 60%B; 8 min, 40% B; 8.5 min, 1%B; 14 min, 1% B. Chromatograms were acquired on scan mode for both positive (+) and negative (-) ionization. The capillary and cone voltage were 1.5 kV and 30 V, respectively. The source and desolvation temperature were 120 and 500 °C, respectively, and the desolvation gas flow was 800 L/h.

2.13.5. Intracellular labelled metabolomic data
The labelled intracellular metabolomic data was all run as targeted analysis and integration of targeted compound peaks was done using TargetLynx (v.4.1, Waters), an application manager. The raw MS data with was then corrected to account for all naturally abundant ^{13}C-glucose isotopes via IsoCor [31]. This provided percentage of isotopes for each molecule that exceeded natural abundance along with corrected isotopolouge distribution.

3. Results

In the following sections, we first used previously defined biomarkers to verify osteogenic differentiation. Next, we used key metabolite markers to track differentiation and define metabolic stages of osteogenic differentiation. We then used untargeted and targeted metabolomic analysis to globally characterize these metabolic shifts. Finally, we reconstructed a gene regulatory network to explore the underlying mechanisms of the observed metabolic shifts.

3.1. Verification of Osteogenic Differentiation

Determination of osteogenic differentiation during the 28-day experiment was performed for all donors using well-established procedures: Alkaline Phosphatase (ALP) activity (performed for four donors at four time points) and Alizarin Red staining (performed for four donors at three time points). Final differentiation was verified through measurements of transcript levels of RUNX2, secreted phosphoprotein 1 (SPP1), and collagen type 1 alpha 2 chain (COL1A2) (performed for three donors at Day 28). ALP activity was higher at all sampling timepoints for all donor samples than in the blank medium (see supplementary figure S1A), though the increase in average ALP level was only significant at Day 14 (Bonferroni-adjusted two-tailed unpaired t-test, $p = 0.1194$ for Day 7, $p = 0.0117$ for Day 14, and $p = 0.6072$ for Day 28). These results follow the typical pattern of ALP activity during osteogenic differentiation [32], [33], with an increase observed at earlier stages of differentiation before a plateau or a decrease in the final stages. Individual measurements, by donor, are presented in Supplementary Table S3 online.

Mineralization, in the form of calcium phosphate accumulation, was verified using Alizarin Red staining of Day 0, 14, and 28 samples, both visually (supplementary figure S1B and supplementary figure S2) and by calculating the change from the Day 0 control (Supplementary Table S4 online). When compared to the control neither day 14 nor day 28 were measured as being statistically significant in difference despite accumulating mineralization. Individual measurements by donor are provided in Supplementary Table S4 online. Advanced stages of osteogenic differentiation are characterized by tissue mineralization; all samples in this study showed an increase in mineralization over time, though the changes were not statistically significant.

Relative expression levels, compared to the housekeeping gene, of RUNX2 and COL1A2 are shown in Supplementary Table S5 online, along with the fold change compared to the Day 0 control. RUNX2 expression increased while COL1A2 decreased over time. In summary, ALP activity, mineralization, and gene expression profiling over the 28-day study period all verified that osteogenic differentiation was initiated by the addition of osteogenic medium (OM).

3.2. Lactate secretion changes during Osteogenic Differentiation

In order to estimate changes in central carbon metabolism we quantified extracellular glucose, lactate, glutamate, glutamine and ammonia concentrations in spent medium from MSCs undergoing osteogenic differentiation (Fig. 1).

To account for differences due to inter-donor variation and analysis batch variation, we fitted a model to these data; model predictions were used in all further analyses. Only extracellular lactate differed significantly from that of the blank medium on Days 19 and 23 (Fig. 1B). Average rates of concentration change (mmol/L/hr) each day can be seen in supplementary Fig. S3B. The average amount of lactate measured was significantly higher during the last 13 days of differentiation than in blank medium, with hourly secretions also higher in those later stages. The concentration changes observed for other metabolites were less apparent. Nevertheless trends were observed in extracellular glucose that dropped following day 12 but did not differ significantly from that in the blank medium (Fig 1A). Glutamine was generally consumed in small amounts each day with an increase in consumption over time, possibly due to an increase in cell number (see Figure 1C) and supplementary Fig. S3C)). Glutamate concentration was little changed in the medium at the beginning of the differentiation period, began to be slightly secreted around Day 15 and showed increasing secretion after Day 21, although the rate of secretion remained low (supplementary Fig. S3D). Ammonia showed an increasing trend towards secretion throughout differentiation, possibly due to variation in cell number (supplementary Fig. S3E). Despite variability, generalized linear modelling revealed patterns in the rates of change of these metabolites during osteogenic differentiation. In order to define these patterns we performed multivariate change point analysis using the normalized data for all five metabolites.

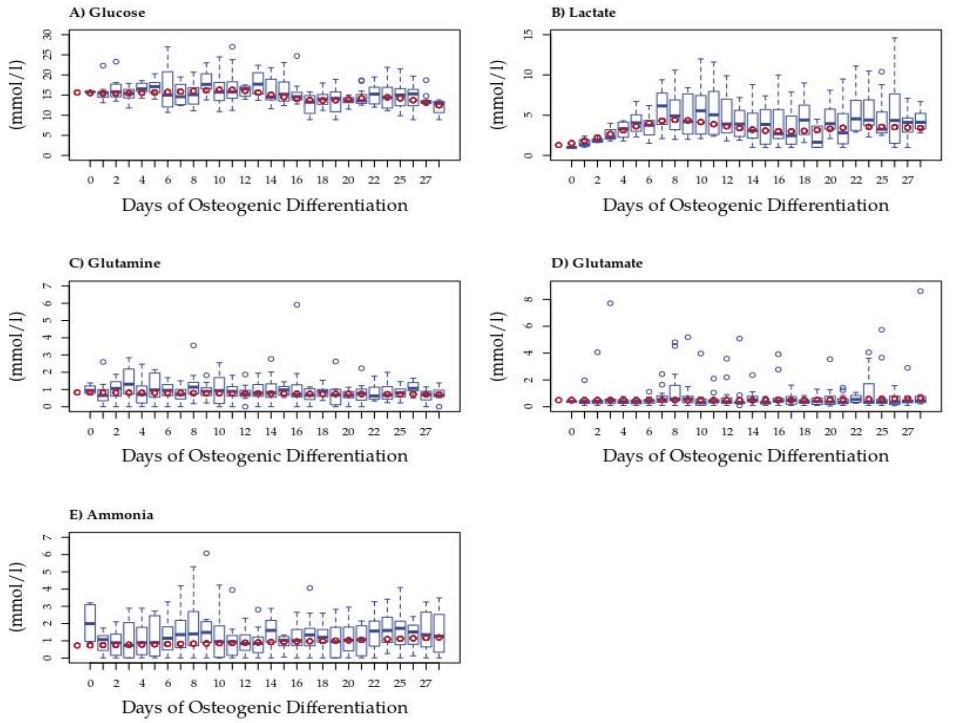

Figure 1. Extracellular metabolite measurements in spent medium from MSCs during osteogenic differentiation*. Box plots show concentrations (mmol/l) of* ***(A)*** *glucose (n = 4),* ***(B)*** *lactate (n = 4),* ***(C)*** *glutamine (n = 4),* ***(D)*** *ammonia (n = 4), and* ***(E)*** *glutamate (n = 4). Dots (◦) show outliers. The ends of whiskers show SEM. Dots (* red shade) represent the model predicted value subsequently used in change point analysis.*

3.4. The utilization and production of essential metabolites are indicative of three stages of osteogenic differentiation.

Multivariate change point analysis was performed using model normalized values converted to hourly rate of change for all five metabolites in the spent medium from osteogenically differentiating MSCs from four donors. We identified two statistically significant change points within the differentiation period ($p < 0.05$), in addition to the beginning and end, defining three metabolic stages of differentiation (**Figure 2**). Phase 1 occurred over Days 1 to 4, Phase 2 was between Days 5 and 15, and Phase 3 was from Day 16 to the end of the study period at Day 28.

We next calculated glucose/lactate ratios within the three phases as a proxy for glycolysis. These ratios were different within the three phases (**Table 1**). During Phase 1, a glucose/lactate ratio of -0.209 was observed that then dropped in phase 2 before increasing to 0.908 during Phase 3 indicating changes to glycoslysis between the three stages. Similarly, glutamine/glutamate and glutamine/ammonia were suggestive of changes to glutaminolysis. These analyses suggest different metabolic phases over the 28 days of osteogenic differentiation that are defined by changes to glycolysis and glutaminolysis.

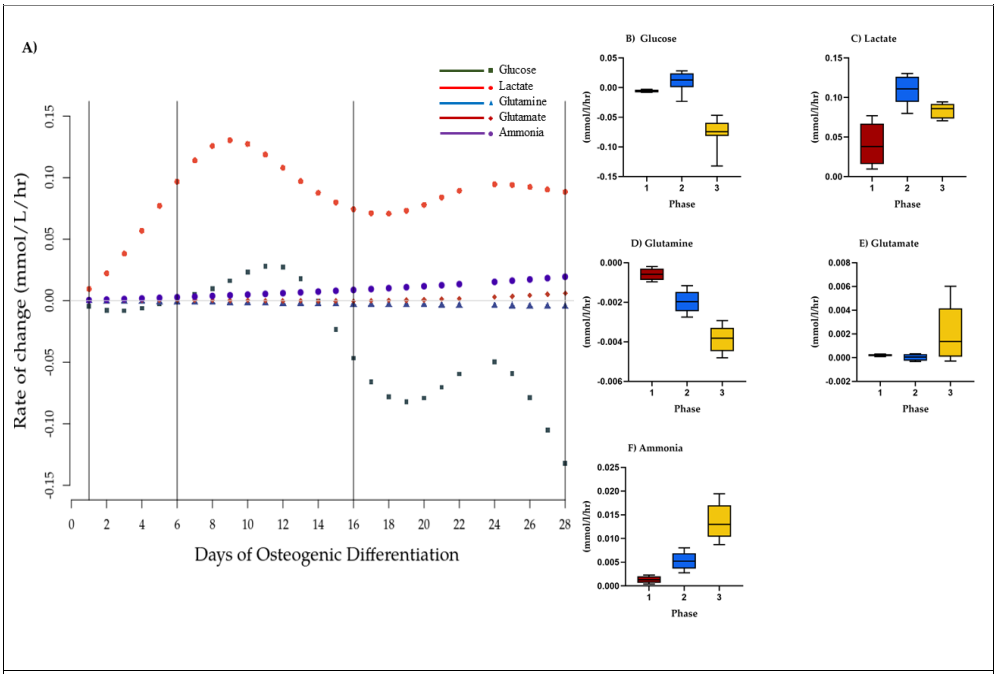

Figure 2. Phases of osteogenic differentiation. A) *Change point analysis for glucose, lactate, glutamine, ammonia, and glutamate in spent medium from osteogenically differentiation MSCs between Days 1 and 28. Vertical lines indicate four possible change points separating the stages of differentiation. Points (various shapes) represent the model normalized rate of change on a given day (mmol/l/hr). Black lines represent the change points detected at less than p = 0.05. Grey line represents 0. Hourly rate of change of concentration of model normalized values (mmol/l/hr) per phase of osteogenic differentiation, mean and SEM of* ***B)*** *glucose,* ***C)*** *lactate* ***D)*** *glutamine,* ***E)*** *ammonia, and* ***F)*** *glutamate. Red = phase 1, blue = phase 2, yellow = phase 3.*

Table 1. *Key metabolite secretion/uptake ratios for all 4 stages of osteogenic differentiation as identified through change point analysis. Mean values are shown for all days in each phase normalized values. Expected perfect ratios (EPRs) are: glucose/lactate EPR = -0.5 with secretion of lactate and uptake of glucose; glutamine/glutamate EPR = -1 with higher number associated with higher use of glutamate, and glutamine/ammonia EPR = -1, with secretion of ammonia and uptake of glutamine. A negative sign is indicative of 1) lacatate secretion and glucose uptake from the medium, 2) Glutamate uptake at a high rate and secretion of glutamine. * = glucose and lactate were measured as secreted over this phase*

Phase	Glucose/Lactate	Glutamine/Glutamate	Glutamine/Ammonia
1 (Days 1-4)	-0.209	-2.620	-0.444
2 (Days 5-15)	0.088*	-38.299	-0.374
3 (Days 16-28)	-0.908	-1.843	-0.284

3.7 ^{13}C-glucose mean label enrichment suggests an anaerobic switch following day 9 of osteogenic differentiation

While offering good temporal resolution, our extracellular data lacked sensitivity. In order to support that altered metabolic phenotypes during osteogenic differentiation are defined by changes to glycolysis we fed cells with uniformly labelled ^{13}C glucose and traced the label to lactate at timepoints that fell within the phases proposed by the changepoint analysis (Figure 5). Label enrichment in glucose was near to 100% (>0.999) and was 95-97 % in spent medium during differentiation. A trend towards lowered glucose uptake into the cells was observed up until day 16 although this was not statistically

significant (Figure 5A). ^{13}C lactate however increased over the first three time points (going from 71.8% to 81%) and dropped at day 16 (65%-72%) indicating an increase and subsequent slow down to glycolysis during differentiation.

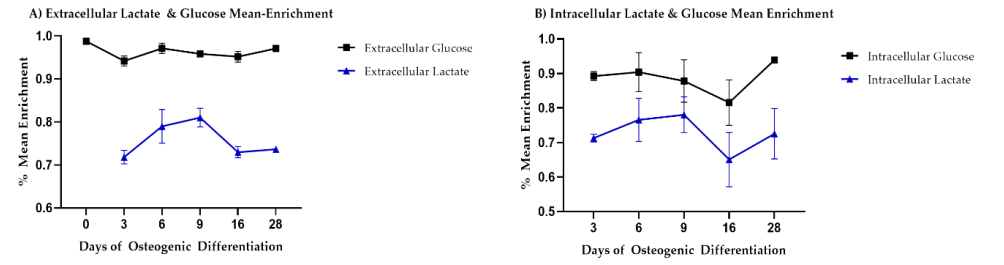

Figure 3. Mean % ^{13}C-glucose label enrichment in intra-and extracellular glucose and lactate. *Day 0 of glucose is label enrichment in unused medium, which is near to 1 or 100%. Shown is average value (n=3) with SD. Data is normalized to cell quantity.*

We also observed ^{13}C label enrichment from glucose in uridine diphosphate glucose (UDP-Glu) that is derived from the glycolytic intermediate glucose-6-phosphate. UDP-glu is substrate for glycogen and glycan synthesis and consists of a pyrophosphate group, pentose sugar ribose, glucose, and the nucleobase uracil. The M+6 and M+11 isotopologues of UDP-Glu can be used to gain insight into glycolytic and pentose phosphate pathway activity on account of the hexose and pentose moieties, respectively. Specifically, the hexose in UDP-glucose originates from glycolysis and because the only source of glucose available to the cells is from the added ^{13}C labelled glucose in the media, the % isotopologue distribution of the M+6 isotopologue of UDP-Glu is an indicator of glycolytic activity. Similarly, the M+11 isotopologue of UDP-Glu consists of both labelled glucose from glycolysis and the ribose originating from the pentose phosphate pathway (PPP).

UPD-Glu concentration fluctuated during differentiation although changes observed were not statistically significant (Figure 6B). Somewhat surprisingly, the mean ^{13}C label enrichment (Figure 6 A) dropped steadily up until day 16, as opposed to lactate although these were not statistically significant. Label enrichment into the M+6 isotopologue however increased steadily up until day 16 (Figure 6C) while the M+11 isotopologue decreased over the same period (Figure 6D) indicating increased glycolytic flux and decreased pentose phosphate pathway flux, respectively.

Like UDP-Glu, UDP-nAcGlu is derived from glycolysis albeit via frucose-6-phosphate and the hexosamine biosynthetic pathway and can be used as a proxy to estimate flux through glycolysis and the PPP. Isotopologue distribution patterns for UDP-nAcGlu mirrored those seen for UDP-Glu (supplementary Figure S4). Combined, the changes observed in lactate excretion during differentiation along with changes to isotopologue enrichment are indicative of glycolytic flux changes and altered flux into peripheral metabolic pathways including glycan synthesis and the pentose phosphate pathway.

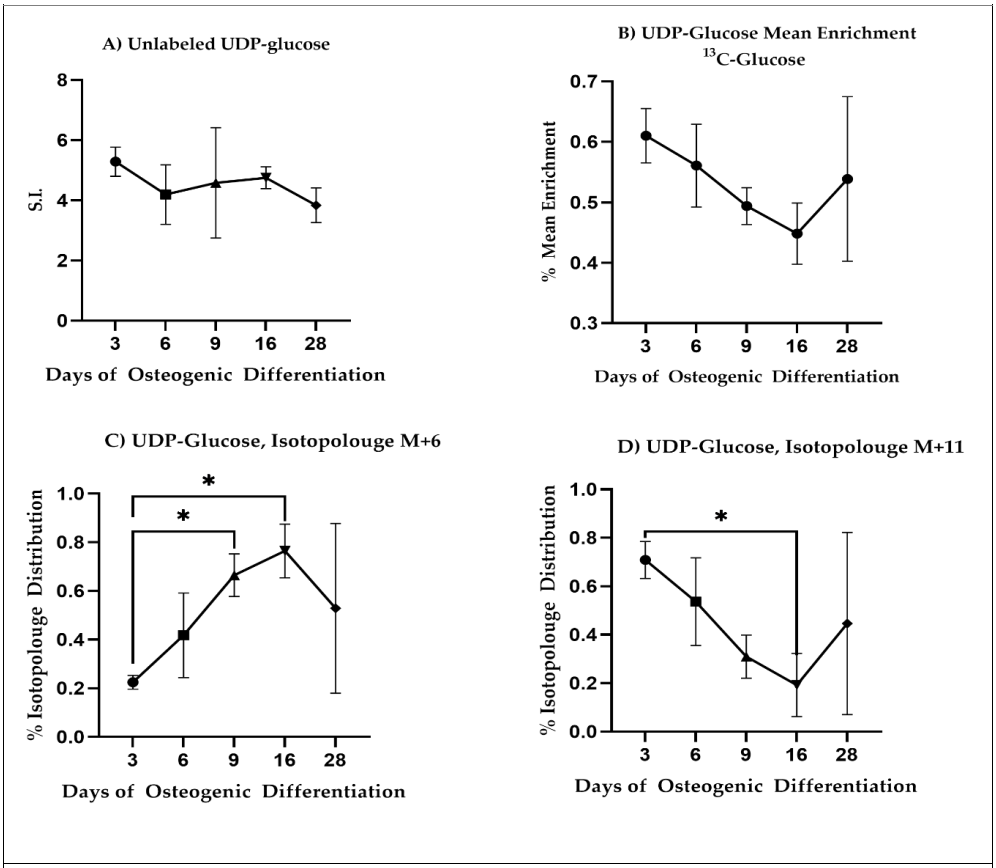

Figure 4. *Isotopologue distribution of UDP-Glucose supports increased glycolysis during osteogenic differentiation. A) Absolute Concentration of UDP-glucose in unlabeled intracellular data (n = 3, SD), B) Mean ^{13}C-glucose label enrichment (n = 3, SD), C) Average % isotopolouge distribution of the M+6 isotopolouge for UDP-glucose (n = 3, SD). D) Average % isotopolouge distribution of the M+11 isotopolouge for UDP-glucose (n = 3, SD). * P <0.05. S.I. = signal intensity.*

3.9 ***Mitochondrial activity increases as differentiation progresses and is significantly different between suggested phases.***

One reason for changes to glycolytic activity is enhanced reliance on TCA cycle driven respiration. Mitochondrial activity and aerobic metabolism have been shown to increase as osteogenic differentiation progresses [11], [12], [15]. Our metabolomics approach did not capture intermediates within the TCA cycle. Therefore we investigated ^{13}C-glucose label enrichment in aspartate and glutamate that can only be derived from glucose via oxaloacetate and alpha ketoglutarate, respectively.

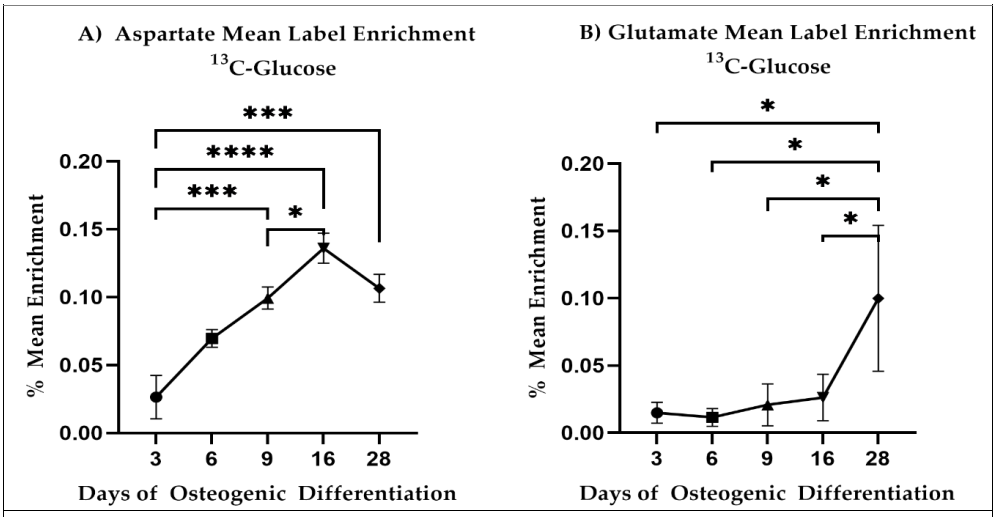

Figure 5. *Mean label enrichment for ^{13}C-Glucose labelled A) Aspartate (n = 3, SD) and B) Glutamate (n = 3, SD),. * P<0.05,, ***P<0.0001, ****P<0.00001*

An increase in ^{13}C incorporation into aspartate was observed with time prior to a slight drop between day 16 and day 28 (Figure 8) consistent with an overall increase in glucose derived carbon flux via oxaloacetate. Changes in enrichment were measured to be significant between the proposed three phases (p-value = 0.0001 day 3 vs. day 9, p-value = 0.0002 day 3 vs. day 28 and p-value = 0.0172 day 9 vs. day 16). ^{13}C label incorporation into glutamate was not as clear although a an increasing trend was observed. In particular however, increased label was observed in glutamate at day 28 and label incorporation was different for the proposed metabolic phases (p-value = 0.0131 day 3 vs day 28, p-value = 0.0199 day 9 vs day 28). See supplementary table S6 for all comparisons. Combined the enrichment patterns of aspartate and glutamate are indicative of changes to TCA cycle flux concomitant with the decrease in glycolysis as osteogenic differentiation progresses.

In order to investigate if these changes were associated with altered glutaminolysis as hypothesised from the changepoint analysis, we fed the cells with uniformly labelled ^{13}C or ^{15}N glutamine and again traced label incorporation to glutamate and aspartate. The mean enrichment of ^{13}C label in intracellular glutamine was quite variable (Figure 6 G)) and no statistically significant changes in label enrichment were observed during differentiation. Nevertheless, a trend in label enrichment in the m+5 isotopologue of glutamine increased up until day 16. This trend was mirrored in the m+5 isotopologue of glutamate (Figure 6 F)) and coincided with a drop in the total intracellular concentrations of glutamine and glutamate (see supplementary figure S6 G)-H)) consistent with enhanced demand for extracellular glutamine. ^{15}N label incorporation into glutamate and aspartate similarly increased at day 16 consistent with altered glutaminolysis (see supplemental figure S5).

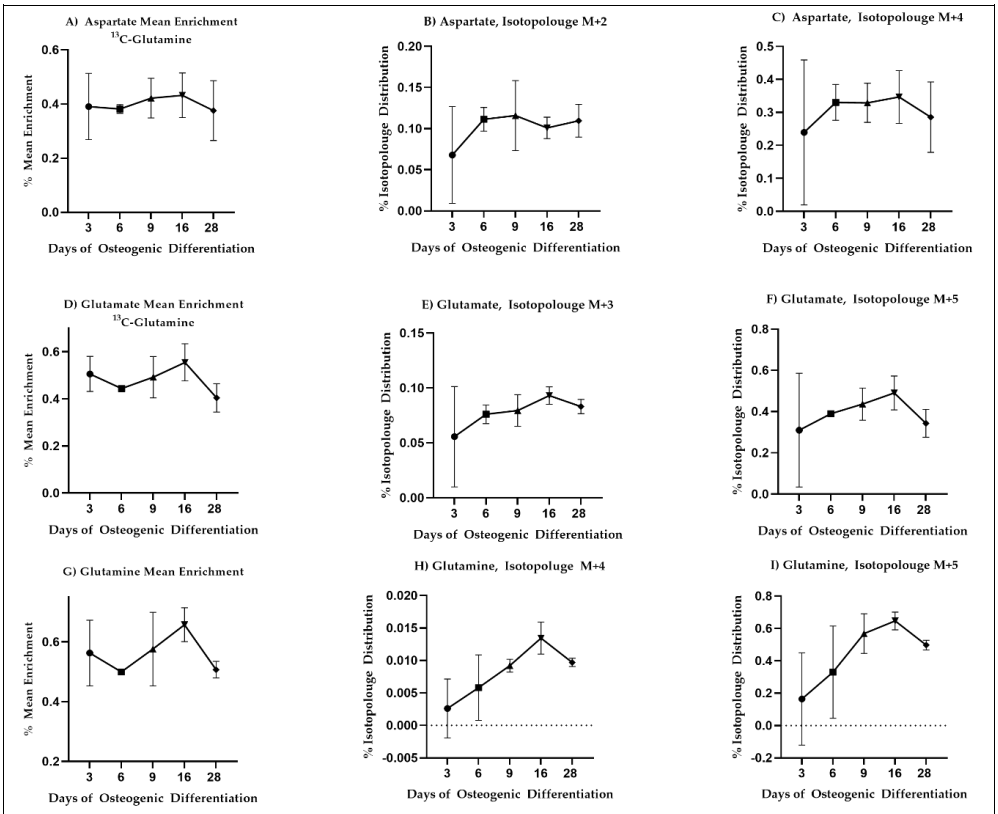

Figure 6 | ^{13}C-glutamine enrichment in glutamate, aspartate and glutamine with isotopolouge distribution is consistent with increased need for extracellular glutamine as differentiation progresses. A) Mean enrichment of ^{13}C-Glutamine in intracellular Aspartate (n = 3, SD), B) ^{13}C-Glutamine m+2 isotopolouge distribution for Aspartate (n = 3, SD), C) ^{13}C-Glutamine m+4 isotopolouge distribution for Aspartate (n = 3, SD), D) Mean enrichment of ^{13}C-Glutamine in intracellular Glutamate (n = 3, SD), E) ^{13}C-Glutamine m+3 isotopolouge distribution for Glutamate (n = 3, SD), F) ^{13}C-Glutamine m+5 isotopolouge distribution for Glutamate (n = 3, SD) , G) Mean enrichment of ^{13}C-Glutamine in intracellular Glutamine (n = 3, SD), H) ^{13}C-Glutamine m+4 isotopolouge distribution for Glutamine (n = 3, SD), I) ^{13}C-Glutamine m+5 isotopolouge distribution for Aspartate (n = 3, SD)

3.5 Intracellular metabolomics validate metabolic stages of osteogenic differentiation

To confirm results from the change point analysis and screen for additional changes in metabolism, we performed untargeted intracellular metabolomic analysis of cells undergoing osteogenic differentiation at the 5 different time points based on the results (n=3 in all instances).

Untargeted peak identification yielded a total 1682 mz values. One way ANOVA statistical analysis yielded a total of 1064 mz values that were significantly enriched ($p<0.05$, data normalised to cell content) between at least one of the comparisons of interest. After using Tukey's HSD post hoc test (THSDpht) analysis to correct for multiple comparisons total number of significant metabolites ($p<0.05$) was reduced to 1041 mz values (Table S3). We visualized these differences by PLSDA (Figure 7). Separation with time was captured by principle component 1. With respect to the three proposed metabolic phases from the changepoint analysis, grouping was observed between day 9 (phase 2) and day 28 (late phase 3). Day 9 (phase 2) however overlapped with day 16 (start of phase 3). A clear

separation between day 3 and 6 (phase 1) with respect to day 28 was also seen. A slight overlap between day 6 and day 16 was also observed. In general the results support discrete metabolic phases during osteogenic differentiation.

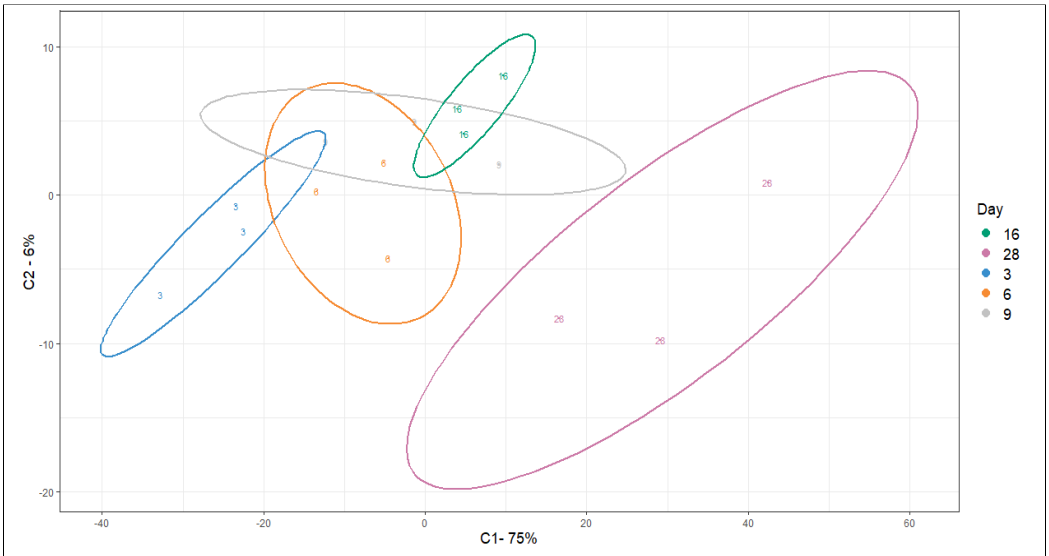

***Figure 7* | PLSDA visualization of m/z values with significantly different ion intensities during osteogenic differentiation**. *Ellipses indicate 95% confidence intervals. An overlap in confidence intervals is present for day 6, day 9 and day 16– however when observing day 3, day 9 and day 28 (timepoints firmly within the suggested phases) the overlap is less prominent. Data were normalized to protein abundance and scaled prior to analysis.*

We next associated identified m/z values with metabolic pathways and specific metabolites using the mummichog algorithm [30]. We filtered the list of statistically significant m/z features due to the workload involved in validating hundreds of m/z feature annotations. Specifically, out of the 1041 significant m/z values identified, different m/z features were found discriminate between the different days. However, a total of 57 common m/z features were found to discriminate day 3 vs. day 28, day 9 vs. day 28 and day 3 vs. day 9. Emphasis was put on annotating the 1041 significant m/z (supplementary table S7) values by manually validating the computationally proposed mummichog annotations by comparison to an in-house spectral library with respect to peak retention time and MSMS fragmentation. The mummichug algorithm provided annotations for 22 of these m/z values (supplementary Table S8). A total of four m/z features could be validated with high confidence corresponding to lysophosphatidyl choline (LPC) 16:0, LPC 18:0 and oxidized and reduced glutathione (Figure 8).

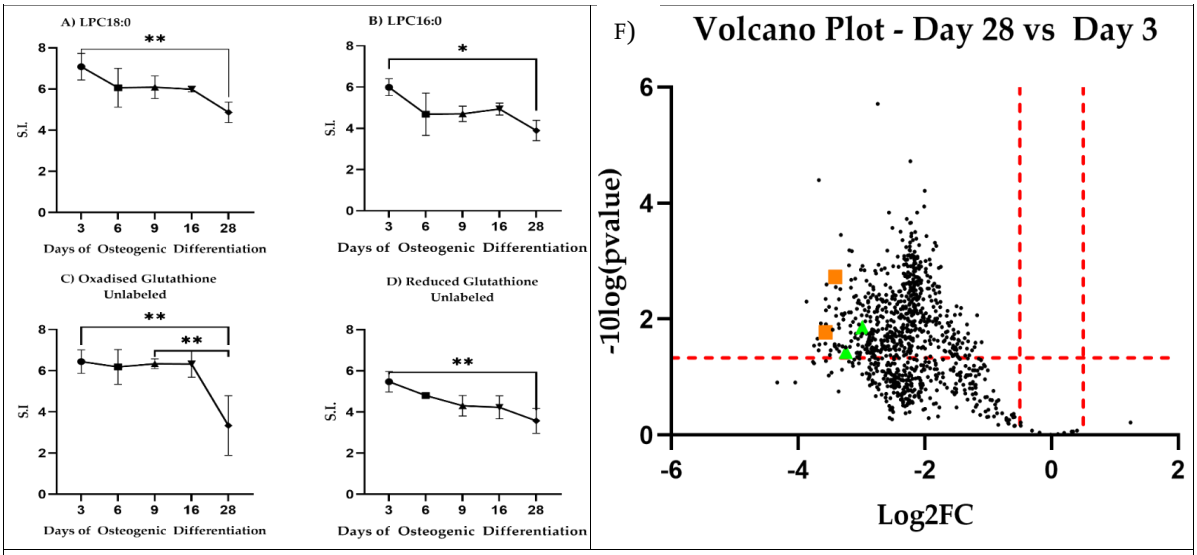

***Figure 8* | Changes in absolute intracellular concentration levels for A) LPC18:0, B) LPC16:0 and C)-D) glutathione during differentiation.** *All metabolites show changed levels across the time observed. * P<0.05, ** P<0.0099. Shown area average values (n=3, SD). S.I. = Signal Intensity. F) Volcano Plot showing fold changes for intracellular untargeted metabolites between day 28 and day 3 during osteogenic differentiation. LPC18:0, LPC16:0 shown as green triangles, glutathione as orange squares. Log2FC = Base 2 logarithmic value of calculated fold change.*

LPC18:0 decreased between day 3 and day 28 (p-value = 0.0083) similar to LPC16:0 (p-value = 0.0131). Reduced glutathione decreased steadily between days 3 and day 28 (p-value = 0.0052) while oxidized glutathione dropped at day 28 as compared to day 3 (p-value = 0.079) and day 9 (p-value = 0.0099). Other p-values can be found in supplementary table S6. Finally, we re-analysed our ^{13}C glucose and ^{13}C glutamine precursor experiments focusing on glutathione. These analyses indicated that glutathione synthesis from glucose derived carbon increased during differentiation (Figure 9A)). Carbon contribution from glutamine remained stable although a similar trend to that observed for glutamate (Figure 6F)) was observed in the m+5 isotopologue of glutathione (Figure 9D)). Combined these results are indicative of altered lipid metabolism and changes to redox potential and are consistent with changes to mitochondrial respiration during differentiation.

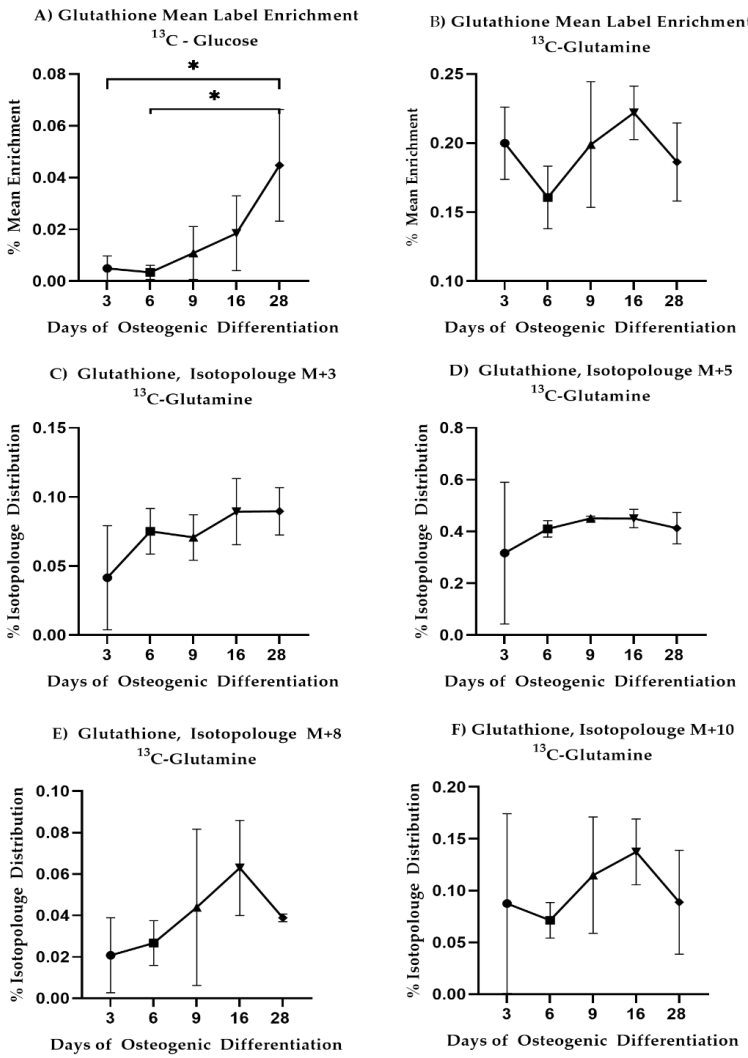

Figure 9 | Mean label enrichment for A) ^{13}C-glucose and B) ^{13}C-glutamine in intracellular glutathione, with C)-F) isotopologue distribution for ^{13}C-glutamine. *Shown area average values (n=3, SD).*

3.10 ***Gene expression analysis indicates major changes in cellular function during osteogenic differentiation***

Towards a better understanding of the molecular mechanisms behind osteogenesis differentiation and observed metabolic changes, we sought to quantify which transcriptional changes occurred along with this transition.

We sampled cell cultures on days 3, 6, 16 and 28 for RNA sequencing. We performed transcriptome quantification and gene differential expression calling with kallisto and DESeq2 respectively[22], [34]. Furthermore, we filtered out differentially expressed genes (DEGs) that (i) were lowly expressed, (ii) showed relatively small fold-change (FC) differences, (iii) had highly variable expression across

biological replicates, and (iv) had inconsistent expression between patients—see Methods for details—resulting in a total set of 1,106 DEGs across all experimental conditions (**Suppl. Info. Table SIT1**).

We sought to investigate the major sources of variation in the set of DEGs. We used principal component analysis (PCA) to project all samples into the two principal components (PCs) that maximized data variance. We found that differentiation time strongly associates with PC1 (52% of total variance), indicating that differentiation trajectory is the major experimental source of transcriptome variation (**Fig. 10A**). PC2 (10% of total variance) discriminates samples from two patients on the last differentiation time point (Day 28), indicative of a smaller divergence in cell differentiation trajectories between these two patients. Therefore, we conclude that cell differentiation is the major source of transcriptome variation and that trajectory divergence between two particular patients accounts for a smaller secondary source of variation.

Next, we pursued to characterize the transcriptional changes associated with the differentiation process. Towards this goal, we identified the set of DEGs and their associated cellular functions between the last and first sampled time points. In later stages of differentiation, we found 488 upregulated DEGs of which 25 are transcription factors (TFs) and 81 metabolic genes (MGs). Similarly, we found a total set of 453 downregulated DEGs containing 12 TFs and 81 MGs (**Fig. 10B** and **Suppl. Info. Table SIT2**). We further explored which cellular pathways are associated with DEGs using gene set ontology enrichment analysis (see Methods).

The top three most upregulated TFs are *FOS*, *RORB* and *NR1D1* with a fold-change of 54, 24 and 15, respectively. Other key upregulated TFs are *PPARG*, *BCL6*, *FOXO1*, *CEBPD* and *NFYB*. Different subsets of these TFs associate with enriched ontologies along three main cellular axes: inhibition of cell death (FOXO-mediated transcription of cell death genes), signalling (interleukin-4 and interleukin-13 signalling) and metabolism (regulation of lipid metabolism by PPARα). **Suppl. Info. Table SIT3** contains all found enriched ontologies. With respect to metabolic genes, the top three most upregulated genes are *ADH1B*, *APOE* and *MAOA* with a fold-change of 52, 50 and 36, respectively. Other upregulated genes encoding influential enzymes are *PTGDS*, *GPX3*, *PDK4*, *SOD2* and *DGAT2*. In this gene set, ontology analysis revealed enriched functions revolving around lipid metabolism (chylomicron clearance, steroid hormone, arachidonic acid and fatty acid metabolisms), compound functionalization and biological oxidation and iron uptake and transport. In addition to TFs and metabolic genes, we identified an upregulated set of 382 other genes. Examples of this set are *IGF2*, *IL1RL1*, *FGF7*, and *TLR3* with a fold-change of 37, 36, 16, and 2, respectively. We would highlight four enriched functions in this set: degradation of the extracellular matrix, interferon and insulin-like growth factor signalling and regulation of the complement cascade. In summary, this set of 488 upregulated DEGs reflects the profound biological shift occurring during the process of osteogenic differentiation.

Just as functionally important as gene upregulation is gene downregulation. Thus, we also determined which genes and biological functions are repressed between the late and early stages of differentiation. The top three downregulated TFs are *MYBL2*, *FOXM1* and *E2F1* with a fold-change of 13, 9 and 8, respectively (**Suppl. Info. Table SIT2**). Other key downregulated TFs are *OSR1*, *HMGA2* and *DNMT1*. The last two genes encode proteins that regulate chromatin accessibility which suggests ongoing chromatin rearrangements. Furthermore, *OSR1* is a direct target of RUNX2 [35] and its negative regulation is key for osteoblastic differentiation[36]. With regard to metabolic genes, the top three most downregulated genes are *RRM2*, *PKMYT1* and *UBE2C*, with a fold-change of 21, 17 and 16, respectively. Collectively, cell cycle-related functions are overwhelmingly enriched in this set of downregulated genes: G2/M transition, mitotic anaphase, regulation of mitotic cell cycle, DNA replication initiation and centrosome maturation are just a few examples of the biological functions significantly enriched in the set of repressed genes in later stages of differentiation (**Suppl. Info. Table SIT3**). Selected examples of downregulated genes that align with these functions are *CDK1*, *CDC25A* and *POLE*. Furthermore,

we noted other enriched functions, e.g., metabolism of carbohydrates, reduction of cytosolic Ca^{2+} levels and solute-carrier mediated transmembrane transport. Particularly interesting is the downregulation of *SLC25A10*, a gene that encodes the mitochondrial dicarboxylate carrier, which transports dicarboxylates such as malonate, malate, and succinate across the inner mitochondrial membrane, thus potentially regulating key metabolic pathways like gluconeogenesis and fatty acid biosynthesis among others. Aside from TFs and metabolic genes, we identified a downregulated set of 360 other genes. This set is also consistently enriched in functions related to cell cycle progression. Moreover, other key factors of this set known to be implicated in osteogenic differentiation are *IL6* and *CXCL12* [37], [38]. In summary, this set of 453 downregulated DEGs reflects a substantial reduction in cell cycle progression during osteogenic differentiation.

Fate decision of mesenchymal stem cells to either adipocytes or osteoblasts is controlled by many factors including the interplay between RUNX2 and PPARγ [39]. Consequently, we sought to quantify the temporal expression profile of *RUNX2* and *PPARG*. We visualized both *RUNX2* and *PPARG* expression levels across time (**Fig. 10C**). We found that *PPARG* expression pattern is increasing, starting from 4 transcripts per million (TPM) on Day 3, to 17 TPM on Day 28 (adjusted $P < 2 \times 10^{-12}$ and adjusted $P < 5 \times 10^{-12}$ for two patients, respectively). *RUNX2* instead, while it also increases from 14 TPM to 27 TPM, its temporal profile is mainly flat with a sharp increase from Day 3 to Day 6. *RUNX2* Day 28 vs Day 3 contrast is significant only for one patient (adjusted $P = 6.00 \times 10^{-2}$ and adjusted $P = 6.44 \times 10^{-3}$ for two patients, respectively) and did not pass our fold-change filter (abs $\log_2$ FC > 1). Altogether, while both genes have a higher expression in the late stages of our experiment, the increasing trend for *PPARG* is more considerable than for *RUNX2*. This observation is in contradiction with the role of RUNX2 as a determinant of osteogenic fate in mesenchymal stromal cells and PPARγ as a counterpoint determining adipogenic fate [40], [41]. We propose several possible scenarios to reconcile this observation: (1) *RUNX2*/*PPARG* transcriptional toggle switch occurred much earlier than Day 3 and therefore we observed a stage already committed for these two master regulators, (2) RUNX2/PPARγ activity may be predominantly controlled by post-transcriptional modifications, e.g., MAPK-dependent phosphorylation status [42], and (3) changes in other activating/repressing factors. For example, we found upregulation of both *CEBPB* and *CEBPD*, which are vital for both adipogenic [43], [44] and osteogenic identity [45], [46]. In parallel, two PPARγ coactivators are differentially expressed, but in opposite directions: *PPARGC1A* is upregulated (from 0 to 8 TPM; $\log_2$ FC = 3.17) and *PPRC1* is downregulated (from 30 to 7 TPM; $\log_2$ FC = -1.95). These findings suggest that mesenchymal stromal cells commitment to either osteogenic or adipogenic fates is a rather complex decision involving multiple molecular regulators and interactions at various regulatory levels, ranging from genomic to transcriptional and post-translational mechanisms.

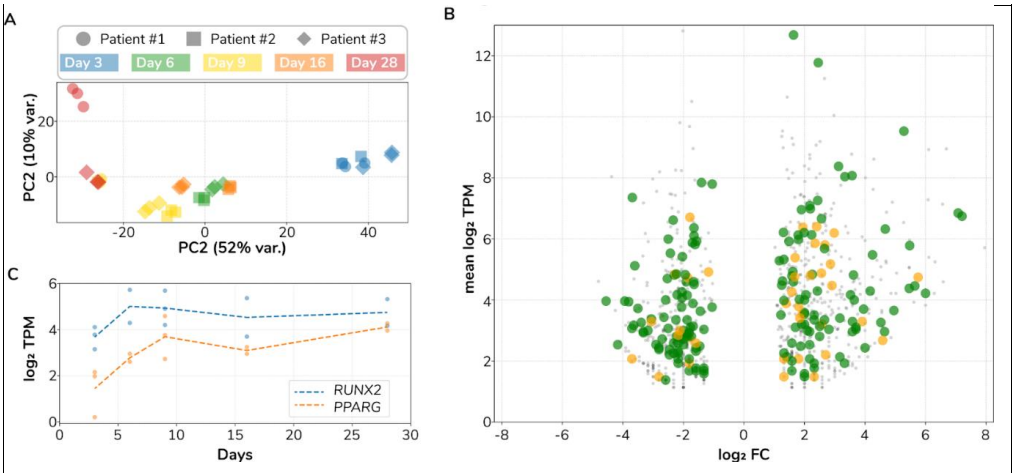

Figure 10 | ***Expression analysis indicates major transcriptional changes.*** ***A****. Principal component analysis projection of sampled transcriptomes. PC, principal component.* ***B****. Scatter plot of differentially expressed genes between last (Day 28) and first sampled (Day 3) time points. Transcription factors are highlighted as large orange dots; metabolic genes as large green dots. FC, fold-change; TPM, transcripts per million.* ***C****. Expression profiles for RUNX2 and PPARG.*

3.11 ***Regulatory influence inference reveals a cell state switch***

Gene regulatory influence inference methods identify regulators of transcriptional response [47]. We took such an approach to infer which regulators, in this case, transcription factors (TFs) control the observed transcriptional changes during osteogenic differentiation. First, we determined regulon memberships. We defined a *regulon* as a set of expression coherent target genes that all share a binding site for a given TF and collectively correlate to such TF expression (see Methods). We identified 111 regulons involving 111 TFs and 469 corresponding target genes. We observed a typical regulon size of nine target genes, ranging from as low as two and up to 123 target genes. We assigned regulons identifiers using the name of the regulator plus the number of target genes separated by a dot, e.g., our largest regulon, E2F8.123, consists of 123 target genes regulated by the transcription factor E2F8. All regulon memberships including their activity across sampled differentiation time points are provided as **Suppl. Info. Table SIT4**. We visualized regulon activity over time (**Fig. 11A**). We observed an evident switch pattern where a set of 60 regulons shifted from active to inactive while 51 other regulons followed the inverse transition. More than 50% of upregulated regulon target genes are controlled by just six TFs: ZNF521, FOXC1, PRRX2, TGIF1, ARID5B and OSR2. ZNF521, the controller of the largest upregulated regulon ZNF521.45, is a negative regulator of the adipogenic differentiation fate in mesenchymal stem cells[48]. FOXC1, PRRX2, TGIF1 and OSR2 are all known regulators of osteogenic differentiation [49]–[52]. However, ARID5B had not been yet implicated as a regulator of osteogenic differentiation to the best of our knowledge. Regarding the downregulation response, just three E2Fs (E2F1, E2F4 and E2F8) control up to 59% of all downregulated regulon target genes. E2Fs are well-known regulators of cell-cycle progression, apoptosis and DNA synthesis [53], which aligns well with our previous findings from the ontology analysis on downregulated DEGs (**Suppl. Info. Table SIT3**). E2Fs role in specifying either osteocyte or adipocyte cell fates is still unclear with positive and negative influences from different family members at different stages of differentiation which complicates a simple interpretation of this finding [54], [55]. Furthermore, we show in **Fig. 11B** selected examples of regulon profiles across time including the TF and their target genes expression. The activity profiles of only three regulons do not strictly match a switch pattern: NFATC4.6, POU6F1.3 and ZFP90.2 display an early strong upregulation with a slower relaxation to near basal levels. From a systems perspective,

we observed a fairly ordered system at both early and late differentiation time points, with regulon activity constrained to either on or off states. On the contrary, intermediate time points manifest a much higher system entropy with regulons exploring a broad range of activity levels. This pattern is consistent with a critical state transition before a bifurcation point [56] and has been experimentally observed in other differentiation systems [57]. Overall, regulatory influence inference revealed a transcriptional state switch in osteogenic differentiation of mesenchymal stromal cells.

TFs regulate target genes which may also be TFs potentially establishing a network of regulatory influences with simple but functionally rich network structures like network motifs [58]. In order to determine the network structure of regulatory influences in the osteogenic differentiation process, we considered a directed edge between two given TFs *A* and *B* if *A* (as the node tail) is the TF of a regulon and *B* (as the head node) is one of its target genes. We built a network of 28 TFs and 26 TF-TF regulatory influence interactions which collectively control 303 target genes (**Fig. 11C**). We observed regulatory cascades, e.g., ZBTB47 ➜ JDP2 ➜ TSC22D1; nodes integrating information from multiple upstream nodes, e.g., CEBPB integrates regulatory influences from four other TFs; subnetworks very close to bi-fans, as FOXC1, TBX15, KLF11 and FOXO1 are one interaction away from the bi-fan motif; and denser and more complex interacting subgraphs, e.g., the downregulation response influence component with nodes integrating information from multiple nodes and concurrently regulating various other nodes. Conclusively, we found a rich network of regulatory influences controlling the osteogenic differentiation of mesenchymal stromal cells. This network has the potential to inform future perturbation experiments to validate the identity of presented master regulators, ultimately facilitating control of the differentiation process.

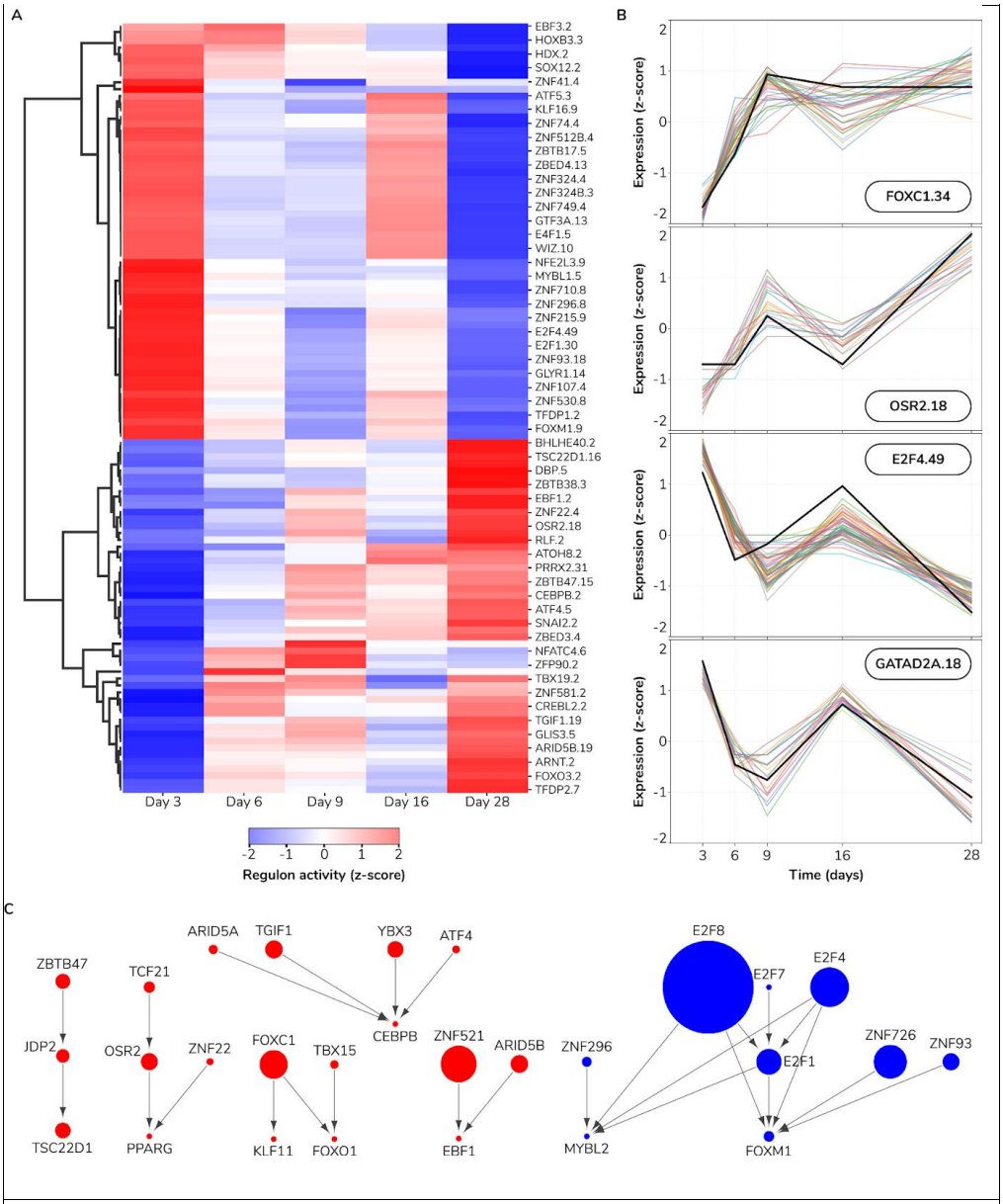

Figure 11 | Gene regulatory influence inference reveals a transcriptional switch in osteogenic differentiation. A*. Regulon activity heatmap.* ***B****. Expression profile of selected regulons. Each line depicts a gene expression profile: black thick lines correspond to the regulon TF, other lines correspond to regulon target genes.* ***C****. TF-TF network. Each node represents a TF. Node size maps to the number of target genes of a particular regulator. Red and blue colours indicate transcriptional upregulation and downregulation, respectively. Directed edges denote inferred transcriptional influences*

4. Discussion

Currently, a barrier to the development of MSC therapeutics is a lack of in depth understanding of the changes occurring within the metabolic processes that are underlying osteogenic differentiation and

proliferation [59]. In this study we utilized limited extracellular metabolites to put forth a hypothesis regarding timepoints of particular metabolic shifts and then used said hypothesis to execute more detailed metabolic studies around those focused time points with the goal of observing where the changes or differences lay.

4.1 Increase in mitochondrial activity following day 9 – a possible point of enhancement?

Through analysis of a limited number of extracellular metabolites an initial hypothesis, based on change point analysis, suggested 2 metabolic switches to be in place over the course of 28 days of osteogenic differentiation (splitting the time into three phases). When looking into broader changes via untargeted analysis of intracellular metabolites, a further support for this initial hypothesis was seen. A separation between days 3, 9 and 28 (see figure 7) was observed, with a clear distinction between day 3 and day 28, and day 9 and day 28. The overlap observed between days 3, 6, and 9, despite going against our original hypothesis, is in concurrence with other reports of metabolic behavior of MSCs during osteogenic differentiation [60]. The clustering of day 16 with the first three time points is unexpected given the knowledge gained from literature and suggests possible benefits in taking a more detailed look at changes occurring between day 16 and day 28.

However, elaborating on these results with more detailed labelling experiments, intracellular metabolomic analysis enabled us to identify one clear switch following day 9. The labelling results confirmed changes in glycolysis and increased mitochondrial activity, with cells diverting more glucose into the TCA cycle, indicative of a switch in metabolism. This shift into aerobic metabolism has been shown in several other studies [11], however the smaller window of change time identified in this paper can help with further focus of more detailed studies and identification of ways to enhance osteogenesis of MSCs and specific timepoints where such intervention may proof most beneficial.

For example, it has been shown that mitochondrial dysfunction impairs osteogenesis, increases the activity of osteoclasts and so can accelerate age related bone loss (i.e. osteoporosis)[61]. A similar observation has been made regarding osteoarthritic (OA) human articular chondrocytes. There mitochondrial mass within OA chondrocytes increased whilst a higher proportion of the cells had de-energized mitochondria, with reduction in activity of complexes II and III observed when compared to normal chondrocytes [62]. Coenzyme Q10 has been observed in research to inhibit aging of MSCs [63], [64] and to improve mitochondrial function and so relieve disease symptoms [65], [66]. It might thus be relevant follow up to this research to see if by supplementation of Coenzyme Q10 around day 9 during osteogenic differentiation the differentiation of MSCs could be enhanced via increased mitochondrial function.

4.2 Increased glycolysis followed by decreased PPP flux as differentiation progresses

Another change observed regarding metabolism of MSCs during osteogenic differentiation was lowered flux through PPP. This was indicated by labelling experiments, when looking at the temporal changes in isotopolouge distribution differences between M+6 and M+11 isotopolouges for ^{13}C-glucose labelling for both UDP-glucose (figure 4) and N-acetyl-UDP glucosamine (supplemental figure S4) both indicated a similar behaviour. In both instances the label enrichment into the M+6 isotopolouge (derived from glycolysis) increased temporally whilst label enrichment into M+11 (which consists of glucose from glycolysis and ribose derived from the PPP) decreased in a significant manner during that same time period, indicating decreased label enrichment coming from the M+5 isotopolouge and so a decreased flux through the PPP.

It has been shown in at least one other paper that for proliferating cells, activation of glycolysis accompanied by high activity of PPP is the preferred metabolic state [67] and as the PPP is responsible for generating NADPH that is used in reductive biosynthesis (e.g. fatty acid and ribose synthesis) its active flux can be reasoned to be necessary for MSC proliferation. One other research has additionally shown that for MSCs undergoing osteogenesis multiple cell layers are formed during the differentiation progression [60], reporting a rapid cell proliferation occurring over the course of the first week before stopping by the end of week 2. This would indicate a necessity for maintenance of high

flux through the PPP at least for the first seven days of differentiation which goes directly against what our label incorporation results indicate. There, flux through glycolysis increases (presented by glucose label incorporation) whilst, seemingly, flux through the PPP decreases. Despite this decrease the total protein amount measured in our BCA assays increased during the differentiation period. Based on these findings and the way they seem to contradict results reported in the already mentioned papers it suggests that further research into the temporal changes to the PPP and its role in osteogenic differentiation and MSC proliferation are necessary.

4.3 Temporal changes in glutaminolysis and TCA-cycle activity

When metabolic pathway analysis was utilized, a shift in redox balance during differentiation was observed with both oxidized and reduced glutathione decreasing over time.

Glutathione plays an important role when it comes to the ability of cells to manage oxidative stress, is important for proper function of oxidative phosphorylation (and thus mitochondrial respiration) and is reliant upon glutaminolysis. Glutathione levels are additionally tied into the activity level of the PPP, but the PPP provides NADPH that enables the maintenance of the reduced form of glutathione and so aids in managing oxidative stress or the redox potential of the cell. It therefore follows that an observation of reduced PPP activity is accompanied by observation of reduction of intracellular glutathione, specifically the reduced form (GSH).

When reanalyzing ^{13}C-glucose label incorporation with respect to glutathione, label incorporation increased as differentiation went on indicating an increased synthesis of glutathione from glucose derived carbons – supportive of the earlier results of an increased glycolytic flux compared to flux through the PPP. An increase into the M+5 isotopolouge of glutathione for ^{13}C-glutamine label enrichment was also seen, similar as the carbon contribution from glutamine into glutamate observed over the course of differentiation. This in conjunction with results for both ^{13}C and ^{15}N labelled glutamine label incorporation into glutamate and aspartate suggest altered glytaminolysis and an increased flux into the TCA cycle as had been suggested before [11]. All suggests increased involvement of mitochondrial respiration which has been reported as essential for successful osteogenesis.

4.4 Unexpected changes in lipolysis suggest next steps

The metabolic pathway analysis revealed a slightly surprising result in that changes to lipolysis during differentiation were observed during untargeted analysis (see figure 8).

No additional lipidomics were performed as a part of the research for this paper but these results suggest it as a tantalizing future direction to take in order to explore other metabolic pathways significantly involved in metabolic changes observed during osteogenic differentiation.

It has been reported that in order for normal skeletal homeostasis to be preserved osteoblasts need to be able to utilize lipids for energy and so mitochondrial long chain fatty acid oxidation has to be active [68]. Additionally, as has been reported, since during osteogenesis MSCs continue proliferating that requires synthesis of new membranes that largely consist of lipids and so changes in lipolytic function and utilization or need for fatty acids are a reasonable expectation. Tied together with a seemingly increased need for energy as osteogenesis progresses fatty acid oxidation during osteogenic differentiation and the temporal changes in lipidomics provide an interesting avenue to look into as a next step.

4.5 Upregulated lipid metabolism and downregulated cell-cycle related anabolic activity observed via DEGs.

The addition of gene expression analysis lent further support to the notion of distinct cell metabotypes existing throughout the differentiation period with clear indicator of differentiation progression being the major experimental source for the transcriptome variation observed. Furthermore, the upregulation observed in the regulation of lipid metabolism (e.g. fatty acid metabolism) on top of the changes in lipolysis gained from metabolomic data highlights the apparent importance of fatty acids as a source of energy for successful osteogenesis reported in literature [68]. With the indications of lipolytic

importance observed from both the data and the literature, addition of lipidomics to the data analysis in order to get a more comprehensive view of what metabolic pathways play a vital role in successful osteogenesis seems of even greater importance. The apparent mismatch between measured protein content (cell mass) throughout the differentiation and the observed downregulation of cell cycle related activity and matching decrease in flux through pathways connected to proliferation also requires further validation. Linking the DEGs with observed changes in metabolite concentrations and metabolic flux to see how coherently gene expression matches enzyme and subsequent protein/metabolite activity may help to identify perturbation experiments that may result in an actual desired phenotypic change.

The regulatory network shown to exist in this paper both highlights the complexity involved in the control of osteogenic differentiation and the importance of accurate identification of master regulators, at the same time as it offers a way to predict downstream metabolic and functional effects that can be gained from well informed perturbation experiments.

5. Conclusions

In conclusion, the changes observed in our study support distinct differences between early- and late-stage osteogenesis on both metabolic and transcriptomic level: there is an initial preparatory and proliferation stage, coinciding with high ALP activity, while later there is a plateau stage with lower ALP activity and possibly higher calcium accumulation. Our metabolomic analysis further supports these two stages, and preliminary results using general differential gene expression analysis indicate the possibility of three stages with a transcriptional state flip occurring between initial and last steps. Future functional work will be needed to fully define the relationships between transcriptomic, metabolic and functional changes. The current experiments also showed a high degree of inter-donor variability, with respect to both metabolism and osteogenic outcome. Further work to understand these differences will hopefully lead to the identification of metabolic biomarkers or master regulators for successful osteogenesis, and possibly to interventions for increasing the success rate. Furthermore, it may be interesting to explore the observed lipolytic changes and related mitochondrial activity in a continuous manner around suggested time points of interest through such technology as Seahorse [69], [70] technique and explore if by impacting the mitochondria in a positive manner can lead to a faster progression of osteogenesis. Such experiments would improve our understanding of how metabolism impacts the ability of cells to differentiate.

References

[1] V. Campana *et al.*, "Bone substitutes in orthopaedic surgery: from basic science to clinical practice," *J. Mater. Sci. Mater. Med.*, vol. 25, no. 10, pp. 2445–2461, Oct. 2014, doi: 10.1007/s10856-014-5240-2.

[2] C. E *et al.*, "Autograft, allograft and bone substitutes in reconstructive orthopedic surgery.," *Aging Clin. Exp. Res.*, vol. 25 Suppl 1, pp. S101-3, Sep. 2013, doi: 10.1007/s40520-013-0088-8.

[3] "Bone Grafts & Substitutes Market Size, Share | Industry Report, 2026." https://www.grandviewresearch.com/industry-analysis/bone-grafts-substitutes-market (accessed Oct. 10, 2020).

[4] R. Marsell and T. A. Einhorn, "THE BIOLOGY OF FRACTURE HEALING," *Injury*, vol. 42, no. 6, pp. 551–555, Jun. 2011, doi: 10.1016/j.injury.2011.03.031.

[5] A. Nauth and E. H. Schemitsch, “Stem cells for the repair and regeneration of bone,” *Indian J. Orthop.*, vol. 46, no. 1, pp. 19–21, 2012, doi: 10.4103/0019-5413.91630.
[6] J. Neman, A. Hambrecht, C. Cadry, and R. Jandial, “Stem cell-mediated osteogenesis: therapeutic potential for bone tissue engineering,” *Biol. Targets Ther.*, vol. 6, pp. 47–57, 2012, doi: 10.2147/BTT.S22407.
[7] R. Vaishya, M. Chauhan, and A. Vaish, “Bone cement,” *J. Clin. Orthop. Trauma*, vol. 4, no. 4, pp. 157–163, Dec. 2013, doi: 10.1016/j.jcot.2013.11.005.
[8] Z. Gazit, G. Pelled, D. Sheyn, N. Kimelman, and D. Gazit, “Chapter 19 - Mesenchymal Stem Cells,” in *Essentials of Stem Cell Biology (Third Edition)*, R. Lanza and A. Atala, Eds. Boston: Academic Press, 2014, pp. 255–266. doi: 10.1016/B978-0-12-409503-8.00019-6.
[9] Z.-L. Deng *et al.*, “Regulation of osteogenic differentiation during skeletal development,” *Front. Biosci. J. Virtual Libr.*, vol. 13, pp. 2001–2021, Jan. 2008, doi: 10.2741/2819.
[10] C.-T. Chen, Y.-R. V. Shih, T. K. Kuo, O. K. Lee, and Y.-H. Wei, “Coordinated changes of mitochondrial biogenesis and antioxidant enzymes during osteogenic differentiation of human mesenchymal stem cells,” *Stem Cells Dayt. Ohio*, vol. 26, no. 4, pp. 960–968, Apr. 2008, doi: 10.1634/stemcells.2007-0509.
[11] G. Pattappa, H. K. Heywood, J. D. de Bruijn, and D. A. Lee, “The metabolism of human mesenchymal stem cells during proliferation and differentiation,” *J. Cell. Physiol.*, vol. 226, no. 10, pp. 2562–2570, Oct. 2011, doi: 10.1002/jcp.22605.
[12] S. Lc, W. Ns, M. Bn, B. Kl, and E. Ra, “Energy Metabolism in Mesenchymal Stem Cells During Osteogenic Differentiation.,” *Stem Cells Dev.*, vol. 25, no. 2, pp. 114–122, Dec. 2015, doi: 10.1089/scd.2015.0193.
[13] M. F. Forni, J. Peloggia, K. Trudeau, O. Shirihai, and A. J. Kowaltowski, “Murine Mesenchymal Stem Cell Commitment to Differentiation is Regulated by Mitochondrial Dynamics,” *Stem Cells Dayt. Ohio*, vol. 34, no. 3, pp. 743–755, Mar. 2016, doi: 10.1002/stem.2248.
[14] A. V. Meleshina *et al.*, “Probing metabolic states of differentiating stem cells using two-photon FLIM,” *Sci. Rep.*, vol. 6, no. 1, Art. no. 1, Feb. 2016, doi: 10.1038/srep21853.
[15] Q. Li, Z. Gao, Y. Chen, and M.-X. Guan, “The role of mitochondria in osteogenic, adipogenic and chondrogenic differentiation of mesenchymal stem cells,” *Protein Cell*, vol. 8, no. 6, pp. 439–445, Jun. 2017, doi: 10.1007/s13238-017-0385-7.
[16] T. Huang *et al.*, “Aging Reduces an ERRalpha-Directed Mitochondrial Glutaminase Expression Suppressing Glutamine Anaplerosis and Osteogenic Differentiation of Mesenchymal Stem Cells,” *Stem Cells Dayt. Ohio*, vol. 35, no. 2, pp. 411–424, 2017, doi: 10.1002/stem.2470.
[17] P. M. Brown, J. D. Hutchison, and J. C. Crockett, “Absence of glutamine supplementation prevents differentiation of murine calvarial osteoblasts to a mineralizing phenotype,” *Calcif. Tissue Int.*, vol. 89, no. 6, pp. 472–482, Dec. 2011, doi: 10.1007/s00223-011-9537-6.
[18] N. Muñoz, J. Kim, Y. Liu, T. M. Logan, and T. Ma, “Gas chromatography-mass spectrometry analysis of human mesenchymal stem cell metabolism during proliferation and osteogenic differentiation under different oxygen tensions,” *J. Biotechnol.*, vol. 169, pp. 95–102, Jan. 2014, doi: 10.1016/j.jbiotec.2013.11.010.
[19] M. E. Klontzas, S. I. Vernardis, M. Heliotis, E. Tsiridis, and A. Mantalaris, “Metabolomics Analysis of the Osteogenic Differentiation of Umbilical Cord Blood Mesenchymal Stem Cells Reveals Differential Sensitivity to Osteogenic Agents,” *Stem Cells Dev.*, vol. 26, no. 10, pp. 723–733, May 2017, doi: 10.1089/scd.2016.0315.
[20] Q. Zhao, H. Ren, and Z. Han, “Mesenchymal stem cells: Immunomodulatory capability and clinical potential in immune diseases,” *J. Cell. Immunother.*, vol. 2, no. 1, pp. 3–20, Mar. 2016, doi: 10.1016/j.jocit.2014.12.001.
[21] L. M. Simon *et al.*, “Human platelet microRNA-mRNA networks associated with age and gender revealed by integrated plateletomics,” *Blood*, vol. 123, no. 16, pp. e37–e45, Apr. 2014, doi: 10.1182/blood-2013-12-544692.

[22] M. I. Love, W. Huber, and S. Anders, "Moderated estimation of fold change and dispersion for RNA-seq data with DESeq2," *Genome Biol.*, vol. 15, no. 12, p. 550, Dec. 2014, doi: 10.1186/s13059-014-0550-8.
[23] L. Garcia-Alonso, C. H. Holland, M. M. Ibrahim, D. Turei, and J. Saez-Rodriguez, "Benchmark and integration of resources for the estimation of human transcription factor activities," *Genome Res.*, vol. 29, no. 8, pp. 1363–1375, Aug. 2019, doi: 10.1101/gr.240663.118.
[24] E. Brunk *et al.*, "Recon3D enables a three-dimensional view of gene variation in human metabolism," *Nat. Biotechnol.*, vol. 36, no. 3, pp. 272–281, Mar. 2018, doi: 10.1038/nbt.4072.
[25] S. Carbon *et al.*, "AmiGO: online access to ontology and annotation data," *Bioinformatics*, vol. 25, no. 2, pp. 288–289, Jan. 2009, doi: 10.1093/bioinformatics/btn615.
[26] P. Shannon *et al.*, "Cytoscape: A Software Environment for Integrated Models of Biomolecular Interaction Networks," *Genome Res.*, vol. 13, no. 11, pp. 2498–2504, Nov. 2003, doi: 10.1101/gr.1239303.
[27] "R: The R Project for Statistical Computing." https://www.r-project.org/ (accessed Oct. 10, 2020).
[28] S. Wood and F. Scheipl, "Package 'gamm4': Generalized Additive Mixed Models using 'mgcv' and 'lme4.'" Apr. 03, 2020. [Online]. Available: https://cran.r-project.org/web/packages/gamm4/gamm4.pdf
[29] N. A. James and D. S. Matteson, "ecp: An R Package for Nonparametric Multiple Change Point Analysis of Multivariate Data," *ArXiv13093295 Stat*, Nov. 2013, Accessed: Oct. 10, 2020. [Online]. Available: http://arxiv.org/abs/1309.3295
[30] S. Li *et al.*, "Predicting Network Activity from High Throughput Metabolomics," *PLOS Comput. Biol.*, vol. 9, no. 7, p. e1003123, Jul. 2013, doi: 10.1371/journal.pcbi.1003123.
[31] "IsoCor: Isotope Correction for mass spectrometry labeling experiments — IsoCor 2.2.0 documentation." https://isocor.readthedocs.io/en/latest/ (accessed Feb. 23, 2021).
[32] M. Bruderer, R. G. Richards, M. Alini, and M. J. Stoddart, "Role and regulation of RUNX2 in osteogenesis," *Eur. Cell. Mater.*, vol. 28, pp. 269–286, Oct. 2014, doi: 10.22203/ecm.v028a19.
[33] E. E. Golub and K. Boesze-Battaglia, "The role of alkaline phosphatase in mineralization:," *Curr. Opin. Orthop.*, vol. 18, no. 5, pp. 444–448, Sep. 2007, doi: 10.1097/BCO.0b013e3282630851.
[34] N. L. Bray, H. Pimentel, P. Melsted, and L. Pachter, "Near-optimal probabilistic RNA-seq quantification," *Nat. Biotechnol.*, vol. 34, no. 5, pp. 525–527, May 2016, doi: 10.1038/nbt.3519.
[35] M. Yamauchi, S. Kawai, T. Kato, T. Ooshima, and A. Amano, "Odd-skipped related 1 gene expression is regulated by Runx2 and Ikzf1 transcription factors," *Gene*, vol. 426, no. 1, pp. 81–90, Dec. 2008, doi: 10.1016/j.gene.2008.08.015.
[36] S. Stricker, S. Mathia, J. Haupt, P. Seemann, J. Meier, and S. Mundlos, "Odd-Skipped Related Genes Regulate Differentiation of Embryonic Limb Mesenchyme and Bone Marrow Mesenchymal Stromal Cells," *Stem Cells Dev.*, vol. 21, no. 4, pp. 623–633, Mar. 2012, doi: 10.1089/scd.2011.0154.
[37] K. L. Pricola, N. Z. Kuhn, H. Haleem-Smith, Y. Song, and R. S. Tuan, "Interleukin-6 maintains bone marrow-derived mesenchymal stem cell stemness by an ERK1/2-dependent mechanism," *J. Cell. Biochem.*, vol. 108, no. 3, pp. 577–588, 2009, doi: 10.1002/jcb.22289.
[38] C. Liu *et al.*, "CXCL12/CXCR4 Signal Axis Plays an Important Role in Mediating Bone Morphogenetic Protein 9-induced Osteogenic Differentiation of Mesenchymal Stem Cells," *Int. J. Med. Sci.*, vol. 10, no. 9, pp. 1181–1192, 2013, doi: 10.7150/ijms.6657.
[39] Q. Chen *et al.*, "Fate decision of mesenchymal stem cells: adipocytes or osteoblasts?," *Cell Death Differ.*, vol. 23, no. 7, pp. 1128–1139, Jul. 2016, doi: 10.1038/cdd.2015.168.
[40] F. Otto *et al.*, "Cbfa1, a Candidate Gene for Cleidocranial Dysplasia Syndrome, Is Essential for Osteoblast Differentiation and Bone Development," *Cell*, vol. 89, no. 5, pp. 765–771, May 1997, doi: 10.1016/S0092-8674(00)80259-7.
[41] E. D. Rosen *et al.*, "PPARγ Is Required for the Differentiation of Adipose Tissue In Vivo and In Vitro," *Mol. Cell*, vol. 4, no. 4, pp. 611–617, Oct. 1999, doi: 10.1016/S1097-2765(00)80211-7.
[42] L. A. Stechschulte and B. Lecka-Czernik, "Reciprocal Regulation of PPARγ and RUNX2 Activities in Marrow Mesenchymal Stem Cells: Fine Balance between p38 MAPK and Protein

Phosphatase 5," *Curr. Mol. Biol. Rep.*, vol. 3, no. 2, pp. 107–113, Jun. 2017, doi: 10.1007/s40610-017-0056-8.
[43] Z. Cao, R. M. Umek, and S. L. McKnight, "Regulated expression of three C/EBP isoforms during adipose conversion of 3T3-L1 cells.," *Genes Dev.*, vol. 5, no. 9, pp. 1538–1552, Sep. 1991, doi: 10.1101/gad.5.9.1538.
[44] Z. Wu *et al.*, "Cross-Regulation of C/EBPα and PPARγ Controls the Transcriptional Pathway of Adipogenesis and Insulin Sensitivity," *Mol. Cell*, vol. 3, no. 2, pp. 151–158, Feb. 1999, doi: 10.1016/S1097-2765(00)80306-8.
[45] H. Tominaga *et al.*, "CCAAT/Enhancer-binding Protein β Promotes Osteoblast Differentiation by Enhancing Runx2 Activity with ATF4," *Mol. Biol. Cell*, vol. 19, no. 12, pp. 5373–5386, Dec. 2008, doi: 10.1091/mbc.e08-03-0329.
[46] M. B. Meyer, N. A. Benkusky, B. Sen, J. Rubin, and J. W. Pike, "Epigenetic Plasticity Drives Adipogenic and Osteogenic Differentiation of Marrow-derived Mesenchymal Stem Cells*," *J. Biol. Chem.*, vol. 291, no. 34, pp. 17829–17847, Aug. 2016, doi: 10.1074/jbc.M116.736538.
[47] M. M. Saint-Antoine and A. Singh, "Network inference in systems biology: recent developments, challenges, and applications," *Curr. Opin. Biotechnol.*, vol. 63, pp. 89–98, Jun. 2020, doi: 10.1016/j.copbio.2019.12.002.
[48] E. Chiarella *et al.*, "ZNF521 Has an Inhibitory Effect on the Adipogenic Differentiation of Human Adipose-Derived Mesenchymal Stem Cells," *Stem Cell Rev. Rep.*, vol. 14, no. 6, pp. 901–914, Dec. 2018, doi: 10.1007/s12015-018-9830-0.
[49] F. Mirzayans, R. Lavy, J. Penner-Chea, and F. B. Berry, "Initiation of Early Osteoblast Differentiation Events through the Direct Transcriptional Regulation of Msx2 by FOXC1," *PLOS ONE*, vol. 7, no. 11, p. e49095, Nov. 2012, doi: 10.1371/journal.pone.0049095.
[50] X. Kang, Y. Sun, and Z. Zhang, "Identification of key transcription factors - gene regulatory network related with osteogenic differentiation of human mesenchymal stem cells based on transcription factor prognosis system," *Exp. Ther. Med.*, vol. 17, no. 3, pp. 2113–2122, Mar. 2019, doi: 10.3892/etm.2019.7170.
[51] H. Saito *et al.*, "TG-interacting factor 1 (Tgif1)-deficiency attenuates bone remodeling and blunts the anabolic response to parathyroid hormone," *Nat. Commun.*, vol. 10, no. 1, p. 1354, Mar. 2019, doi: 10.1038/s41467-019-08778-x.
[52] S. Kawai, M. Yamauchi, S. Wakisaka, T. Ooshima, and A. Amano, "Zinc-Finger Transcription Factor Odd-Skipped Related 2 Is One of the Regulators in Osteoblast Proliferation and Bone Formation," *J. Bone Miner. Res.*, vol. 22, no. 9, pp. 1362–1372, 2007, doi: 10.1359/jbmr.070602.
[53] H.-Z. Chen, S.-Y. Tsai, and G. Leone, "Emerging roles of E2Fs in cancer: an exit from cell cycle control," *Nat. Rev. Cancer*, vol. 9, no. 11, pp. 785–797, Nov. 2009, doi: 10.1038/nrc2696.
[54] L. Fajas, R. L. Landsberg, Y. Huss-Garcia, C. Sardet, J. A. Lees, and J. Auwerx, "E2Fs Regulate Adipocyte Differentiation," *Dev. Cell*, vol. 3, no. 1, pp. 39–49, Jul. 2002, doi: 10.1016/S1534-5807(02)00190-9.
[55] S. Flowers, F. Xu, and E. Moran, "Cooperative Activation of Tissue-Specific Genes by pRB and E2F1," *Cancer Res.*, vol. 73, no. 7, pp. 2150–2158, Apr. 2013, doi: 10.1158/0008-5472.CAN-12-1745.
[56] M. Scheffer *et al.*, "Anticipating Critical Transitions," *Science*, vol. 338, no. 6105, pp. 344–348, Oct. 2012, doi: 10.1126/science.1225244.
[57] N. Moris, C. Pina, and A. M. Arias, "Transition states and cell fate decisions in epigenetic landscapes," *Nat. Rev. Genet.*, vol. 17, no. 11, pp. 693–703, Nov. 2016, doi: 10.1038/nrg.2016.98.
[58] S. S. Shen-Orr, R. Milo, S. Mangan, and U. Alon, "Network motifs in the transcriptional regulation network of Escherichia coli," *Nat. Genet.*, vol. 31, no. 1, pp. 64–68, May 2002, doi: 10.1038/ng881.
[59] Þ. Sigmarsdóttir, S. McGarrity, Ó. Rolfsson, J. T. Yurkovich, and Ó. E. Sigurjónsson, "Current Status and Future Prospects of Genome-Scale Metabolic Modeling to Optimize the Use of Mesenchymal Stem Cells in Regenerative Medicine," *Front. Bioeng. Biotechnol.*, vol. 8, Mar. 2020, doi: 10.3389/fbioe.2020.00239.

[60] H. Hanna, L. M. Mir, and F. M. Andre, "In vitro osteoblastic differentiation of mesenchymal stem cells generates cell layers with distinct properties," *Stem Cell Res. Ther.*, vol. 9, no. 1, p. 203, Jul. 2018, doi: 10.1186/s13287-018-0942-x.
[61] P. F. Dobson *et al.*, "Mitochondrial dysfunction impairs osteogenesis, increases osteoclast activity, and accelerates age related bone loss," *Sci. Rep.*, vol. 10, no. 1, Art. no. 1, Jul. 2020, doi: 10.1038/s41598-020-68566-2.
[62] E. Maneiro *et al.*, "Mitochondrial respiratory activity is altered in osteoarthritic human articular chondrocytes," *Arthritis Rheum.*, vol. 48, no. 3, pp. 700–708, Mar. 2003, doi: 10.1002/art.10837.
[63] D. Zhang *et al.*, "Coenzyme Q10 Inhibits the Aging of Mesenchymal Stem Cells Induced by D-Galactose through Akt/mTOR Signaling," *Oxid. Med. Cell. Longev.*, vol. 2015, p. e867293, Feb. 2015, doi: 10.1155/2015/867293.
[64] D. Zheng *et al.*, "Coenzyme Q10 promotes osteoblast proliferation and differentiation and protects against ovariectomy-induced osteoporosis," *Mol. Med. Rep.*, vol. 17, no. 1, pp. 400–407, Jan. 2018, doi: 10.3892/mmr.2017.7907.
[65] K. Luo *et al.*, "Therapeutic potential of coenzyme Q 10 in mitochondrial dysfunction during tacrolimus-induced beta cell injury," *Sci. Rep.*, vol. 9, no. 1, Art. no. 1, May 2019, doi: 10.1038/s41598-019-44475-x.
[66] G. Tian *et al.*, "Ubiquinol-10 Supplementation Activates Mitochondria Functions to Decelerate Senescence in Senescence-Accelerated Mice," *Antioxid. Redox Signal.*, vol. 20, no. 16, pp. 2606–2620, Jun. 2014, doi: 10.1089/ars.2013.5406.
[67] K. Ito and T. Suda, "Metabolic requirements for the maintenance of self-renewing stem cells," *Nat. Rev. Mol. Cell Biol.*, vol. 15, no. 4, pp. 243–256, Apr. 2014, doi: 10.1038/nrm3772.
[68] N. S. Alekos, M. C. Moorer, and R. C. Riddle, "Dual Effects of Lipid Metabolism on Osteoblast Function," *Front. Endocrinol.*, vol. 11, Sep. 2020, doi: 10.3389/fendo.2020.578194.
[69] "How Agilent Seahorse XF Analyzers Work | Agilent." https://www.agilent.com/en/products/cell-analysis/how-seahorse-xf-analyzers-work (accessed Jan. 13, 2021).
[70] D. Nicholas *et al.*, "Advances in the quantification of mitochondrial function in primary human immune cells through extracellular flux analysis," *PLOS ONE*, vol. 12, no. 2, p. e0170975, Feb. 2017, doi: 10.1371/journal.pone.0170975.

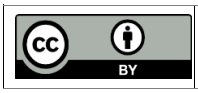

Paper II

frontiers in Cell and Developmental Biology

ORIGINAL RESEARCH
published: 04 June 2021
doi: 10.3389/fcell.2021.642681

Analyzing Metabolic States of Adipogenic and Osteogenic Differentiation in Human Mesenchymal Stem Cells via Genome Scale Metabolic Model Reconstruction

Thora Bjorg Sigmarsdottir[1], Sarah McGarrity[1,2], James T. Yurkovich[3], Óttar Rolfsson[2] and Ólafur Eysteinn Sigurjónsson[1,4,]*

[1] School of Science and Engineering, Reykjavík University, Reykjavík, Iceland, [2] Center for Systems Biology, University of Iceland, Reykjavík, Iceland, [3] Department of Bioengineering, University of California, San Diego, La Jolla, CA, United States, [4] The Blood Bank, Landspitali – The National University Hospital of Iceland, Reykjavík, Iceland

OPEN ACCESS

Edited by:
Cesare Indiveri, University of Calabria, Italy

Reviewed by:
Teresita Padilla-Benavides, Wesleyan University, United States
Yang Bi, Children's Hospital of Chongqing Medical University, China

***Correspondence:**
Ólafur Eysteinn Sigurjónsson
oes@ru.is

Specialty section:
This article was submitted to Cellular Biochemistry, a section of the journal Frontiers in Cell and Developmental Biology

Received: *08 January 2021*
Accepted: *29 April 2021*
Published: *04 June 2021*

Citation:
Sigmarsdottir TB, McGarrity S, Yurkovich JT, Rolfsson Ó and Sigurjónsson ÓE (2021) Analyzing Metabolic States of Adipogenic and Osteogenic Differentiation in Human Mesenchymal Stem Cells via Genome Scale Metabolic Model Reconstruction. Front. Cell Dev. Biol. 9:642681. doi: 10.3389/fcell.2021.642681

Since their initial discovery in 1976, mesenchymal stem cells (MSCs) have been gathering interest as a possible tool to further the development and enhancement of various therapeutics within regenerative medicine. However, our current understanding of both metabolic function and existing differences within the varying cell lineages (e.g., cells in either osteogenesis or adipogenesis) is severely lacking making it more difficult to fully realize the therapeutic potential of MSCs. Here, we reconstruct the MSC metabolic network to understand the activity of various metabolic pathways and compare their usage under different conditions and use these models to perform experimental design. We present three new genome-scale metabolic models (GEMs) each representing a different MSC lineage (proliferation, osteogenesis, and adipogenesis) that are biologically feasible and have distinctive cell lineage characteristics that can be used to explore metabolic function and increase our understanding of these phenotypes. We present the most distinctive differences between these lineages when it comes to enriched metabolic subsystems and propose a possible osteogenic enhancer. Taken together, we hope these mechanistic models will aid in the understanding and therapeutic potential of MSCs.

Keywords: GEM, MSCs, osteogenesis, metabolic reconstruction, adipogenesis, metabolic differences

INTRODUCTION

Mesenchymal stem cells (MSCs) originate in the mesenchymal germ layer of the embryo and can be isolated from various adult tissues, including bone marrow, adipose tissue and skeletal tissue to name a few. *In vitro* MSCs are a heterogeneous population of cells that can be expanded and differentiated to chondrocyte, adipocyte and osteocyte lineages (Liu et al., 2006). MSCs have been used as tissue replacements with mixed results but recent studies suggest that their paracrine effect

may be of greater clinical importance (Rosenbaum et al., 2008; Duijvestein et al., 2010; Mohyeddin Bonab et al., 2012; Campana et al., 2014; Goldberg et al., 2017; Sigmarsdóttir et al., 2020). The differentiation of MSCs is characterized by chemical and mechanical signals (such as changes to available metabolites, Croitoru-Lamoury et al., 2011; Buravkova et al., 2013) and changing metabolic capabilities (Chen et al., 2008).

This study focuses on MSCs during expansion, early osteogenesis and early adipogenesis because of the potential utility of the cells as immune-modulators (Aggarwal and Pittenger, 2005; Gan et al., 2008; Waterman et al., 2010; Neman et al., 2012; Valencia et al., 2016; Wang et al., 2018; de Castro et al., 2019) and the intricate inverse relationship that seems to exist between adipogenesis and osteogenesis. Osteoporosis is a common and sometimes a severe age related disease condition that can go on undiagnosed until a major fracture occurs. "Malfunctioning" of MSCs in osteoporosis pushes cells toward adipose accretion in the bone marrow at the expense of osteoblast formation – indicating that under this condition MSC behavior is altered and the microenvironment disturbed. A similar shift has been observed to happen under microgravity conditions, as are seen during space flights (Zayzafoon et al., 2004; Pino et al., 2012; Phetfong et al., 2016; Han et al., 2019). Understanding metabolic aspects of this shift may aid in preventing it. Moreover, understanding metabolic differences between MSCs in expansion and in osteogenic differentiation will allow optimization of *in vitro* expansion and initial *in vitro* osteogenic differentiation of MSCs needed for therapeutic techniques to succeed.

Over the past decade as the rate of biological data generation has increased, data analysis and interpretation has become a bottleneck of biological discovery (Yurkovich and Palsson, 2016), necessitating improved modeling and analysis approaches to organize and interpret data (Becker et al., 2007; Thiele and Palsson, 2010; Noronha et al., 2018). By creating a framework to integrate multiple data types (e.g., metabolomics, transcriptomics, proteomics, and genomics), genome scale metabolic models (GEMs) provide a more nuanced understanding of how the cell achieves a given metabolic state (Oberhardt et al., 2009; Thiele and Palsson, 2010; Aurich et al., 2015, 2016; Yurkovich and Palsson, 2016) that can be further tailored to specific physiological conditions using a variety of constraint-based reconstruction and analysis (COBRA) methods (Becker et al., 2007; Orth et al., 2010; Heirendt et al., 2019).

Genome scale metabolic models have been applied to various biological problems including drug resistance and biomarker identification and have been explored using these approaches (Oberhardt et al., 2009; Motamedian et al., 2015; Väremo et al., 2015). Previously, a GEM of MSC metabolism (iMSC1255) was developed (Fouladiha et al., 2015) and used to assess the effects of metabolic environmental changes on chondrogenesis and proliferation (Fouladiha et al., 2018). However, iMSC1255 is limited by only including transcriptomic data from proliferating MSCs and has not considered osteogenesis or adipogenesis explicitly. Furthermore iMSC1255 was based on Recon1 (Duarte et al., 2007), a base human metabolic reconstruction that has been superseded by Recon3 (Brunk et al., 2018). Recon3 includes greater detail of lipid metabolism and glycan metabolism that are known to be key to the processes of differentiation that these models will be used to study. To provide an improved modeling framework to study MSC osteogenic and adipogenic differentiation this paper describes a new set of three models that separately describe the metabolism of expanding MSCs (iMSC_E_1972), osteogenically differentiating MSCs (iMSC_O_1900), and adipogenically differentiating MSCs (iMSC_A_2036). These models provide improved metabolic coverage by using an updated base model from Recon3 (Brunk et al., 2018). The new models were constructed with publicly available lineage specific transcriptomic data, and new metabolomics data produced in house from each lineage. By creating this set of equivalent but separate models, it is possible to create an *in silico* laboratory that helps to design experiments for the cell culture laboratory with a higher probability of success.

Here, we describe three parallel GEMs of MSC metabolism: during expansion, iMSC-E-1972; osteogenic differentiation, iMSC-O-1900; and adipogenic differentiation, iMSC-A-2036. We have benchmarked these models against generic human metabolic functions, the existing model of MSC metabolism, iMSC1255, and known metabolic differences between lineages. We then used these benchmarked models to propose ideas for optimizing osteogenic differentiation of MSCs that will hopefully improve our understanding of the mechanisms underlying these processes.

MATERIALS AND METHODS

Transcriptomic Data Sets

Transcriptomic data were obtained from ArrayExpress (Kolesnikov et al., 2015). Data sets were selected based on their relevance to the experimental conditions described below for collection of uptake and secretion data. The most important considerations having been lineage of differentiation and the length of time since the start of differentiation (7 days). See **Table 1** for details of the data sets.

The selected data sets were processed using MATLAB (Mathworks, Natick, Massachusetts, United States). First, the data set IDs were converted to Entrez IDs using either DAVID (Huang et al., 2009; Agarwala et al., 2018) or the chip data from array expression in combination with MATLAB. These numbers were then normalized within each data set and re-scaled so that the magnitude of the range of expression values was like the starting range (all the data sets had maximal expression values of around 1000 to begin with and this range was approximately maintained) allowing the data to be pooled.

Metabolic Data Collection

Mesenchymal stem cells were obtained from 5 to 6 different donors from LONZA (Basel, Switzerland, donors with National Bioethics committee number VSN19-189). Cells were stored in liquid nitrogen, thawed and seeded in 175cm^2 flask in basal medium in an incubator at 5% CO2, 37°C and 95% humidity. For experiments cells were seeded in 75cm^2 flasks at 6000cells/cm^2. Cells were either grown in basal growth medium or osteogenic differentiation medium. 5000 IU/ml of heparin (LEO Pharma

TABLE 1 | List of data sets used to create the computational models.

# of set	iMSC-E-1972	iMSC-O-1900	iMSC-A-2036
1	Samples and Data < E-MEXP-3046 < Browse < ArrayExpress < EMBL-EBI, 2018	Samples and Data < E-MEXP-3046 < Browse < ArrayExpress < EMBL-EBI, 2018[30]	E-MEXP-858
2	E-MEXP-858	E-TABM-318 ("E-TABM-318 < Experiments Matching " 'Mesenchymal Stem Cell' " < ArrayExpress < EMBL-EBI," n.d.; Ng et al., 2008)	E-TABM-("E-TABM-318 < Experiments Matching " 'Mesenchymal Stem Cell' " < ArrayExpress < EMBL-EBI," n.d.; Ng et al., 2008)
3	E-TABM-318	NA	NA

A/Sm Ballerup, Denmark), 1% Penicillin/Streptomycin (Gibco, Grand Island, NY, United States), and 10% Platelet lysate (Platome Reykjavik, Iceland) into DMEM/F12 + Glutamax growth medium (Gibco, Grand Island, NY, United States). This mixture will hereby be referred to as the basal growth-medium. The platelet lysate (PIPL) was centrifuged at 5000rpm/4975g for ten minutes before the supernatant being added to the medium to remove platelet debris and coagulation. The differentiation medium also with the addition of dexamethasone (50 μl, Sigma, Missouri, SL, United States), BMP-2 (50 μl, Peprotech, Rocky Hill, United States), β-glycerophosphate (108 mg, Sigma, Missouri, SL, United States), and ascorbic acid (50 μl, Sigma, Missouri, SL, United States). Cells were used between passage 2 and 6 and care was taken to ensure that at least 5 of the same donors were used for each lineage. Medium was changed on average every 48 h.

Baseline and spent medium samples were assayed for glucose and lactate concentration using an ABL90 blood gas analyzer (Radiometer Medical ApS, Bronshøj, Denmark). In addition, medium samples were analyzed by high pressure liquid chromatography mass spectrometry as described below.

Cell number was determined by trypan blue exclusion and counting in a hemocytometer and an approximate doubling time calculated, this was confirmed with estimates from the literature (Milo et al., 2010). An estimate of dry cell weight was obtained from the literature (Milo et al., 2010) and the changes in metabolite concentration per hour per gram of dry weight were calculated using linear regression in MATLAB. The resulting estimates of uptake and secretion rate of the measured metabolites were applied as constraints to the metabolic model as described below.

Mass Spectrometry

UPLC-MS Analyses were performed with an UPLC system (UPLC Acquity, Waters, MA, United Kingdom) coupled in line with a quadrupole-time of flight hybrid mass spectrometer (Synapt G2, Waters, MA, United Kingdom) as described in Paglia et al. (2012).

Model Construction

Model construction was performed using the Constraint-based reconstruction and analysis (COBRA) Toolbox version 3 in MATLAB, 2017b (Mathworks, Natick, MA, United States). The GEM Recon3 (Brunk et al., 2018) was used as a base reconstruction of the global human metabolic network. We further modified the model to more closely represent MSC metabolism (e.g., extracellular bile acid metabolism and drug metabolism) and to include a greater range of glycan metabolism and lipid metabolism (see **Supplementary Table 1**). The version of Recon3 downloaded from VMH.life (Virtual Metabolic Human n.d.) had already been constrained to be thermodynamically feasible. We used standard quality checks from the COBRA Toolbox (Thiele and Fleming, n.d.) to ensure that the model remained mathematically and biologically feasible as transcriptomic data were integrated.

We constrained the base model using known medium composition, the list of additional metabolites detected by mass spectrometry in basal medium, and data on cell weight and growth using the Metabotools suite within the COBRA Toolbox (Heirendt et al., 2019). This was done separately for proliferating and osteogenically and adipogenically differentiating MSCs. These three media-constrained models were further constrained using the transcriptomic data described above with core reactions those considered important based on the literature (see **Supplementary Table 2**) increased to maximal expression and the GIMME algorithm implemented in the COBRA Toolbox (Becker and Palsson, 2008). GIMME was selected as it retains the model growth function. This was considered appropriate because during the process of expansion and the initial stages of differentiation modeled here, MSCs are growing. It was ensured that these models remained mathematically and biologically feasible and that core reactions were all included. Those core reactions that were not included were manually added along with reactions to link them into the model. These transcriptomically constrained models then had uptake and secretion constraints added based on mass spectrometry data with minimal relaxation of these added constraints to allow a feasible model (the list of rates can be found in Method labeled Supplementary Data Sheet, see *Rxn_fluxes_for_O_model, Rxn_fluxes_for_E_model*, and *Rxn_fluxes_for_A_model*). Finally, these models were pruned to give fully functional condition specific models. The models were then checked for the inclusion of core reactions and biological feasibility. We validated the three new reconstructions against the original Recon3 model using Memote (Lieven et al., 2020).

The model iMSC1255 was downloaded (Fouladiha et al., 2015) and used for comparison, for some comparisons the constraints on uptake and secretion of metabolites were altered to create three models; expansion, osteogenic differentiation and adipogenic differentiation.

Model Comparison

Lethal genes and reactions - those essential to produce flux through the biomass reaction - were determined for each model using the relevant functions in the COBRA Toolbox. Random sampling of the solution space for between 50 and 100% of the optimal biomass reaction flux using the "gpSampler" function in the COBRA Toolbox (Schellenberger and Palsson, 2009), in combination with flux variability analysis (FVA) (Gudmundsson and Thiele, 2010) and flux balance analysis (FBA) (Orth et al., 2010) with the biomass function as the objective were used to determine, the range, probability of distribution, and optimal fluxes through all the model reactions in each model. These were all performed in the COBRA Toolbox. To explore possible reactions needed to optimize osteogenesis the relax reactions function was used. Intersect models including the reactions of either osteogenesis and expansion or osteogenesis and adipogenesis were created, the mean random sampled fluxes for the osteogenic model (with zeros for reactions not in that model) were assigned as the target state and the intersect model with expansion or adipogenic bounds was used as the initial state. An alpha 0.99 was used except where this gave only over 100 reactions to relax, in which case 0.75 was used to achieve lists of reactions to relax that were of a length that could be easily explored. Results from these analyses were assessed by subsystem and gene rule using flux enrichment analysis in the COBRA Toolbox in MATLAB.

RESULTS

Three comparable models of MSC metabolism representing expansion, osteogenesis and adipogenesis were built using publicly available transcriptomic data and parameterized with newly generated metabolomic data. It was shown that these models could recapitulate known metabolic differences among the three cell subtypes and that has allowed the proposal of novel interventions to optimize osteogenesis that will guide future investigations.

Metabolomics Data Analysis Indicates Functional Difference

In order to parameterize the three models of MSC differentiation extracellular metabolomic data (UPLC-MS) was generated for each cell lineage. The estimates of uptake and secretion rate of the measured metabolites were applied as constraints to the metabolic model, enabling them to be analyzed in the context of previously published data on metabolic network structure as summarized in Recon 3 (add in relevant reference), and MSC transcripts from cells at the relevant stage and lineage of differentiation (add in references for the array express data sets).

A total of 59 unique metabolites were detected across the three cell culture lineages. Of these metabolites, 42 were detected in the expansion samples, 50 were detected in the osteogenic samples, and 44 were detected in the adipogenic samples. Interestingly, some metabolites showed opposite trends in the different cell lineages. For example, asparagine, folate, and fumarate were taken up only in expanding cells. Ascorbate, aspartate (measured only in O), glycerol 2 phosphate, glycl groups, palmitate, histidine, pantothenate, proline and threonine (only measurable in O) were taken up only in osteogenic cells. Oxoproline, acetyl carnitine, adenine, adenosine, biotin, phosphocholine, guanine, phenylalanine, riboflavin, and spermine were taken up only in adipogenic cells (rate lists can be found in **Supplementary Material**). These data were analyzed by applying them as constraints to the prior knowledge contained in metabolic networks based on Recon 3 and previously published transcriptomics data. This allowed us to leverage prior knowledge to gain greater insights into the likely metabolic changes to MSCs during differentiation than would have been obtained by statistical methods.

Newly Reconstructed Models Expand Coverage of Metabolic Pathways and Accurately Represent Core Metabolic Fluxes

Model reconstruction is an iterative process where multiple type of -omic data are combined and results from experiments based on model predictions are used to make future predictions more accurate (**Figure 1**). As shown in **Table 2** the three models were of similar size with a mean of 6517 reactions, 3674 metabolites and 1969 genes, an increase in size of almost 3-fold compared iMSC1255 (2288 reactions, 1850 metabolites, and 1259 genes). The three models had a combined total of 7478 unique reactions, of which 212 reactions were unique to iMSC-E-1972, 151 reactions were unique to iMSC-O-1900, and 457 reactions were unique to iMSC-A-2036. The ability to produce extracellular calcium phosphate—an important function for osteogenic MSCs—was added to the osteogenic model.

iMSC-O-1900 contained fewer genes, reactions and metabolites compared to the other two final models, a difference first apparent after implementing the transcriptomic constraint.

The base model, adapted from Recon3D, and the three new iMSC models were assessed using the memote tool (Lieven et al., 2020). The iMSC1255 (Fouladiha et al., 2015) scored 31% overall. This reflected high scores for model consistency but low scores on annotation. iMSC-E-1972 scored 37%, iMSC-O-1900 48% and iMSC-A-2036. Again scores were higher for consistency than annotation, however, annotation was improved. All of the new models include around 2100 stoichiometrically balanced cycles, however, given the size of the models this was unsurprising. The models do not erroneously produce ATP, NAD, or NADP (threshold 1e-10) and a fast leak test from the Cobratoolbox found no leaking metabolites.

None of the newly constructed MSC models showed biologically infeasible behaviors such as creating ATP from water alone or leaking metabolites when uptake was prevented (see

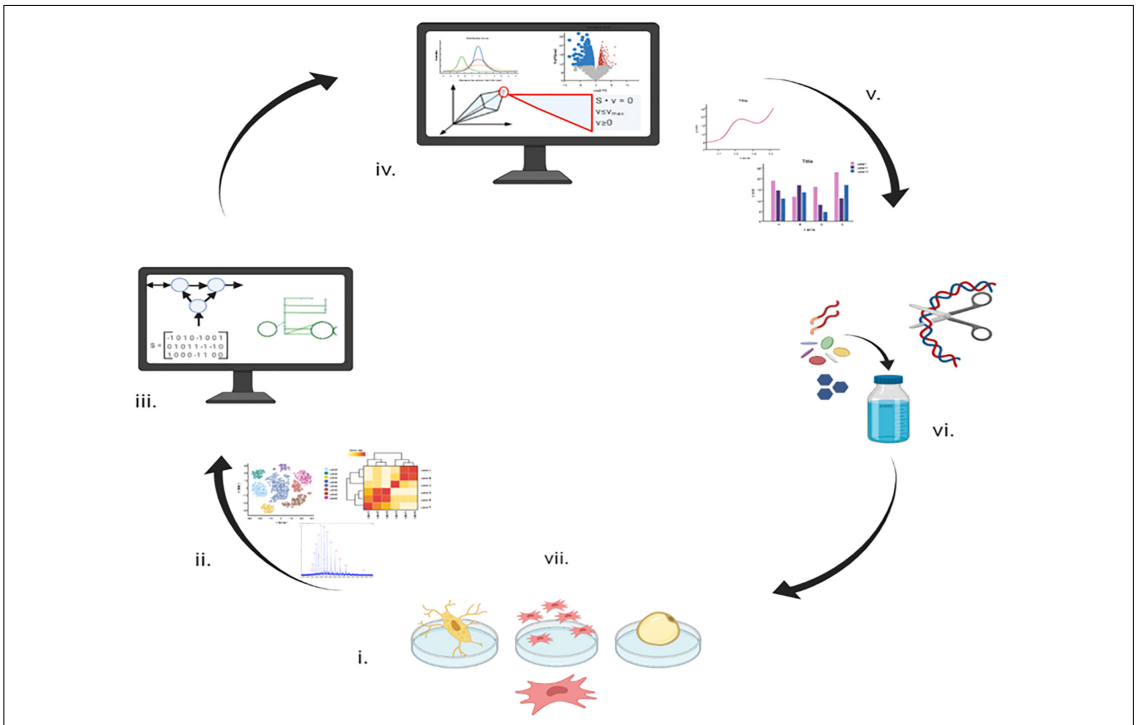

FIGURE 1 | A schematic drawing showing how metabolic modeling can integrate data to contribute to planning future experiments and potential utilization. **Stage (i)** Initial metabolomics and transcriptomics data acquisition from *in vitro* culture. **Stage (ii)** Statistical analysis of metabolomic and transcriptomic data. **Stage (iii)** Reconstruction of the human metabolic network from the literature and previous knowledge. **Stage (iv)** Application of metabolic and transcriptomic data to the metabolic network to produce context specific models. **Stage (v)** Analysis of the differences between the three biological models. **Stage (vi)** Verification of novel findings of the models initially through comparison to the results of published experiments (presented in this manuscript) and then through new experiments. **Stage (vii)** Improved knowledge of the biological system enabling optimized growth and differentiation that may be applied to improve healthcare or industrial outcomes.

Supplementary Table 1). It should be noted that the previously published iMSC1255 generally also fulfilled these criteria but does include some duplicated reactions, possibly due to the treatment of reversible reactions.

The three new MSC models presented here were all capable of producing approximately the correct number of ATP molecules per molecule of both glucose (32 aerobic and 2 anaerobic for all three models) and glutamine (22.5 aerobic and 1 anaerobic all three models) under both aerobic and anaerobic conditions. There were slight differences in theoretical ATP production in the literature and existing models but around 31 from aerobic glucose, 2 from anaerobic glucose, 23 from aerobic glutamine and anaerobic glutamine are common figures obtained in other models including those specifically curated for central energy metabolism (Smith et al., 2017; Mazat and Ransac, 2019). However, the estimates of these values for iMSC1255 were often very different (423 glucose aerobic, 400 glucose anaerobic, 415 glutamine aerobic, and 399 glutamine anaerobic). These large values for ATP production from glucose and glutamine in iMSC1255 were explained by increased activity in the mitochondrial ATPsynthase reaction. The presented new and updated models therefore better captured the energetics of central carbon, fatty acid, and amino acid metabolism.

ATP production from other important carbon sources was also generally close to theoretical values (see **Figure 2**) in the three new MSC models. The initial values for medium fatty acid composition had a large effect on these values and the differences are likely due to the composition chosen.

The uptake and secretion fluxes of amino acids in the proliferation model and the original iMSC1255 values were compared (see **Supplementary Table 2** for details). Nine of the amino acids with uptake/secretion values reported in Fouladiha et al. (2015) were included in the constraints for our model based on our own measurements. These were generally in accordance with the reported constraints. Leucine and lysine fluxes were not based on mass spectrometry measurements, but the range of random sampled fluxes falls at least partially within the same range as the iMSC1255 estimates. Another six amino acids had fluxes in the same predicted direction as iMSC1255 but overestimated the magnitude of uptake or secretion. Two amino acids are predicted as secreted in our random sampling but taken up by iMSC1255.

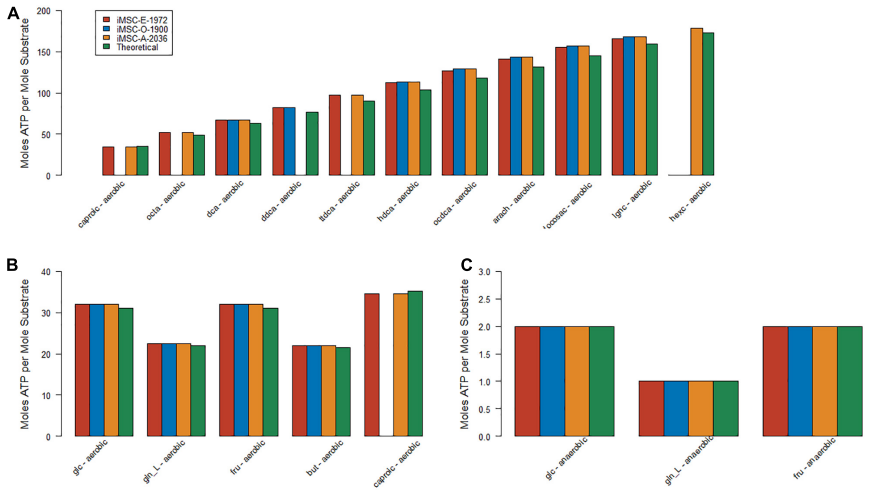

FIGURE 2 | Estimates of optimal fluxes for ATP production from various key carbon sources – **(A)** Aerobic metabolism of the most energy dense substrates **(B)** Aerobic metabolism of the least energy dense substrates **(C)** Anaerobic metabolism.

Mitochondrial Function Separates Proliferating and Differentiating MSCs and Pentose Phosphate Pathway Flux Differentiates Osteogenesis and Adipogenesis

To determine the quality of the models, model predictions were compared to data about MSC metabolism from the literature. Proliferating, osteogenically and adipogenically differentiating bone marrow derived MSC models were examined and compared to the outputs from the re-constrained versions of iMSC1255 (Fouladiha et al., 2015). The newly produced models matched the data very well for the relative levels of *beta hydroxylase* activity, but iMSC1255 does not include beta hydroxylase reactions. The new models qualitatively predicted differences in flux between proliferating MSCs and one or other of the differentiating lineages but not both in *lactate dehydrogenase, creatine kinase, glyceraldyhyde-3-phosphate dehydrogenase, phosphofructokinase* and *glutathione reductase* with only a slight mis-estimation in the other differentiation lineage. iMSC1255 estimated very similar fluxes across all three models for all of these reactions. *Isocitrate dehydrogenase* appeared to be well estimated in the adipogenic and proliferation models but underestimated in the osteogenic model, iMSC1255 estimated little difference in this reaction.

Various studies have analyzed metabolism in osteogenic and adipogenic differentiation of cells, sometimes in MSCs and sometimes in other cell types (Pattappa et al., 2011; Meleshina et al., 2016; Shum et al., 2016). The new models were compared to several of these studies. Random sampling of the new models with a flux of between 50 and 100% of the biomass function showed that both iMSC-O-1900 and iMSC-A-2036 show increased flux through mitochondrial ATPsynthase, marked as highly significant using the Wilcoxon statistic in MATLAB (ranksum, p-Values ~0 for O vs. E and 5.40 e-81 for E vs. A). Both differentiating models had mean predicted values twice as high as the proliferating model. The minimum values for the iMSC-A and –O were around ten times than in iMSC-E. However, the maximum value in iMSC-E was approximately 10% higher than either differentiating model, indicating that differentiating models showed increased mitochondrial function (**Figure 3A**). It has also been reported that suppression of ornithine decarboxylase activity increases osteogenesis in human bone marrow MSCs (Tsai et al., 2015). This is supported by the mean flux from random sampling iMSC-E-1972 for ORNDC being greater over 10 times greater than the value of that in iMSC-O-1900 (**Figure 3B**, $p \sim 0$ Wilcoxon rank test).

TABLE 2 | Model size at various stages of construction (E) refers to iMSC-E-1972, (O) refers to iMSC-O-1900, and (A) refers to the iMSC-A-2036.

Model	Genes	Reactions	Metabolites
Recon3D	3697	13543	8399
Base Model	2280	9151	4900
GIMME Models *(medium and growth and transcriptomic)*		6693(E) 6061(O) 6933(A)	3792(E) 3472(O) 3884(A)
Corrected Models *(GIMME plus literature)*		6741(E) 6134(O) 7006(A)	3830(E) 3526(O) 3939(A)
Final Models *(Corrected plus metabolomics)*	1972(E) 1900(O) 2036(A)	6600(E) 5975(O) 6876(A)	3740(E) 3428(O) 3855(A)
iMSC1255 model *(used for comparison)*	1259 (E)	2288 (E)	1850 (E)

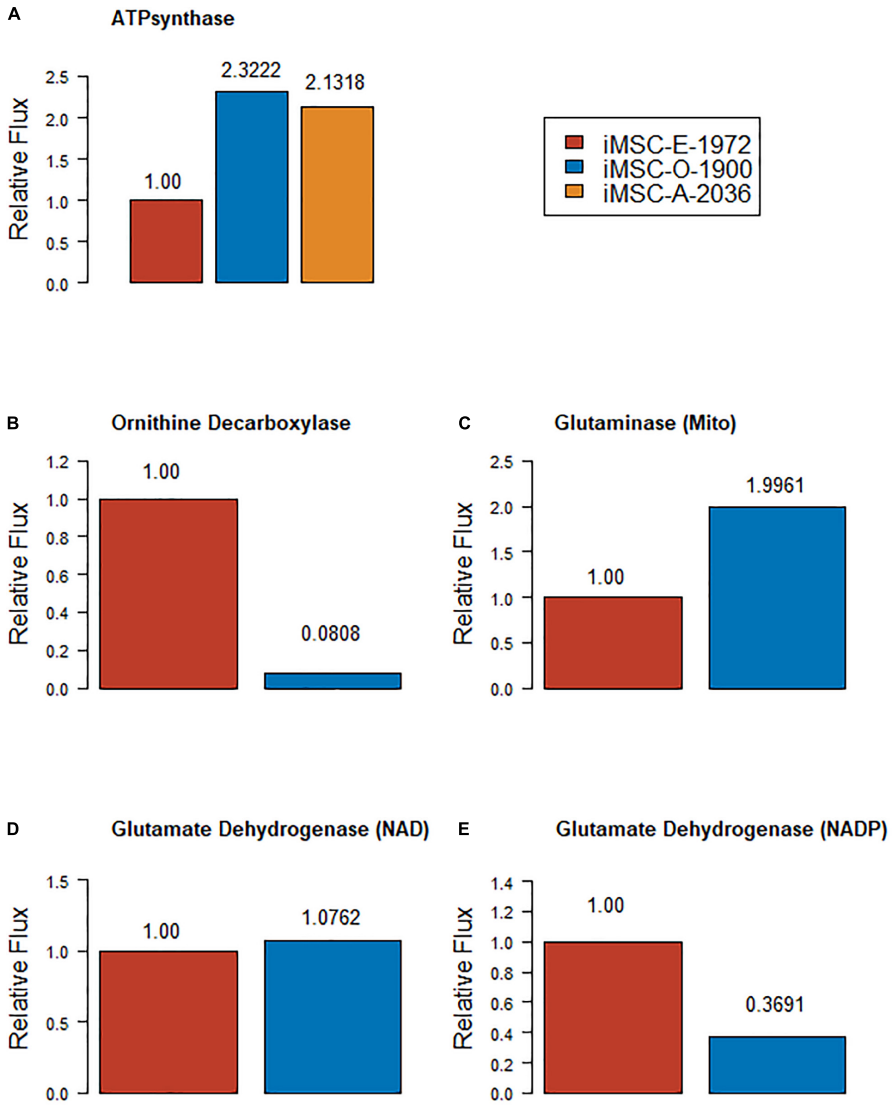

FIGURE 3 | Relative mean fluxes (compared to expansion model) from various reactions – **(A)** ATPsynthase **(B)** Ornithine decarboxylase **(C)** Mitochondrial glutaminase **(D)** NAD dependent glutamate dehydrogenase **(E)** NADP dependent glutamate dehydrogenase.

Conversely, it has been shown that suppressing glutaminase activity and the contribution of glutamine to the TCA cycle prevents osteogenesis (Huang et al., 2017; Chen et al., 2019). iMSC-O-1900 showed lower mitochondrial glutaminase (**Figure 3C**) but higher cytoplasmic glutaminase (not seen in iMSC-E-1972) and overall glutaminase activity more than twice as high as the proliferation model. However, the contribution of glutamine to the TCA cycle via glutamate dehydrogenase (anaplerosis) was slightly higher in the proliferation than the osteogenic model (**Figures 3D,E**). Other uses of glutamate account for the rest of the osteogenic model's glutaminase activity. This result indicates that this central area of metabolism may be lacking in sub-cellular location specificity in the models, however, it substantially agrees with the literature on a whole cell basis. Furthermore, it has been shown that the production of kyneurine via indoalamine dioxygenase

is increased in osteogenesis compared to proliferation of MSCs (Vidal et al., 2015). A key enzyme in this pathway L-Tryptophan:Oxygen 2, 3-Oxidoreductase (Decyclizing), that produces L formyl-kyneurine is absent from iMSC-E-1972 but present in iMSC-O-1900 (and iMSC-A-2036).

A key feature of adipogenesis is the upregulation of glucose 6 phosphate dehydrogenase activity. G6PDH forms 6-Phosphonoglucono-D-lactone (6PGL) and NADPH. 6PGL contributes to the pentose phosphate pathway and therefore the production of nucleotides and reducing potential via NAPDH. NADPH contributes to the synthesis of fatty acids by supplying a reducing agent. This is a key metabolic coupling between glucose and fatty acid utilization and storage (Park et al., 2005). Overall, the formation of NADPH by this reaction was much higher in iMSC-A-2036, around ten times higher than iMSC-E and almost twice that of iMSC-O (**Figure 4D**). This was partially due to the higher endoplasmic reticulum G6PDH forward activity in iMSC-A-2036 but also due to the presence of some reverse activity being predicted in iMSC-O-1900 and -E-1972.

To assess metabolic differences between MSCs undergoing expansion, osteogenic differentiation, and adipogenic differentiation, Markov chain Monte Carlo (MCMC, Schellenberg et al., 1992) sampling was used to generate a uniform random sampling of the solution space of each of the three the models. A set of predictions for each reaction was obtained and these sets of predictions compared across the three models. Specifically, the fold changes in the means for each reaction were compared, 5-fold change being considered

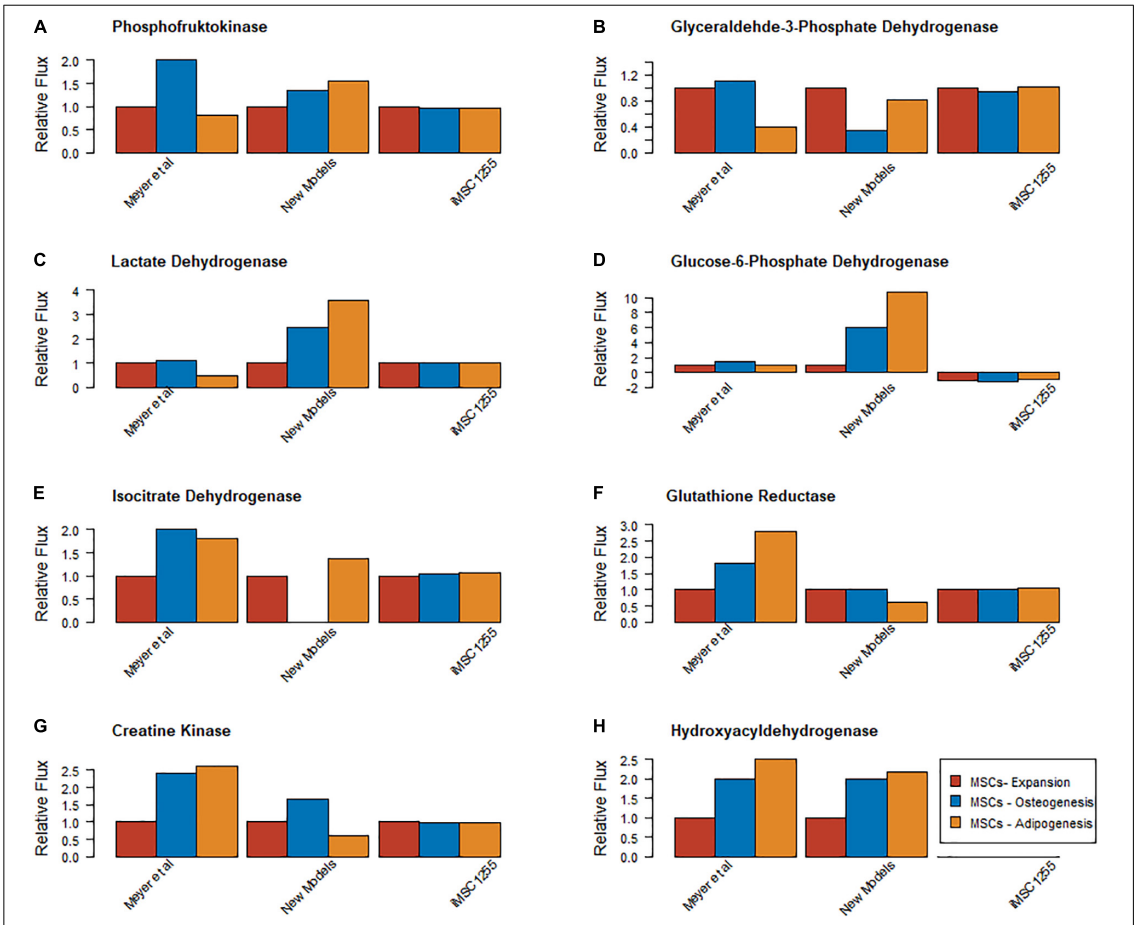

FIGURE 4 | Comparison of relative magnitude of metabolic fluxes found at day 7 of expansion, osteogenic and adipogenic differentiation in Meyer et al. (2018), iMSC1255 er-constrained with MS data collected in Iceland and the new models **(A)** Phosphofructokinase **(B)** Glyceraldyhyde 3 phosphate dehydrogenase **(C)** Lactate dehydrogenase **(D)** Glucose 6 phosphate dehydrogenase **(E)** Isocitrate dehydrogenase **(F)** Glutathione reductase **(G)** Creatine kinase **(H)** Beta hydroxyl acyl dehydrogenase. E, Expansion; O, Osteogenesis; A, Adipogenesis.

of interest, and a two tailed *t*-test was performed using 1e-12 as a *p*-Value cut-off; see *Metabolic_difference_rxn_pred* in **Supplementary Data Sheet** for a full list of these reactions.

Reactions in the model were grouped by metabolic subsystem enabling an enrichment analysis to be performed on lists of up regulated reactions (predicted to carry more flux) in each cell type compared to each of the others, shown in **Table 3**. Enrichment analysis compares which subsytems (areas of metabolism) show more reactions that are up regulated compared to the expected distribution of changes if all changes occurred by chance across the whole of metabolism. This demonstrates those areas of metabolism that are more important to one lineage than another. This enrichment analysis showed that the areas of metabolism that are significantly more active in proliferating cells than in either of the differentiating cell types include biotin metabolism, vitamin A metabolism, sphingolipid metabolism, fatty acid oxidation and fatty acid synthesis as well as mitochondrial transport and exchange/demand reactions. This upregulation showed higher activity in areas of metabolism related to fatty acid signaling (vitamin A and sphingolipids). Sphingolipid metabolism may also indicate the need for new cell membranes. In adipogenic differentiation, fatty acid oxidation and as would be expected fatty acid synthesis were over represented in increased activity along with exchange/demand reactions. Fatty acid oxidation and exchange demand reactions were over represented in increased activity reactions in osteogenesis compared to the other pathways studied, see **Figure 5**.

TABLE 3 | Showing subsystems that have a significantly overrepresented (adjusted p-value < 0.05) number of more active reactions in the relevant model compared to the other differentiation lineage in the case of osteogenesis/adipogenesis or compared to the two differentiation models in the case of expansion.

Expansion			
Adjusted p-Value	*Enriched set size*	*Total set size*	*Groups Increased*
0.000254	98	1368	Exchange/demand reaction
0.001831	65	961	Fatty acid oxidation
0.003348	9	242	Cholesterol metabolism
0.003348	9	240	Fatty acid synthesis
0.003348	1	105	Transport, lysosomal
0.003348	25	453	Transport, mitochondrial
0.006098	3	133	Sphingolipid, metabolism
0.011893	7	185	Bile acid synthesis
0.017589	11	47	Vitamin A metabolism
0.019096	5	12	Biotin metabolism
Osteogenesis			
Adjusted p-Value	*Enriched set size*	*Total set size*	*Groups Increased*
7.09E-07	12	961	Fatty acid oxidation
8.6E-06	28	1368	Exchange/demand reaction
Adipogenesis			
Adjusted p-Value	*Enriched set size*	*Total set size*	*Groups Increased*
1.64E-05	26	1368	Exchange/demand reaction
0.000253	16	961	Fatty acid oxidation
0.012651	1	240	Fatty acid synthesis

Model-Driven Experimental Design for Engineering Osteogenesis

Metabolic modeling allows the generation of hypotheses about means of optimizing one cell lineage over another. To propose means of improving osteogenesis desirable for regenerative medicine, combined models of either expansion-and-osteogenesis or adipogenesis-and-osteogenesis were created. Two of each of these models were produced, one representing the constraints on reactions from each lineage with other reactions blocked. These models were then subjected to relaxation analyses.

The results of relaxing the model to find a solution intermediate between either the expansion model or the adipogenic model and the osteogenic model produced lists of key reactions to modify to move towards osteogenesis (see *Relaxed_rxn_lists,* **Supplementary Data Sheet**, for the more extensive lists required for full transition). The transport reactions to relax to move from expansion to osteogenesis were transport from extracellular to cytosol of serotonin, urea and 13-Docosenoic Acid, in all case the changes moved these metabolites from being taken up to being either not active or in the case of 13-Docosenoic Acid to being secreted. To transform from adipogenic to osteogenic by modifying transport reactions Bilirubin Beta-Diglucuronide uptake should be prevented along with the blocking of leukotriene C4 reduced glutathione transport, thromboxane B2 transport, leukotriene E4 transport and Mono (Glucosyluronic Acid) Bilirubin transport while inward transport of citrate and ribosomal transport of bilirubin should be encouraged. The non-transport reactions (including demand and exchange reactions) to alter to encourage osteogenesis from expansion are: 'EX_cspg_e[e],' 'KAS8,' 'r0797,' 'RE0344C,' 'RE0577C,' 'RE0578C,' 'RE1845C,' 'EX_aicar[e],' 'EX_gudac[e],' 'EX_stcrn[e],' 'EX_Lhcystin[e],' 'EX_mal_L[e],' 'MYELIN_HSSYN,' and 'DM_myelin_hs[c].' These reactions include amino acid uptake and formation of lipid and glyco lipids. The equivalent reactions for encouraging osteogenesis from adipogenesis are: 'EX_retfa[e],' 'EX_mal_L[e],' 'EX_taur[e],' and 'DM_na1[r].' Again, this includes alterations to the necessary amino acids as well as fatty acid retinol involved in developmental signaling. The relaxation required of truly non-transport reactions to bring the expansion model close to the osteogenic model are 'KAS8,' 'r0797,' 'RE0344C,' 'RE0577C,' 'RE0578C,' and 'RE1845C.' These reactions are all involved in fatty acid and CoA metabolism and are generally moving from being active (sometimes in the reverse direction) to being less active or inactive. The equivalent relaxation (with an alpha value of 0.75) produced no necessary changes from adipogensis to osteogenesis however with and alpha of 0.9 '3SALACBOXL,' 'CBPPer,' 'GGNG,' 'GLBRAN,' 'GLGNS1,' 'KAS8,' 'LCYSTCBOXL,' 'r0060,' 'IDL_HSSYN,' 'IDL_HSDEG,' 'HMR_3422,' and 'HMR_6647.' These reactions become more active or move from a negative to a positive direction while 'LPS3e,' 'NDP7er,' 'PCHOL2LINL_HSPLA2,' and 'PE203_HSPLA2' more from the reverse direction to inactivity. Many of these reactions are glycosylating enzymes

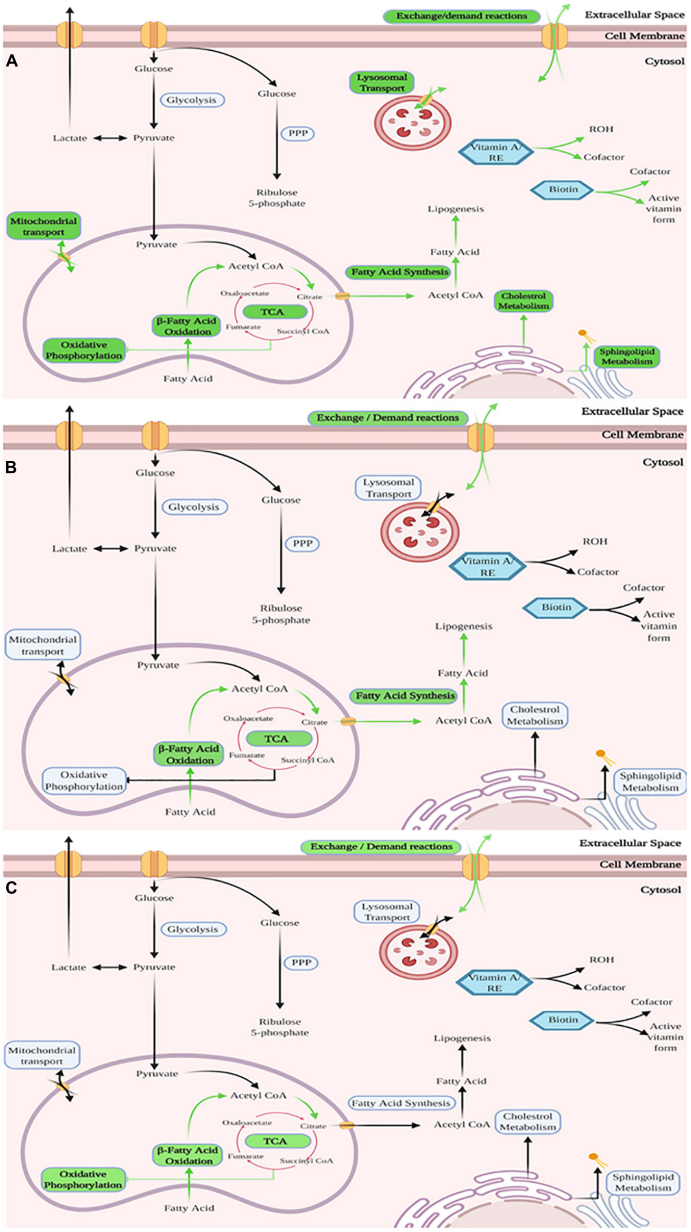

FIGURE 5 | Graphical representation of the enriched subsystems between the cell lineages based on the new reconstructed models – The three figures show in a graphical manner the subsystems (a group of related metabolic reactions representing a specific aspect of metabolism) in each model that were found to contain significantly more changed reactions than other subsystems of the model. Shown is – **(A)** Proliferation of MSCs, with various subsystems identified as enriched. This mirrors expectations as expansion requires energy and synthesis of new material (e.g., cell wall and DNA). **(B)** Adipogenesis of MSCs, with subsystems related to synthesis and breakdown of fatty acids identified as enriched as well as exchange/demand reactions **(C)** Osteogenesis of MSCs, with subsystems related to fatty acid breakdown and TCA-cycle activity identified as enriched as well as exchange/demand reactions. For detailed list with included *p*-Values for each listed subsystem see **Table 3**. Green arrows and labels indicate enriched pathways.

likely accounting for the alterations in the cells' outer glycan layer between these two states.

DISCUSSION

The driving factor behind this study was to improve understanding of the metabolic underpinnings of MSC differentiation with hopes that that will enable further application of them in regenerative medicine. To achieve that three metabolic networks were reconstructed from varied -omics and experimental data and compared. The models achieved to recapitulate key metabolic phenotypic features characteristic for each cell state, to showcase the major metabolic differences and to propose a possible way to improve osteogenesis.

Measurements of Metabolism

The metabolomic data used in the reconstruction of the presented models was specifically generated and analyzed in order to parametrize the models in accordance to very specific experimental conditions known to the authors to influence the cells in a specific desired manner. The mass spectrometry data shows differences in metabolism between the 3 lineages of cells. These changes in the extracellular milieu support different metabolism during cell growth and differentiation of MSCs. In order to better understand how these extracellular changes reflected intracellular metabolic changes during MSC expansion and differentiation, these data were analyzed in the context of changes in gene transcription within their respective metabolic models.

Reconstruction of Metabolic Models for Three States of MSCs

Three constraint-based models of MSC metabolism (iMSC-E-1972, iMSC-O-1900, and iMSC-A-2036 describing expansion, osteogenesis, and adipogenesis, respectively) were reconstructed, from the global human metabolic network (Recon3), publicly available transcriptomic data and metabolomic data generated here. These models largely share reactions (2.0 - 6.1% of total reaction number are unique to a model), an expected result considering the transcriptomic data seem to have had the strongest effect on inclusion/exclusion of reactions as demonstrated by showing the biggest change in the number of reactions included in each model (**Table 2**). These transcriptomics data, and the metabolomics data, represent MSCs at day 7 after first exposure to differentiation medium. Day 7 is still considered as an early stage of the two differentiation processes that take between 21 and 28 days, respectively, and increased lineage differences are expected to be seen at later time points, however, there was insufficient data available for those later time points in a suitable format at the time that this project began. The publicly available transcriptomic data used to generated these models had lower coverage of metabolic genes for the osteogenic state, resulting in a smaller number of reactions included in this model (iMSC-O-1900) when compared to the other two (iMSC-E-1972 and iMSC-A-2036). The osteogenic transcript was missing any call, present or absent for 5.19% of base model genes whilst proliferation and adipogenesis were missing information for only 2.35 and 2.38%, respectively. These models can be continually upgraded and expanded using specifically generated RNAseq data from cells collected at later stages of osteogenesis and adipogenesis in order to further improve the predictive capabilities of the models. The use of RNAseq data in the place of microarray-based data is also likely to improve the coverage of enzyme expression data.

Verification of Metabolic Function in Comparison to iMSC1255

This comparison is in some ways limited to broad comments as the enzyme activity assays in the paper presented by Fouladiha et al. (2015) were performed to determine maximal activity in cell extracts, not fluxes in living cell situations as simulated by the models.

The new MSC models all pass key metabolic sanity checks and manage an almost 3-fold increase in metabolic coverage compared to iMSC1255, roughly a proportional increase to that between the base model and Recon1. This similarity suggests retention of similar level of cell specificity compared to iMSC1255 despite the great increase in metabolic coverage. However, the models reported here are able to more correctly capture the production of ATP from various substances and are additionally able to perform more metabolic functions compared to the previously existing MSC model, iMSC1255 (originally reconstructed for cells exclusively in the state of proliferation). One of the areas of metabolic function that the models presented in this paper are more adept at in comparison to iMSC1255 is fatty acid metabolism. This is illustrated by the example of iMSC1255 lacking beta hydroxylase activity (**Figure 4**), but the activity of beta hydroxylase has been shown to be present in MSCs, as well as its much smaller number of human functions assessed by the COBRA Toolbox (**Supplementary Table 1**).

As fatty acid metabolism is key to adipogenesis, the additional detail of beta hydroxylase inclusion in the new presented models will likely prove important to the utility of their predictions. The increased coverage of fatty acid and lipid metabolism that is seen in them is in large part due to the updated base reconstruction used for the model's reconstruction (i.e., using Recon 3 instead of Recon 1). Additionally, when the iMSC1255 model was constrained using the same metabolomic data sets as were used to reconstruct the presented three new MSC models, the new models (iMSC-E-1972, iMSC-O-1900 and iMSC-A-1972) were better able to match the results of Meyer et al. (2018) compared to iMSC1255 (**Figure 4**). This indicates that by specifically constraining the models with transcriptomics data from various differentiation lineages the models created are better able to show the differences in metabolism between the different lineages.

Verification of Lineage Specific Metabolic Functions

A good qualitative fit between known metabolic differences between the three lineages studied and the relationships between the predicted fluxes in the three new models was observed. Key metabolic features, such as the production of ATP changing in osteogenesis, are reflected in the differences between the

models, indicative of a realistic reconstruction reflecting expected biological behavior. Differences in amino acid metabolism, ornithine and to a lesser extent glutamine and tryptophan, are shown between osteogenesis and expansion in ways that reflect known differences in metabolism during osteogenic differentiation.

G6PDH expression is known to be key to producing NADPH for fatty acid synthesis and overall activity of this enzyme is greater in the adipogenic model than the other two cell lineage models, an observation suggesting that these models reflect this aspect of metabolism well. However, comments on the activity of G6PDH in relation to this paper are complicated by the reversibility of this reaction and the presence in the models of multiple forms of this enzyme. In iMSC1255, the flux is only predicted to be in the reverse direction, creating NADP not NADPH. This does not agree with the previous consensus, our models suggest a mix, specifically our adipogenic model favors NADPH production in accordance with the literature (Park et al., 2005; Melis et al., 2013; Lee et al., 2017; Meyer et al., 2018). These contradictions might suggest that this may be either premature or reflective of the limitations of measuring activity in an isolated enzyme.

Overall, these results demonstrate that this key area of metabolism is well reflected in the models which gives a good ground for building the iMSC-O-1900 model into the later and potentially more metabolically diverse later stages of osteogenesis.

Observation of Main Metabolic Differences Between the Models

The groups of metabolic reactions that are upregulated in each of the lineages reflect the changes in function of cells during expansion and differentiation. The metabolic subsystems upregulated in expansion are varied, reflecting the necessity of the cells for varied reaction activity to be able to produce cell biomass, membranes, and nucleic acids in order to grow. On the other hand, the changes in adipogenesis are more concentrated around fatty acids and fatty acid synthesis. This is to be expected, especially the increased activity of fatty acid synthesis, which is a key feature of adipocytes. The areas of metabolism with the most concentrated changes in osteogenesis is fatty acid oxidation, which reflects increased oxidative metabolism in the differentiating cells – a phenomenon previously reported by multiple studies (Chen et al., 2008; Pattappa et al., 2011; Buravkova et al., 2013; Shum et al., 2016). All of the cell lines show changes to the exchange reaction activity, which may partially be due to exchange reaction alterations that happen during the model reconstruction process but since many of these observed differences reflect actual measured differences this is unlikely to be problematic.

Proposed Method to Increase Osteogenesis

The results of the relaxation of reactions between adipogensis or expansion and osteogenesis suggest that alterations in the need for malate are changed, with either reduced uptake or a switch to secretion being observed in both cases. Fatty acid and lipids, particularly those involved in signaling (i.e., retinoic acids and fatty acids) and those involved in cell membranes and glycosylation (i.e., myelin_HS) are altered as well. These are key metabolites for the rearrangement of cell membranes and transmembrane glycoproteins as well as cell signaling and therefore seem plausible as metabolic markers of differentiation. One of the reactions highlighted is the need to increase transport of citrate from the extracellular space to the cytosol. It has been shown that growing cells on citrate rich materials encourages osteogenesis (Wang et al., 2013; Irizarry et al., 2017), this match with the literature is encouraging. This discovery regarding citrate in combination with the enrichment of the exchange/demand reactions subsystem also suggests that other transporters may be interesting targets for future investigation when it comes to searching for new ways to increase osteogenesis of MSCs.

CONCLUSION

We present three new genome-scale metabolic models of MSC metabolism, representing expansion, osteogenesis and adipogenesis differentiation. These newly reconstructed models are increased in scope compared to previous models of this cell type both in terms of the coverage of multiple lineages in models produced specifically for two new lineages and with the models due to usage of a new and much improved base human metabolic reconstruction (Recon3). We computed a variety of metabolic phenotypes, demonstrating that the models presented here accurately represent qualitative and quantitative cellular characteristics and important differences between the cell types. Having validated these models, we used them for model-driven experimental design with the goal to optimize *in vitro* osteogenesis. One of predicted solutions, the citrate transporter, concurs with a previously identified target which encourages further possibilities of similar predictions. Through the use of mechanistic models such as are presented here, we provide a blueprint for the application and engineering of regenerative medicine therapies where promising therapeutics like MSCs can be made more efficient and attainable.

DATA AVAILABILITY STATEMENT

The data presented in the study are deposited in the MetaboLights repository (https://www.ebi.ac.uk/metabolights/MTBLS2844), accession number MTBLS2844.

ETHICS STATEMENT

The studies involving human participants were reviewed and approved by the National Bioethics committee number VSN19-189. Written informed consent for participation was not required for this study in accordance with the national legislation and the institutional requirements.

AUTHOR CONTRIBUTIONS

TS and SMcG designed the study, analyzed the data, and drafted the manuscript. JY, ÓR, and ÓS designed the study and reviewed the manuscript. All authors gave their final approval of the submitted version.

FUNDING

This research was supported by the Icelandic Research Fund (Grant Number 217005).

ACKNOWLEDGMENTS

The authors would like to thank the staff of the Blood bank and Davíð Ingvi Snorrason who collected media samples used for adipogenic MS analysis.

SUPPLEMENTARY MATERIAL

The Supplementary Material for this article can be found online at: https://www.frontiersin.org/articles/10.3389/fcell.2021.642681/full#supplementary-material

REFERENCES

Agarwala, R., Barrett, T., Beck, J., Benson, D. A., Bollin, C., Bolton, E., et al. (2018). Database resources of the national center for biotechnology information. *Nucleic Acids Res.* 46(D1), D8–D13. doi: 10.1093/nar/gkx1095

Aggarwal, S., and Pittenger, M. F. (2005). Human mesenchymal stem cells modulate allogeneic immune cell responses. *Blood* 105, 1815–1822. doi: 10.1182/blood-2004-04-1559

Aurich, M. K., Fleming, R. M. T., and Thiele, I. (2016). MetaboTools: a comprehensive toolbox for analysis of genome-scale metabolic models. *Front. Physiol.* 7:327. doi: 10.3389/fphys.2016.00327

Aurich, M., Paglia, G., Rolfsson, Ó, Hrafnsdóttir, S., Magnúsdóttir, M., Stefaniak, M., et al. (2015). Prediction of intracellular metabolic states from extracellular metabolomic data. *Metabolomics* 11, 603–619. doi: 10.1007/s11306-014-0721-3

Becker, S. A., and Palsson, B. O. (2008). Context-Specific metabolic networks are consistent with experiments. *PLoS Comput. Biol.* 4:e1000082. doi: 10.1371/journal.pcbi.1000082

Becker, S., Feist, A., Mo, M., Hannum, G., Palsson, B., and Herrgard, M. (2007). Quantitative prediction of cellular metabolism with constraint-based models: the COBRA toolbox. *Nat. Protocol.* 2, 727–738. doi: 10.1038/nprot.2007.99

Brunk, E., Sahoo, S., Zielinski, D. C., Altunkaya, A., Dräger, A., Mih, N., et al. (2018). Recon3D enables a three-dimensional view of gene variation in human metabolism. *Nat. Biotechnol.* 36, 272–281. doi: 10.1038/nbt.4072

Buravkova, L. B., Rylova, Y. V., Andreeva, E. R., Kulikov, A. V., Pogodina, M. V., Zhivotovsky, B., et al. (2013). Low ATP level is sufficient to maintain the uncommitted state of multipotent mesenchymal stem cells. *Biochim. Biophys. Acta General Sub.* 1830, 4418–4425. doi: 10.1016/j.bbagen.2013.05.029

Campana, V., Milano, G., Pagano, E., Barba, M., Cicione, C., Salonna, G., et al. (2014). Bone substitutes in orthopaedic surgery: From basic science to clinical practice. *J. Mater. Sci. Mater. Med.* 25, 2445–2461. doi: 10.1007/s10856-014-5240-2

Chen, C.-T., Shih, Y.-R. V., Kuo, T. K., Lee, O. K., and Wei, Y.-H. (2008). Coordinated changes of mitochondrial biogenesis and antioxidant enzymes during osteogenic differentiation of human mesenchymal stem cells. *Stem Cells (Dayton, Ohio)* 26, 960–968. doi: 10.1634/stemcells.2007-0509

Chen, Y., Yang, Y. R., Fan, X. L., Lin, P., Yang, H., Chen, X. Z., et al. (2019). MiR-206 inhibits osteogenic differentiation of bone marrow mesenchymal stem cells by targetting glutaminase. *Biosci. Rep.* 39:BSR20181108. doi: 10.1042/BSR20181108

Croitoru-Lamoury, J., Lamoury, F. M. J., Caristo, M., Suzuki, K., Walker, D., Takikawa, O., et al. (2011). Interferon-γ regulates the proliferation and differentiation of mesenchymal stem cells via activation of indoleamine 2,3 dioxygenase (IDO). *PLoS One* 6:e14698. doi: 10.1371/journal.pone.0014698

de Castro, L. L., Lopes-Pacheco, M., Weiss, D. J., Cruz, F. F., and Rocco, P. R. M. (2019). Current understanding of the immunosuppressive properties of mesenchymal stromal cells. *J. Mol. Med.* 97, 605–618. doi: 10.1007/s00109-019-01776-y

Duarte, N., Becker, S., Jamshidi, N., Thiele, I., Mo, M., Vo, T., et al. (2007). Global reconstruction of the human metabolic network based on genomic and bibliomic data. *PNAS* 104, 1777–1782. doi: 10.1073/pnas.0610772104

Duijvestein, M., Vos, A. C. W., Roelofs, H., Wildenberg, M. E., Wendrich, B. B., Verspaget, H. W., et al. (2010). Autologous bone marrow-derived mesenchymal stromal cell treatment for refractory luminal Crohn's disease: Results of a phase I study. *Gut* 59, 1662–1669. doi: 10.1136/gut.2010.215152

Fouladiha, H., Marashi, S.-A., and Shokrgozar, M. (2015). Reconstruction and validation of a constraint-based metabolic network model for bone marrow-derived mesenchymal stem cells. *Cell Proliferat.* 48, 475–485. doi: 10.1111/cpr.12197

Fouladiha, H., Marashi, S.-A., Shokrgozar, M. A., Farokhi, M., and Atashi, A. (2018). Applications of a metabolic network model of mesenchymal stem cells for controlling cell proliferation and differentiation. *Cytotechnology* 70, 331–338. doi: 10.1007/s10616-017-0148-6

Gan, Y., Dai, K., Zhang, P., Tang, T., Zhu, Z., and Lu, J. (2008). The clinical use of enriched bone marrow stem cells combined with porous beta-tricalcium phosphate in posterior spinal fusion. *Biomaterials* 29, 3973–3982. doi: 10.1016/j.biomaterials.2008.06.026

Goldberg, A., Mitchell, K., Soans, J., Kim, L., and Zaidi, R. (2017). The use of mesenchymal stem cells for cartilage repair and regeneration: a systematic review. *J. Orthop. Surg. Res.* 12:39. doi: 10.1186/s13018-017-0534-y

Gudmundsson, S., and Thiele, I. (2010). Computationally efficient flux variability analysis. *BMC Bioinform.* 11:489. doi: 10.1186/1471-2105-11-489

Han, L., Wang, B., Wang, R., Gong, S., Chen, G., and Xu, W. (2019). The shift in the balance between osteoblastogenesis and adipogenesis of mesenchymal stem cells mediated by glucocorticoid receptor. *Stem Cell Res. Ther.* 10:377. doi: 10.1186/s13287-019-1498-0

Heirendt, L., Arreckx, S., Pfau, T., Mendoza, S. N., Richelle, A., Heinken, A., et al. (2019). Creation and analysis of biochemical constraint-based models using the COBRA Toolbox v.3.0. *Nat. Protocol.* 14, 639–702. doi: 10.1038/s41596-018-0098-2

Huang, D. W., Sherman, B. T., and Lempicki, R. A. (2009). Systematic and integrative analysis of large gene lists using DAVID bioinformatics resources. *Nat. Protocol.* 4, 44–57. doi: 10.1038/nprot.2008.211

Huang, T., Liu, R., Fu, X., Yao, D., Yang, M., Liu, Q., et al. (2017). Aging Reduces an ERRalpha-directed mitochondrial glutaminase expression suppressing glutamine anaplerosis and osteogenic differentiation of mesenchymal stem cells. *Stem Cells (Dayton, Ohio)* 35, 411–424. doi: 10.1002/stem.2470

Irizarry, A. R., Yan, G., Zeng, Q., Lucchesi, J., Hamang, M. J., Ma, Y. L., et al. (2017). Defective enamel and bone development in sodium-dependent citrate transporter (NaCT) Slc13a5 deficient mice. *PLoS One* 12:e0175465. doi: 10.1371/journal.pone.0175465

Kolesnikov, N., Hastings, E., Keays, M., Melnichuk, O., Tang, Y. A., Williams, E., et al. (2015). ArrayExpress update—Simplifying data submissions. *Nucleic Acids Res.* 43(D1), D1113–D1116. doi: 10.1093/nar/gku1057

Lee, W.-C., Guntur, A. R., Long, F., and Rosen, C. J. (2017). Energy metabolism of the osteoblast: implications for osteoporosis. *Endocrine Rev.* 38, 255–266. doi: 10.1210/er.2017-00064

Lieven, C., Beber, M. E., Olivier, B. G., Bergmann, F. T., Ataman, M., Babaei, P., et al. (2020). MEMOTE for standardized genome-scale metabolic model testing. *Nat. Biotechnol.* 38, 272–276. doi: 10.1038/s41587-020-0446-y

Liu, T. M., Martina, M., Hutmacher, D. W., Hui, J. H. P., Lee, E. H., and Lim, B. (2006). Identification of common pathways mediating differentiation of bone marrow- and adipose tissue-derived human mesenchymal stem cells into three mesenchymal lineages. *Stem Cells* 25, 750–760. doi: 10.1634/stemcells.2006-0394

Mazat, J. P., and Ransac, S. (2019). The fate of glutamine in human metabolism. The interplay with glucose in proliferating cells. *Metabolites* 9:81. doi: 10.3390/metabo9050081

Meleshina, A. V., Dudenkova, V. V., Shirmanova, M. V., Shcheslavskiy, V. I., Becker, W., Bystrova, A. S., et al. (2016). Probing metabolic states of differentiating stem cells using two-photon FLIM. *Sci. Rep.* 6:21853. doi: 10.1038/srep21853

Melis, D., Pivonello, R., Cozzolino, M., Della Casa, R., Balivo, F., Puente, A. D., et al. (2013). Impaired bone metabolism in glycogen storage disease type 1 is associated with poor metabolic control in type 1a and with granulocyte colony-stimulating factor therapy in type 1b. *Horm. Res. Paediatr.* 81, 55–62. doi: 10.1159/000351022

Meyer, J., Salamon, A., Mispagel, S., Kamp, G., and Peters, K. (2018). Energy metabolic capacities of human adipose-derived mesenchymal stromal cells *in vitro* and their adaptations in osteogenic and adipogenic differentiation. *Exp. Cell Res.* 370, 632–642. doi: 10.1016/J.YEXCR.2018.07.028

Milo, R., Jorgensen, P., Moran, U., Weber, G., and Springer, M. (2010). BioNumbers—The database of key numbers in molecular and cell biology. *Nucleic Acids Res.* 38, D750–D753.

Mohyeddin Bonab, M., Ali Sahraian, M., Aghsaie, A., Ahmadi Karvigh, S., Massoud Hosseinian, S., Nikbin, B., et al. (2012). Autologous mesenchymal stem cell therapy in progressive multiple sclerosis: an open label study. *Curr. Stem Cell Res. Ther.* 7, 407–414. doi: 10.2174/157488812804484648

Motamedian, E., Ghavami, G., and Sardari, S. (2015). Investigation on metabolism of cisplatin resistant ovarian cancer using a genome scale metabolic model and microarray data. *Iran. J. Basic Med. Sci.* 18, 267–276.

Neman, J., Hambrecht, A., Cadry, C., and Jandial, R. (2012). Stem cell-mediated osteogenesis: therapeutic potential for bone tissue engineering. *Biol. Targets Ther.* 6, 47–57. doi: 10.2147/BTT.S22407

Ng, F., Boucher, S., Koh, S., Sastry, K. S., Chase, L., Lakshmipathy, U., et al. (2008). PDGF, TGF-beta, and FGF signaling is important for differentiation and growth of mesenchymal stem cells (MSCs): Transcriptional profiling can identify markers and signaling pathways important in differentiation of MSCs into adipogenic, chondrogenic, and osteogenic lineages. *Blood* 112, 295–307. doi: 10.1182/blood-2007-07-103697

Noronha, A., Modamio, J., Jarosz, Y., Guerard, E., Sompairac, N., Preciat, G., et al. (2018). The Virtual Metabolic Human database: integrating human and gut microbiome metabolism with nutrition and disease. *Nucleic Acids Res.* 47(D1), D614–D624. doi: 10.1093/nar/gky992

Oberhardt, M. A., Palsson, B. Ø, and Papin, J. A. (2009). Applications of genome-scale metabolic reconstructions. *Mol. Syst. Biol.* 5:320. doi: 10.1038/msb.2009.77

Orth, J., Thiele, I., and Palsson, B. (2010). What is flux balance analysis? *Nat. Biotechnol.* 28, 245–248. doi: 10.1038/nbt.1614

Paglia, G. G., Magnúsdóttir, M. M., Thorlacius, S. S., Sigurjónsson, O., Guðmundsson, S. S., Palsson, B. B. Ø, et al. (2012). Intracellular metabolite profiling of platelets: evaluation of extraction processes and chromatographic strategies. *J. Chromatogr. B Analyt. Technol. Biomed. Life Technol.* 898, 111–120. doi: 10.1016/j.jchromb.2012.04.026

Park, J., Rho, H. K., Kim, K. H., Choe, S. S., Lee, Y. S., and Kim, J. B. (2005). Overexpression of glucose-6-phosphate dehydrogenase is associated with lipid dysregulation and insulin resistance in obesity. *Mol. Cell. Biol.* 25, 5146–5157. doi: 10.1128/mcb.25.12.5146-5157.2005

Pattappa, G., Heywood, H. K., de Bruijn, J. D., and Lee, D. A. (2011). The metabolism of human mesenchymal stem cells during proliferation and differentiation. *J. Cell. Physiol.* 226, 2562–2570. doi: 10.1002/jcp.22605

Phetfong, J., Sanvoranart, T., Nartprayut, K., Nimsanor, N., Seenprachawong, K., Prachayasittikul, V., et al. (2016). Osteoporosis: the current status of mesenchymal stem cell-based therapy. *Cell. Mol. Biol. Lett.* 21:12. doi: 10.1186/s11658-016-0013-1

Pino, A. M., Rosen, C. J., and Rodríguez, J. P. (2012). In Osteoporosis, differentiation of mesenchymal stem cells (MSCs) improves bone marrow adipogenesis. *Biol. Res.* 45, 279–287. doi: 10.4067/S0716-97602012000300009

Rosenbaum, A. J., Grande, D. A., and Dines, J. S. (2008). The use of mesenchymal stem cells in tissue engineering. *Organogenesis* 4, 23–27. doi: 10.4161/org.6048

Schellenberg, G. D., Bird, T. D., Wijsman, E. M., Orr, H. T., Anderson, L., Nemens, E., et al. (1992). Genetic linkage evidence for a familial Alzheimer's disease locus on chromosome 14. *Science (New York, N.Y.)* 258, 668–671. doi: 10.1126/science.1411576

Shum, L. C., White, N. S., Mills, B. N., Bentley, K. L., and Eliseev, R. A. (2016). Energy metabolism in mesenchymal stem cells during osteogenic differentiation. *Stem Cells Devel.* 25, 114–122. doi: 10.1089/scd.2015.0193

Sigmarsdóttir, Þ., McGarrity, S., Rolfsson, Ó., Yurkovich, J. T., and Sigurjónsson, Ó. E. (2020). Current status and future prospects of genome-scale metabolic modeling to optimize the use of mesenchymal stem cells in regenerative medicine. *Front. Bioeng. Biotechnol.* 8:239. doi: 10.3389/fbioe.2020.00239

Smith, A. C., Eyassu, F., Mazat, J.-P., and Robinson, A. J. (2017). MitoCore: a curated constraint-based model for simulating human central metabolism. *BMC Syst. Biol.* 11:114. doi: 10.1186/s12918-017-0500-7

Samples and Data < E-MEXP-3046 < Browse < ArrayExpress < EMBL-EBI (2018). Available online at: https://www.ebi.ac.uk/arrayexpress/experiments/E-MEXP-3046/samples/?s_page=1&s_pagesize=50 (accepted May 17, 2021).

Thiele, I., and Fleming, R. (n.d.). *Testing Basic Properties of A Metabolic Model (aka Sanity Checks)—The COBRA Toolbox*. Available online at: https://opencobra.github.io/cobratoolbox/stable/tutorials/tutorialModelSanityChecks.html (accessed June 3, 2019).

Thiele, I., and Palsson, B. (2010). A protocol for generating a high-quality genome-scale metabolic reconstruction. *Nat. Protocol.* 5, 93–121. doi: 10.1038/nprot.2009.203

Tsai, Y.-H., Lin, K.-L., Huang, Y.-P., Hsu, Y.-C., Chen, C.-H., Chen, Y., et al. (2015). Suppression of ornithine decarboxylase promotes osteogenic differentiation of human bone marrow-derived mesenchymal stem cells. *FEBS Lett.* 589, 2058–2065. doi: 10.1016/j.febslet.2015.06.023

Valencia, J., Blanco, B., Yáñez, R., Vázquez, M., Herrero Sánchez, C., Fernández-García, M., et al. (2016). Comparative analysis of the immunomodulatory capacities of human bone marrow– and adipose tissue–derived mesenchymal stromal cells from the same donor. *Cytotherapy* 18, 1297–1311. doi: 10.1016/j.jcyt.2016.07.006

Väremo, L., Scheele, C., Broholm, C., Mardinoglu, A., Kampf, C., Asplund, A., et al. (2015). Proteome- and transcriptome-driven reconstruction of the human myocyte metabolic network and its use for identification of markers for diabetes. *Cell Rep.* 11, 921–933. doi: 10.1016/j.celrep.2015.04.010

Vidal, C., Li, W., Santner-Nanan, B., Lim, C. K., Guillemin, G. J., Ball, H. J., et al. (2015). The Kynurenine pathway of tryptophan degradation is activated during osteoblastogenesis. *Stem Cells* 33, 111–121. doi: 10.1002/stem.1836

Wang, M., Yuan, Q., and Xie, L. (2018). Mesenchymal stem cell-based immunomodulation: properties and clinical application. *Stem Cells Int.* 2018:e3057624. doi: 10.1155/2018/3057624

Wang, W., Chen, Q., Li, X., Zhang, W., Peng, L., Wang, L., et al. (2013). Enhancement of bone formation with a synthetic matrix containing bone morphogenetic protein-2 by the addition of calcium citrate. *Knee Surg. Sports Traumatol. Arthroscopy* 21, 456–465. doi: 10.1007/s00167-012-1953-2

Waterman, R. S., Tomchuck, S. L., Henkle, S. L., and Betancourt, A. M. (2010). A new mesenchymal stem cell (MSC) paradigm: polarization into a pro-inflammatory MSC1 or an immunosuppressive MSC2 phenotype. *PLoS One* 5:e10088. doi: 10.1371/journal.pone.0010088

Yurkovich, J. T., and Palsson, B. O. (2016). "Solving puzzles with missing pieces: the power of systems biology [Point of View]," in *In Proceedings of the IEEE*, Vol. 104, (New York, NY: Institute of Electrical and Electronics Engineers Inc), doi: 10.1109/JPROC.2015.2505338

Zayzafoon, M., Gathings, W. E., and McDonald, J. M. (2004). Modeled microgravity inhibits osteogenic differentiation of human mesenchymal stem cells and increases adipogenesis. *Endocrinology* 145, 2421–2432. doi: 10.1210/en.2003-1156

Conflict of Interest: The authors declare that the research was conducted in the absence of any commercial or financial relationships that could be construed as a potential conflict of interest.

Paper III

frontiers in Bioengineering and Biotechnology

REVIEW
published: 31 March 2020
doi: 10.3389/fbioe.2020.00239

Current Status and Future Prospects of Genome-Scale Metabolic Modeling to Optimize the Use of Mesenchymal Stem Cells in Regenerative Medicine

Þóra Sigmarsdóttir[1,2†], Sarah McGarrity[2,3†], Óttar Rolfsson[3], James T. Yurkovich[4] and Ólafur E. Sigurjónsson[1,2]*

[1] The Blood Bank, Landspitali – The National University Hospital of Iceland, Reykjavik, Iceland, [2] School of Science and Engineering, Reykjavik University, Reykjavik, Iceland, [3] Faculty of Medicine, School of Health Sciences, University of Iceland, Reykjavik, Iceland, [4] Institute for Systems Biology, Seattle, WA, United States

OPEN ACCESS

Edited by:
Martin James Stoddart, AO Research Institute Davos, Switzerland

Reviewed by:
Ngan F. Huang, Stanford University, United States
Ron June, Montana State University, United States

****Correspondence:***
Ólafur E. Sigurjónsson
oes@ru.is

†These authors have contributed equally to this work

Specialty section:
This article was submitted to Tissue Engineering and Regenerative Medicine, a section of the journal Frontiers in Bioengineering and Biotechnology

Received: *11 July 2019*
Accepted: *09 March 2020*
Published: *31 March 2020*

Citation:
Sigmarsdóttir Þ, McGarrity S, Rolfsson Ó, Yurkovich JT and Sigurjónsson ÓE (2020) Current Status and Future Prospects of Genome-Scale Metabolic Modeling to Optimize the Use of Mesenchymal Stem Cells in Regenerative Medicine. Front. Bioeng. Biotechnol. 8:239. doi: 10.3389/fbioe.2020.00239

Mesenchymal stem cells are a promising source for externally grown tissue replacements and patient-specific immunomodulatory treatments. This promise has not yet been fulfilled in part due to production scaling issues and the need to maintain the correct phenotype after re-implantation. One aspect of extracorporeal growth that may be manipulated to optimize cell growth and differentiation is metabolism. The metabolism of MSCs changes during and in response to differentiation and immunomodulatory changes. MSC metabolism may be linked to functional differences but how this occurs and influences MSC function remains unclear. Understanding how MSC metabolism relates to cell function is however important as metabolite availability and environmental circumstances in the body may affect the success of implantation. Genome-scale constraint based metabolic modeling can be used as a tool to fill gaps in knowledge of MSC metabolism, acting as a framework to integrate and understand various data types (e.g., genomic, transcriptomic and metabolomic). These approaches have long been used to optimize the growth and productivity of bacterial production systems and are being increasingly used to provide insights into human health research. Production of tissue for implantation using MSCs requires both optimized production of cell mass and the understanding of the patient and phenotype specific metabolic situation. This review considers the current knowledge of MSC metabolism and how it may be optimized along with the current and future uses of genome scale constraint based metabolic modeling to further this aim.

Keywords: MSCs, metabolism, personalized/precision medicine, metabolomics, metabolic modeling, tissue engineering

INTRODUCTION

In recent years, there has been increasing interest in the possibilities offered by regenerative medicine (Maienschein, 2011; Sampogna et al., 2015), a field which seeks solutions for the restoration of the structure and functions of organs and tissues that have become permanently damaged. While regenerative medicine has enjoyed success in some areas, treatment can result in

danger to patients or in therapeutic inefficiency (Neman et al., 2012; Campana et al., 2014; Goldberg et al., 2017; Moreira et al., 2017; Cunningham et al., 2018; Solarte et al., 2018) that have pushed researchers to continuously search for novel approaches to address limitations.

One important area of regenerative medicine is the use of stem cells to enhance available therapeutic applications and to further the development of new ones (Mahla, 2016). In particular, mesenchymal stem cells, or mesenchymal stromal cells (MSCs) (Rosenbaum et al., 2008; Ullah et al., 2015; Fitzsimmons et al., 2018), are of interest. MSCs are multipotent cell types with stem cell-like abilities that can be isolated from various adult and neonatal tissues (Nombela-Arrieta et al., 2011; Alberts et al., 2014). MSCs maintain proliferation abilities while possessing the ability to undergo trilineage differentiation (adipogenic, chondrogenic, and osteogenic differentiation) and remarkable immunomodulatory capabilities (Rosenbaum et al., 2008; Lin et al., 2013). These properties offer the possibility of furthering treatment options for various ailments, such as metabolic and autoimmune diseases like multiple sclerosis (Bonab et al., 2012), Alzheimer's disease (Rosenbaum et al., 2008; Mahla, 2016), diabetes (Ullah et al., 2015; Fitzsimmons et al., 2018), Crohn's disease (Duijvestein et al., 2010), and cancer (Qin et al., 2016).

For the past decade, MSCs metabolism has received growing interest due to mounting evidence suggesting that the manipulation of metabolism allows enhanced therapeutic uses of these cells (e.g., cell retention, cell survival, immunoregulation, differentiation) in cell-based medicine and tissue engineering (Chen et al., 2008; Croitoru-Lamoury et al., 2011; Pattappa et al., 2011; Buravkova et al., 2013; Beegle et al., 2015; Shum et al., 2016; Li et al., 2017; Meyer et al., 2018; Vigo et al., 2019; Zhu and Thompson, 2019). Cellular metabolism is an intricate and complex network of pathways, enzymatic reactions, metabolites, and co-factors with numerous effects on the cell and its immediate surroundings. Due to the complexity of metabolism and its effects, research into the possibilities of manipulating metabolism in these cells has been slow.

The advent of high-throughput -omic technologies (Henry et al., 2010; Resendis-Antonio, 2013) has allowed for the detailing of genome-scale metabolic networks (Yurkovich and Palsson, 2016). This holistic systems biology approach acknowledges that biological systems are made up of a network of networks (Reed and Palsson, 2003; Resendis-Antonio, 2013; Bordbar et al., 2014). Genome-scale models (GEMs) of metabolism (Rocha et al., 2008) provide a framework for the computation of the genotype-phenotype relationship in which various types of -omics data can be integrated along with organism-specific network reconstructions to generate tissue, cell, or organism specific *in silico* models (Feist et al., 2009; Chang et al., 2010; Agren et al., 2014; Fouladiha et al., 2015). These models can then be constrained by experimental measurements and computed in order to explore possible therapeutic applications, making use of the newest RNA sequencing and metabolomic data or *in vitro* experimentation. Such models will aid further understanding of MSCs metabolism under various external or internal conditions. Thus far, metabolic modeling has not been applied to the study of MSCs, but this area offers great possibilities for enhancing both research and therapeutic application of these cells.

In this review, we describe how the study of human MSC (hMSC) metabolism can be used to answer the fundamental question: "How can GEMs be used to optimize MSC therapeutics?" First, we describe the biology of MSCs, their differentiation and immunomodulation properties and their applications and limitations in regenerative medicine. Next, we detail how metabolism affects or can be used to manipulate these functions. We then discuss how mathematical modeling of hMSC metabolism can aid in developing pre-clinical and clinical experiments. Finally, we give our vision for the future of using metabolic modeling to study hMSCs and how the resulting insights could prove transformative for the field of regenerative medicine.

BIOLOGY OF MESENCHYMAL STEM CELLS (MSCs)

Mesenchymal stromal cells comprise non-hematopoietic cells originating from the mesodermal germ layer and are capable of both self-renewal and multilineage differentiation into various tissues of mesodermal origin (Gazit et al., 2014). These multipotent cells can be isolated both from various adult tissues (e.g., skin, peripheral blood, bone marrow) and neonatal tissues (e.g., Wharton's jelly, umbilical cord blood) (Nombela-Arrieta et al., 2011; Alberts et al., 2014). Despite the historical lack of consensus on methods for isolation, expansion, and characterization of hMSCs, the International Society for Cellular Therapy (ISCT) has produced minimal criteria to define hMSCs (Rosenbaum et al., 2008; Lin et al., 2013). The cells must be able to:

- Adhere to plastic and develop as fibroblast colony-forming units and differentiate into cells of mesodermal origin (i.e., osteocytes, chondrocytes, and adipocytes). See **Figure 1**.
- Express the surface markers CD73, CD90, and CD105 during *in vitro* culture expansion
- Lack expression of CD11b, CD14, CD34, CD45, CD19, and HLA-DR surface markers during *in vitro* culture expansion

It is likely that this definition will continue to evolve to account for new findings.

Differentiation of MSCs

One of the identifying characteristics of MSCs is their ability to differentiate into cells of mesodermal origin (Nombela-Arrieta et al., 2011; Gazit et al., 2014). In addition to this hallmark trilineage differentiation, there have also been reports of differentiation toward other cell types of the ectodermal and endodermal origins, including tenocytes, cardiomyocytes, skeletal myocytes, smooth muscle cells, and neurons (Tatard et al., 2007; Galli et al., 2014; Ullah et al., 2015; Youngstrom et al., 2016). The actual functionality of the end product in this transdifferentiation is still debated.

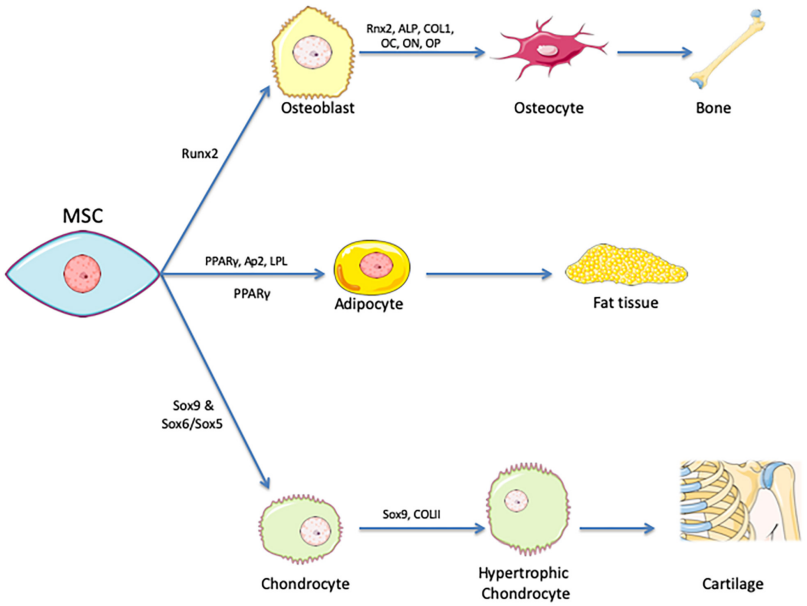

FIGURE 1 | Tri-lineage encompasses differentiation of MSCs. Mesenchymal stem cells are identified by their ability to differentiate into chondrocytes, adipocytes, and osteoblasts that in turn develop into cartilage, fat tissue and bone. PPARγ is the master regulator of adipogenesis, Runx2 for osteogenesis and Sox9 for chondrogenesis. Various expression markers are used as indicators of successful differentiation.

Differentiation of MSCs is primarily induced through media supplementation (and, in some instances, mechanical stimulation), with different supplements being required for the various differentiations. Adipogenesis, for example, is induced through supplementation with dexamethasone, indomethacin, insulin, and isobutyl methyl xanthine. Osteogenic differentiation is induced by dexamethasone, ascorbic acid, β-glycerophosphate, and sometimes bone morphogenic protein 2 (BMP-2) (Ullah et al., 2015). The completion of differentiation is verified by checking the expression of characteristic cell type markers, such as lipoprotein lipase (LPL) for adipogenesis and alkaline phosphatase (ALP) activity for osteogenesis (Ullah et al., 2015). More detailed lists of differentiation-promoting components and the most characteristic markers used to measure level of differentiation are shown in **Table 1**.

Differentiation is controlled by an interlinked set of regulatory molecules forming complex signaling pathways. These pathways are somewhat distinct between differentiation lineages, although there are important areas of overlap. This phenomenon is demonstrated by the inverse relationship that exists between pathways relating to adipogenic and osteogenic differentiation (**Figure 2**). Most differentiation pathways revolve around regulation of peroxisome proliferator-activated receptor (PPAR), which is the master regulator of adipogenesis, and runt-related transcription factor 2 (RUNX2), which is the master regulator of osteogenesis (Muruganandan et al., 2009; Neve et al., 2011; James, 2013; Hu et al., 2018). Further details on the most relevant reported signaling pathways and molecules for each type of differentiation are provided in **Table 1**.

Immunomodulation of MSCs

Beyond their potential for differentiation, hMSCs have remarkable immunomodulatory properties; they possess the ability to inhibit or promote the immune response of the host's body though mediated immunosuppression. These mechanisms include direct inhibitory effects and other indirect regulatory effects. This regulatory response involves inhibition of B and T cell proliferation, cytokine production inhibition, decreased natural killer (NK) cell activation, and dendritic cell maturation (**Figure 3**; Deng et al., 2005; Ma and Chan, 2016; Cunningham et al., 2018; Wang et al., 2018).

The immunomodulatory response of hMSCs is activated by inflammatory cytokines (e.g., IFN-γ, IL-1α, IL-1β, and TNF-α) that are secreted by T cells and other antigen-presenting cells (Ren et al., 2008; Németh et al., 2009). In response to their activation, MSCs secrete soluble immune factors capable of affecting both the innate and adaptive immune systems by mediating the subsequent regulatory responses of target cells (**Figure 4**; Kaundal et al., 2018; Wang et al., 2018). The immunoregulatory effects mediated in each instance are dependent on one or more of these secreted factors.

Indoleamine 2,3-dioxygenase (IDO) is one of the well-known paracrine factors released by hMSCs and has been shown to promote kidney allograft tolerance (Lan et al., 2010). It

TABLE 1 | Summary of various inducing components, expression markers, and signaling pathways related to differentiation.

Cell type resulting from differentiation	Differentiation-inducing components	Culturing time	Relevant expression markers	Most relevant reported signaling pathways and molecules	References
Adipocytes	Dexamethasone Indomethacin Insulin Isobutylmethyl xanthine	14–21 days, with 2 phases (determination and terminal differentiation)	ap2 LPL PPARγ	β-catenin dependent Wnt (anti) Hedgehog (anti) NELL-1 (anti) BMP (pro)	James, 2013
Cardiomyocytes	5-azacytidine	28 days	α-MHC α-cardiac actin ANP cTnT Desmin	miR1-2 + Wnt/β-catening (pro) HDAC TGF-β VR-1 5-aza	Solchaga et al., 2011; Guo et al., 2018
Chondrocytes	Ascorbate 2-phosphate Dexamethasone Insulin Linoleic acid Selenious pyruvate Selenium TGF-βIII Transferrin	21 days, with 2 phases (pre – induction and terminal differentiation)	*Phase 1:* Collagen types I and II *Phase 2:* L-Sox5 Sox6 Sox9	*Phase 1 expression dependent upon:* TGF-β1,2 and 3 *Phase 2 expression dependent upon:* BMP2 IGF-I TGF-β1 Wnt/β-catenin (pro) PTHrp (anti)	Mackay et al., 1998; Antonitsis et al., 2008; Li and Dong, 2016
Hepatocytes	*Phase 1:* bFGF EGF Nicotinamide *Phase 2:* Dexamethasone Insulin Oncostatin M Selenium Transferrin	2 phases: differentiation (7 days) and maturation			Ullah et al., 2015
Neuronal cells	bFGF BME EGF FGF HGF Insulin LMX1A* NGF Retinoic acid Valproic acid				Ullah et al., 2015
Osteocytes	β-glycerophosphate Ascorbic acid BMP-2 Dexamethasone	21–35 days	ALP COL1 OC ON OP RUNX2	β-catenin dependent Wnt (pro) BMP (pro) Hedgehog (pro) NELL-1 (pro) TGF-β1 + Wnt/β-catening (anti)	Neve et al., 2011; James, 2013
Pancreocytes	Actavin A Nicotinaminde Sodium butyrate Taurine				Ullah et al., 2015
Skeletal/smooth muscle	NICD TGF-β				Ullah et al., 2015

Note that this is not an exhaustive list.

suppresses proliferation and activity of NK and T cells by its metabolic activity – converting tryptophan into kynurenine. In humans, IDO synthesis has been reported as a response of MSCs to pro-inflammatory cytokine production that suppresses the inflammatory response (Bernardo and Fibbe, 2013; Mbongue et al., 2015; Gao et al., 2016; Kaundal et al., 2018; Wang et al., 2018).

Another reported soluble factor with immunoregulatory effects is the unstable oxidative molecule nitric oxide (NO), which is generated by NO synthase. Inducible NO synthase (iNOS) is responsible for the immunomodulatory effect of NO. Increased secretion of NO results in modulation of both the proliferation and function of T cells. At very high concentrations, it can lead to the apoptosis of immune cells (Bernardo and Fibbe, 2013; Gao et al., 2016; Kaundal et al., 2018; Wang et al., 2018). A list of the known soluble paracrine factors secreted by hMSCs that are involved in immunoregulation is provided in **Table 2**, along with their related effects.

Homing Effects of MSCs

Mesenchymal stromal cells secrete paracrine factors that promote tissue repair. In response to physical tissue damage, MSCs secrete factors that allow them to navigate to the site of injury, referred to as homing (Ullah et al., 2015). An example of a homing molecules used by MSCs are the chemokine receptors CXCR4 and CXCR7, which both bind to stromal cell-derived factor (SDF-1) on endothelial cells; this is a critical step in facilitating homing of MSCs to various tissues (Ullah et al., 2019). Homing is generally considered to be beneficial for tissue repair (Ullah et al., 2015) due to the interaction of the cells with the host tissue via secretion of trophic and paracrine factors (Ullah et al., 2015; Moreira et al., 2017). Engrafting or migration of hMSCs in experimental settings relies in part on this phenomenon in combination with the direct delivery of cells.

The homing effect and subsequent migration of hMSCs has been observed. However, the mechanisms behind it are not well understood. Only a small percentage of systemically administered cells manage to reach target tissue and remain there (De Becker and Riet, 2016; Moreira et al., 2017). For the most part, this low success rate has been ascribed to low expression levels of homing molecules, loss of expression of homing molecules during *in vitro* expansion, and cultural heterogeneity of the hMSCs. Cells derived from different sources seem to express different profiles of the homing molecules (De Becker and Riet, 2016; Moreira et al., 2017).

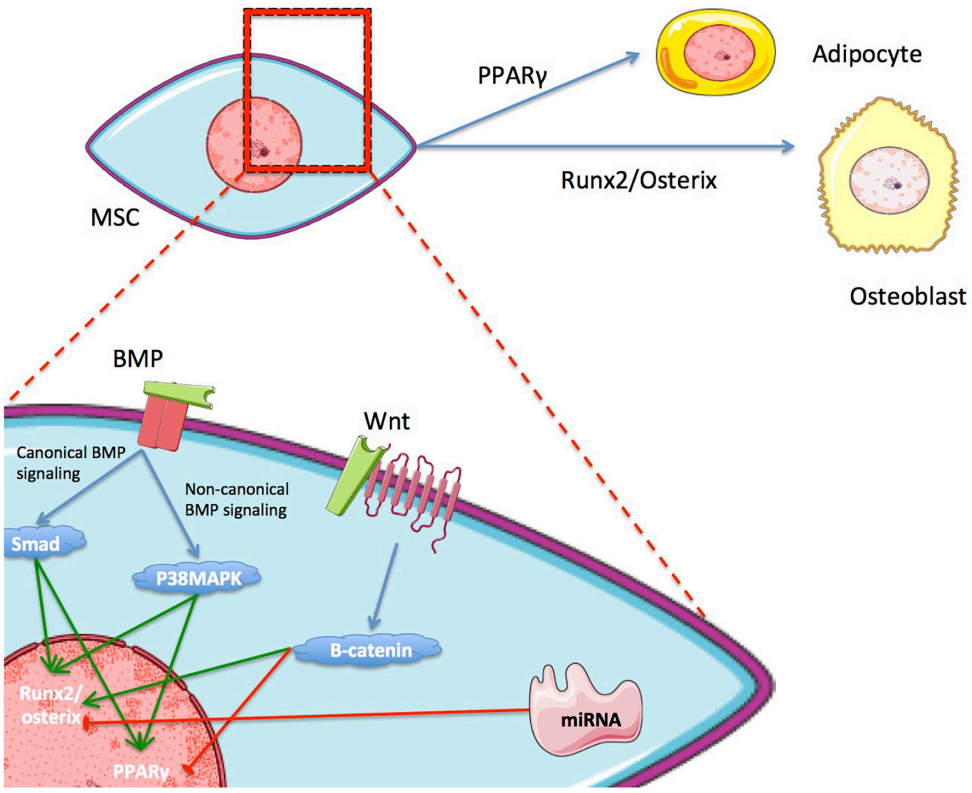

FIGURE 2 | The inverse relationship of the main metabolic pathways in OD and AD. Differentiation toward one lineage can inhibit differentiation toward the other.

MSCs as a Novel Tool in Regenerative Medicine

Regenerative medicine is considered a novel frontier in medical research (Maienschein, 2011; Sampogna et al., 2015). It combines the knowledge and application of various fields such as tissue engineering, cell transplantation, stem cell biology, biomechanics, prosthetics, nanotechnology, and biochemistry to replace or restore human cells, tissues, or organs to their normal functions (Sampogna et al., 2015). A variety of regenerative medicine therapies are available (see Lonner et al., 2000; Blais et al., 2013; Zhang X. et al., 2013; Trushina and Mielke, 2014; Björnson et al., 2016; Moreira et al., 2017), but their success has been limited by functional obstacles that increase the risk of harm to patients and reduce their efficacy as a therapeutic (Neman et al., 2012; Campana et al., 2014; Goldberg et al., 2017; Cunningham et al., 2018; Solarte et al., 2018). Despite recent progress, there is obvious room for improvements regarding both the safety and efficacy of therapies for patients. The multipotency, high proliferation potential, paracrine effect, and immunomodulatory activity of hMSCs (Rosenbaum et al., 2008; Ullah et al., 2015; Fitzsimmons et al., 2018) have led to development of MSCs as a tool for use in regenerative medicine. Thus, MSCs are considered ideal candidates for immunotherapy and tissue engineering.

Recent advancements have allowed researchers to overcome initial obstacles in the use of MSCs. Numerous clinical trials have assessed their safety and found that transfusions using these cells are safe (Neman et al., 2012; Zhao et al., 2016). Various studies have developed isolation and culture approaches along with various possible mechanisms of delivery. These studies have shown that long-term culture of MSCs is possible without losing the cells functional, phenotypical, or morphological features (Bernardo et al., 2007).

Further, MSCs are becoming readily available for biomedical research. There is growing interest in the use of placental- and umbilical cord-derived hMSCs due to the relatively high availability of discarded tissue associated with births (Moreira et al., 2017); however, the variance in phenotypic properties (if any) between hMSCs derived from different sources is an important open question. Bone marrow- (BM-) and adipose tissue-derived (Ad-) hMSCs are the most favored stem cell

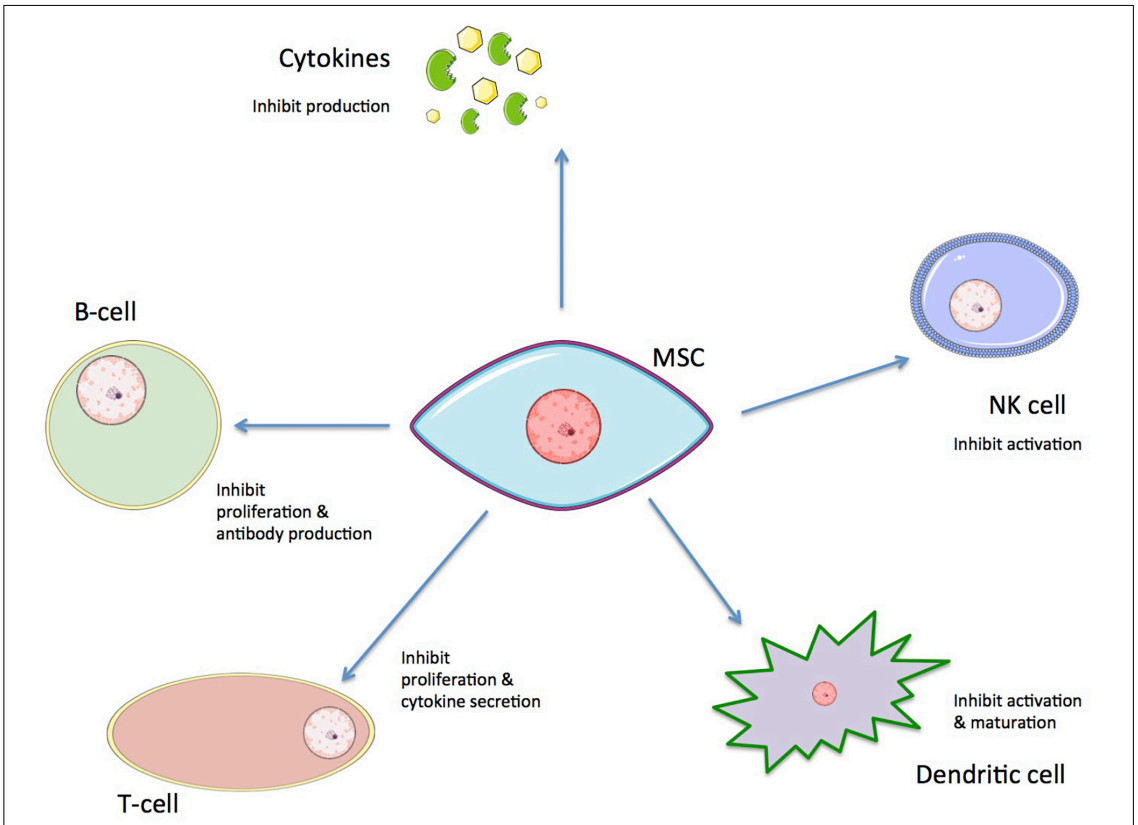

FIGURE 3 | The immunoregulatory effects of hMSCs on immune cells.

types in both tissue engineering and cell-based medicine for a variety of reasons, despite the invasive procedures required for tissue collection (Fitzsimmons et al., 2018): (1) the total cell number that can be harvested each time is higher than with other stem cells; (2) the frequency of cells of interest is higher than with other stem cells; and (3) Ad-hMSC harvesting can be performed as part of some elective cosmetic surgeries (e.g., liposuction) (Fitzsimmons et al., 2018). Ad-hMSCs have been shown to have increased capacity for adipogenic differentiation *in vitro*, while BM-hMSCs have increased capacity for osteogenic and chondrogenic differentiation (Liu et al., 2007). Through a comparative study on the immunomodulatory abilities of cells derived from the same donor bit different tissues, Valencia et al. (2016) determined that Ad-hMSCs have a higher capacity for inhibiting dendritic cell differentiation than do BM-hMSCs, while BM-hMSCs displayed a higher capacity for inhibition of NK cell cytotoxic activity; these results have been corroborated by several independent groups (Ivanova-Todorova et al., 2009; Blanco et al., 2016). These observations—whether relating to proliferation potential or direct therapeutic application abilities—highlight the importance of choosing the optimal cell source for a particular clinical circumstance.

Efficacy of Cell Engraftment vs. Paracrine Factors

For the last several decades, the therapeutic potential of hMSCs has been focused on cell transplantation, adding hMSCs to a recipient donor site for repair via regeneration, differentiation, and immunomodulation (Lukomska et al., 2019). Co-culturing in animal studies has shown that hMSCs can induce tissue regeneration to some extent in the heart (Rose et al., 2008), kidneys (Qian et al., 2008), and liver (Cho et al., 2009) through infiltration and replacement in damaged or injured tissue by multipotent hMSCs (see **Figure 5**). Increasing attention, however, has lately been given to the immunomodulatory and suppressive capabilities of hMSCs, especially with regards to their paracrine factors (Németh et al., 2009; Cunningham et al., 2018; Kaundal et al., 2018). Currently, approximately 10% of the clinical trials registered in the United States are using MSCs to study immunological disease. Through their ability to decrease inflammation and general inhibitory functions, hMSCs have been utilized as contributing factors for various immune disorders for

TABLE 2 | A list of inflammatory cytokines that activate immunoregulatory state of hMSCs, major known soluble paracrine factors secreted by hMSCs, and a summary of their biological functions.

Immunosuppressive factors secreted by MSCs	Summary of biological function	Activating inflammatory cytokines
CCL2	Promotion of monocyte migration. Suppression of activation and mitigation of TH17 cells.	IFN-γ, IL-1α, IL-1β, TNF-α
Galectins	Suppression of the immunomodulatory effects of T cells.	
IDO	Suppression of the effects and proliferation of immune cells.	
IL-10	Suppression of immune cell apoptosis.	
NO	Promotion of immune cell apoptosis. Suppression of proliferation and modulation of T cells.	
PGE2	Suppression of NK cell cytolytic activity and T cell proliferation.	
TSG6	Overall anti-inflammatory effect.	
TGF-β	Inhibition of mast cell degranulation, NK cell activation and proliferation, and Treg induction.	

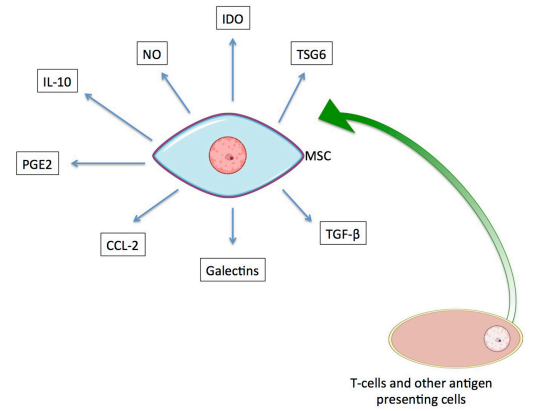

FIGURE 4 | The immunoregulatory secretome of hMSCs. Known soluble factors secreted by MSCs upon activation by T cells and other antigen presenting cells are shown.

symptom relief. Such disorders include type 1 and type 2 diabetes (Moreira et al., 2017), acute graft versus host disease (GvHD) (Gao et al., 2016), arthritis (Burke et al., 2016), allograft rejection (Munir and McGettrick, 2015), and Crohn's disease (Ibraheim et al., 2018). The possible immunomodulatory effects of hMSCs have been found to be dependent upon the source of the hMSCs as well as their immediate microenvironment (Bortolotti et al., 2015). The microenvironment is dependent upon the individual inflammatory profile of the host, which is potentially related to any disease pathogenesis present. This variability leads to varied cytokine profiles that are, at least in part, responsible for the difficulties of using MSC therapy effectively in both preclinical and clinical situations (Kaundal et al., 2018). Some of these challenges may be overcome by personalizing each case (i.e., tailoring each therapy to the inflammatory environment of the recipient patient).

There has been a recent paradigm shift away from the primary aim of hMSC transplantation being tissue repair by engraftment toward the use of hMSCs to promote healing via their secretion of paracrine factors. In many therapeutic contexts, it is now recognized that MSCs exert their healing effects through paracrine signaling and cell-to-cell contact, not by replacing cells (Fitzsimmons et al., 2018). There are a few notable examples using hSMCs as paracrine-mediated treatment currently in development (Amorin et al., 2014; Hofer and Tuan, 2016; Archambault et al., 2017; Moreira et al., 2017; Cunningham et al., 2018; Ibraheim et al., 2018; Solarte et al., 2018). The reported success of these studies indicates that the MSC secretome exerts beneficial effects that may be exploited by therapeutic applications.

Existing Challenges and Problems

Despite the initial successes demonstrated in animal and early clinical trials regarding the safety and efficacy of hMSCs, a number of challenges, problems, and unanswered questions remain. In order for *in vitro* cultured MSCs to engraft after implantation or to secrete their beneficial factors, they must be able to survive. The transplantation procedure itself exerts various direct mechanical and chemical stresses on the cells, and the treated tissue offers a comparatively much harsher environment than the standard culture surroundings that cells experience *in vitro*. In tissues *in vivo*, there are various negatively impacting stressors, such as hypoxia, inflammation, decreased energy/nutritional availability, and high acidity. Various strategies to enhance survival and overcome these adverse conditions have been developed, including preconditioning, genetic modification, and supportive biomaterials as a delivery device (Baldari et al., 2017; Moreira et al., 2017).

It is possible that donor variability and differences in isolation site have an effect on experimental outcomes, though the extent of these effects is not yet well understood. This uncertainty may be exacerbated by heterogeneity in the origins of MSCs used in tests (Bortolotti et al., 2015; Lukomska et al., 2019). Further, there is a lack of knowledge of the optimal dose and frequency required for hMSC transplantation (Lee, 2018; Lukomska et al., 2019). In addition, generating high doses of hMSCs requires cellular expansion on a large scale. Despite being proven to retain their characteristics over long term expansion (Bernardo et al., 2007), MSCs eventually become senescent (Turinetto et al., 2016). Senescent cells have undergone functional changes. Firstly, differentiation potential usually decreases due to accumulation of oxidative stress and dysregulation of key differentiation

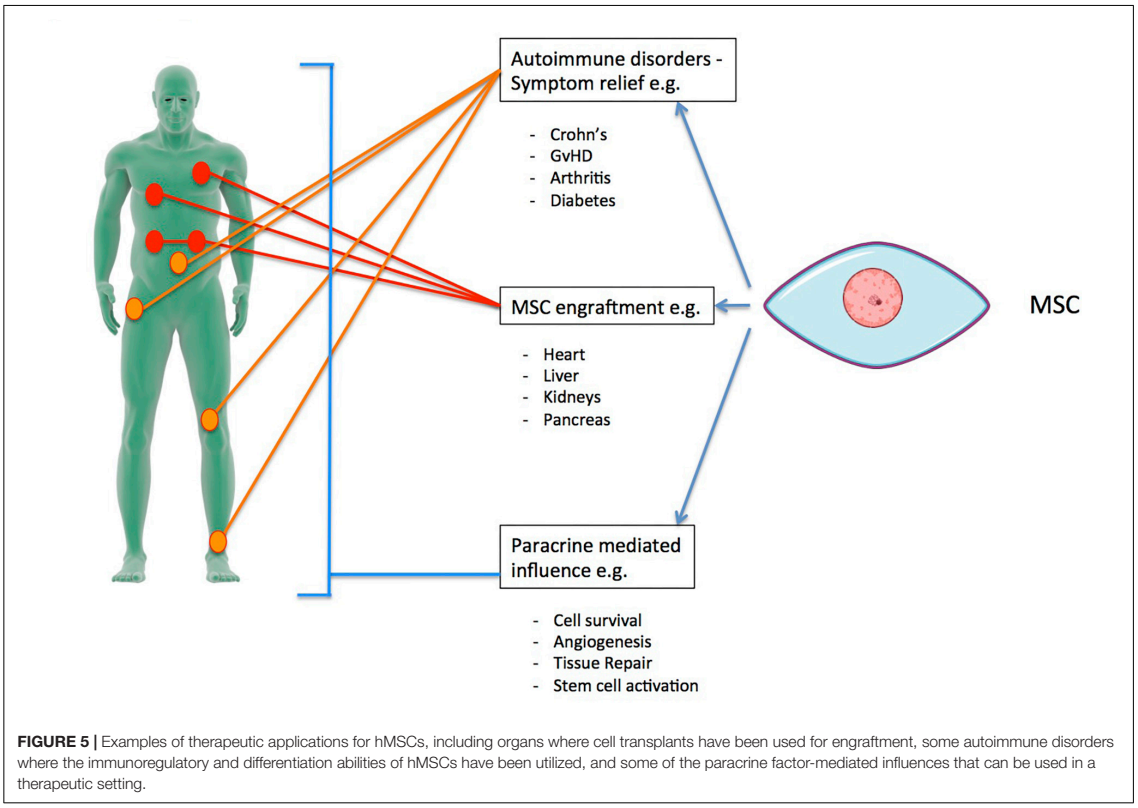

FIGURE 5 | Examples of therapeutic applications for hMSCs, including organs where cell transplants have been used for engraftment, some autoimmune disorders where the immunoregulatory and differentiation abilities of hMSCs have been utilized, and some of the paracrine factor-mediated influences that can be used in a therapeutic setting.

regulatory factors. Secondly, both migratory- and homing-related abilities of hMSCs are reduced as they move into senescence. Finally, the secretome of hMSCs becomes compromised in senescence. Many of the factors that are present in the senescent MSC secretome can exacerbate an inflammatory response at a systemic level and so promote either migration or proliferation of cancer cells (Turinetto et al., 2016).

In many cases of MSC transplantation, there is little to no integration of the transplanted cells, and cells that are retained are observed to have a short survival time in some cases (Li et al., 2016; Lukomska et al., 2019). Even though more than two thousand patients have received either autologous or culture expanded allogeneic MSCs, long-lasting observations are lacking in many cases (Lukomska et al., 2019). This lack of data indicates that more progress is difficult. Tumor support due to the immunosuppressive effects of MSCs and the related possibility of tumorigenicity of such a therapy has been reported (Barkholt et al., 2013). There have also been reports of BM-hMSC-induced liver fibrosis (Russo et al., 2006). These issues must be addressed by long-term studies regarding safety of use.

While the use of hMSCs holds great promise in regenerative medicine, the hurdles and unanswered questions outlined in this section still linger. perhaps the greatest barrier preventing widespread and successful implementation of hMSCs as tools to enhance and develop therapeutics is the critical gap in knowledge of hMSC metabolism. During differentiation, we can observe a metabolic shift in hMSCs from using only glycolysis to a mix of glycolysis, oxidative phosphorylation, and beta fatty acid oxidation to produce energy. However, in order to have immunomodulatory effects (via paracrine factors) on a host's immune system, hMSCs must be mainly in a glycolytic state. Further, it is not well understood to what extent energy metabolism is mixed at different stages of differentiation (early versus late) or whether it is dependant upon the type of differentiation the cells are undergoing. An understanding of how cell source and age affects differentiation and if different states affect the survival and function and, therefore, usability of cells *in vivo*. In the following section, we delve into some of these gaps and discuss how acquiring a deep understanding of underlying mechanisms can help unlock the therapeutic potential of hMSCs in regenerative medicine.

METABOLISM OF MSCs

MSC Function Is Linked to Metabolism

The proliferation, differentiation, and immunomodulatory functions of hMSCs are linked to cellular metabolism

(dos Santos et al., 2010; Estrada et al., 2012; Beegle et al., 2015). Emerging evidence suggests that hMSCs are metabolically heterogeneous and that these differing metabolic states impact both differentiation ability and capacity for immunomodulation (Agathocleous and Harris, 2013; Liu et al., 2019). To date, studies have focused primarily on BM-hMSCs and Ad-hMSCs.

There is strong evidence suggesting that, in their undifferentiated state (while undergoing proliferation), hMSCs rely primarily on glycolysis for energy production. This phenotype has been demonstrated in BM-hMSCs, which show a preference for glycolysis during proliferation (Pattappa et al., 2011; Buravkova et al., 2013; Shum et al., 2016; Zhu and Thompson, 2019) but shift to a more oxidative phosphorylation (OxPhos)-dependent metabolism during osteogenic and adipogenic differentiation (OD, AD) (Meleshina et al., 2016; Shum et al., 2016). Similar findings have been reported for Ad-hMSCs (Meleshina et al., 2016; Meyer et al., 2018). Proliferating Ad-hMSCs were found to have a preference for glycolysis even under aerobic conditions, while during OD the cells increased both glycolysis and mitochondrial metabolism, including the processes of OxPhos and fatty acid β-oxidation. However, when Ad-hMSCs underwent AD, they showed a decreased capacity for the pentose phosphate pathway (PPP) and glycolysis, while mitochondrial enzyme activities increased, indicating an increased capacity for oxidative phosphorylation and β-oxidation (Meleshina et al., 2016; Meyer et al., 2018).

The ability of BM-hMSCs to differentiate has also been shown to be affected by mitochondrial functions (Zhang Y. et al., 2013; Li et al., 2017). Consistent with reports that proliferating hMSCs have a glycolytic phenotype, undifferentiated cells have high levels of hypoxia-inducible factor 1 (HIF-1), a transcriptional regulator central to regulation of genes that are involved in hypoxic responses. It is also a crucial physiological regulator of anaerobic metabolism (Gaspar and Velloso, 2018). Cells undergoing OD downregulate HIF-1. Downregulation of HIF-1 seems to be required for the activation of mitochondrial OxPhos, an oxygen-dependent pathway (Shum et al., 2016).

The mitochondria of hMSCs seem to be primarily inactive while cells remain in their proliferation stage, during which metabolic pathways related to glycolysis and its associated signaling pathways required for adenosine triphosphate (ATP) generation and general anabolitic activity are most active (see **Table 3**). Glycolytic metabolism also seems to be a requirement for hMSCs to be able to sustain immunosuppressive factor secretion (Liu et al., 2019). Secretion of immunomodulatory factors is only possible when hMSCs have been activated, such as by IFN-γ (Waterman et al., 2010). Liu et al. (2019) utilized IFN-γ treatment to cause immune polarization in hMSCs leading to remodeling of metabolic pathways toward glycolysis (reducing TCA cycle metabolism), a requirement for sustained immunosuppressive factor secretion. The activated cells were measured to have increased lactate levels, glucose consumption, and acidification rate. Increased expression of glucose transporter 1 and hexokinase isoform 2 (key enzymes in glycolysis), along with reduced electron transport and OxPhos, was also observed. These are all indicators of increased glycolytic activity (Liu et al., 2019). MSCs with a glycolytic phenotype are also able to sustain IDO production and the exposure to IFN-γ inhibited activity of the mitochondrial electron transport chain (complexes I or III), blocking OxPhos and reducing mitochondria-related reactive oxygen species (mROS). This reduces the effects of mROS that are key to metabolic remodeling in differentiation. Liu et al. (2019) further showed that Akt/mTOR signaling pathway activation is required to induce metabolic reconfiguration, specifically IDO and Prostaglandin E2 (PGE2) production. PGE2 increases in response to increased aerobic glycolysis. The immune response of hMSCs treated with IFN-γ is altered if the metabolic reconfiguration induced by Akt/mTOR is disrupted.

TABLE 3 | List of common signals in metabolism and the major metabolic pathways effected.

Signal	Metabolic pathways regulated by the signal
AMPK	Inhibition of glycolysis and fatty acid synthesis. Promotion of fatty acid oxidation.
Hedgehog	Stimulation of glycolysis.
HIF	Redirection of energy metabolism from OXPhos to glycolysis.
mTOR	Stimulation of glycolysis, lipid synthesis, protein synthesis, and pyrimidine synthesis.
Myc	Stimulation of glycolysis, glutaminolysis, and nucleotide synthesis.
PI3K	Stimulation of glucose uptake, fatty acid synthesis, and glycolysis.
Ras	Stimulation of glucose uptake and PPP. Regulation of glutaminolysis.
Sirtuins	Regulation of TCA cycle, glycolysis, and fatty acid oxidation.

The effect of interferon regulation on hMSC metabolism can be varied. IFN-γ has also been used to inhibit proliferation and alter AD, OD, and neural differentiation (ND) by activating IDO (Croitoru-Lamoury et al., 2011). The kynurenine pathway (KP), along with IDO1 and IDO2, is expressed in hMSCs and highly regulated by both IFN-γ and IFN-β. IFN-γ licensing of hMSCs results in inhibited proliferation via activation of the KP and subsequently IDO, and inhibits the cell potential for OD and AD. In contrast to IFN-γ licensing, IFN-β treatment managed to increase expression of adipogenic markers (Croitoru-Lamoury et al., 2011).

IFN-β has been shown to enhance immunomodulatory functions of hMSCs in other reports. Vigo et al. (2019) demonstrated IFN-γ induced expression of secretory leukocyte protease inhibitor (SLPI) and hepatocyte growth factor (HGF), soluble mediators that are involved in both immune and regenerative functions of hMSCs. Simultaneously, IFN-β induced the activity of mTOR, increasing the glycolytic capacity of the cells. This energy metabolic modification improved the cells' ability to control T cell proliferation, yet another indication of a link between high glycolytic capacity and immunomodulatory capabilities (Vigo et al., 2019).

Overall reports discussing hMSC metabolism seem to, for the most part, agree that during proliferation the cells primarily generate ATP through glycolysis. However, upon initiation of differentiation, cells seem to turn toward mitochondrial metabolism, with reported increases in metabolism and

biogenesis indicating the importance of mitochondrial activity when it comes to hMSC functionality (Shum et al., 2016).

There is not much known about whether amino acid metabolism is affected during functional progression of hMSCs or what effects they induce if modified through metabolic changes. For example, El Refaey et al. (2015) studied the aromatic amino acids tryptophan and tyrosine, finding that oxidation (via cell senescence) disrupted their anabolic effects on BM-MSCs. By using mouse BM-MSCs, they were able to examine effects of oxidized dityrosine and kynurenine of proliferation and differentiation and found that these oxides inhibited BM-MSC proliferation, ALP expression and activity and expression of osteogenic markers. Yue et al. (2018) studied fatty acid related gene expression and compositions of fatty acids during adipogenesis of bovine Ad-MSCs and found that lipid-related gene expression and fatty acid composition changed noticeably during the early stages of differentiation (e.g., there was increased expression of *de novo* lipogenesis-related genes, and thus *de novo* lipogenesis produced fatty acid elongation and desaturation) before returning to normal (e.g., proportions of saturated fatty acids, monounsaturated fatty acids, and polyunsaturated fatty acids returned to initial levels in later stages). Their conclusion was that *de novo* lipogenesis and desaturation comprised the major fatty acid flux during adipogenic differentiation of bovine Ad-MSCs.

Ornithine decarboxylase (ODC) and polyamine biosynthesis are important in the proliferation of stem cells (Tsai et al., 2015). The role of ODC regarding differentiation has not been fully explored but is considered to be diverse. Through the study of inhibition of ODC's irreversible inhibitor, α-difluoromethylornithine, Tsai et al. (2015) hypothesized that inhibition of ODC and the accompanying depletion of exogenous polyamines might be correlated with the osteogenic induction of BM-hMSCs, and demonstrated (in BM-hMSCs) that decreases in the expression of PPAR- γ and ODC along with an accompanying reduction in polyamines, are responsible for enhanced osteogenesis.

MSC Functionality Is Greatly Impacted by Mitochondrial Activity

As suggested in section "MSC Function Is Linked to Metabolism," active mitochondria are necessary for successful differentiation. Accumulating evidence indicates that mitochondrial enzymes and regulatory pathways are of great importance for MSCs in proliferative and differentiating states (Chen et al., 2008; Buravkova et al., 2013; Li et al., 2017). Mitochondria have been found to be crucial for sufficient ATP production to support OD, in addition to other mechanisms. Active mitochondria support OD by promoting β-catenin acetylation and, therefore, its activity. β-catenin is an important signaling pathway in osteogenesis (Shares et al., 2018). In osteogenesis, a mechanism of OD induction is to induce mitochondrial OxPhos by replacing glucose with galactose. This switch also stimulates β-catenin signaling and β-catenin acetylation. Increased β-catenin acetylation is the mechanism of osteogenesis driven by mitochondrial OxPhos (Shares et al., 2018). This acetylation increases during osteogenesis (BM-hMSCs). Active mitochondria may also support other osteogenic pathways by providing acetyl groups.

Other enzymatic activity has been confirmed that further supports the importance of mitochondrial activation for MSC functionality. Creatine kinase (CK) activity, which is involved in buffering and recovery of ATP, has been reported in Ad-hMSCs. It stimulates glycogenolysis by increasing cytoplasmic concentration of inorganic phosphate. Activity of CK was found in both differentiated and proliferating Ad-hMSCs, with more mitochondrial CK activity in AD cells. This further supports the theory of a shift toward oxidative metabolism/mitochondrial metabolism during differentiation of MSCs (Meyer et al., 2018).

Through the reversible mitochondrial nicotinamide adenine dinucleotide phosphate (NADP)-dependent reaction of isocitrate dehydrogenase (NADP-IDH), an anaplerotic pathway exists that forms isocitrate from glutamine through a process called glutaminolysis. Through this pathway, glutamine can compensate for the lack of glucose for both ATP production and anabolic precursor supply (Smolková and Ježek, 2012). This pathway is active in MSCs during OD, indicating yet another important role that mitochondria play when it comes to provision of sufficient ATP to ensure successful differentiation.

Reactive oxygen species (ROS) are known to serve as signaling molecules capable of regulating biochemical pathways that are a part of normal cell function. They are particularly important in metabolism and inflammatory signaling (Forrester et al., 2018). Regulation of mROS levels also contributes to determination of differentiation outcome. For a long time, these molecules were considered to be harmful to cells, inducing organismal death and dysfunction, but more recent reports suggest that excess mROS impair OD and promote AD by inhibiting Hedgehog signaling (a pathway essential for bone development and maintenance) (Li et al., 2017).

Possible Ways to Achieve Metabolic Manipulation

Since functionality and survival of hMSCs is affected by changes in their metabolism, there is the potential to enhance the efficacy of hMSC therapies through manipulation of metabolism. hMSCs can effectively reconfigure metabolism to respond to the biochemical demands of tissue repair, be it secretion of immunomodulatory factors or integration and differentiation toward tissue specific cell types (Mylotte et al., 2008; Zhu et al., 2014; Yuan et al., 2019). Currently, the most extensively studied subtypes are BM-hMSCs and Ad-hMSCs, but even these subtypes have not been exhaustively studied. Evidence indicating the importance of both the enzymes and mitochondrial pathways support its significance for proliferation and differentiation of hMSCs (Chen et al., 2008; Buravkova et al., 2013; Li et al., 2017). In addition, several critical MSC functions are not only influenced by internal cellular mechanisms, but also by external ones (mechanical and biochemical) such as the composition of its microenvironment (Bloom and Zaman, 2014). Previous work has explored various ways of affecting the mechanisms controlling MSC metabolic function (see **Figure 6**).

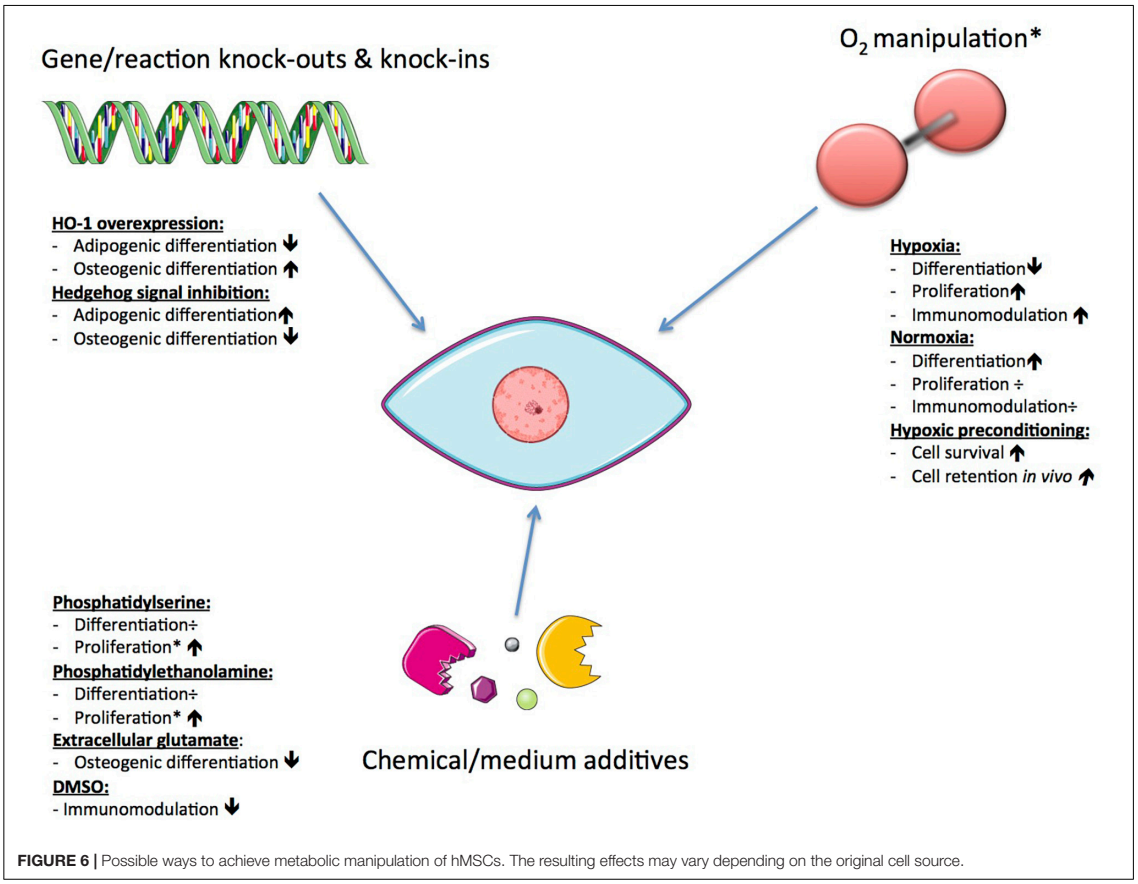

FIGURE 6 | Possible ways to achieve metabolic manipulation of hMSCs. The resulting effects may vary depending on the original cell source.

One such approach is to alter the functional capacity of MSCs through oxygen manipulation, due to the importance of mitochondria and mROS discussed above. Muñoz et al. (2014) investigated the effect of oxygen levels on metabolic phenotypes of hMSCs. Oxygen is a ubiquitous regulator of cellular metabolic activity and of the survival, function, and differentiation of hMSCs. Using both normoxic and hypoxic conditions, they found contrasting metabolic profiles for hMSCs during proliferation versus OD. The key difference was found in the coupling of glycolysis to the TCA cycle, glutaminolysis, and malate-aspartate shuttle. In response to low oxygen levels, undifferentiated hMSCs showed increased consumption of both glucose and glutamine that activated the malate-aspartate shuttle in order to accommodate increased cytosolic production of nicotinamide adenine dinucleotide + hydrogen (NADH) and transport glutamate and reducing equivalents into the mitochondrial matrix for oxidation (Muñoz et al., 2014). Low oxygen also activates HIF-1, reducing pyruvate dehydrogenase activity so that transport of glucose derived carbons into the TCA cycle decreases (Estrada et al., 2012). These metabolic characteristics allow increased proliferation under hypoxic circumstances, allowing cells to survive in an ischemic environment.

Similar findings were reported for proliferation of cells grown under hypoxia (dos Santos et al., 2010). For cells in OD, hypoxia induces a more significant block of carbon flow from glycolysis into the TCA cycle, compared to undifferentiated cells. This is demonstrated by a greater rise in lactate levels. The carbon flow blockage results in lower citrate levels and less production of reduced cofactors [e.g., NADH and flavin adenine dinucleotide ($FADH_2$)] involved in OxPhos. The lower citrate levels indicate a more pronounced metabolic uncoupling of glycolysis and TCA cycle for cells in OD compared to undifferentiated cells (Muñoz et al., 2014). This observation of a tight coupling of glycolysis and TCA cycle in cells undergoing OD compared to proliferating hMSCs suggests a stronger dependence on oxygen during OD (Muñoz et al., 2014). This dependency has been shown independently (Buravkova et al., 2013). Permanent oxygen deprivation resulted in the attenuation of cellular ATP levels, leading to diminished mitochondrial ATP production and stimulation of glycolytic ATP production. The attenuated cellular ATP levels stimulated a proliferation state of the hMSCs and

reduced the differentiation capacity, indicating that low ATP levels (arising from glycolysis only) are sufficient to maintain the cells' uncommitted state (Buravkova et al., 2013). Hypoxia has also been used to precondition MSCs to enhance their survival and cell retention *in vivo* via induction of metabolic changes (Beegle et al., 2015).

Reactive oxygen species are known to play a role in the mediation of both pathophysiological and physiological signal transduction (Forrester et al., 2018). The subcompartments in cells (e.g., peroxisome and mitochondria) that produce ROS are often associated with metabolism. Mitochondria-related ROS are able to influence metabolic processes on their own, and so have an effect on differentiation and immunomodulation of hMSCs. Studies have shown that by using mitochondrial-targeted antioxidants, AD may be inhibited; however, as mentioned in section "MSC Functionality Is Greatly Impacted by Mitochondrial Activity," excess mROS impair OD and promote AD by inhibiting Hedgehog signaling (Li et al., 2017). The role of mROS in chondrogenic differentiation (CD) is less well known (Li et al., 2017). Takarada-Iemata et al. (2011) found that through sustained exposure to glutamate, a significant decrease in osteoblastic marker expression could be induced. This happened in association with a reduction of intracellular glutathione (GSH) levels, but without affecting adipogenic marker expression. This finding suggests that extracellular glutamate preferentially suppresses osteoblastogenesis over adipogenesis in MSCs through the cysteine/glutamate antiporter (Takarada-Iemata et al., 2011).

The effects of other chemical stimuli have also been reported. In contrast to the inhibiting effects of extracellular glutamate on OD, it was reported that by inducing overexpression of heme oxygenase-1 (HO-1) OD of BM-hMSCs may be enhanced and adipogenesis decreased (although no mechanism was determined) (Barbagallo et al., 2010). HO-1 is a nuclear factor erythroid 2-related factor 2 (Nrf2)-regulated gene that plays a critical role in preventing vascular inflammation. It also has important antioxidant, anti-inflammatory, antiproliferative, and antiapoptotic effects in vascular cells (Araujo et al., 2012). Recent reports suggest that frozen or cryopreserved hMSCs are therapeutically less effective than freshly harvested MSCs (François et al., 2012). It seems that dimethyl sulfoxide (DMSO), a commonly used cryopreservative solution, decreases metabolic and immunosuppressive properties of hMSCs, while valproic acid (VPA) pre-treatment enhances both (François et al., 2012). Moreover, the T cell suppressive capacity of hMSCs *in vivo* is related to the cells' glycolytic and respiratory capacity, in contrast to their IDO dependence *in vitro*. This observation, therefore, leads to speculation that hMSCs may only be able to induce immunoregulatory effects when undifferentiated.

Metabolism in MSCs is a complex and dynamic system. We have outlined several gaps in the collective knowledge of MSC metabolism that are actively being addressed by the community. As we gain insights into questions regarding the primary energy-generating pathway(s) utilized during differentiation, we will move closer to manipulating these systems. However, we will need a holistic perspective that integrates knowledge at the various biological levels of MSC differentiation.

MATHEMATICAL MODELING OF HUMAN METABOLISM

A bottom-up systems biology approach allows for a mechanistic understanding of a system (Westerhoff and Palsson, 2004). Such mathematical models can predict potential interventions, potentially providing insights into how to successfully manipulate MSCs for therapeutic applications. Over the last few decades, many individual components of MSC biology have been studied in detail. However, to predict a cell's phenotype, it is necessary to understand all of the systemic interactions of environmental and cellular components that contribute to that phenotype (Bordbar et al., 2014). A combination of high-throughput -omics technologies, enabling the collection of large data sets, and improved computational modeling methods to holistically analyze that data have made systems biology possible (Henry et al., 2010; Resendis-Antonio, 2013).

The first step in modeling metabolism at the genome-scale is to reverse engineer the network structure (Reed and Palsson, 2003; Resendis-Antonio, 2013; Bordbar et al., 2014; Yurkovich and Palsson, 2016). This reconstruction process starts with collecting all annotated components of the genome and experimental evidence of biochemical reactions for the organism of interest (Thiele and Palsson, 2010). Further constraints are placed on the network based on biochemical knowledge—including stoichiometric constraints (e.g., mass and charge balance of reactions), thermodynamic constraints, and enzymatic capacity constraints (Reed and Palsson, 2003; Rocha et al., 2008; Oberhardt et al., 2009; Thiele and Palsson, 2010)—eventually resulting in a genome-scale model (GEM) of metabolism (see **Figure 7**). Transcriptomic and proteomic data is then used to select which of these reactions are active in a given phenotype, based on the presence of the enzyme that catalyzes the reaction. Metabolomic data may be used to constrain which metabolites should be produced or consumed by the cell being modeled (Bordbar et al., 2017). The resulting GEM can then be used with a variety of computational approaches, such as flux balance analysis (FBA), to determine the flux state (i.e., pathway usage) of the entire metabolic network (see **Figure 8**).

This ability to integrate information from multiple types of -omic data with previously acquired detailed biochemical data makes metabolic modeling a powerful technique to answer biological questions regarding how phenotypes occur due to genetic mutation or environmental perturbations (Thiele and Palsson, 2010). As further data is obtained, the model will more closely represent the intended physiological conditions. An updated model may produce novel hypotheses which can suggest new experimental directions. Establishing this feedback between experimental design and computational evaluation is valuable and enables a better understanding of how cells—including MSCs—organize their metabolic system in response to shifts in environment and functional demands (Reed and Palsson, 2003; Resendis-Antonio, 2013). Furthermore, the ability to contextualize models based on information at various levels from genomic to environmental has the potential to allow models

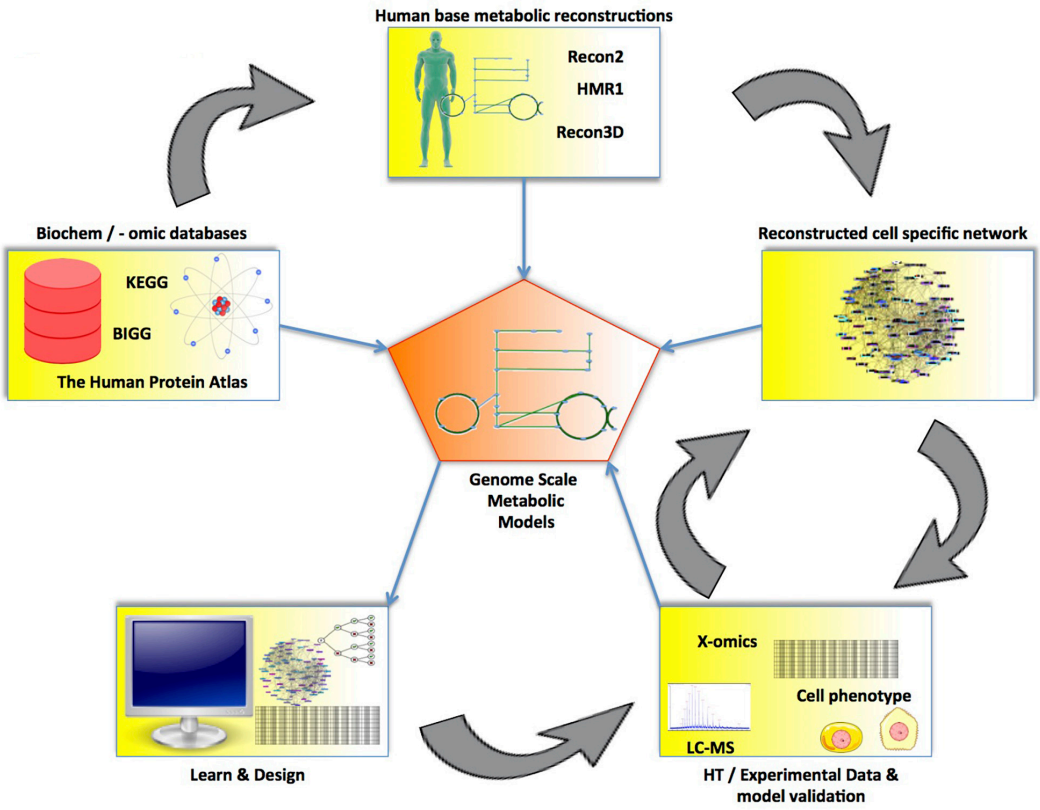

FIGURE 7 | The process of reconstructing a genome-scale metabolic model (GEM). Using a base human metabolic reconstruction along with experimental data and biochemical databases (e.g., KEGG or BiGG), a constraint-based model can be created. From this model, a GEM is derived, from which cellular functions can be studied. Newly acquired knowledge from the GEM can be used to create cell experiments to further validate or improve the model. The validated GEMs can then be used to further study cells for use in regenerative medicine.

to inform personalization of medicine, for example by predicting potential genetic markers of a successful MSC donor.

Existing Human Models

Genome Annotation Efforts Led to the First Human Metabolic Reconstructions

Various community-driven efforts have led to several reconstructions of the global human metabolic network (Romero et al., 2004; Duarte et al., 2007; Ma et al., 2007; Agren et al., 2012; Thiele et al., 2013; Mardinoglu et al., 2014). Compiling data on all reactions that have been linked to genes annotated in the human genome from various databasesas having metabolic activity is a substantial task, and important to the quality of subsequent work (Kanehisa et al., 2016; Norsigian et al., 2020). This production of annotated human genomes allowed, for the first time, metabolic networks that cover the entire human metabolic repertoire to be produced. Between 2005 and 2012, the first four human metabolic reconstructions were produced; humanCyc (Romero et al., 2004), Recon1 (Duarte et al., 2007), Edinburgh Human Metabolic Network (EHMN) (Ma et al., 2007), and Human Metabolic Reconstruction (HMR) (Agren et al., 2012). Each of these networks expanded on the previous work, including more reactions and better links between reactions and genes, allowing for improved analysis of expression data. Further improvements were made in Recon2 (Thiele et al., 2013) and HMR2 (Mardinoglu et al., 2014) and their updates (Smallbone et al., 2013; Quek et al., 2014; Sahoo et al., 2014, 2015; Swainston et al., 2016). By expanding the extent of the reaction coverage, increasing the detail of the available gene-to-reaction links, and placing more emphasis on the inclusion of good thermodynamic and stoichiometric information, better possibilities for accurate simulations were afforded; thus, these models represent significant steps forward. In addition, tools such as PathwayBooster and Path2Models have allowed the utilization of data bases such as KEGG in the automated reconstruction of new or custom built networks.

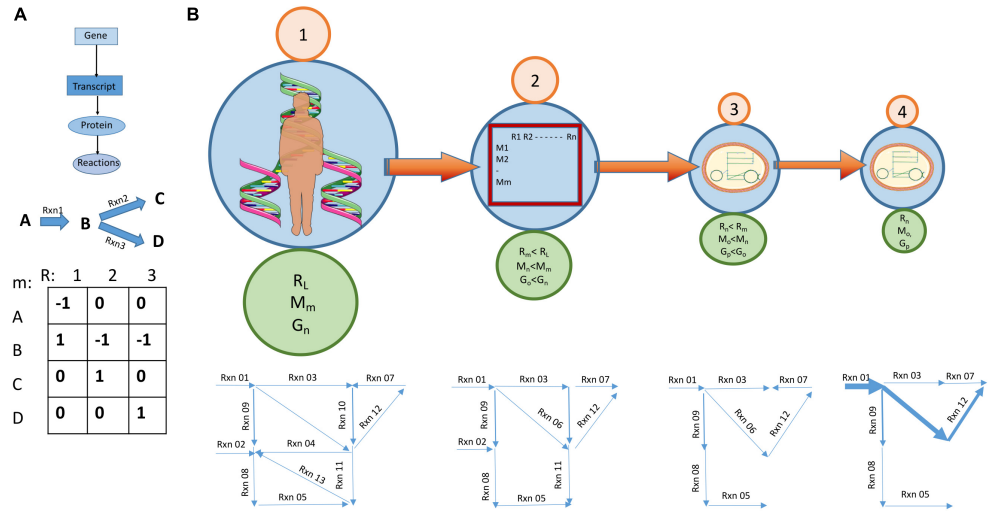

FIGURE 8 | Going from a large base model to a cell specific GEM. **(A)** Genome scale metabolic models build on the gene-protein reaction association and represent a set of reactions as a matrix with linked genes. Synthesis of metabolites is designated by a positive number and breakdown with a negative number. **(B)** Going from a large base model to a cell/condition specific model. (1) A relevant base model is chosen. This model is a summary of known metabolic reactions and forms a species specific metabolic reconstruction. This base model usually has the highest count of genes, reactions and metabolites. (2) A process aiming at reducing the size of the model starts. By considering biochemical and biophysical constraints, e.g., thermodynamic feasibility, some reactions stop being reversable and the reconstruction becomes a model. Other constraints applied at this stage relate to stoiciometricity and enzyme capacity. The number of genes, reactions and metabolites is reduced. (3) Data about transcripts and proteins present in a cell type and the availability of nutrients in medium lead to the removal of yet more reactions. A cell specific model is created. (4) Metabolomic data specific to the condition the cell is supposed to represent allows the magnitude of reactions to be predicted. Some will have higher flux rates than others. More reactions may be removed at this stage. The model now becomes condition specific.

The Latest Human Metabolic Reconstructions Contain New Dimensions of Information

Recon3D is the latest update of the Recon family of human metabolic network reconstructions (Brunk et al., 2018). The key novel attribute of this reconstruction is that it includes information regarding protein and metabolite structures. In addition, the number of reactions included in the reconstruction has almost doubled from the previous version, to 13,453 total reactions. The inclusion of three-dimensional (3D) structural information has allowed Recon3D to be used to show that deleterious mutations map to specific areas of the genome. By using this information, improved predictions of cancer-related mutations may be made compared to previous Recon models, which include a less detailed mapping of genes. The 3D aspect of the protein and metabolite information in Recon3D has also been used to investigate the metabolic effects of various drugs; this analysis revealed that drug effect signatures often contained disparate functional domains and metabolites, indicating that many drug effects are due to compensatory downstream metabolic effects (Brunk et al., 2018). Recon3D has been constructed in such a way as to allow for integration with the AGORA platform for modeling the gut microbiome by using a consistent set of identifiers (Magúsdóttir et al., 2017). As it becomes increasingly clear that the microbiome plays an important part in human health, being able to include cometabolism by human and microbial cells is a very useful feature (Magúsdóttir et al., 2017). A global network reconstruction can then provide the starting point for the production of tissue-, cell-, or condition-specific GEMs.

Current State-of-the-Art Applications

Generic Human Metabolic Reconstructions Can Be Analyzed to Gain General Metabolic Insights

A base GEM may be utilized to produce general predictions about whole human metabolism, providing useful insights into both human health and predictions of currently unknown human metabolic functions.

The various human models have been used to predict biomarkers for inborn errors of metabolism (the accuracy of previous predictions feeds into improving these models) (Kell and Goodacre, 2014). Inborn errors of metabolism (IEMs) are a collection of hereditary metabolic defects found in most of the main human metabolic pathways. These defects are usually screened for in infants by way of biofluid metabolomics (i.e., metabolomics analysis of either dried blood samples or urine). Early recognition and treatment of IEMs is very important. The current method detects specific biomarkers that have altered concentrations due to known genomic mutations. Identifying good biomarkers is key to successful early diagnosis. With the advent of the human metabolism genome-scale network model, a novel computational approach was developed that could systematically predict altered or affected metabolic biomarkers.

This possible use of GEMs has the potential to extend the information that can be inferred from the data, enabling accurate diagnosis for each individual patient, further insight of hot spots in human metabolism with respect to IEMs, and discovery of novel IEMs (expanding the range of disease-associated metabolites). By making use of the GEM, gene-protein-reaction (GPR) metabolic pathways relevant to a specific genotype-phenotype pair can become more feasible, meaning that disease-specific biological insights can be derived (Shlomi et al., 2009; Sahoo et al., 2012; Mandal et al., 2018; Mussap et al., 2018).

By analyzing reactions in Recon1 that were defined as being present due to genome annotation or literature data, but that were not predicted to be active, and then adding surrounding reactions to activate them, predictions have been made about previously unknown human metabolic functions such as that of iduronic acid following glycan degradation, N-acetylglutamate in amino acid metabolism, and the human activity of gluconokinase (Rolfsson et al., 2011; Paglia et al., 2016). Such information will improve future metabolic studies both computationally and in the laboratory.

Reconstructions can be made specific by integrating -omics data

Once a base GEM has been selected, there are a variety of methods available to make the model specific to a particular cell type and circumstance by integrating transcriptomic, proteomic, and metabolomics data. These context-specific models are able to provide more detailed insights into human metabolism in a particular cell type, and comparison of models is particularly useful. Previous context-specific human models have produced useful insights into healthy and diseased metabolism.

A cell's metabolic capabilities are defined by which enzymes it expresses. Transcriptomic and proteomic data provide information about the enzymes expressed under certain circumstances. Both of these data types correlate to enzyme activity, although not perfectly (Munir and McGettrick, 2015; Ibraheim et al., 2018). Several methods to prune a GEM based on expression data, mostly transcriptomics, have been developed. Although there are numerous technical differences, all seek to balance the retention of reactions known to be or likely to be present in a particular cell type, based on expression data or prior knowledge, while removing extraneous reactions. GIMME (Moreira et al., 2017), iMAT and INIT (Antonitsis et al., 2008; Vigo et al., 2019), and MBA, Fastcore, and mCADRE (Ullah et al., 2015; Archambault et al., 2017; Fitzsimmons et al., 2018) are all commonly used (Rosenbaum et al., 2008; Neman et al., 2012).

Another way to make models more context specific is to use metabolomic data collected by mass spectrometry or NMR to constrain what the model takes up or secretes to realistic values. By either measuring changes in the concentration of various metabolites in the medium over time or by comparing the relative values of metabolites at different times, the rate of uptake or secretion of a range of metabolites is determined. These rates can be applied to the model as additional constraints that will restrict the model predictions to those consistent with the metabolic dataset (Bordbar et al., 2017). These additional constraints help to predict different sets of active and inactive intracellular reactions based on extracellular data. This process may follow a protocol such as Metabotools. This protocol has been used to obtain metabolic insights into the metabolic differences between different leukemic cell lines (Aurich et al., 2015, 2016; von Bomhard et al., 2016).

Models can also be used to analyze isotope labeling data and this data can, in turn, contribute better constraints to improve the model. Cells may be fed on medium containing glucose or glutamine labeled with heavy isotopes of carbon or nitrogen. The proportions of various metabolites labeled with these heavy isotopes in cells that are sampled and analyzed at different time points after this treatment allows inferences to be made about the production of the labeled metabolites. Sholmi et al. used this technique to elucidate the differences in the TCA cycle during the cell cycle. Further information may be obtained if the cells are fractionated into different organelles before analysis (Ahn et al., 2017). For example, the subcellular localization of glutamine metabolism in cancer has been elucidated using this technique (Lee et al., 2019).

Using the model building algorithm (MBA) (Jerby et al., 2010), which generates tissue-specific models, a focused model for cancer metabolism has been created containing a core set of reactions known to be common for 60 variant cancer cell lines. Using this model and the knowledge that uncontrolled cell growth and altered metabolism are characterizing hallmarks for cancer cells, it was possible to identify two different types of drug targets (Hanahan and Weinberg, 2011; Dougherty et al., 2017). The first target type was growth-supporting genes (found via *in silico* gene deletion screens) that resulted in identification of 52 metabolic drug targets; 8 of these currently correspond to cancer therapeutics. In addition, a set of genes were identified in the healthy cell model network that were downregulated in the cancer model. By inhibiting the genes more highly expressed in cancer cells, targeting could be achieved (Dougherty et al., 2017).

More specific cancer models have also been produced. For example, a model has been created for hepatocellular carcinoma by Agren et al. (2014). They evaluated the presence of proteins in 27 patients and from that reconstructed personalized GEMs for six. These reconstructions were then used to identify anticancer drugs by observing the inhibition of reactions around each metabolite in a network and the subsequent effects on cellular growth within the models. By conceptualizing drugs as structural analogs to metabolites, and so capable of interfering with target enzymes and enzymatic activity, 101 antimetabolites were predicted as possible drug targets (Agren et al., 2014). Similar approaches have been applied to breast cancer undergoing epithelial-to-mesenchymal transition in order to identify targets to reduce this pro-metastatic process (Halldorsson et al., 2017).

Comparing Models of Cells in Different Circumstances Can Produce Useful Insights Into Metabolism

Many constraint-based metabolic analyses have historically relied upon an objective function, which is defined as a metabolic objective of a cell; flux through this reaction is either maximized or minimized to compute the flux state (i.e., pathway usage) across the entire network. For metabolic states that do not

have as well-defined objective functions as cancer does (i.e., gross cellular growth), algorithms that are able to create tissue- or cell-specific models without a specific objective function are needed. An algorithm often used for this purpose is the metabolic transformation algorithm (MTA) (Yizhak et al., 2013), an algorithm that uses GEMs to predict genetic perturbations that are able to shift a diseased metabolic state toward a healthy one. This algorithm has been used to determine reactions capable of shifting "old" muscle into "young" (providing potential targets that can help reducing metabolic shifts related to aging) and to determine key reactions that, when removed from a GEM modeling Alzheimer's disease, resulted in a network reconstruction more similar to that of a healthy state (Stempler et al., 2014; Wone et al., 2018).

Obesity has been addressed through the use of the human metabolic reconstruction by identifying pathways implicated in the disease process. As with many diseases, pinpointing a specific genetic or environmental marker as a cause for obesity, making the determination of progression, and deciding on a "treatment" a difficult task. Using the HMR and transcriptomic data from both healthy and obese individuals, a GEM with the objective function defined as acetyl-CoA production and formation of lipid droplets was produced. Through this analysis, two possible drug targets were identified by considering reactions with significantly changed flux values, and a potential biomarker for obesity was identified through reporter metabolites, which is an algorithm allowing the analysis of transcriptomic data in the light of the metabolic network structure to predict highly affected metabolites (Bordbar et al., 2011; Väremo et al., 2013; Levian et al., 2014; Dougherty et al., 2017).

Drug toxicity levels and side effects over both short and long periods of usage can also be identified in an easier and more cost-efficient manner using GEMs. It is possible to make predictions on system-wide perturbations using previously determined information on how protein structural analysis can be used to determine off-target binding of drugs, in combination with metabolic networks, as was done by Chang et al. (2010).

Metabolic Models Can Be Used to Uncover Changes Over Time

Biological systems often change dynamically over time. Analyzing how these changes occur can be challenging but is being addressed through the integration of time-course experimental data. One approach, dynamic flux balance analysis (dFBA) {ref 10.1016/j.celrep.2017.07.04}, integrates time-course measurements of the major inputs and outputs of the system to provide more accurate flux predictions. dFBA provides a continuous prediction based on these changing inputs and outputs (e.g., end products of pathways). This method has been applied to murine embryonic stem cells and revealed changes to mitochondrial metabolism and one carbon metabolism during priming (Shen et al., 2019). more recently, time-course -omic measurements have been integrated with metabolic models. One such method, unsteady-state flux balance analysis (uFBA), integrates absolutely quantified time-course metabolomic data to model cellular dynamics. uFBA was used to explore how temporal dynamics impact the cellular metabolism of stored red blood cells, which led to the proposal of better storage solutions that could potentially increase the storage time and quality of this key medical product. Such methods may be applied to other cell types and phenotypes in the future where dynamics play a key role. In MSCs, for example, key metabolic shifts that occur during trilineage differentiation may be examined and compared as a function of time.

A Metabolic Model of MSCs Has Already Predicted Better Ways to Expand MSC Cultures

A GEM of MSCs, iMSC1255, was recently created to improve understanding of the function of MSC metabolism. This model is based upon publicly available transcriptomic data sets from proliferating, early passage bone marrow MSCs. The data was used with the mCADRE algorithm to generate a tissue-specific version of the global human model Recon1, which was then manually curated by comparison to proteomic data and the literature to ensure that all desirable reactions were included to account for known MSC metabolic functions (Wang et al., 2012). Further metabolic constraints were added based on the composition of the commonly used medium alpha MEM, which meant that the modeled cells were able to take up metabolites known to be available in alpha MEM. This model was compared to previous models created with the same algorithm for adipose, bone marrow, and blood (using tissue-based, rather than cell-based, models). These previous models were shown to be less specific than iMSC1255. iMSC1255 was also shown to be able to produce amino acid uptake and secretion and growth rate predictions consistent with data available in the literature (Fouladiha et al., 2015).

iMSC1255 has subsequently been used to computationally predict metabolic interventions to optimize proliferation and chondrogenic differentiation of MSCs. By analyzing the maximum growth rate predicted FBA with and without allowing the uptake of a range of nutrients, it was proposed that supplementing the MSC medium with the phospholipids phosphoethanolamine and phosphoserine would improve proliferation. This was confirmed experimentally (Fouladiha et al., 2018). This paper also describes how MTA was used along with transcriptomic data from chondrocytes to determine likely metabolic changes during chondrocyte differentiation. This analysis suggested that mitochondrial transport reactions are key to chondrocyte differentiation, a finding that has yet to be experimentally confirmed. Further, the authors also examined the effects of hypoxia on proliferating MSCs by assessing the range of possible metabolic activities when the models use different levels of oxygen and glucose availability. The predicted metabolic changes to lactate and glucose uptake and secretion, G6P isomerase, and pyruvate transport were generally correct, with the exception of superoxide dismutase, according to the literature (Fouladiha et al., 2018). This study showed that a model of MSC metabolism can provide useful insights into their proliferation under different circumstances. This will allow the optimization of MSC growth that may be useful for large scale production of MSC-based therapeutics. Follow-up work has begun to examine the potential of GEMs to predict changes necessary for successful differentiation (Fouladiha et al., 2018).

By expanding upon such techniques, including by using models constrained with metabolic data from differentiating cells, this can be built upon.

LOOKING AHEAD

Since 2007, when the very first global GEM for humans was reconstructed (Duarte et al., 2007), researchers have been exploring the clinical application possibilities of GEMs. Some of the possible ways GEMs can be of use in furthering the clinical application of cell-based medicine include: (1) trials with *in silico* metabolic engineering (gene knock-outs and knock-ins); (2) identifying biomarkers of diseases; (3) predicting drug targets and therapeutic windows; and (4) optimization of cellular functions without the cost of wet lab experimentation. Some success has already been reported, as mentioned in section "Current State-of-the-Art Applications."

Manipulation of the Metabolic State

Building on the various uses of existing cell- or tissue-specific human GEMs and the most up-to-date version of the human reconstruction (Brunk et al., 2018), the potential use of GEMs to explore methods to maintain or manipulate a desired metabolic state for hMSCs (in order to provide a specific function or desired effect) has been the subject of work done by Fouladiha et al. They demonstrated the potential of GEMs to gain insight into how MSCs may be manipulated by means of nutrient supplementation (Fouladiha et al., 2018). By adding nutrients into the growth medium or manipulating oxygen concentration *in silico*, the number of experiments needed to optimize growth conditions may be reduced. This may be an interesting avenue to explore for each cell type and cell state, since different responses may be observed. Such testing is more feasible to explore *in silico* than *in vitro*. Even though time and money will have to be spent on reconstruction of the GEMs themselves, the savings in experimental time and material costs afforded by the use of validated reconstructions will likely outweigh these costs. Promising *in silico* outcomes can then be taken further, being validated or explored *in vitro* and later *in vivo*. Positive results would further validate the models and perhaps further that particular avenue of cell-based medicine or that particular use of the cells in regenerative medicine.

Exploration of Metabolic Differences

One potential use for GEMs would be to explore the different metabolic capacities of hMSCs from different sources. There have been some reports, albeit limited, explaining possible differences in the proliferative, differentiation, and immunomodulatory abilities of hMSCs isolated from various tissues (Liu et al., 2007; Hass et al., 2011; Secunda et al., 2015; Tachida et al., 2015). As hMSCs are isolated from disparate microenvironments, some with large differences in their surroundings, their optimal survival conditions and, possibly, utilization potential may differ. For example, by comparing models created using transcriptomics data from a study of MSCs from various sources such as ArrayExpress (EMBL-EBI, 2014; Athar et al., 2019) and then subjecting them to comparative flux analysis, different metabolic patterns may be discovered and linked to previously reported functional differences, such as the ability to form hematopoietic cells. Results could be verified or supplemented with data from independent proteomics experiments such as can be found via PRIDE Archive (Billing et al., 2016).

The creation and study of GEMs of MSCs undergoing each of the three classical differentiation (adipo-, osteo- and chondrogenic) could be approached in various ways. uFBA could be used as a framework to examine MSC metabolomics data collected at different timepoints during each of the differentiation lineages (Bordbar et al., 2017). The study of other stem cell types over time has already provided useful insights into differentiation from a transcriptional viewpoint. uFBA would allow a better understanding of the metabolic changes to be reached (Bordbar et al., 2017).

Experimental Cost Reduction via *in silico* Result Prediction

As expansion and differentiation of MSCs is a time-consuming and potentially expensive process, it would be desirable to be able to predict in advance the success of cells from a particular donor. For example, a signature pattern of gene features could be tested before donation. To this end, a model of successful and unsuccessful cells created with Recon3D could be used to analyze the genes relevant to an ideally differentiated model *in silico* (Strober et al., 2019). Single and combined gene deletion to find genes essential to each form of differentiation would be useful as a secondary way of finding a genetic signature for successful differentiation. This process could provide a means of reducing the necessary number of *in vitro* analyses.

It would also be desirable to confirm adequate differentiation by measuring a few metabolites before attempting implantation. The reporter metabolites algorithm (Çakır, 2015; Schultz and Qutub, 2016) applied to a model of well- differentiated MSCs would determine exometabolomic biomarkers that are indicative of successful levels of differentiation.

Multi-Cell Models

Community models or multi-cell models are another avenue to be explored as a potential use for GEMs to enhance the use of hMSCs in regenerative medicine. These models can provide insight into the metabolic functions of possible interacting organisms or the various cell types residing within the same organism (Levy and Borenstein, 2013; Dougherty et al., 2017). Given that hMSCs are intended to be integrated into a host system for clinical application (Han et al., 2012; Levy and Borenstein, 2013; Burke et al., 2016; Archambault et al., 2017; Goldberg et al., 2017; Moreira et al., 2017; Cunningham et al., 2018; Hu et al., 2018; Ibraheim et al., 2018; Solarte et al., 2018), this could provide useful insights.

Recently, more attention has been given to the hMSC secretome and its possible therapeutic effect; this might be well explored through the use of multi-cellular GEMs. The secretome of hMSCs might be manipulated via some of the previously mentioned methods, and the effect of composition changes on

the targeted organism, cell, and/or environment observed. This could help to find novel directions in which to expand the use of hMSCs in regenerative medicine.

Age Related Exploration

Yet another aspect that could more easily be explored through the use of GEMs covering hMSCs is the effect of donor age. This is not the same as cell senescence, but effects due to age have been observed in hMSCs lines through *in vitro* experiments (Choudhery et al., 2014; Narbonne, 2018). This appears in the way that cells are able to perform with regard to proliferation speed, differentiation ability, and immunomodulation. There have been numerous attempts to return functionality to stem cells from aged donors, with some degree of success (Neves et al., 2017). However, with the application of GEMs, the significant changes and the reasons behind them may be more systematically documented and attempts to return function performed in a more cost-effective and time-saving manner.

Overall, the use of GEMs to further the use of hMSCs in regenerative medicine is increasing, but, as of yet, is a relatively unexplored avenue that holds a lot of promise. We anticipate that *in silico* metabolic modeling will help to elucidate the differentiation process of hMSCs, ultimately providing crucial insights into novel therapies in the field of regenerative medicine.

AUTHOR CONTRIBUTIONS

ÞS and SM were the main authors of the manuscript. All additional authors (ÓR, JY, and ÓS) also contributed to the writing and editing of the manuscript.

FUNDING

This research was supported by the Icelandic Research Fund (grant number 217005) and by the Institute for Systems Biology's Translational Research Fellows Program (JY).

REFERENCES

Agathocleous, M., and Harris, W. A. (2013). Metabolism in physiological cell proliferation and differentiation. *Trends Cell Biol.* 23, 484–492. doi: 10.1016/j.tcb.2013.05.004

Agren, R., Bordel, S., Mardinoglu, A., Pornputtapong, N., Nookaew, I., and Nielsen, J. (2012). Reconstruction of genome-acale active metabolic networks for 69 human cell types and 16cancer types using INIT. *PLoS Comput. Biol.* 8:e1002518. doi: 10.1371/journal.pcbi.1002518

Agren, R., Mardinoglu, A., Asplund, A., Kampf, C., Uhlen, M., and Nielsen, J. (2014). Identification of anticancer drugs for hepatocellular carcinoma through personalized genome-scale metabolic modeling. *Mol. Syst. Biol.* 10:721. doi: 10.1002/msb.145122

Ahn, E., Kumar, P., Mukha, D., Tzur, A., and Shlomi, T. (2017). Temporal fluxomics reveals oscillations in TCA cycle flux throughout the mammalian cell cycle. *Mol. Syst. Biol.* 13:953. doi: 10.15252/msb.20177763

Alberts, B., Bray, D., Hopkin, K., Johnson, A., Lewis, J., Raff, M., et al. (2014). "Chapter 13: how cells obtain energy from food," in *Essential Cell Biology*, ed. K. Mesa (New York, NY: Garland Science), 419–437.

Amorin, B., Alegretti, A. P., Valim, V., Pezzi, A., Laureano, A. M., da Silva, M. A. L., et al. (2014). Mesenchymal stem cell therapy and acute graft-versus-host disease: a review. *Hum. Cell* 27, 137–150. doi: 10.1007/s13577-014-0095-x

Antonitsis, P., Ioannidou-Papagiannaki, E., Kaidoglou, A., Charokopos, N., Kalogeridis, A., Kouzi-Koliakou, K., et al. (2008). Cardiomyogenic potential of human adult bone marrow mesenchymal stem cells in vitro. *Thorac. Cardiovasc. Surg.* 56, 77–82. doi: 10.1055/s-2007-989328

Araujo, J. A., Zhang, M., and Yin, F. (2012). Heme oxygenase-1, oxidation, inflammation, and atherosclerosis. *Front. Pharmacol.* 3:119. doi: 10.3389/fphar.2012.00119

Archambault, J., Moreira, A., McDaniel, D., Winter, L., Sun, L., and Hornsby, P. (2017). Therapeutic potential of mesenchymal stromal cells for hypoxic ischemic encephalopathy: a systematic review and meta-analysis of preclinical studies. *PLoS One* 12:e0189895. doi: 10.1371/journal.pone.0189895

Athar, A., Füllgrabe, A., George, N., Iqbal, H., Huerta, L., Ali, A., et al. (2019). ArrayExpress update - from bulk to single-cell expression data. *Nucleic Acids Res.* 47, D711–D715. doi: 10.1093/nar/gky964

Aurich, M. K., Fleming, R. M. T., and Thiele, I. (2016). MetaboTools: a comprehensive toolbox for analysis of genome-scale metabolic models. *Front. Physiol.* 7:327. doi: 10.3389/fphys.2016.00327

Aurich, M. K., Paglia, G., Rolfsson, Ó., Hrafnsdóttir, S., Magnúsdóttir, M., Stefaniak, M. M., et al. (2015). Prediction of intracellular metabolic states from extracellular metabolomic data. *Metabolomics* 11, 603–619. doi: 10.1007/s11306-014-0721-3

Baldari, S., Di Rocco, G., Piccoli, M., Pozzobon, M., Muraca, M., and Toietta, G. (2017). Challenges and strategies for improving the regenerative effects of mesenchymal stromal cell-based therapies. *Int. J. Mol. Sci.* 18:2087. doi: 10.3390/ijms18102087

Barbagallo, I., Vanella, A., Peterson, S. J., Kim, D. H., Tibullo, D., Giallongo, C., et al. (2010). Overexpression of heme oxygenase-1 increases human osteoblast stem cell differentiation. *J. Bone Miner. Metab.* 28, 276–288. doi: 10.1007/s00774-009-0134-y

Barkholt, L., Flory, E., Jekerle, V., Lucas-Samuel, S., Ahnert, P., Bisset, L., et al. (2013). Risk of tumorigenicity in mesenchymal stromal cell-based therapies–bridging scientific observations and regulatory viewpoints. *Cytotherapy* 15, 753–759. doi: 10.1016/j.jcyt.2013.03.005

Beegle, J., Lakatos, K., Kalomoiris, S., Stewart, H., Isseroff, R. R., Nolta, J. A., et al. (2015). Hypoxic preconditioning of mesenchymal stromal cells induces metabolic changes, enhances survival, and promotes cell retention in vivo. *Stem Cells* 33, 1818–1828. doi: 10.1002/stem.1976

Bernardo, M. E., and Fibbe, W. E. (2013). Mesenchymal stromal cells: sensors and switchers of inflammation. *Cell Stem Cell* 13, 392–402. doi: 10.1016/j.stem.2013.09.006

Bernardo, M. E., Zaffaroni, N., Novara, F., Cometa, A. M., Avanzini, M. A., Moretta, A., et al. (2007). Human bone marrow derived mesenchymal stem cells do not undergo transformation after long-term in vitro culture and do not exhibit telomere maintenance mechanisms. *Cancer Res.* 67, 9142–9149. doi: 10.1158/0008-5472.can-06-4690

Billing, A. M., Ben Hamidane, H., Dib, S. S., Cotton, R. J., Bhagwat, A. M., Kumar, P., et al. (2016). Comprehensive transcriptomic and proteomic characterization of human mesenchymal stem cells reveals source specific cellular markers. *Sci. Rep.* 6:21507. doi: 10.1038/srep21507

Björnson, E., Borén, J., and Mardinoglu, A. (2016). Personalized cardiovascular disease prediction and treatment—a review of existing strategies and novel systems medicine tools. *Front. Physiol.* 7:2. doi: 10.3389/fphys.2016.00002

Blais, M., Parenteau-Bareil, R., Cadau, S., and Berthod, F. (2013). Concise review: tissue-engineered skin and nerve regeneration in burn treatment. *Stem Cells Transl. Med.* 2, 545–551. doi: 10.5966/sctm.2012-0181

Blanco, B., Herrero-Sánchez, M. D. C., Rodríguez-Serrano, C., García-Martínez, M. L., Blanco, J. F., Muntión, S., et al. (2016). Immunomodulatory effects of bone marrow versus adipose tissue-derived mesenchymal stromal cells on NK cells: implications in the transplantation setting. *Eur. J. Haematol.* 97, 528–537. doi: 10.1111/ejh.12765

Bloom, A. B., and Zaman, M. H. (2014). Influence of the microenvironment on cell fate determination and migration. *Physiol. Genomics* 46, 309–314. doi: 10.1152/physiolgenomics.00170.2013

Bonab, M. M., Sahraian, M. A., Aghsaie, A., Karvigh, S. A., Hosseinian, S. M., Nikbin, B., et al. (2012). Autologous mesenchymal stem cell therapy in progressive multiple sclerosis: an open label study. *Curr. Stem Cell Res. Ther.* 7, 407–414. doi: 10.2174/157488812804484648

Bordbar, A., Feist, A. M., Usaite-Black, R., Woodcock, J., Palsson, B. O., and Famili, I. (2011). A multi-tissue type genome-scale metabolic network for analysis of whole-body systems physiology. *BMC Syst. Biol.* 5:180. doi: 10.1186/1752-0509-5-180

Bordbar, A., Monk, J. M., King, Z. A., and Palsson, B. O. (2014). Constraint-based models predict metabolic and associated cellular functions. *Nat. Rev. Genet.* 15, 107–120. doi: 10.1038/nrg3643

Bordbar, A., Yurkovich, J. T., Paglia, G., Rolfsson, O., Sigurjónsson, Ó. E., and Palsson, B. O. (2017). Elucidating dynamic metabolic physiology through network integration of quantitative time-course metabolomics. *Sci. Rep.* 7:46249. doi: 10.1038/srep46249

Bortolotti, F., Ukovich, L., Razban, V., Martinelli, V., Ruozi, G., Pelos, B., et al. (2015). In vivo therapeutic potential of mesenchymal stromal cells depends on the source and the isolation procedure. *Stem Cell Rep.* 4, 332–339. doi: 10.1016/j.stemcr.2015.01.001

Brunk, E., Sahoo, S., Zielinski, D. C., Altunkaya, A., Dräger, A., Mih, N., et al. (2018). Recon3D enables a three-dimensional view of gene variation in human metabolism. *Nat. Biotechnol.* 36, 272–281. doi: 10.1038/nbt.4072

Buravkova, L. B., Rylova, Y. V., Andreeva, E. R., Kulikov, A. V., Pogodina, M. V., Zhivotovsky, B., et al. (2013). Low ATP level is sufficient to maintain the uncommitted state of multipotent mesenchymal stem cells. *Biochim. Biophys. Acta* 1830, 4418–4425. doi: 10.1016/j.bbagen.2013.05.029

Burke, J., Hunter, M., Kolhe, R., Isales, C., Hamrick, M., and Fulzele, S. (2016). Therapeutic potential of mesenchymal stem cell based therapy for osteoarthritis. *Clin. Transl. Med.* 5:27. doi: 10.1186/s40169-016-0112-7

Çakır, T. (2015). Reporter pathway analysis from transcriptome data: metabolite-centric versus reaction-centric approach. *Sci. Rep.* 5:14563. doi: 10.1038/srep14563

Campana, V., Milano, G., Pagano, E., Barba, M., Cicione, C., Salonna, G., et al. (2014). Bone substitutes in orthopaedic surgery: from basic science to clinical practice. *J. Mater. Sci. Mater. Med.* 25, 2445–2461. doi: 10.1007/s10856-014-5240-2

Chang, R. L., Xie, L., Xie, L., Bourne, P. E., and Palsson, B. Ø. (2010). Drug off-target effects predicted using structural analysis in the context of a metabolic network model. *PLoS Comput. Biol.* 6:e1000938. doi: 10.1371/journal.pcbi.1000938

Chen, C.-T., Shih, Y.-R. V., Kuo, T. K., Lee, O. K., and Wei, Y.-H. (2008). Coordinated changes of mitochondrial biogenesis and antioxidant enzymes during osteogenic differentiation of human mesenchymal stem cells. *Stem Cells* 26, 960–968. doi: 10.1634/stemcells.2007-0509

Cho, K.-A., Ju, S.-Y., Cho, S. J., Jung, Y.-J., Woo, S.-Y., Seoh, J.-Y., et al. (2009). Mesenchymal stem cells showed the highest potential for the regeneration of injured liver tissue compared with other subpopulations of the bone marrow. *Cell Biol. Int.* 33, 772–777. doi: 10.1016/j.cellbi.2009.04.023

Choudhery, M. S., Badowski, M., Muise, A., Pierce, J., and Harris, D. T. (2014). Donor age negatively impacts adipose tissue-derived mesenchymal stem cell expansion and differentiation. *J. Transl. Med.* 12:8. doi: 10.1186/1479-5876-12-8

Croitoru-Lamoury, J., Lamoury, F. M. J., Caristo, M., Suzuki, K., Walker, D., Takikawa, O., et al. (2011). Interferon-γ regulates the proliferation and differentiation of mesenchymal stem cells via activation of indoleamine 2,3 dioxygenase (IDO). *PLoS One* 6:e14698. doi: 10.1371/journal.pone.0014698

Cunningham, C. J., Redondo-Castro, E., and Allan, S. M. (2018). The therapeutic potential of the mesenchymal stem cell secretome in ischaemic stroke. *J. Cereb. Blood Flow Metab.* 38, 1276–1292. doi: 10.1177/0271678X18776802

De Becker, A., and Riet, I. V. (2016). Homing and migration of mesenchymal stromal cells: how to improve the efficacy of cell therapy? *World J. Stem Cells* 8, 73–87. doi: 10.4252/wjsc.v8.i3.73

Deng, W., Han, Q., Liao, L., You, S., Deng, H., and Zhao, R. C. H. (2005). Effects of allogeneic bone marrow-derived mesenchymal stem cells on T and B lymphocytes from BXSB mice. *DNA Cell Biol.* 24, 458–463. doi: 10.1089/dna.2005.24.458

dos Santos, F., Andrade, P. Z., Boura, J. S., Abecasis, M. M., da Silva, C. L., and Cabral, J. M. S. (2010). Ex vivo expansion of human mesenchymal stem cells: a more effective cell proliferation kinetics and metabolism under hypoxia. *J. Cell. Physiol.* 223, 27–35. doi: 10.1002/jcp.21987

Dougherty, B. V., Moutinho, T. J., and Papin, J. (2017). "Accelerating the drug development pipeline with genome-scale metabolic network reconstructions," in *Systems Biology*, eds J. Nielsen and S. Hohmann (Hoboken, NJ: John Wiley & Sons, Ltd), 139–162. doi: 10.1002/9783527696130.ch5

Duarte, N. C., Becker, S. A., Jamshidi, N., Thiele, I., Mo, M. L., Vo, T. D., et al. (2007). Global reconstruction of the human metabolic network based on genomic and bibliomic data. *Proc. Natl. Acad. Sci. U.S.A.* 104, 1777–1782. doi: 10.1073/pnas.0610772104

Duijvestein, M., Vos, A. C. W., Roelofs, H., Wildenberg, M. E., Wendrich, B. B., Verspaget, H. W., et al. (2010). Autologous bone marrow-derived mesenchymal stromal cell treatment for refractory luminal Crohn's disease: results of a phase I study. *Gut* 59, 1662–1669. doi: 10.1136/gut.2010.215152

El Refaey, M., Watkins, C. P., Kennedy, E. J., Chang, A., Zhong, Q., Ding, K.-H., et al. (2015). Oxidation of the aromatic amino acids tryptophan and tyrosine disrupts their anabolic effects on bone marrow mesenchymal stem cells. *Mol. Cell. Endocrinol.* 410, 87–96. doi: 10.1016/j.mce.2015.01.034

EMBL-EBI (2014). *Array Express: E-GEOD-57151 - Epigenetic and In Vivo Comparison of Diverse Mesenchymal Stromal Cell Sources Reveals an Endochondral Signature for Human Hematopoietic Niche Formation*. Hinxton: European Bioinformatics Institute.

Estrada, J. C., Albo, C., Benguría, A., Dopazo, A., López-Romero, P., Carrera-Quintanar, L., et al. (2012). Culture of human mesenchymal stem cells at low oxygen tension improves growth and genetic stability by activating glycolysis. *Cell Death Differ.* 19, 743–755. doi: 10.1038/cdd.2011.172

Feist, A. M., Herrgard, M. J., Thiele, I., Reed, J. L., and Palsson, B. O. (2009). Reconstruction of biochemical networks in microbial organisms (supplementary table 1). *Nat. Rev. Microbiol.* 7, 129–143. doi: 10.1038/nrmicro1949

Fitzsimmons, R. E. B., Mazurek, M. S., Soos, A., and Simmons, C. A. (2018). Mesenchymal stromal/stem cells in regenerative medicine and tissue engineering. *Stem Cells Int.* 2018:8031718. doi: 10.1155/2018/8031718

Forrester, S. J., Kikuchi, D. S., Hernandes, M. S., Xu, Q., and Griendling, K. K. (2018). Reactive oxygen species in metabolic and inflammatory signaling. *Circ. Res.* 122, 877–902. doi: 10.1161/CIRCRESAHA.117.311401

Fouladiha, H., Marashi, S.-A., and Shokrgozar, M. A. (2015). Reconstruction and validation of a constraint-based metabolic network model for bone marrow-derived mesenchymal stem cells. *Cell Prolif.* 48, 475–485. doi: 10.1111/cpr.12197

Fouladiha, H., Marashi, S.-A., Shokrgozar, M. A., Farokhi, M., and Atashi, A. (2018). Applications of a metabolic network model of mesenchymal stem cells for controlling cell proliferation and differentiation. *Cytotechnology* 70, 331–338. doi: 10.1007/s10616-017-0148-6

François, M., Copland, I. B., Yuan, S., Romieu-Mourez, R., Waller, E. K., and Galipeau, J. (2012). Cryopreserved mesenchymal stromal cells display impaired immunosuppressive properties as a result of heat-shock response and impaired interferon-γ licensing. *Cytotherapy* 14, 147–152. doi: 10.3109/14653249.2011.623691

Galli, D., Vitale, M., and Vaccarezza, M. (2014). Bone marrow-derived mesenchymal cell differentiation toward myogenic lineages: facts and perspectives. *Biomed Res. Int.* 2014:762695. doi: 10.1155/2014/762695

Gao, F., Chiu, S. M., Motan, D. A. L., Zhang, Z., Chen, L., Ji, H.-L., et al. (2016). Mesenchymal stem cells and immunomodulation: current status and future prospects. *Cell Death Dis.* 7:e2062. doi: 10.1038/cddis.2015.327

Gaspar, J. M., and Velloso, L. A. (2018). Hypoxia inducible factor as a central regulator of metabolism – implications for the development of obesity. *Front. Neurosci.* 12:813. doi: 10.3389/fnins.2018.00813

Gazit, Z., Pelled, G., Sheyn, D., Kimelman, N., and Gazit, D. (2014). "Chapter 19 - mesenchymal stem cells," in *Essentials of Stem Cell Biology*, eds R. Lanza and A. Atala (Cambridge, MA: Academic Press), 255–266. doi: 10.1016/B978-0-12-409503-8.00019-6

Goldberg, A., Mitchell, K., Soans, J., Kim, L., and Zaidi, R. (2017). The use of mesenchymal stem cells for cartilage repair and regeneration: a systematic review. *J. Orthop. Surg. Res.* 12:39. doi: 10.1186/s13018-017-0534-y

Guo, X., Bai, Y., Zhang, L., Zhang, B., Zagidullin, N., Carvalho, K., et al. (2018). Cardiomyocyte differentiation of mesenchymal stem cells from bone marrow: new regulators and its implications. *Stem Cell Res. Ther.* 9:44. doi: 10.1186/s13287-018-0773-9

Halldorsson, S., Rohatgi, N., Magnusdottir, M., Choudhary, K. S., Gudjonsson, T., Knutsen, E., et al. (2017). Metabolic re-wiring of isogenic breast epithelial cell lines following epithelial to mesenchymal transition. *Cancer Lett.* 396, 117–129. doi: 10.1016/j.canlet.2017.03.019

Han, Z., Jing, Y., Zhang, S., Liu, Y., Shi, Y., and Wei, L. (2012). The role of immunosuppression of mesenchymal stem cells in tissue repair and tumor growth. *Cell Biosci.* 2:8. doi: 10.1186/2045-3701-2-8

Hanahan, D., and Weinberg, R. A. (2011). Hallmarks of cancer: the next generation. *Cell* 144, 646–674. doi: 10.1016/j.cell.2011.02.013

Hass, R., Kasper, C., Böhm, S., and Jacobs, R. (2011). Different populations and sources of human mesenchymal stem cells (MSC): a comparison of adult and neonatal tissue-derived MSC. *Cell Commun. Signal.* 9:12. doi: 10.1186/1478-811X-9-12

Henry, C. S., DeJongh, M., Best, A. A., Frybarger, P. M., Linsay, B., and Stevens, R. L. (2010). High-throughput generation, optimization and analysis of genome-scale metabolic models. *Nat. Biotechnol.* 28, 977–982. doi: 10.1038/nbt.1672

Hofer, H. R., and Tuan, R. S. (2016). Secreted trophic factors of mesenchymal stem cells support neurovascular and musculoskeletal therapies. *Stem Cell Res. Ther.* 7:131. doi: 10.1186/s13287-016-0394-0

Hu, L., Yin, C., Zhao, F., Ali, A., Ma, J., and Qian, A. (2018). Mesenchymal stem cells: cell fate decision to osteoblast or adipocyte and application in osteoporosis treatment. *Int. J. Mol. Sci.* 19:360. doi: 10.3390/ijms19020360

Ibraheim, H., Giacomini, C., Kassam, Z., Dazzi, F., and Powell, N. (2018). Advances in mesenchymal stromal cell therapy in the management of Crohn's disease. *Expert Rev. Gastroenterol. Hepatol.* 12, 141–153. doi: 10.1080/17474124.2018.1393332

Ivanova-Todorova, E., Bochev, I., Mourdjeva, M., Dimitrov, R., Bukarev, D., Kyurkchiev, S., et al. (2009). Adipose tissue-derived mesenchymal stem cells are more potent suppressors of dendritic cells differentiation compared to bone marrow-derived mesenchymal stem cells. *Immunol. Lett.* 126, 37–42. doi: 10.1016/j.imlet.2009.07.010

James, A. W. (2013). Review of signaling pathways governing MSC osteogenic and adipogenic differentiation. *Scientifica* 2013:684736. doi: 10.1155/2013/684736

Jerby, L., Shlomi, T., and Ruppin, E. (2010). Computational reconstruction of tissue-specific metabolic models: application to human liver metabolism. *Mol. Syst. Biol.* 6:401. doi: 10.1038/msb.2010.56

Kanehisa, M., Sato, Y., Kawashima, M., Furumichi, M., and Tanabe, M. (2016). KEGG as a reference resource for gene and protein annotation. *Nucleic Acids Res.* 44, D457–D462. doi: 10.1093/nar/gkv1070

Kaundal, U., Bagai, U., and Rakha, A. (2018). Immunomodulatory plasticity of mesenchymal stem cells: a potential key to successful solid organ transplantation. *J. Transl. Med.* 16:31. doi: 10.1186/s12967-018-1403-0

Kell, D. B., and Goodacre, R. (2014). Metabolomics and systems pharmacology: why and how to model the human metabolic network for drug discovery. *Drug Discov. Today* 19, 171–182. doi: 10.1016/j.drudis.2013.07.014

Lan, Z., Ge, W., Arp, J., Jiang, J., Liu, W., Gordon, D., et al. (2010). Induction of kidney allograft tolerance by soluble CD83 associated with prevalence of tolerogenic dendritic cells and indoleamine 2,3-dioxygenase. *Transplantation* 90, 1286–1293. doi: 10.1097/TP.0b013e3182007bbf

Lee, S. H. (2018). The advantages and limitations of mesenchymal stem cells in clinical application for treating human diseases. *Osteoporos. Sarcopenia* 4:150. doi: 10.1016/j.afos.2018.11.083

Lee, W. D., Mukha, D., Aizenshtein, E., and Shlomi, T. (2019). Spatial-fluxomics provides a subcellular-compartmentalized view of reductive glutamine metabolism in cancer cells. *Nat. Commun.* 10:1351. doi: 10.1038/s41467-019-09352-1

Levian, C., Ruiz, E., and Yang, X. (2014). The pathogenesis of obesity from a genomic and systems biology perspective. *Yale J. Biol. Med.* 87, 113–126.

Levy, R., and Borenstein, E. (2013). Metabolic modeling of species interaction in the human microbiome elucidates community-level assembly rules. *Proc. Natl. Acad. Sci. U.S.A.* 110, 12804–12809. doi: 10.1073/pnas.1300926110

Li, J., and Dong, S. (2016). The signaling pathways involved in chondrocyte differentiation and hypertrophic differentiation. *Stem Cells Int.* 2016:2470351. doi: 10.1155/2016/2470351

Li, L., Chen, X., Wang, W. E., and Zeng, C. (2016). How to improve the survival of transplanted mesenchymal stem cell in ischemic heart? *Stem Cells Int.* 2016:9682757. doi: 10.1155/2016/9682757

Li, Q., Gao, Z., Chen, Y., and Guan, M.-X. (2017). The role of mitochondria in osteogenic, adipogenic and chondrogenic differentiation of mesenchymal stem cells. *Protein Cell* 8, 439–445. doi: 10.1007/s13238-017-0385-7

Lin, C.-S., Xin, Z.-C., Dai, J., and Lue, T. F. (2013). Commonly used mesenchymal stem cell markers and tracking labels: limitations and challenges. *Histol. Histopathol.* 28, 1109–1116. doi: 10.14670/HH-28.1109

Liu, T. M., Martina, M., Hutmacher, D. W., Hui, J. H. P., Lee, E. H., and Lim, B. (2007). Identification of common pathways mediating differentiation of bone marrow- and adipose tissue-derived human mesenchymal stem cells into three mesenchymal lineages. *Stem Cells* 25, 750–760. doi: 10.1634/stemcells.2006-0394

Liu, Y., Yuan, X., Muñoz, N., Logan, T. M., and Ma, T. (2019). Commitment to aerobic glycolysis sustains immunosuppression of human mesenchymal stem cells. *Stem Cells Transl. Med.* 8, 93–106. doi: 10.1002/sctm.18-0070

Lonner, J. H., Hershman, S., Mont, M., and Lotke, P. A. (2000). Total knee arthroplasty in patients 40 years of age and younger with osteoarthritis. *Clin. Orthop. Relat. Res.* 380, 85–90. doi: 10.1097/00003086-200011000-00012

Lukomska, B., Stanaszek, L., Zuba-Surma, E., Legosz, P., Sarzynska, S., and Drela, K. (2019). Challenges and controversies in human mesenchymal stem cell therapy. *Stem Cells Int.* 2019:9628536. doi: 10.1155/2019/9628536

Ma, H., Sorokin, A., Mazein, A., Selkov, A., Selkov, E., Demin, O., et al. (2007). The Edinburgh human metabolic network reconstruction and its functional analysis. *Mol. Syst. Biol.* 3:135. doi: 10.1038/msb4100177

Ma, O. K.-F., and Chan, K. H. (2016). Immunomodulation by mesenchymal stem cells: interplay between mesenchymal stem cells and regulatory lymphocytes. *World J. Stem Cells* 8, 268–278. doi: 10.4252/wjsc.v8.i9.268

Mackay, A. M., Beck, S. C., Murphy, J. M., Barry, F. P., Chichester, C. O., and Pittenger, M. F. (1998). Chondrogenic differentiation of cultured human mesenchymal stem cells from marrow. *Tissue Eng.* 4, 415–428. doi: 10.1089/ten.1998.4.415

Magúsdóttir, S., Heinken, A., Kutt, L., Ravcheev, D. A., Bauer, E., Noronha, A., et al. (2017). Generation of genome-scale metabolic reconstructions for 773 members of the human gut microbiota. *Nat. Biotechnol.* 35, 81–89. doi: 10.1038/nbt.3703

Mahla, R. S. (2016). Stem cells applications in regenerative medicine and disease therapeutics. *Int. J. Cell Biol.* 2016:6940283. doi: 10.1155/2016/6940283

Maienschein, J. (2011). Regenerative medicine's historical roots in regeneration, transplantation, and translation. *Dev. Biol.* 358, 278–284. doi: 10.1016/j.ydbio.2010.06.014

Mandal, R., Chamot, D., and Wishart, D. S. (2018). The role of the human metabolome database in inborn errors of metabolism. *J. Inherit. Metab. Dis.* 41, 329–336. doi: 10.1007/s10545-018-0137-8

Mardinoglu, A., Agren, R., Kampf, C., Asplund, A., Uhlen, M., and Nielsen, J. (2014). Genome-scale metabolic modelling of hepatocytes reveals serine deficiency in patients with non-alcoholic fatty liver disease. *Nat. Commun.* 5:3083. doi: 10.1038/ncomms4083

Mbongue, J. C., Nicholas, D. A., Torrez, T. W., Kim, N.-S., Firek, A. F., and Langridge, W. H. R. (2015). The role of indoleamine 2, 3-dioxygenase in immune suppression and autoimmunity. *Vaccines* 3, 703–729. doi: 10.3390/vaccines3030703

Meleshina, A. V., Dudenkova, V. V., Shirmanova, M. V., Shcheslavskiy, V. I., Becker, W., Bystrova, A. S., et al. (2016). Probing metabolic states of differentiating stem cells using two-photon FLIM. *Sci. Rep.* 6:21853. doi: 10.1038/srep21853

Meyer, J., Salamon, A., Mispagel, S., Kamp, G., and Peters, K. (2018). Energy metabolic capacities of human adipose-derived mesenchymal stromal cells in vitro and their adaptations in osteogenic and adipogenic differentiation. *Exp. Cell Res.* 370, 632–642. doi: 10.1016/j.yexcr.2018.07.028

Moreira, A., Kahlenberg, S., and Hornsby, P. (2017). Therapeutic potential of mesenchymal stem cells for diabetes. *J. Mol. Endocrinol.* 59, R109–R120. doi: 10.1530/JME-17-0117

Munir, H., and McGettrick, H. M. (2015). Mesenchymal stem cell therapy for autoimmune disease: risks and rewards. *Stem Cells Dev.* 24, 2091–2100. doi: 10.1089/scd.2015.0008

Muñoz, N., Kim, J., Liu, Y., Logan, T. M., and Ma, T. (2014). Gas chromatography–mass spectrometry analysis of human mesenchymal stem cell metabolism during proliferation and osteogenic differentiation under different oxygen tensions. *J. Biotechnol.* 169, 95–102. doi: 10.1016/j.jbiotec.2013.11.010

Muruganandan, S., Roman, A. A., and Sinal, C. J. (2009). Adipocyte differentiation of bone marrow-derived mesenchymal stem cells: cross talk with the osteoblastogenic program. *Cell. Mol. Life Sci.* 66, 236–253. doi: 10.1007/s00018-008-8429-z

Mussap, M., Zaffanello, M., and Fanos, V. (2018). Metabolomics: a challenge for detecting and monitoring inborn errors of metabolism. *Ann. Transl. Med.* 6:338. doi: 10.21037/atm.2018.09.18

Mylotte, L. A., Duffy, A. M., Murphy, M., O'Brien, T., Samali, A., Barry, F., et al. (2008). Metabolic flexibility permits mesenchymal stem cell survival in an ischemic environment. *Stem Cells* 26, 1325–1336. doi: 10.1634/stemcells.2007-1072

Narbonne, P. (2018). The effect of age on stem cell function and utility for therapy. *Cell Med.* 10:2155179018773756. doi: 10.1177/2155179018773756

Neman, J., Hambrecht, A., Cadry, C., and Jandial, R. (2012). Stem cell-mediated osteogenesis: therapeutic potential for bone tissue engineering. *Biologics* 6, 47–57. doi: 10.2147/BTT.S22407

Németh, K., Leelahavanichkul, A., Yuen, P. S. T., Mayer, B., Parmelee, A., Doi, K., et al. (2009). Bone marrow stromal cells attenuate sepsis via prostaglandin E(2)-dependent reprogramming of host macrophages to increase their interleukin-10 production. *Nat. Med.* 15, 42–49. doi: 10.1038/nm.1905

Neve, A., Corrado, A., and Cantatore, F. P. (2011). Osteoblast physiology in normal and pathological conditions. *Cell Tissue Res.* 343, 289–302. doi: 10.1007/s00441-010-1086-1

Neves, J., Sousa-Victor, P., and Jasper, H. (2017). Rejuvenating strategies for stem cell-based therapies in aging. *Cell Stem Cell* 20, 161–175. doi: 10.1016/j.stem.2017.01.008

Nombela-Arrieta, C., Ritz, J., and Silberstein, L. E. (2011). The elusive nature and function of mesenchymal stem cells. *Nat. Rev. Mol. Cell Biol.* 12, 126–131. doi: 10.1038/nrm3049

Norsigian, C. J., Pusarla, N., McConn, J. L., Yurkovich, J. T., Dräger, A., Palsson, B. O., et al. (2020). BiGG models 2020: multi-strain genome-scale models and expansion across the phylogenetic tree. *Nucleic Acids Res.* 48, D402–D406. doi: 10.1093/nar/gkz1054

Oberhardt, M. A., Palsson, B. Ø., and Papin, J. A. (2009). Applications of genome-scale metabolic reconstructions. *Mol. Syst. Biol.* 5:320. doi: 10.1038/msb.2009.77

Paglia, G., Sigurjónsson, Ó. E., Bordbar, A., Rolfsson, Ó., Magnusdottir, M., Palsson, S., et al. (2016). Metabolic fate of adenine in red blood cells during storage in SAGM solution. *Transfusion* 56, 2538–2547. doi: 10.1111/trf.13740

Pattappa, G., Heywood, H. K., de Bruijn, J. D., and Lee, D. A. (2011). The metabolism of human mesenchymal stem cells during proliferation and differentiation. *J. Cell. Physiol.* 226, 2562–2570. doi: 10.1002/jcp.22605

Qian, H., Yang, H., Xu, W., Yan, Y., Chen, Q., Zhu, W., et al. (2008). Bone marrow mesenchymal stem cells ameliorate rat acute renal failure by differentiation into renal tubular epithelial-like cells. *Int. J. Mol. Med.* 22, 325–332. doi: 10.3892/ijmm_00000026

Qin, J., Zhao, Y., Wang, Y., Betzler, C., Popp, F., Sen Gupta, A., et al. (2016). Therapeutic potential of mesenchymal stem cells in gastrointestinal cancers - current evidence. *Gastrointest. Cancer Targets Ther.* 2016, 41–47.

Quek, L.-E., Dietmair, S., Hanscho, M., Martínez, V. S., Borth, N., and Nielsen, L. K. (2014). Reducing recon 2 for steady-state flux analysis of HEK cell culture. *J. Biotechnol.* 184, 172–178. doi: 10.1016/j.jbiotec.2014.05.021

Reed, J. L., and Palsson, B. Ø. (2003). Thirteen years of building constraint-based in silico models of *Escherichia coli*. *J. Bacteriol.* 185, 2692–2699. doi: 10.1128/JB.185.9.2692-2699.2003

Ren, G., Zhang, L., Zhao, X., Xu, G., Zhang, Y., Roberts, A. I., et al. (2008). Mesenchymal stem cell-mediated immunosuppression occurs via concerted action of chemokines and nitric oxide. *Cell Stem Cell* 2, 141–150. doi: 10.1016/j.stem.2007.11.014

Resendis-Antonio, O. (2013). "Constraint-based modeling," in *Encyclopedia of Systems Biology*, eds W. Dubitzky, O. Wolkenhauer, K.-H. Cho, and H. Yokota (New York, NY: Springer), 494–498. doi: 10.2147/GICTT.S54121

Rocha, I., Förster, J., and Nielsen, J. (2008). "Design and application of genome-scale reconstructed metabolic models," in *Microbial Gene Essentiality: Protocols and Bioinformatics Methods in Molecular BiologyTM*, Vol. 416, eds A. L. Osterman and S. Y. Gerdes (Totowa, NJ: Humana Press), 409–431. doi: 10.1007/978-1-59745-321-9_29

Rolfsson, O., Palsson, B. Ø., and Thiele, I. (2011). The human metabolic reconstruction recon 1 directs hypotheses of novel human metabolic functions. *BMC Syst. Biol.* 5:155. doi: 10.1186/1752-0509-5-155

Romero, P., Wagg, J., Green, M. L., Kaiser, D., Krummenacker, M., and Karp, P. D. (2004). Computational prediction of human metabolic pathways from the complete human genome. *Genome Biol.* 6:R2. doi: 10.1186/gb-2004-6-1-r2

Rose, R. A., Jiang, H., Wang, X., Helke, S., Tsoporis, J. N., Gong, N., et al. (2008). Bone marrow-derived mesenchymal stromal cells express cardiac-specific markers, retain the stromal phenotype, and do not become functional cardiomyocytes in vitro. *Stem Cells* 26, 2884–2892. doi: 10.1634/stemcells.2008-0329

Rosenbaum, A. J., Grande, D. A., and Dines, J. S. (2008). The use of mesenchymal stem cells in tissue engineering. *Organogenesis* 4, 23–27. doi: 10.4161/org.6048

Russo, F. P., Alison, M. R., Bigger, B. W., Amofah, E., Florou, A., Amin, F., et al. (2006). The bone marrow functionally contributes to liver fibrosis. *Gastroenterology* 130, 1807–1821. doi: 10.1053/j.gastro.2006.01.036

Sahoo, S., Aurich, M. K., Jonsson, J. J., and Thiele, I. (2014). Membrane transporters in a human genome-scale metabolic knowledgebase and their implications for disease. *Front. Physiol.* 5:91. doi: 10.3389/fphys.2014.00091

Sahoo, S., Franzson, L., Jonsson, J. J., and Thiele, I. (2012). A compendium of inborn errors of metabolism mapped onto the human metabolic network. *Mol. Biosyst.* 8, 2545–2558. doi: 10.1039/c2mb25075f

Sahoo, S., Haraldsdóttir, H. S., Fleming, R. M. T., and Thiele, I. (2015). Modeling the effects of commonly used drugs on human metabolism. *FEBS J.* 282, 297–317. doi: 10.1111/febs.13128

Sampogna, G., Guraya, S. Y., and Forgione, A. (2015). Regenerative medicine: historical roots and potential strategies in modern medicine. *J. Microsc. Ultrastruct.* 3, 101–107. doi: 10.1016/j.jmau.2015.05.002

Schultz, A., and Qutub, A. A. (2016). Reconstruction of tissue-specific metabolic networks using CORDA. *PLoS Comput. Biol.* 12:e1004808. doi: 10.1371/journal.pcbi.1004808

Secunda, R., Vennila, R., Mohanashankar, A. M., Rajasundari, M., Jeswanth, S., and Surendran, R. (2015). Isolation, expansion and characterisation of mesenchymal stem cells from human bone marrow, adipose tissue, umbilical cord blood and matrix: a comparative study. *Cytotechnology* 67, 793–807. doi: 10.1007/s10616-014-9718-z

Shares, B. H., Busch, M., White, N., Shum, L., and Eliseev, R. A. (2018). Active mitochondria support osteogenic differentiation by stimulating β-catenin acetylation. *J. Biol. Chem.* 293, 16019–16027. doi: 10.1074/jbc.RA118.004102

Shen, F., Cheek, C., and Chandrasekaran, S. (2019). Dynamic network modeling of stem cell metabolism. *Methods Mol. Biol.* 1975, 305–320. doi: 10.1007/978-1-4939-9224-9_14

Shlomi, T., Cabili, M. N., and Ruppin, E. (2009). Predicting metabolic biomarkers of human inborn errors of metabolism. *Mol. Syst. Biol.* 5:263. doi: 10.1038/msb.2009.22

Shum, L. C., White, N. S., Mills, B. N., de Mesy Bentley, K. L., and Eliseev, R. A. (2016). Energy metabolism in mesenchymal stem cells during osteogenic differentiation. *Stem Cells Dev.* 25, 114–122. doi: 10.1089/scd.2015.0193

Smallbone, K., Messiha, H. L., Carroll, K. M., Winder, C. L., Malys, N., Dunn, W. B., et al. (2013). A model of yeast glycolysis based on a consistent kinetic characterisation of all its enzymes. *FEBS Lett.* 587, 2832–2841. doi: 10.1016/j.febslet.2013.06.043

Smolková, K., and Ježek, P. (2012). The role of mitochondrial NADPH-dependent isocitrate dehydrogenase in cancer cells. *Int. J. Cell Biol.* 2012:273947. doi: 10.1155/2012/273947

Solarte, V. A., Bayona, S. B., Aranguren, L. S., Sossa, C. L., Meana, A., Lloves, J. M., et al. (2018). Function and therapeutic potential of mesenchymal stem cells and their acellular derivatives on non-healing chronic skin ulcers. *J. Stem Cell Res. Ther.* 8:423. doi: 10.4172/2157-7633.1000423

Solchaga, L. A., Penick, K. J., and Welter, J. F. (2011). Chondrogenic differentiation of bone marrow-derived mesenchymal stem cells: tips and tricks. *Methods Mol. Biol.* 698, 253–278. doi: 10.1007/978-1-60761-999-4_20

Stempler, S., Yizhak, K., and Ruppin, E. (2014). Integrating transcriptomics with metabolic modeling predicts biomarkers and drug targets for Alzheimer's disease. *PLoS One* 9:e105383. doi: 10.1371/journal.pone.0105383

Strober, B. J., Elorbany, R., Rhodes, K., Krishnan, N., Tayeb, K., Battle, A., et al. (2019). Dynamic genetic regulation of gene expression during cellular differentiation. *Science* 364, 1287–1290. doi: 10.1126/science.aaw0040

Swainston, N., Smallbone, K., Hefzi, H., Dobson, P. D., Brewer, J., Hanscho, M., et al. (2016). Recon 2.2: from reconstruction to model of human metabolism. *Metabolomics* 12:109.

Tachida, Y., Sakurai, H., Okutsu, J., Suda, K., Sugita, R., Yaginuma, Y., et al. (2015). Proteomic comparison of the secreted factors of mesenchymal stem cells from bone marrow, adipose tissue and dental pulp. *J. Proteomics Bioinform.* 8, 266–273. doi: 10.4172/jpb.1000379

Takarada-Iemata, M., Takarada, T., Nakamura, Y., Nakatani, E., Hori, O., and Yoneda, Y. (2011). Glutamate preferentially suppresses osteoblastogenesis than adipogenesis through the cystine/glutamate antiporter in mesenchymal stem cells. *J. Cell. Physiol.* 226, 652–665. doi: 10.1002/jcp.22390

Tatard, V. M., D'Ippolito, G., Diabira, S., Valeyev, A., Hackman, J., McCarthy, M., et al. (2007). Neurotrophin-directed differentiation of human adult marrow stromal cells to dopaminergic-like neurons. *Bone* 40, 360–373. doi: 10.1016/j.bone.2006.09.013

Thiele, I., and Palsson, B. Ø. (2010). A protocol for generating a high-quality genome-scale metabolic reconstruction. *Nat. Protoc.* 5, 93–121. doi: 10.1038/nprot.2009.203

Thiele, I., Swainston, N., Fleming, R. M. T., Hoppe, A., Sahoo, S., Aurich, M. K., et al. (2013). A community-driven global reconstruction of human metabolism. *Nat. Biotechnol.* 31, 419–425. doi: 10.1038/nbt.2488

Trushina, E., and Mielke, M. M. (2014). Recent advances in the application of metabolomics to Alzheimer's disease. *Biochim. Biophys. Acta Mol. Basis Dis.* 1842, 1232–1239. doi: 10.1016/j.bbadis.2013.06.014

Tsai, Y.-H., Lin, K.-L., Huang, Y.-P., Hsu, Y.-C., Chen, C.-H., Chen, Y., et al. (2015). Suppression of ornithine decarboxylase promotes osteogenic differentiation of human bone marrow-derived mesenchymal stem cells. *FEBS Lett.* 589, 2058–2065. doi: 10.1016/j.febslet.2015.06.023

Turinetto, V., Vitale, E., and Giachino, C. (2016). Senescence in human mesenchymal stem cells: functional changes and implications in stem cell-based therapy. *Int. J. Mol. Sci.* 17:1164. doi: 10.3390/ijms17071164

Ullah, I., Subbarao, R. B., and Rho, G. J. (2015). Human mesenchymal stem cells - current trends and future prospective. *Biosci. Rep.* 35:e00191. doi: 10.1042/BSR20150025

Ullah, M., Liu, D. D., and Thakor, A. S. (2019). Mesenchymal stromal cell homing: mechanisms and strategies for improvement. *iScience* 15, 421–438. doi: 10.1016/j.isci.2019.05.004

Valencia, J., Blanco, B., Yáñez, R., Vázquez, M., Herrero Sánchez, C., Fernández-García, M., et al. (2016). Comparative analysis of the immunomodulatory capacities of human bone marrow- and adipose tissue-derived mesenchymal stromal cells from the same donor. *Cytotherapy* 18, 1297–1311. doi: 10.1016/j.jcyt.2016.07.006

Väremo, L., Nookaew, I., and Nielsen, J. (2013). Novel insights into obesity and diabetes through genome-scale metabolic modeling. *Front. Physiol.* 4:92. doi: 10.3389/fphys.2013.00092

Vigo, T., La Rocca, C., Faicchia, D., Procaccini, C., Ruggieri, M., Salvetti, M., et al. (2019). IFNβ enhances mesenchymal stromal (stem) cells immunomodulatory function through STAT1-3 activation and mTOR-associated promotion of glucose metabolism. *Cell Death Dis.* 10:85.

von Bomhard, A., Elsässer, A., Ritschl, L. M., Schwarz, S., and Rotter, N. (2016). Cryopreservation of endothelial cells in various cryoprotective agents and media - vitrification versus slow freezing methods. *PLoS One* 11:e0149660. doi: 10.1371/journal.pone.0149660

Wang, M., Yuan, Q., and Xie, L. (2018). Mesenchymal stem cell-based immunomodulation: properties and clinical application. *Stem Cells Int.* 2018:3057624. doi: 10.1155/2018/3057624

Wang, Y., Eddy, J. A., and Price, N. D. (2012). Reconstruction of genome-scale metabolic models for 126 human tissues using mCADRE. *BMC Syst. Biol.* 6:153. doi: 10.1186/1752-0509-6-153

Waterman, R. S., Tomchuck, S. L., Henkle, S. L., and Betancourt, A. M. (2010). A new mesenchymal stem cell (MSC) paradigm: polarization into a pro-inflammatory MSC1 or an Immunosuppressive MSC2 phenotype. *PLoS One* 5:e10088. doi: 10.1371/journal.pone.0010088

Westerhoff, H. V., and Palsson, B. O. (2004). The evolution of molecular biology into systems biology. *Nat. Biotechnol.* 22, 1249–1252. doi: 10.1038/nbt1020

Wone, B. W. M., Kinchen, J. M., Kaup, E. R., and Wone, B. (2018). A procession of metabolic alterations accompanying muscle senescence in *Manduca sexta*. *Sci. Rep.* 8:1006. doi: 10.1038/s41598-018-19630-5

Yizhak, K., Gabay, O., Cohen, H., and Ruppin, E. (2013). Model-based identification of drug targets that revert disrupted metabolism and its application to ageing. *Nat. Commun.* 4:2632. doi: 10.1038/ncomms3632

Youngstrom, D. W., LaDow, J. E., and Barrett, J. G. (2016). Tenogenesis of bone marrow-, adipose-, and tendon-derived stem cells in a dynamic bioreactor. *Connect. Tissue Res.* 57, 454–465. doi: 10.3109/03008207.2015.1117458

Yuan, X., Logan, T. M., and Ma, T. (2019). Metabolism in human mesenchymal stromal cells: a missing link between hMSC biomanufacturing and therapy? *Front. Immunol.* 10:977. doi: 10.3389/fimmu.2019.00977

Yue, Y., Zhang, L., Zhang, X., Li, X., and Yu, H. (2018). De novo lipogenesis and desaturation of fatty acids during adipogenesis in bovine adipose-derived mesenchymal stem cells. *In Vitro Cell. Dev. Biol. Anim.* 54, 23–31. doi: 10.1007/s11626-017-0205-7

Yurkovich, J. T., and Palsson, B. O. (2016). Solving puzzles with missing pieces: the power of systems biology. *Proc. IEEE* 104, 2–7. doi: 10.1109/JPROC.2015.2505338

Zhang, X., Zhang, L., Xu, W., Qian, H., Ye, S., Zhu, W., et al. (2013). Experimental therapy for lung cancer: umbilical cord-derived mesenchymal stem cell-mediated interleukin-24 delivery. *Curr. Cancer Drug Targets* 13, 92–102. doi: 10.2174/1568009611309010092

Zhang, Y., Marsboom, G., Toth, P. T., and Rehman, J. (2013). Mitochondrial respiration regulates adipogenic differentiation of human mesenchymal stem cells. *PLoS One* 8:e77077. doi: 10.1371/journal.pone.0077077

Zhao, Q., Ren, H., and Han, Z. (2016). Mesenchymal stem cells: immunomodulatory capability and clinical potential in immune diseases. *J. Cell. Immunother.* 2, 3–20. doi: 10.1016/j.jocit.2014.12.001

Zhu, H., Sun, A., Zou, Y., and Ge, J. (2014). Inducible metabolic adaptation promotes mesenchymal stem cell therapy for ischemia: a hypoxia-induced and glycogen-based energy prestorage strategy. *Arterioscler. Thromb. Vasc. Biol.* 34, 870–876. doi: 10.1161/ATVBAHA.114.303194

Zhu, J., and Thompson, C. B. (2019). Metabolic regulation of cell growth and proliferation. *Nat. Rev. Mol. Cell Biol.* 20, 436–450. doi: 10.1038/s41580-019-0123-5

Conflict of Interest: The authors declare that the research was conducted in the absence of any commercial or financial relationships that could be construed as a potential conflict of interest.

6. Appendix

6.1. Appendix A.

Table A1. Summary of various methods of inducing varying differentiations, expression marker and signalling pathways related to differentiation. Adapted from [73]. *Not an exhaustive list*

Cell type resulting from differentiation	Differentiation via media additives	Differentiation via mechanical stimulation	Differentiation via scaffold/culture surface modification	Culturing time	Relevant expression markers	Most relevant reported pathways and molecules	References
Adipocytes	Dexamethasone, Indomethacin, Insulin, Isobutilmethyl xanthine		Nanopatterning of bulk metallic glass, soft scaffold (pro)	14-21 days, with 2 phases (determination and terminal differentiation)	Ap2, LPL, PPARγ	B-catenin dependent Wnt (anti), Hedgehog, (anti), NELL-1 (anti), BMP (pro)	[76], [81]
Cardiomyocytes	5-azacytidine	Equiaxial cyclic strain		28 days	α-MHC, α-cardiac actin, ANP, cTnT, Desmin	miR1-2 + Wnt/β-catenin (pro) HDAC, TGF-β, VR-1, 5-aza	[279]–[281]
Chondrocytes	Ascorbate-2-phosphate, Dexamethasone, Insulin, Linoleic Acid, Selenious pyruvate, Selenium, TGF-βIII, Transferrin		Soft scaffold (pro)	21 days, with 2 phases (pre-induction and terminal differentiation)	*Phase I*: Collagen types I and II *Phase II:* L-Sox5 Sox6 Sox9	*Phase 1 expression dependent upon:* TGF-β1, 2 and 3 *Phase 2 expression dependent upon:* BMP2, IGF-I, TGF-β1, Wnt/β-catenin (pro), PTHrp(anti)	[75], [77]–[79]
Hepatocytes	*Phase I:* bFGF, EGF, Nicotinamide *Phase II:* Dexamethasone, Insulin, Oncostatin, M-Selenium, Transferrin		3D environment sustains differentiation functions better	2 phases: differentiation (7 days) and maturation			[18], [282]
Neuronal cells	bFGF, BME, EGF, FGF, HGF, Insulin, LMX1A, NGF, Retinoic acid, Valproic acid						[18]
Osteocytes	B-glycerolphosphate, Ascorbic acid, BMP-2, Dexamethasone	Cyclic stretching (tensile loading), hydrostatic pressure (compressive loading), fluid flow (shear stress)	Nanopatterning of bulk metallic glass, stiff scaffold (pro)	21-35 days	ALP, COL1, OC, ON, OP, RUNX2	B-catenin dependent Wnt (pro), BMP (pro), Hedgehog (pro), NELL-1 (pro), TGF-β1 + Wnt/β-catenin (anti)	[74], [75], [81], [283]
Pancreocytes	Actavin A, Nicotnamide, Sodium butyrate, Taurine						[18]
Skeletal/smooth muscle	NICD, TGF-β	Cyclic stretching (tensile loading)					[18], [74]

Table A2. Akaike Information Criteria from models fitted with the gamm4 function in R, all models are for each metabolite varying by day with the combinations of random effects considered below.

	Donor + Analysis Batch	PIPL/Donor + Analysis Batch	Passage/Donor + Analysis Batch	PIPL/Passage/Donor + Analysis Batch	Donor + Media + Analysis Batch	Donor
Glucose	1543.795	1545.795	1545.795	1547.795	1545.795	1558.992
Lactate	1168.993	1170.993	1170.993	1172.993	1167.776	1227.897
Glutamine	587.1644	589.1644	588.3329	591.1644	595.5849	591.5849
Glutamate	292.9485	294.9485	293.2039	296.9485	381.4727	377.9853
Ammonia	757.6984	759.3254	758.5992	761.3254	820.5771	816.5771

Appendix A

Table A1. Summary of various methods of inducing varying differentiations, expression marker and signalling pathways related to differentiation. Adapted from [73]. *Not an exhaustive list*

Cell type resulting from differentiation	Differentiation via media additives	Differentiation via mechanical stimulation	Differentiation via scaffold/culture surface modification	Culturing time	Relevant expression markers	Most relevant reported pathways and molecules	References
Adipocytes	Dexamethasone, Indomethacin, Insulin, Isobutilmethyl xanthine		Nanopatterning of bulk metallic glass, soft scaffold (pro)	14-21 days, with 2 phases (determination and terminal differentiation)	Ap2, LPL, PPARγ	B-catenin dependent Wnt (anti), Hedgehog, (anti), NELL-1 (anti), BMP (pro)	[76], [81]
Cardiomyocytes	5-azacytidine	Equiaxial cyclic strain		28 days	α-MHC, α-cardiac actin, ANP, cTnT, Desmin	miR1-2 + Wnt/β-catenin (pro) HDAC, TGF-β, VR-1, 5-aza	[279]–[281]
Chondrocytes	Ascorbate-2-phosphate, Dexamethasone, Insulin, Linoleic Acid, Selenious pyruvate, Selenium, TGF-βIII, Transferrin		Soft scaffold (pro)	21 days, with 2 phases (pre-induction and terminal differentiation)	*Phase I*: Collagen types I and II *Phase II:* L-Sox5 Sox6 Sox9	*Phase 1 expression dependent upon:* TGF-β1, 2 and 3 *Phase 2 expression dependent upon:* BMP2, IGF-I, TGF-β1, Wnt/β-catenin (pro), PTHrp(anti)	[75], [77]–[79]
Hepatocytes	*Phase I:* bFGF, EGF, Nicotinamide *Phase II:* Dexamethasone, Insulin, Oncostatin, M-Selenium, Transferrin		3D environment sustains differentiation functions better	2 phases: differentiation (7 days) and maturation			[18], [282]
Neuronal cells	bFGF, BME, EGF, FGF, HGF, Insulin, LMX1A, NGF, Retinoic acid, Valproic acid						[18]
Osteocytes	B-glycerolphosphate, Ascorbic acid, BMP-2, Dexamethasone	Cyclic stretching (tensile loading), hydrostatic pressure (compressive loading), fluid flow (shear stress)	Nanopatterning of bulk metallic glass, stiff scaffold (pro)	21-35 days	ALP, COL1, OC, ON, OP, RUNX2	B-catenin dependent Wnt (pro), BMP (pro), Hedgehog (pro), NELL-1 (pro), TGF-β1 + Wnt/β-catenin (anti)	[74], [75], [81], [283]
Pancreocytes	Actavin A, Nicotnamide, Sodium butyrate, Taurine						[18]
Skeletal/smooth muscle	NICD, TGF-β	Cyclic stretching (tensile loading)					[18], [74]

Table A2. Akaike Information Criteria from models fitted with the gamm4 function in R, all models are for each metabolite varying by day with the combinations of random effects considered below.

	Donor + Analysis Batch	PIPL/Donor + Analysis Batch	Passage/Donor + Analysis Batch	PIPL/Passage/Donor + Analysis Batch	Donor + Media + Analysis Batch	Donor
Glucose	1543.795	1545.795	1545.795	1547.795	1545.795	1558.992
Lactate	1168.993	1170.993	1170.993	1172.993	1167.776	1227.897
Glutamine	587.1644	589.1644	588.3329	591.1644	595.5849	591.5849
Glutamate	292.9485	294.9485	293.2039	296.9485	381.4727	377.9853
Ammonia	757.6984	759.3254	758.5992	761.3254	820.5771	816.5771

ORCID:0000-0002-4737-4646.
ISBN 978-9935-9620-1-0 electronic version.
ISBN 978-9935-9620-0-3 printed version.